DEPARTAMENTO DE BIOLOGÍA CELULAR Y ECOLOGÍA
ÁREA DE BIOLOGÍA CELULAR
FACULTAD DE BIOLOGÍA

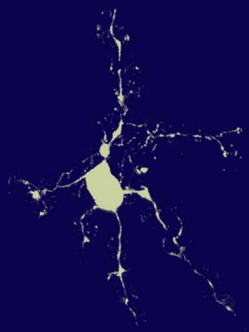

Developmental study of the cerebellum in cartilaginous fishes: Towards the identification of primitive features of the cerebellar formation in gnathostomes

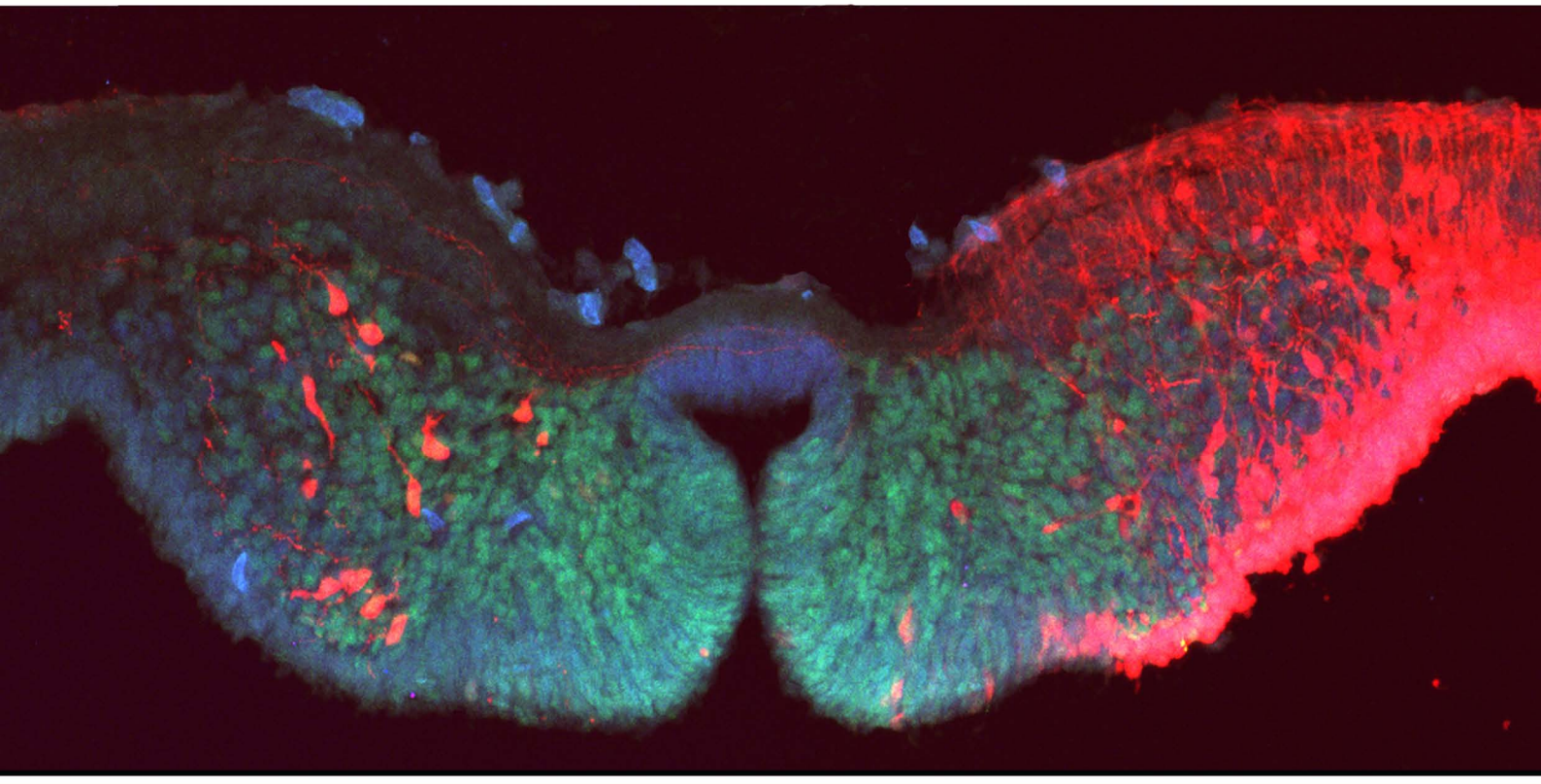

TESIS DOCTORAL

SOL M. POSE MÉNDEZ

Santiago de Compostela, 2013

UNIVERSIDAD DE SANTIAGO DE COMPOSTELA
DEPARTAMENTO DE BIOLOGÍA CELULAR Y ECOLOGÍA
FACULTAD DE BIOLOGÍA

PROGRAMA DE DOCTORADO INTERUNIVERSITARIO EN NEUROCIENCIA
(UNIVERSIDAD DE SANTIAGO DE COMPOSTELA, UNIVERSIDAD DE VIGO,
UNIVERSIDAD DE A CORUÑA)

DEVELOPMENTAL STUDY OF THE CEREBELLUM IN CARTILAGINOUS FISHES: TOWARDS THE IDENTIFICATION OF PRIMITIVE FEATURES OF THE CEREBELLAR FORMATION IN GNATHOSTOMES

MEMORIA

Para optar al Grado de Doctor por la Universidad de Santiago de Compostela presentada por

SOL M. POSE MÉNDEZ

Santiago de Compostela, 2013

USC
UNIVERSIDADE
DE SANTIAGO
DE COMPOSTELA

Santiago de Compostela, 2013

ISABEL RODRÍGUEZ-MOLDES REY, CATEDRÁTICA DEL ÁREA DE BIOLOGÍA CELULAR Y EVA CANDAL SUÁREZ, PROFESORA CONTRATADA DOCTORA DEL DEPARTAMENTO DE BIOLOGÍA CELULAR Y ECOLOGÍA DE LA UNIVERSIDAD DE SANTIAGO DE COMPOSTELA,

CERTIFICAN:

Que la presente memoria titulada Developmental study of the cerebellum in cartilaginous fishes: Towards the identification of primitive features of the cerebellar formation in gnathostomes, para optar al Grado de Doctor por la Universidad de Santiago de Compostela presentada por Dña. SOL M. POSE MÉNDEZ, ha sido realizada bajo nuestra dirección. Y considerando que constituye trabajo de tesis, autorizamos su presentación a la Comisión Académica correspondiente.

Y para que así conste, expedimos el presente certificado en Santiago de Compostela, a 3 de junio del 2013.

La Doctoranda Las Directoras de la Tesis

Fdo.: Sol M. Pose Méndez Fdo.: Isabel Rodríguez-Moldes Rey Fdo.: Eva Candal Suárez

USC
UNIVERSIDADE
DE SANTIAGO
DE COMPOSTELA

FINANCIACIÓN DE LA INVESTIGACIÓN

La realización de esta Tesis ha sido posible gracias a la financiación de los siguientes organismos:

Ministerio de Educación y Ciencia- Dirección General de Investigación-FEDER (BFU2007-61154). *Título del proyecto:* Formación del patrón del encéfalo en condrictios (peces cartilaginosos)

Ministerio de Ciencia e Innovación- Dirección General de Investigación-FEDER (BFU2010-15816). *Título del proyecto:* Buscando la condición ancestral de la organización cerebral de gnatóstomos: regionalización, migración, proyecciones y asimetrías en el cerebro en desarrollo de un tiburón

Dirección Xeral de I+D - Xunta de Galicia (10PXIB200051PR). *Título del proyecto:* Control de la expresión génica in ovo durante el desarrollo del sistema nervioso de peces. Identificación de los mecanismos conservados evolutivamente

Consellería de Economía – Programa xeral de Consolidación e estruturación das unidades de investigación do sistema galego de I+D+I. INCITE09ENA200048ES (Año 2009)

Consellería de Economía e Industria – Programa xeral de Consolidación e estruturación das unidades de investigación do sistema galego de I+D+I. IN845B-2010/159 (Año 2010).

Conselleria de Cultura, Educación e Ordenación Universitaria – Proxectos Plan Galego IDT- Consolidación e Estruturación de Unidades de Investigación competitivas (GPC). CN 2012/237. Año 2012.

CONTRATOS Y BECAS

La realización de esta Tesis ha sido posible gracias a la concesión de las siguientes becas y contratos:

- Beca/contrato del programa predoctoral María Barbeito de la Xunta de Galicia.
- Contrato asociado al proyecto: BFU2010-15816.

- Contrato asociado al proyecto: CN 2012/237.
- Beca para la realización de la estancia realizada en la Universidad Técnica de Braunschweig (Alemania), concedida por COST Action BM0804 (EuFishBioMed).

DISPONIBILIDAD DE EMBRIONES DE LA PINTARROJA

La disponibilidad de embriones ha sido posible gracias a la financiación de European Community – Research Infrastructure Action under the FP7 "Capacities" Specific Programme (ASSEMBLE grant agreement no. 227799) y a la colaboración de la Estación de Bioloxía Mariña da Graña, y de los acuarios de Gijón, O Grove y A Coruña (España).

DISPONIBILIDAD DE LAS SONDAS DE GENES DE PINTARROJA

La disponibilidad de las sondas de los genes ha sido posible gracias al proyecto de secuenciacion EST del genoma de pintarroja, coordinado por la Dra. Sylvie Mazan, financiado por Génoscope, Evry (Francia).

Esta etapa de tese foi unha gran e tan grata experiencia que se dispuxese dunha máquina do tempo, volvería a empezar outra vez. Tamén coñecín e compartín con tanta e tan boa xente que non me cansarei de repetir a mesma palabra unha chea de veces, gracias. Gracias a todos aqueles que me ensinaron e dos cales tanto aprendín.

Gracias Isa, por darme esta gran oportunidade de coñecer tan maravilloso mundo. Porque gracias a ti me acabaron cautivando os misterios da neurociencia, e as ganas de querer saber sempre máis. Gracias por estar sempre ahí, atopar sempre solución a todos ós problemas, e por ensinarme tanto e sempre con tanto entusiasmo.

Gracias Eva, por toda a túa dedicación, por tantas cousas que me ensinaches, por tanto que me axudaches e tantos problemas que me solucionaches.

Gracias a Isa e a Eva por compartir tan bos momentos conmigo, por guiarme, animarme sempre, por tanta paciencia e comprensión, e por tantos e tan bos consellos.

A Ramón, pola súa axuda incondicional. Por estar sempre ahí, sempre disposto a solucionar todas as dúbidas e cuestións.

A Idoia, por compartir tantos momentos e experiencias xuntas, codo con codo, dende o principio ata o final.

A Iván por axudarme e guiarme nos primeiros pasos durante esta etapa de tese.

A todos os compañeiros/as do laboratorio. Gabriel, por compartir e alegrarme tantas mañás e tardes. Nuria, por toda a paciencia, sobre todo nesta etapa final. Susana por tantas cousas que me ensinaches. David e Alba, por esa alegría e optimismo contaxiosos. Santi por tan grata compañía. Así como todos os demáis compañeiros/as que tamén compartiron moi bos momentos.

A Miguel e Fátima, porque alegran o laboratorio cada vez que entran. Fátima, gracias por estar aí sempre axudándome cando o necesitaba.

Ós lampreólogos polo seu gran compañerismo, Antón, Verona, Blanca e Maru, gracias.

A todos os demais compañeiros e membros do departamento, tamén gracias.

Merche e Raquel pola súa axuda e tan bos consellos no mundo do confocal.

A todos os meus/miñas amigos/as, en especial Ana y Lucía, porque sei que sempre estaredes aí.

A todos os cadarsianos/as, os cales non olvidarei, nin esquecerei tan bos momentos que pasamos como unha gran familia, e que o seguirá sendo.

I am also very grateful for the opportunity that the Professor Köster gave me being in his laboratory, and his kindness. Thanks to Hideaki for being so kind and teaching me so many things. And thanks to all members of the lab who have been very friendly.

Dear all in Braunschweig, danke schön.

E en especial a miña familia, que tanto me apoian e comprenden, meu irmán Adrián, meus pais e meus avós.

GRACIAS A TODOS.

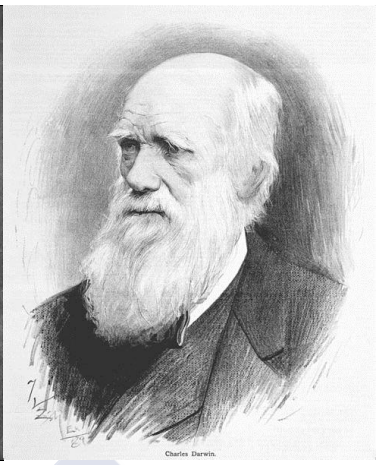

Santiago Ramón y Cajal *Charles Darwin*

También a ellos, gracias.

USC
UNIVERSIDADE
DE SANTIAGO
DE COMPOSTELA

INDEX

GENERAL INTRODUCTION

USC
UNIVERSIDADE
DE SANTIAGO
DE COMPOSTELA

GENERAL INTRODUCTION

The cerebellum and its functions

The cerebellum (the Latin word for *little brain*) has largely been one of the most studied structures of the brain (Glickstein et al., 2009). A considerable part of our knowledge on cerebellar cellular structure and histogenesis is due to Ramón y Cajal (for a deep review, see Puelles, 2009), who is considered one of the founding fathers in the study of the cerebellum (see Fig. 1). From the time of his discoveries up to now, much of what is known about the development, structure and function of the cerebellum is based on classical anatomical tools such as Golgi staining, neuroanatomical tract tracing, immunostaining and a number of genetic tools.

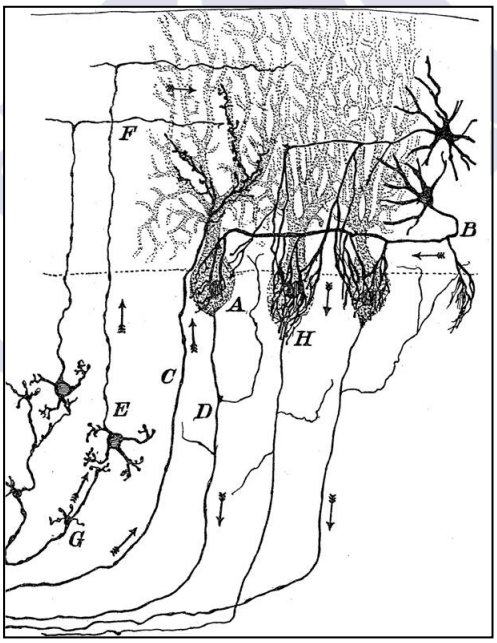

Figure 1. The elements of the cerebellar cortex. A, Purkinje cell; B, basket cell; C, climbing fiber; D, Purkinje cell axon with collaterals; E, granule cell; F, parallel fiber; G, mossy fiber rosette; H, basket of the basket cells axon. From Ramon y Cajal's Croonian Lecture (Ramon y Cajal, 1894). Taken from Glickstein et al. (2009).

The cerebellum displays several features that make it highly amenable to study the genetic specification and morphogenetic processes that are at the basis of the

structural complexity of the adult brain. First, it represents 10% of the total brain's volume, but contains more than half of its neurons, which become organized in a discrete number of cell layers and give rise to a highly organized circuitry (see below). Second, the cerebellum presents a protracted development that allows a detailed study of its early regionalization and morphogenesis, which in turn helps to understand how the adult cerebellar architecture is achieved. Third, the understanding of these morphogenetic processes will help to know the basis of a large spectrum of cerebellar disorders.

Other of the reasons that explain why the cerebellum is attracting a growing number of scientists is the increasing awareness of its multiple roles (Manto and Haines, 2012). It is well known that the cerebellum integrates sensorial and motor information (for review, see Delgado-García, 2001). It is involved in the coordination of voluntary movements (by controlling the timing and pattern of muscle activation), in the regulation of muscle tone and in the maintenance of body balance and posture. The cerebellum is also involved in motor learning, i.e., it plays a major role in adapting and fine-tuning motor programs to make accurate movements through a trial-and-error process (see Thach, 1998). A well-known example of motor learning is the vestibulo-ocular reflex (Ito, 1984; Allman, 2003; Yoshikawa et al., 2004), in which the cerebellum allows the retinal image getting stabilized (i.e., not blurred by the movement). More recently described functions include the involvement of the cerebellum in cognitive and emotional processes such as associative learning, emotional conditioning, relational memory or spatial cognition. Motor learning and cognitive processes were observed not only in mammals, but also in other vertebrate groups as bony fishes (Rodríguez et al., 2005). Furthermore, the cerebellum is also responsible for the analysis of the lateral line information in most of anamniota vertebrates (Puzdrowski

and Leonard, 1993), as well as in the electroreception in fishes that generate electrical fields and those who have electroreceptors (Butler and Hodos, 2005).

Cerebellar gross anatomy

The mammalian cerebellum consists of two major parts (Fig. 2): the cerebellar deep nuclei (or cerebellar nuclei) and the cerebellar cortex, which contains almost all of the neurons in the cerebellum. Two major fissures run mediolaterally dividing the cerebellar cortex into three primary subdivisions. The posterolateral fissure separates the flocculonodular lobe from the cerebellar body, and the primary transverse fissure separates the cerebellar body into a posterior lobe and an anterior lobe.

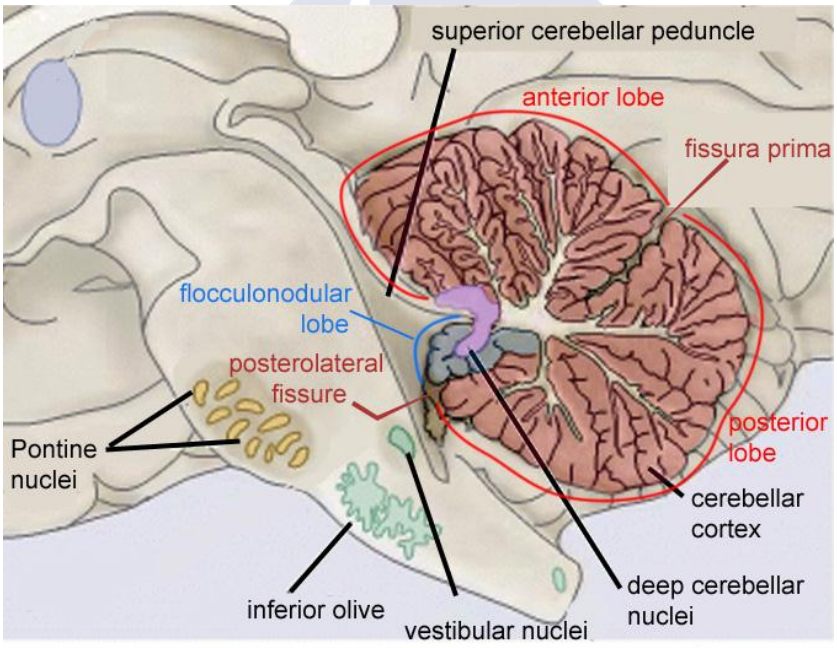

Figure 2. Drawing of a sagittal section to show the major structures of the cerebellar system in mammals, including the deep cerebellar nuclei and the cerebellar cortex. Adapted from Purves et al. (2001).

In birds and mammals, the cerebellum is also divided sagittally into different zones that run from medial to lateral (Fig. 3). The cerebellar body (central vermis) is

located along the midsagittal plane of the cerebellum while two paired hemispheres are located laterally. These anatomical subdivisions correspond to the three major functional subdivisions of the cerebellum, as illustrated by Larsell (1937) and Dow (1942). The vestibulocerebellum is constituted by the floculonodular lobe (or auricle) and mostly receives inputs from the vestibular and reticular systems. It is responsible for maintaining body balance and eye movements. The spinocerebellum corresponds to the cerebellar body or central vermis and is mainly connected with the spinal cord. It controls the axial musculature (body movements and proximal regions of the limbs). The pontocerebellum correspond to the lateral hemispheres. It is involved in the planning and timing of movements of the distal parts of the limbs and in the cognitive functions of the cerebellum (Sarnat and Netsky, 1981; Pollok et al., 2006).

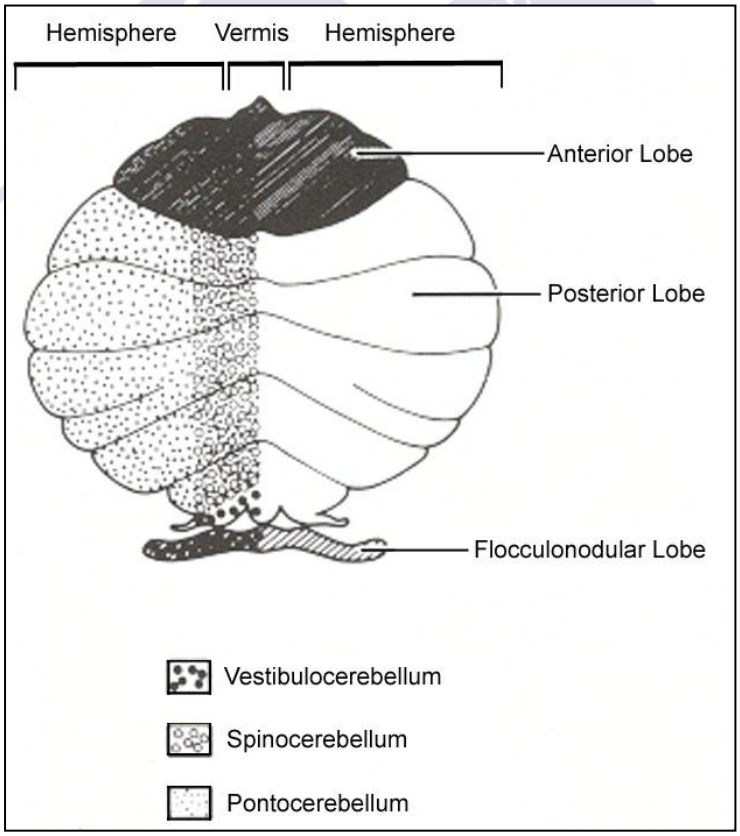

Figure 3. Anatomy and organization of the cerebellum, using the Larsell's nomenclature (Larsell, 1967). Taken from Walker et al. (1990).

Histology and connectivity of the cerebellar cortex

The cerebellar cortex is the superficial gray matter of the cerebellum. It contains cell bodies, dendrites and axons of different cell types that are organized in three cell layers (for review, see Butler and Hodos, 2005). In amniota, the outermost layer is named molecular layer and contains stellate and basket cells, the latter located at basal (inner) positions. It is followed by the Purkinje layer, which contains Purkinje cells. The granular layer is located next and contains granule and Golgi cells. Inner to these three cell layers is the fibrous layer or white matter (for review, see Delgado-García, 2001). In addition to this, there are a few cell types which are only present in some groups of gnathostomes, such as Lugaro, brush, candelabrum, and eurydendroid cells (Lainé and Axelrad, 1994; Pushchina and Varaksin, 2001; Ito, 2006; Campbell et al, 2007; Meek et al, 2008).

The cerebellum is able to carry out all of its functions due to all the information that receives from multiple pathways and from different regions of the brain. Cerebellar input from different precerebellar nuclei can be divided into three major cerebellar afferents: mossy fibers, climbing fibers and fibers of diffuse termination. Mossy fibers originate in the pontine nuclei, the spinal cord, the brainstem reticular formation, and the vestibular nuclei (see Fig. 2) and they project onto the cerebellar nuclei and onto granule cells in the cerebellar cortex. The granule cells send axons up toward the cortical surface. Each axon bifurcates in opposite directions in the molecular layer. These parallel fibers run parallel to the folds of the cerebellar cortex, where they make excitatory synapses with Purkinje cells along the way. The firing of each Purkinje cell can be influenced by thousands of mossy fibers. Climbing fibers originate exclusively in the contralateral inferior olive (see Fig. 2) and project onto the cerebellar nuclei and

onto the Purkinje cells of the cerebellar cortex. Each Purkinje cell receives a single input from a single climbing fiber. Fibers of diffuse termination originate mainly from locus coeruleus (noradrenergic), pedunculopontine nucleus (cholinergic) and raphe nucleus (serotoninergic). Their endings were described in the three layers of the cerebellar cortex (for review, see Delgado-García, 2001; Sillitoe et al., 2012).

Purkinje cells are considered key cells in the cerebellum, since they constitute the sole output of the cerebellar cortex. Their action is regulated directly or indirectly by cerebellar interneurons and afferent fibers. Then Purkinje cells send the integrated information to the deep cerebellar nuclei, which in turn constitute the output of the cerebellum.

Evolutionary history of the cerebellum

It has largely been a matter of debate whether a cerebellar anlage is present in agnatha or jawless vertebrates. To date, there is no complete agreement about whether the cellular extension in myxinoids or the small plate in adult petromyzonts over the fourth ventricle would correspond to a cerebellar anlage or not (Johnston, 1902a,b; for review, see Larsell, 1947; Nieuwenhuys, 1967; Schnitzlein and Faucette, 1969; Butler and Hodos, 2005; Murakami and Watanabe, 2009). However, a true cerebellum with functional subdivisions, typical stratification and main cell types (see above) is observed only in gnathostomes (jawed vertebrates). Tracing studies further support the absence of cerebellum in agnatha (for a review, see Northcutt, 2002). Therefore, the cerebellum is recognized as an evolutionary innovation at the agnathan-gnathostome transition. The appearance of the cerebellum is concurrent with that of the jaw and, consequently, with the appearance of new ways of feeding and more active locomotion (for a review, see Northcutt, 2002).

All gnathostomes present a vestibulocerebellar subdivision constituted by the cerebellar auricle (Fig. 4A), also named caudal lobe, or vestibulolateral lobe. In land vertebrates, the cerebellar auricle is known as flocculonodular lobe, and it is generally downsized because of the disappearance of the lateral line system (Larsell, 1967; Schnitzlein and Faucette, 1969; for review, see also Nieuwenhuys, 1967).

The spinocerebellar subdivision corresponds to the cerebellar body, which shows a huge variability in size, shape and complexity among different groups of gnathostomes and also within the same group, in part due to the existence of hypertrofies and regressions through evolution (Eccles, 1969). The cerebellar body in amphibians and reptiles shows a very simple structure, which consists on a flat plate or a plate with a small curvature (Butler and Hodos, 2005). In contrast, the cerebellum of fishes appears more complex than that of amphibians and reptiles. Fishes generally develop a folded cerebellar body (Fig. 4B), including cases of double-folded (as in dogfish), multifolded (as in the sting ray) and hyperfolded (as in mormyrids) cerebellar bodies. In addition, the rostral part of the cerebellar body of bony fishes grows to give rise to the cerebellar valvula (Nieuwenhuys, 1967; Pouwels, 1978; Butler and Hodos, 2005; Candal et al., 2005), which is absent in other gnathostomes. Much higher degree of complexity is found in birds and mammals, who in addition to a multifolded cerebellar body (known as central vermis; see above) present a pontocerebellum consisting of lateral hemispheres.

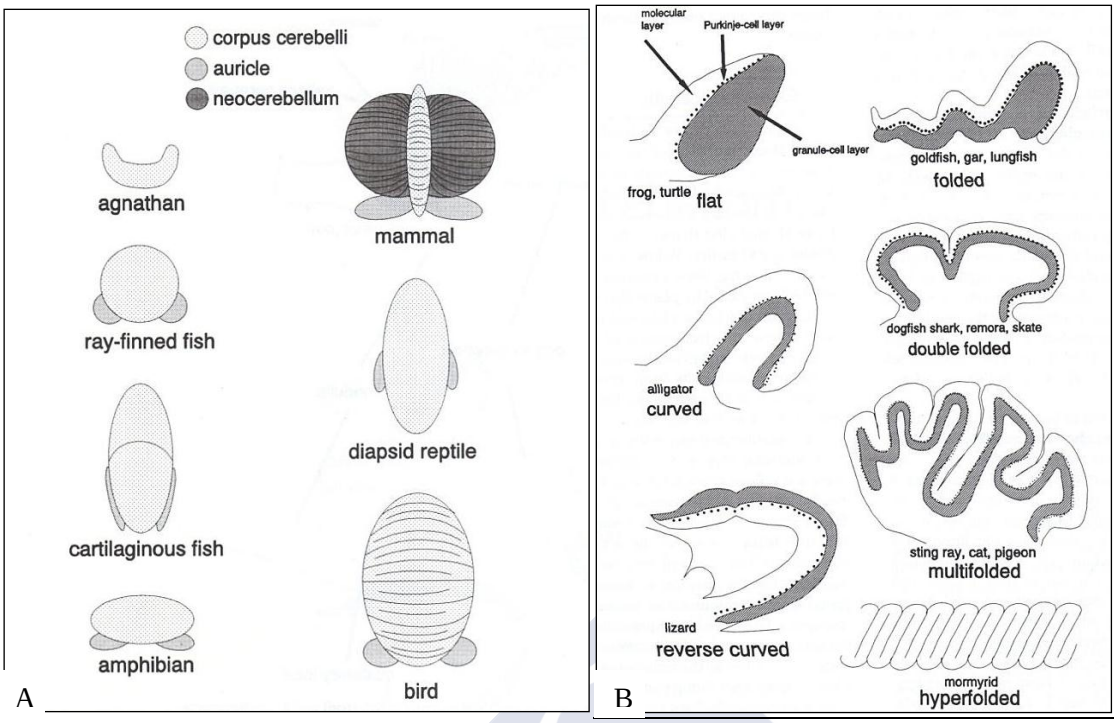

Figure 4. A. Schematic representations of the main parts of the cerebellum in different groups of vertebrates. Note that lateral hemispheres were not illustrated in birds. **B.** Schematic representations of sagittal sections of the cerebellar cortex in different groups of vertebrates, showing different degrees of folding. Taken from Butler and Hodos (2005).

The cerebellum of cartilaginous fishes

Chondrichthyans or cartilaginous fishes include holocephala (as chimaera) and elasmobranchs, which include sharks, skates and rays (Fig. 5). Cartilaginous fishes are at the base of the gnathostome lineage. Because the cerebellum is considered an evolutionary innovation that occurred at the agnatha-gnathostome transition, cartilaginous fishes are recognized as the gnathostome group that present a cerebellum with the most primitive features and, therefore, they represent a key phylogenetic group to study the ancestral condition of the cerebellum.

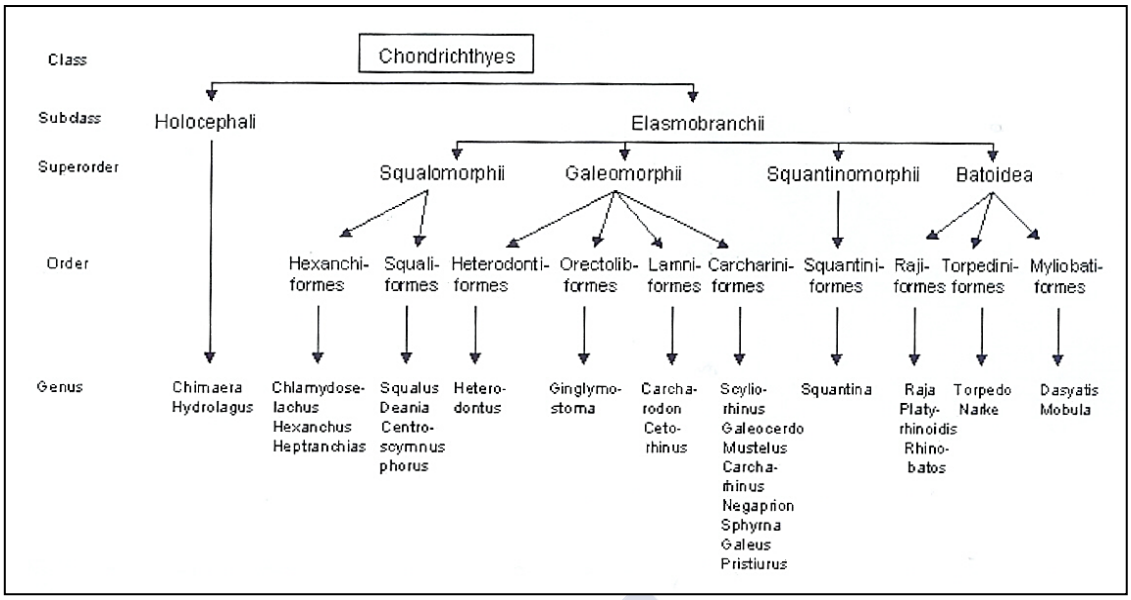

Figure 5. Taxonomic classification of chondrichthyans. Taken from Compagno (1977).

Gross anatomy of the cerebellum

Among elasmobranchs, a large variety has been observed as regards the allometry of the cerebellar system (Yopak and Montgomery, 2008). In spite of this variety, two main divisions are present in the cerebellum of all elasmobranch fishes: the cerebellar auricle and the cerebellar body, which are separated by the posterolateral fissure. This fissure is present in all groups of gnathostomes (Larsell, 1967). The cerebellar auricle is related with the ocatovolateral or acoustic-lateral system, which includes auditory, vestibular and lateral line systems. Although most fishes show a caudal lobe or vestibulolateral lobe, auricles as lateral projections with ear-like shape are only observed in chondrichthyans (Fig. 6), chondrosteans and urodele amphibians. The cerebellar auricle in these groups is mostly subdivided into upper and lower leaves, anteromedially and caudolaterally located each other respectively. Both are joined rostrolaterally, forming the lateral recess of the fourth ventricle, covered by the choroid plexus.

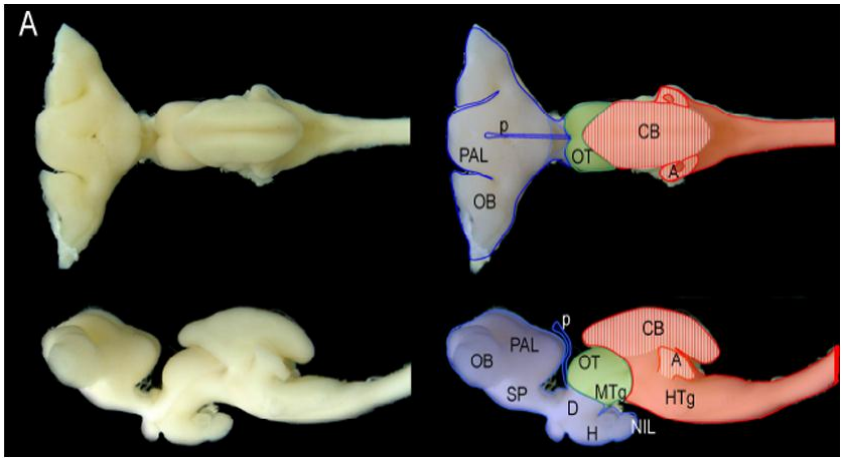

Figure 6. Dorsal and lateral views of adult brain in the shark *Scyliorhinus canicula*, showing the cerebellar body and paired auricles. Taken from Rodríguez-Moldes (2011).

A high variety was also found as regards the degree of folding of the cerebellar body (Lisney et al., 2008; Figure 7). While rays show a highly folded cerebellar body (Hoffman, 1999), in other elasmobranchs a bilobed cerebellar body is common, which is divided by the primary transverse fissure or *fissura prima* (Larsell, 1967). Different degrees of folding are not only affected by the phylogeny, but also by the ecology of different species. For instance, benthic species have a smoother cerebellum (schematic drawings in Fig. 7), as has been described by Lisney et al. (2008). In addition, the cerebellar body is bilaterally divided by a longitudinal fissure (Fig. 7). In contrast to other gnathostomes, the inner part of the cerebellum shows a wide ventricle, which corresponds to an expansion of the fourth ventricle.

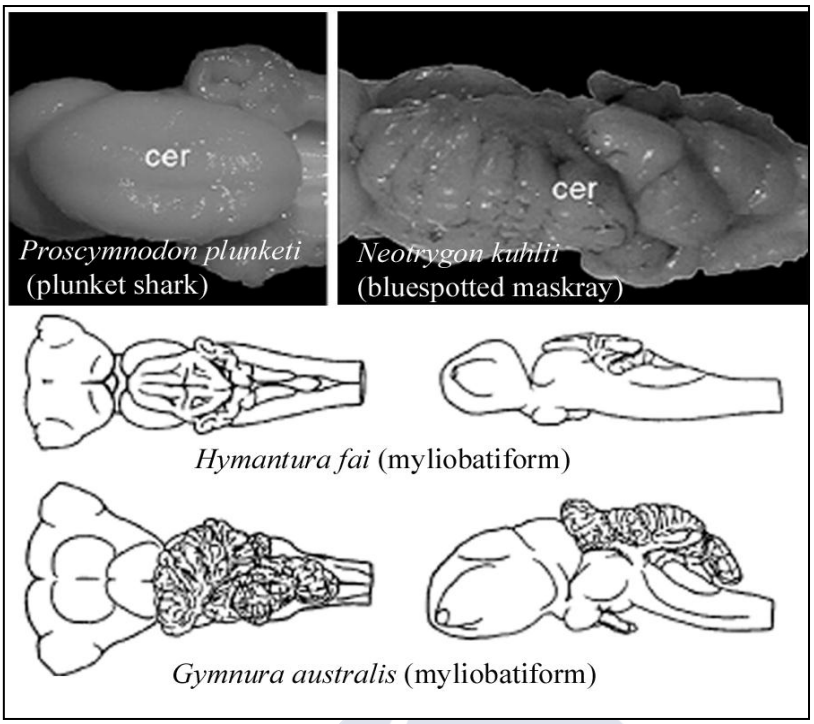

Figure 7. Dorsal and lateral views of cerebellum in four different species of chondrichthyans showing different degrees of folding. Adapted from Lisney et al. (2008) and Yopak et al. (2010).

Histology and connectivity of the cerebellar cortex

A wide number of studies have contributed to what is known about the gross anatomy, histology and connectivity of the cerebellar cortex in adult cartilaginous fishes (Schaper, 1898; Houser, 1901; Ariëns Kappers et al., 1936; Larsell, 1967; Nieuwenhuys, 1967; Nicholson et al., 1969; Kuhlenbeck, 1975; Smeets et al., 1983; Álvarez-Otero, 1990; Álvarez-Otero et al., 1995; Anadón et al., 2009). Several cell layers are distinguished, from marginal to ependymal levels, in the cerebellar cortex: the molecular layer (containing stellate cells), the Purkinje layer (with Purkinje cells), and the fibrous layer (containing axons of Purkinje cells and processes of cerebellar afferents). The granular layer (containing Golgi and granule cells) is restricted to paramedian levels, where cells are grouped into a pair of paramedian eminences, also known as granular eminences (for review, see New, 2001; Álvarez-Otero, 1990). These

eminences are rostrocaudally extended from the anterior medullary velum up to most caudal levels, and continued in the auricle (Fig. 8).

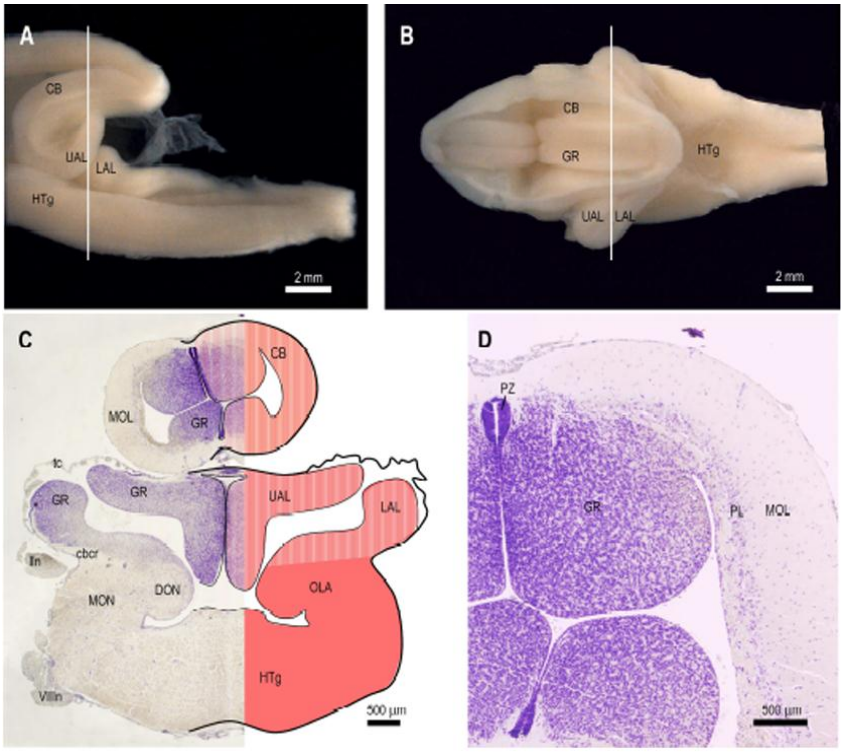

Figure 8. A. Lateral view of the hindbrain of the shark *Scyliorhinus canicula* sectioned longitudinally (A), horizontally (B; the dorsal part of the cerebellar body has been removed) and transversally (C, D). CB, cerebellum; DON, dorsal octaval nucleus; GR, granular layer; LAL, lower auricle leaf; MOL, molecular layer; MON, medial octaval nucleus; OLA, octavolateral area; PL, Purkinje layer; UAL, upper auricle leaf. Taken from Rodríguez-Moldes (2011).

The fibrous layer is not well defined in the auricle leaves. A few dissimilarities also exist between them. The upper auricle leaf shows three layers: molecular (marginal), Purkinje (intermediate) and granule (ventricular) layers. The granular layer of this auricle leaf is grouped in two paramedian eminences (continuation from those of the cerebellar body), which are fused in the median plane as a bridge over the fourth ventricle. Instead, the lower auricle leaves are not fused in the median plane. The molecular layer is located marginally, they present relatively low quantity of Purkinje cells, and the granular layer is located in the ventricular zone. The molecular layer is continuous with the cerebellar crest over the octavolateral area or lateral line lobe.

A similar histology to that of the cerebellar cortex is also present in other structures known as cerebellar-like structures, which mainly include parts of the octavolateral and electrosensory systems (Montgomery et al., 2012).

The neurochemical signature of different cell types in the cerebellar cortex of the shark *Scyliorhinus canicula* has also been previously described by our group, including Pax6-immunoreactive (-ir) granule cells (Rodríguez-Moldes et al., 2008), Glycine-ir Golgi cells (Anadón et al., 2013), or calretinin-ir Golgi and stellate cells (Anadón et al., 2009). Components of GABAergic, cholinergic and serotoninergic systems were also described in the cerebellar cortex (Álvarez-Otero and Anadón, 1992; Álvarez-Otero et al., 1995; Anadón et al., 2000; Carrera et al., 2008). Furthermore, different subtypes of cells in the cerebellar nucleus were described in detail (Álvarez-Otero et al., 1996).

These studies have contributed to verify that main cellular components of the mammalian cerebellum (Purkinje, stellate, granule and Golgi cells) are represented primarily in cartilaginous fishes and that intercellular connectivity appear to be very similar to that of other gnathostomes (for review, see Álvarez-Otero, 1990).

Origin and development of cerebellum and cerebellar connections

Classical anatomical studies combined with current molecular techniques are excellent complementary tools to gain knowledge about early regionalization and morphogenesis of the cerebellum, which in turn is crucial to understand how the adult cerebellar architecture is achieved. Some developmental studies about the cerebellum of the shark *S. canicula* (the lesser spotted dogfish) have been carried out recently (Rodríguez-Moldes et al, 2008; Chaplin et al., 2010). This species is now considered a model species in Evo-Devo studies (Coolen et al., 2009), a relatively new field that relates evolutionary and developmental studies.

Early specification of the cerebellum

The genoarchitectonic analysis has revealed as an essential tool to define the embryonic origin of specific regions of the adult brain (Puelles and Ferrán, 2012; Sillitoe et al., 2012). Distinct domains are specified under the influence of local environmental signals located at specific locations of the developing neural primordium. Initially, the neural tube is divided into three vesicles: forebrain (prosencephalon), midbrain (mesencephalon), and hindbrain (rhombencephalon). Thus, the hindbrain becomes organized into a series of repeated segments (rhombomeres) which exhibit individual identities by expression of a unique combination of genes. By contrast, immediately anterior to the hindbrain, the midbrain is patterned by a graded signal from an organiser tissue (the isthmus) located at the boundary between midbrain and hindbrain (reviewed by Irving and Mason, 2000). The development of the cerebellum depends on the isthmic organizer (IsO), which controls anterior hindbrain and midbrain regionalization (for review, see Sato and Joyner, 2009).

There is a broad network of genes related to the IsO (Fig. 9). Among them the transcription factors *Otx2* and *Gbx2* are particularly relevant, because they determine the location of the organizer (Simeone, 2000), where the main signaling molecule will correspond to *Fgf8*. This signaling molecule is responsible for the formation of the cerebellum by activating the expression of several genes involved in the early patterning of this structure, such as *Engrailed2* (for review, see Hidalgo-Sánchez et al., 2005).

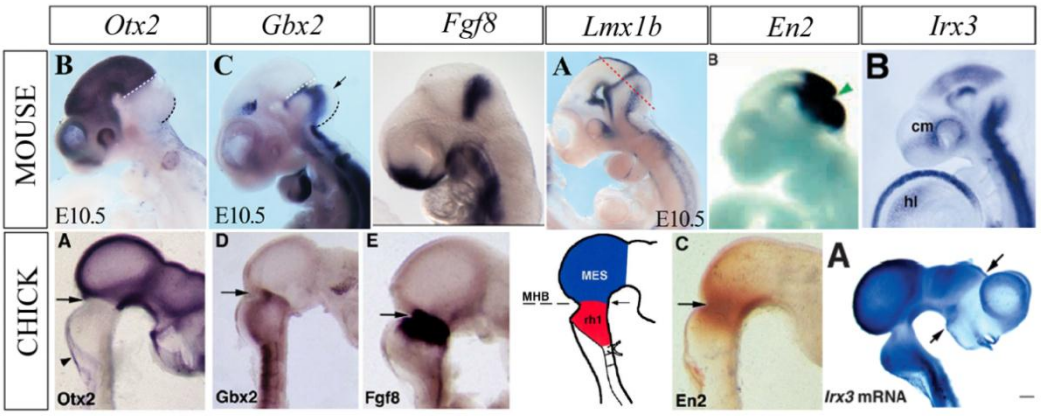

Figure 9. Expression pattern of the *Otx2*, *Gbx2*, *Fgf8*, *Lmx1b*, *En2* and *Irx3* genes in mouse and chick embryos. Taken from: Liu et al., 1999; Cohen et al., 2000; Kobahashi et al., 2002; Hidalgo-Sánchez et al., 2005; Guo et al., 2010; and Liu et al., 2010.

The cerebellum originates from the alar part of the most rostral hindbrain. However, there is no complete agreement whether the cerebellum is exclusively formed form the first rhombomere, or also partially from the caudal midbrain and the second rhombomere (Marín and Puelles, 1995; Wingate and Hatten, 1999; Sotelo, 2004; Tümpel et al., 2008).

The regionalization map of the isthmus outlined by the expression of these genes appears well conserved throughout evolution (Urbach, 2007). Outlining the IsO in elasmobranch fishes based on gene expression will be extremely useful to define the embryonic origin of the adult cerebellum of elasmobranch. Since the cerebellum is an evolutionary innovation of gnathostomes (see above), commonness or dissimilarities found in the IsO of chondrichthyans with respect to other vertebrates could explain what genetic changes in this organizer are at the base of the evolutionary origin of the cerebellum.

Cerebellar morphogenesis

The study of cerebellar development in cartilaginous fishes from the time of its early specification to the acquisition of mature features- is also essential to assess the

degree of evolutionary conservation of cerebellar morphogenesis. In gnathostomes, once the location where the cerebellum will be formed becomes determined, two thickenings (rhombic lips) of the alar part of the rostral hindbrain grow and fuse in the median plane (Fig. 10), to form first the cerebellar plate and then the cerebellar body and auricles.

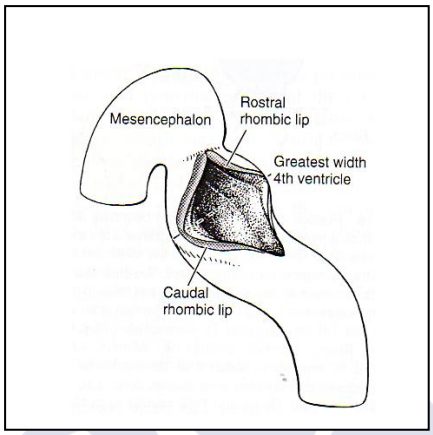

Figure 10. Schematic drawing of the rhombic lips. Taken from Glikstein et al. (2007).

The cerebellar anlage is firstly distinguished by the presence of anatomical boundaries as the isthmic fissure (rostral boundary). Then the posterolateral fissure (the boundary between the cerebellar body and the cerebellar auricle) appears, followed by the primary transverse fissure (the boundary between the rostral and caudal lobes of the cerebellar body), as illustrated in Figure 11. These fissures are maintained throughout development and they still delimit the main subdivisions of the adult cerebellum (see above). Depending on the species, more fissures can also appear in the cerebellar cortex (for review, see Nieuwenhuys, 1967).

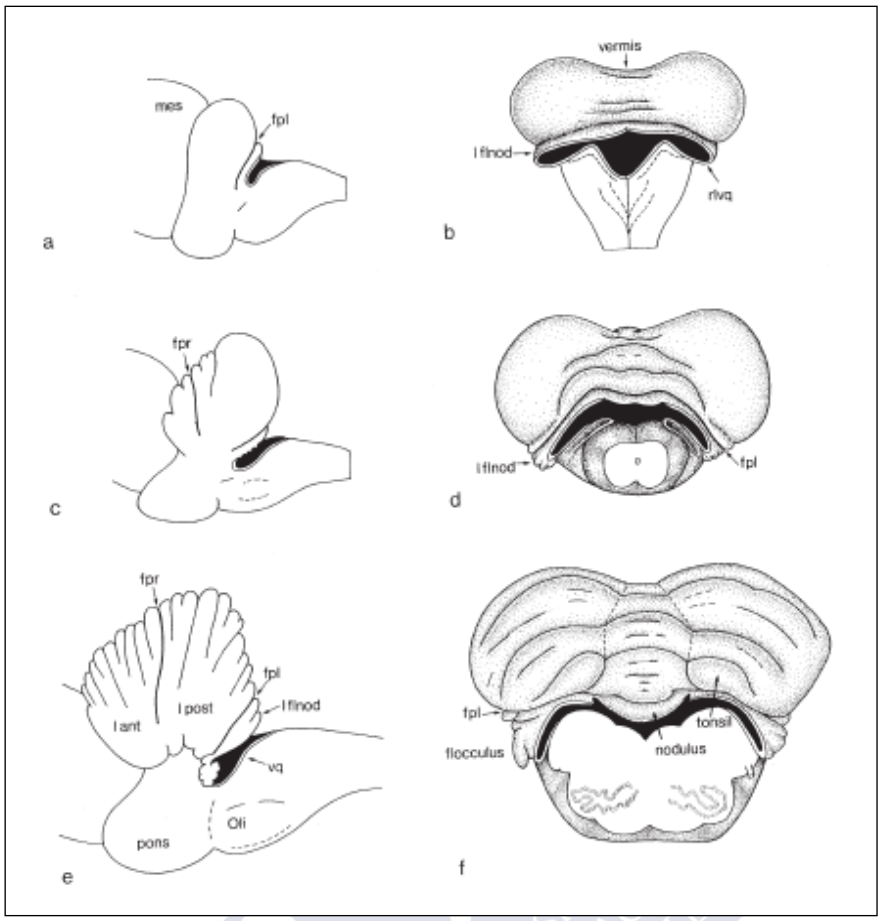

Figure 11. Schematic representation of the cerebellar development in humans. Taken from ten Donkelaar et al., 2003.

As development progresses the different cell types become organized by multiple migrations from two independent proliferative regions: the ventricular zone, which is the source of cells of the deep cerebellar nuclei, Purkinje cells and interneurons; and the external granular layer, which is the source of granular cells (for review, see Sotelo, 2004). Although the existence of the external granular layer in fishes has been questioned (Chaplin et al., 2010), there is evidence of its existence in teleosts (Wullimann et al., 2011) and cartilaginous fishes, as previously described by our group (Rodríguez-Moldes et al., 2008). In fishes, neurogenesis continues throughout life, as has been described in teleosts (Candal et al., 2005; Zupanc et al., 2005; Kaslin et al., 2009) and cartilaginous fishes (Margotta, 2007; Rodríguez-Moldes et al., 2008).

Late in cerebellar development, different territories also appear in the median-lateral axis of the cerebellar cortex. This process, known as compartmentalization, gives rise to a zebra-like pattern with multiple parasagittal bands, which is related to the topography of cerebellar afferents (Sillitoe et al., 2010). This zebra-like pattern was described in amniota species (for review, see Herrup and Kuemerle, 1997) but, to date, there is no evidence of this multiple banding pattern in fishes (Vecino and Ekström, 1991; Puzdrowski, 1997).

Recent studies made evident that *S. canicula* is especially suitable for developmental studies about the cerebellum under an evolutionary perspective (Rodríguez-Moldes et al., 2008; Chaplin et al., 2010): first, they are at a key phylogenetic position to analyse changes that occur at the agnathan-gnathostome transition; second, despite its basal position in the gnathostome lineage, the cerebellum presents the basic anatomical subdivisions (cerebellar auricles and cerebellar body), which eases the understanding of the morphogenetic processes that lead to most complex cerebellar organizations as those found in mammals; third, they present a protracted development and through life neurogenesis, which allows a detailed study of such morphogenetic processes. Despite these advantages, studies about cerebellar morphogenesis in elasmobranch fishes are scarcer than in other vertebrate groups. To our knowledge, these studies are limited to a few classical reports (for review, see Larsell, 1967) and two recent works on neurogenic processes (Rodríguez-Moldes et al., 2008; Chaplin et al., 2010).

Cerebellar connections: New perspectives in cartilaginous fishes

Afferent and efferent cerebellar connections appear to be conserved throughout evolution (New, 2001). Some studies in adults of different species of cartilaginous

fishes (reviewed in Nieuwenhuys, 1967; Northcutt, 1978; Smeets et al., 1983; Schmidt and Bodznick, 1987; Fiebig, 1988; Smeets, 1998; Puzdrowski and Gruber, 2009) revealed that precerebellar nuclei were comparable to those of mammals (Fig. 12). However, developmental studies are lacking, though they are essential for understanding the origin and evolution of precerebellar nuclei. The lesser spotted dogfish represents an adequate species for studying the development of cerebellar connections because its cerebellum is simpler and smother than that of batoids, in which cerebellar connections were previously reported; Fiebig, 1988; Puzdrowski and Gruber, 2009. Understanding the development of these connections in gnathostomes with relatively simple cerebellums can provide insight into basic principles of cerebellar connectivity.

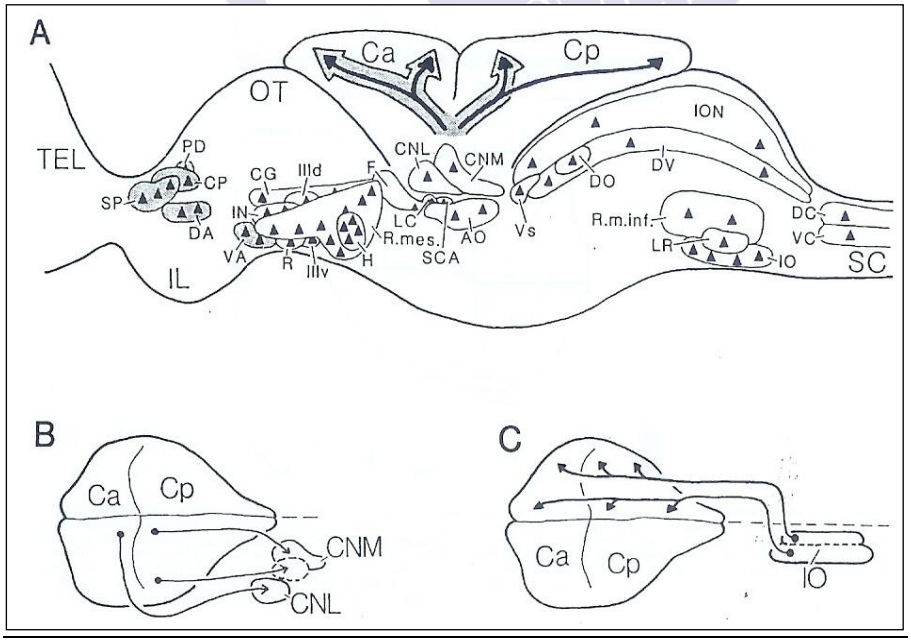

Figure 12. Schematic representation of the cerebellar afferents (a, c) and efferents (b) of the cerebellar body in an elasmobranch (*Platyrhinoidis triseriata*). Taken from Fiebig (1988).

The origin of precerebellar nuclei: rhombic lip derivatives

Precerebellar nuclei of the hindbrain emerge mainly from the upper rhombic lips and also from caudal or lower rhombic lips. Then, precursors of different precerebellar nuclei reach their final position by several complex migrating pathways (Fig. 13), which have been well described in amniota (for review, see Sotelo, 2004; and Sotelo and Chedotal, 2005) and bony fishes (Wullimann et al., 2011), but not in basal gnathostomes. If similar pathways occur early in gnathostomate evolution warrants further research.

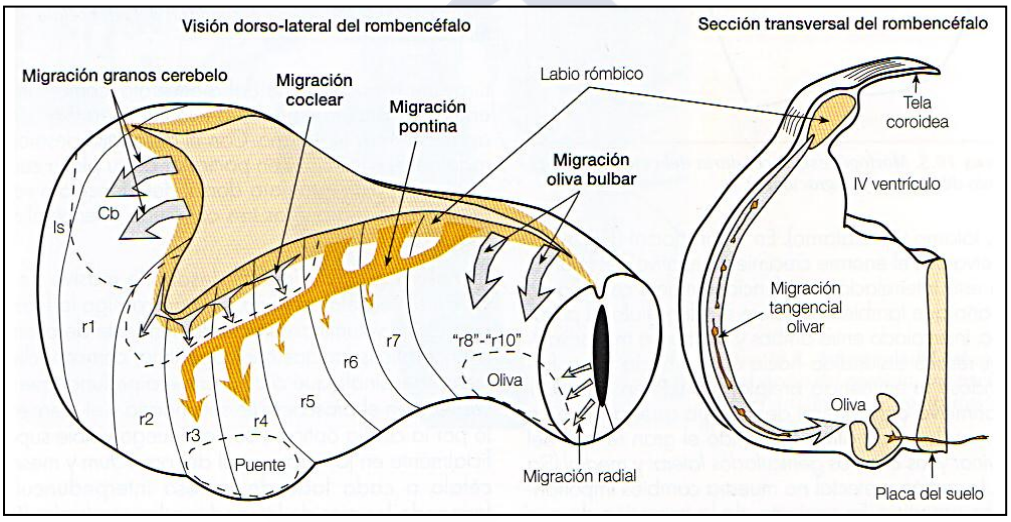

Figure 13. Schematic drawings of migrating pathways from rhombic lips. Taken from Puelles et al. (2008).

LITERATURE CITED

Allman JM. 2003. El cerebro en evolución. Ariel Neurociencia 86.

Álvarez-Otero R. 1990. Estudio citarquitectónico y ultraestructural del cerebelo de la pintarroja, *Scyliorhinus canicula L.* Doctoral Thesis, University of Santiago de Compostela, Spain.

Álvarez-Otero R, Anadón R. 1992. Golgi cells of the cerebellum of the dogfish, *Scyliorhinus canicula* (Elasmobranchs): a Golgi and ultrastructural study. J Hirnforsch 33:321-327.

Álvarez-Otero R, Díaz Regueira S, Anadón R. 1993. New structural aspects of the synaptic contacts on Purkinje cells in an elasmobranch cerebellum. J Anat 182: 13-21.

Álvarez-Otero R, Pérez SE, Rodríguez MA, Adrio F, Anadón R. 1995. GABAergic neuronal circuits in the cerebellum of the dogfish *Scyliorhinus canicula* (Elasmobranchs): an immunocytochemical study. Neurosci Lett 187:87-90.

Álvarez-Otero R, Pérez SE, Rodríguez MA, Anadón R. 1996. Organisation of the cerebellar nucleus of the dogfish, *Scyliorhinus canicula L.*: a light microscopic, immnuhistochemical, and ultrastructural study. J Comp Neurol 368:487-502.

Anadón R, Molist P, Rodríguez-Moldes I, López JM, Quintela I, Cerviño MC, Barja P, González A. 2000. Distribution of choline acetyltransferase immunoreactivity in the brain of an elasmobranch, the lesser spotted dogfish (*Scyliorhinus canicula*). J Comp Neurol 420:139-170.

Anadón R, Ferreiro-Galve S, Sueiro C, Graña P, Carrera I, Yáñez J, Rodríguez-Moldes I. 2009. Calretinin-immunoreactive systems in the cerebellum and cerebellum-related lateral-line medullary nuclei of an elasmobranch, *Scyliorhinus canicula*. J Chem Neuroanat 37:46-54.

Anadón R, Rodríguez-Moldes I, Adrio F. 2013. Glycine immunoreactive neurons in the brain of a shark (*Scyliorhinus canicula L.*). J Comp Neurol doi: 10.1002/cne.23332.

Ariëns Kappers CU, Huber GC, Crosby EC. 1936. The comparative anatomy of the nervous system of vertebrates including man. Vol. 1, New York: Hafner Publishing Company.

Butler A, Hodos W. 2005. Comparative vertebrate neuroanatomy, evolution and adaption. Wiley-Liss. p. 180-197.

Campbell HR, Meek J, Zhang J, Bell CC. 2007. Anatomy of the posterior caudal lobe of the cerebellum and the eminentia granularis posterior in a mormyrid fish. J Comp Neurol 502:714-35.

Candal E, Anadón R, Bourrat F, Rodríguez-Moldes I. 2005. Cell proliferation in the developing and adult hindbrain and midbrain of trout and medaka (teleosts): a segmental approach. Dev Brain Res 160:157-175.

Carrera I, Molist P, Anadón R, Rodríguez-Moldes I. 2008. Development of the serotoninergic system in the central nervous system of a shark, the lesser spotted dogfish Scyliorhinus canicula. J Comp Neurol 511:804-831.

Chaplin N, Tendeng C, Wingate RJT. 2010. Absence of an external layer in zebrafish and shark reveals a distinct, anamniote ground plan of cerebellum development. J Neurosci 30:3048-3057.

Cohen DR, Cheng CW, Cheng SH, Hui CC. 2000. Expression of two novel mouse *Iroquois* homeobox genes during neurogenesis. Mech Dev 91:317-21.

Compagno LJV. 1977. Phyletic relationships of living sharks and rays. Am Zool 17: 303-322.

Coolen M, Menuet A, Chassoux D, Compagnucci C, Henry S, Lévèque L, Da Silva C, Gavory F, Samain S, Wincker P, Thermes C, D'Aubenton-Carafa Y, Rodriguez-Moldes I, Naylor G, Depew M, Sourdaine P, Mazan S. 2009. The dogfish *Scyliorhinus canicula*, a reference in jawed vertebrates. In: Behringer RR, Johnson AD, Krumlauf RE, editors. Emerging model organisms. A laboratory manual. Vol. 1. Cold Spring Harbor, NY: Cold Spring Harbor Laboratory Press. p 431-446.

Delgado-García JM. 2001. Structure and function of the cerebellum. Rev Neurol 33:635-642.

Dow R. 1942. The evolution and anatomy of the cerebellum. Bol Rev 17:179-220.

Eccles JC. 1969. The development of the cerebellum of vertebrates in relation to the control of movement. Naturwissenschaften 56:525-34.

Fiebig E. 1988. Connections of the corpus cerebelli in the Thornback guitarfish, *Platyrhinoidis triseriata* (Elasmobranchii): a study with WGA-HRP and extracellular granule cell recording. J Comp Neurol 268:567-83.

Glickstein M, Oberdick J, Voogd J. 2007. Evolution of the cerebellum. In: Kaas JH, Krubitzer LA, Editors. Evolution of the nervous system. A comprehensive reference. Vol. 3, Elsevier. p. 413-442.

Glickstein M, Strata P, Voogd J. 2009. Cerebellum: history. Neuroscience 162:549-59.

Guo Q, Li K, Sunmonu NA, Li JY. 2010. *Fgf8b*-containing spliceforms, but not *Fgf8a*, are essential for *Fgf8* function during development of the midbrain and cerebellum. Dev Biol 338:183-92.

Herrup K, Kuemerle B. 1997. The compartmentalization of the cerebellum. Annu Rev Neurosci 20:61-90.

Hidalgo-Sánchez M, Millet S, Bloch-Gallego E, Alvarado-Mallart RM. 2005 Specification of the meso-isthmo-cerebellar region: the *Otx2/Gbx2* boundary. 49:134-149.

Hoffmann MH. 1999. Nervous system. In: Hamlett WC, editor. Sharks, skates and rays. The Biology of elasmobranch fishes. Baltimore and London: The Johns Hopkins University Press.

Houser GL. 1901. The neurones and supporting elements of the brain of a selachian. J Comp Neurol 11:65-175.

Irving C, Mason I. 2000. Signalling by FGF8 from the isthmus patterns anterior hindbrain and establishes the anterior limit of *Hox* gene expression. Development 127:177-86.

Ito M. 1984. The cerebellum and neural control. Raven Press.

Ito M. 2006. Cerebellar circuitry as a neuronal machine. Prog Neurobiol 78:272-303.

Johnston J. 1902a. The brain of *Petromyzon*. J Comp Neurol 12:1-82.

Johnston J. 1902b. An attempt to define the primitive functional divisions of the central nervous system. J Comp Neurol 12:87-106.

Kaslin J, Ganz J, Geffarth M, Grandel H, Hans S, Brand M. 2009. Stem cells in the adult zebrafish cerebellum: initiation and maintenance of a novel stem cell niche. J Neurosci 29:6142-6153.

Kobayashi D, Kobayashi M, Matsumoto K, Ogura T, Nakafuku M, Shimamura K. 2002. Early subdivisions in the neural plate define distinct competence for inductive signals. Development 129:83-93.

Kuhlenbeck H. 1975. The central nervous system of vertebrates: spinal cord and deuterencephalon. Vol. 4, S. Karger, Basel.

Lainé J, Axelrad H. 1994. The candelabrum cell: a new interneuron in the cerebellar cortex. J Comp Neurol 8:159-173.

Larsell O. 1937. The cerebellum. A review and interpretation. Arch Neurol Psychiatr (Chic) 38:580-607.

Larsell O. 1947. The cerebellum of myxinoids and petromyzonts including developmental stages in the lampreys. J Comp Neurol 86:395-445.

Larsell O. 1967. The comparative anatomy and histology of the cerebellum from myxinoids through birds. Minneapolis: University Minnesota Press. p. 37-61.

Lisney T, Yopak K, Montgomery J, Collin S. 2008. Variation in brain organization and cerebellar foliation in Chondrichthyans: batoids. Brain Behav Evol 72:262-282.

Liu A, Losos K, Joyner AL. 1999. FGF8 can activate *Gbx2* and transform regions of the rostral mouse brain into a hindbrain fate. Development 126:4827-38.

Liu ZR, Shi M, Hu ZL, Zheng MH, Du F, Zhao G, Ding YQ. 2010. A refined map of early gene expression in the dorsal rhombomere 1 of mouse embryos. Brain Res Bull 82:74-82.

Manto M, Haines D. 2012. Cerebellar research: two centuries of discoveries. Cerebellum 11:446-448.

Margotta V. 2007. PCNA immunoreactivity revealing normal proliferative activity in the brain of an adult elasmobranch, *Torpedo marmorata*. Ital J Anat Embryol 112:145-155.

Marín F, Puelles L. 1995. Morphological fate of rhombomeres in quail/chick chimeras: a segmental analysis of hindbrain nuclei. Eur J Neurosci 7:14-38.

Meek J, Yang JY, Han VZ, Bell CC. 2008. Morphological analysis of the mormyrid cerebellum using immunohistochemistry with emphasis on the unusual neuronal organization of the valvula. J Comp Neurol 510:396-421.

Montgomery JC, Bodznick D, Yopak KE. 2012. The cerebellum and cerebellum-like structures of cartilaginous fishes. Brain Behav Evol 80:152-165.

Murakami Y, Watanabe A. 2009. Development of the central and peripheral nervous systems in the lamprey. Dev Growth Differ 51:197-205.

New JG. 2001. Comparative neurobiology of the elasmobranch cerebellum: theme and variations on a sensorimotor interface. Environ Biol Fish 60:93-108.

Nicholson CR, Llinás R, Precht W. 1969. Neural elements of the cerebellum in elasmobranch fishes. Structure and functional characteristic. In: Llinás R, editor. Neurobiology of cerebellar evolution and development. Chicago: Am Med Assoc. p. 215-243.

Nieuwenhuys R. 1967. Comparative anatomy of the cerebellum. Prog Brain Res 25:1-93.

Northcutt RG. 1978. Brain organization in the cartilaginous fishes. In: Hodgson ES, Mathewson RF, editors. Sensory biology of sharks, skates, and rays. Arlington, VA: Office of Naval Research, Department of the Navy. p. 117-193.

Northcutt RG. 2002. Understanding vertebrate brain evolution. Integr Comp Biol 42:743-756.

Pollok B, Butz M, Gross J, Südmeyer M, Timmermann L, Schnitzler A. 2006. Coupling between cerebellar hemispheres: behavioural, anatomic, and functional data. Cerebellum 5:212-219.

Pouwels E. 1978. On the development of the cerebellum of the trout, *Salmo gairdneri. I.* Patterns of cell migration. Anat Embryol (Berl) 152:291-308.

Puelles L. 2009.Contributions to neuroembryology of Santiago Ramón y Cajal (1852- 1934) and Jorge F. Tello (1880-1958). Int J Dev Biol 53:1145-1160.

Puelles L, Ferrán JL. 2012. Concept of neural genoarchitecture and its genomic fundament. Front Neuroanat 6:47. Puelles López L, Martínez Pérez S, Martínez de la Torre M. 2008. Morfogénesis secundaria del SNC. In: Neuroanatomía. Medica Panamericana. p. 53-57.

Purves D, Augustine GJ, Fitzpatrick D, Katz LC, LaMantia AS, McNamara JO, Williams SM. 2001. Neuroscience. Sunderland (MA): Sinauer Associates.

Pushchina EV, Varaksin AA. 2001. Argyrophilic and nitroxydergic bipolar neurons (Lugaro cells) in the cerebellum of *Pholidapus dybowskii*. Zh Evol Biokhim Fiziol 37:437-41.

Puzdrowski RL. 1997. Anti-Zebrin II immunopositivity in the cerebellum and octavolateral nuclei in two species of stingrays. Brain Behav Evol 50:358-368.

Puzdrowski RL, Gruber S. 2009. Morphologic features of the cerebellum of the Atlantic stingray, and their possible evolutionary significance. Integr Zool 4:110-122.

Puzdrowski R, Leonard R. 1993. The octavolateral systems in the stingray, *Dasyatis Sabina. I.* Primary projections of the octaval and lateral line nerves. J Comp Neurol 332:21-37.

Rodríguez F, Durán E, Gómez A, Ocaña FM, Álvarez E, Jiménez-Moya F, Broglio C, Salas C. 2005. Cognitive and emotional functions of the teleost fish cerebellum. Brain Res Bull 66:365-370.

Rodríguez-Moldes I. 2011. Functional morphology of the brains of cartilaginous fishes. In: Farrell AP, editor. Encyclopedia of Fish Physiology: From Genome to Environment. Vol. 1, San Diego: Academic Press. p. 26-36.

Rodríguez-Moldes I, Ferreiro-Galve, S.; Carrera, I.; Sueiro, C.; Candal, E.; Manzan, S.; Anadón, R. 2008. Development of the cerebellar body in sharks: spatiotemporal relations of Pax6-expression, cell proliferation and differentiation. Neurosci Lett 432:105-110.

Sarnat H, Netsky M. 1981. Evolution of the nervous system. Oxford University Press.

Sato T, Joyner AL. 2009. The duration of *Fgf8* isthmic organizer expression is key to patterning different tectal-isthmo-cerebellum structures. Development 136:3617-3626.

Schaper A. 1898. The fine structure of the selachian cerebellum (*Mustelus vulgaris*) as shown by chrome-silver impregnation. J Comp Neurol 8:1-20.

Schmidt AW, Bodznick D. 1987. Afferent and efferent connections of the vestibulolateral cerebellum of the little skate, *Raja erinacea*. Brain Behav Evol 30:282-302.

Schnitzlein HN, Faucette JR. 1969. General morphology of the fish cerebellum. En: Neurobiology of cerebellar evolution and development. Llinás R, editor, Chicago:Am Med Assoc. p.77-106.

Sillitoe RV, Vogel MW, Joyner AL. 2010. *Engrailed* homeobox genes regulate establishment of the cerebellar afferent circuit map. J Neurosci 30:10015-24.

Sillitoe RV, YuHong F, Watson C. 2012. Cerebellum. In: Watson C, Paxinos G, Puelles L, editors. The mouse nervous system. Elsevier. p. 360-390.

Simeone A. 2000. Positioning the isthmic organizer where *Otx2* and *Gbx2* meet. Trends Genet 16:237-40.

Smeets WJAJ. 1998. Cartilaginous fish. In: Nieuwenhuys R, Ten Donkelaar HJ, Nicholson C, editors. The central nervous system of vertebrates. Vol. 1, Berlin: Springer-Verlag. p. 551-654.

Smeets WJAJ, Nieuwenhuys R, Roberts BL. 1983. The central nervous system of cartilaginous fishes. Berlin: Springer-Verlag.

Sotelo C. 2004. Cellular and genetic regulation of the development of the cerebellar system. Prog Neurobiol 72:295-339.

Sotelo C, Chedotal A. 2005. Development of the olivocerebellar system: migration and formation of cerebellar maps. Prog Brain Res 148:1-20.

Thach WT. 1998. A role for the cerebellum in learning movement coordination. Neurobiol Learn Mem 70:177-88.

ten Donkelaar HJ, Lammens M, Wesseling P, Thijssen HO, Renier WO. 2003. Development and developmental disorders of the human cerebellum. J Neurol 250:1025-1036.

Tümpel S, Cambronero F, Sims C, Krumlauf R, Wiedemann LM. 2008. A regulatory module embedded in the coding region of *Hoxa2* controls expression in rhombomere 2. Proc Natl Acad Sci USA 105:20077-82.

Urbach R. 2007. A procephalic territory in *Drosophila* exhibiting similarities and dissimilarities compared to the vertebrate midbrain/hindbrain boundary region. Neural Dev 2:23.

Vecino E, Ekström P. 1991. Expression of the homeobox *engrailed* gene during the embryonic development of the nervous system of the trout (*Salmo fario L*.). Neurosci Lett 129:311-314.

Walker HK, Hall WD, Hurst JW. 1990. The cerebellum. In: Clinical Methods: The History, Physical, and Laboratory Examinations. Boston: Butterworths.

Wingate RJ, Hatten ME. 1999. The role of the rhombic lip in avian cerebellum development. Development 126:4395-4404.

Wullimann MF, Mueller T, Distel M, Babaryka A, Grothe B, Köster RW. 2011. The long adventurous journey of rhombic lip cells in jawed vertebrates: a comparative developmental analysis. Front Neuroanat 5:1-27.

Yopak KE, Montgomery JC. 2008. Brain organization and specialization in deep sea chondrychtians. Brain Behav Evol 71:287-304.

Yopak KE, Lisney TJ, Darlington RB, Collin SP, Montgomery JC, Finlay BL. 2010. A conserved pattern of brain scaling from sharks to primates. Proc Natl Acad Sci USA 107:12946-51.

Yoshikawa A, Yoshida M, Hirata Y. 2004. Capacity of the horizontal vestibuloocular reflex motor learning in goldfish. Conf Proc IEEE Eng Med Biol Soc 1:478-81.

Zupanc GK, Hinsch K, Gage FH. 2005. Proliferation, migration, neuronal differentiation, and long-term survival of new cells in the adult zebrafish brain. J Comp Neurol 488:290-319.

RATIONALE AND AIMS OF THE THESIS

USC
UNIVERSIDADE
DE SANTIAGO
DE COMPOSTELA

RATIONALE AND AIMS OF THE THESIS

The cerebellar development has been widely studied, not only because it is crucial for a better understanding of the complex structure of the adult cerebellum and the origin of many cerebellar disorders, but also because of its importance in evolutionary studies. Indeed, the identification of similarities and differences among species throughout development is essential in comparative studies. These studies have led to know that, while the cerebellum is the structure of the brain with highest variability as regards gross morphology at maturity, all jawed vertebrates appear to present similar developmental processes and a basic (common) cellular network. Thus, understanding the simplest morphogenetic processes and resulting structures, may serve as an essential framework to understand the most complex developmental outcomes.

Cartilaginous fishes, which are at the base of the gnathostome lineage, appear especially suitable for studying the development of the cerebellum. Since the cerebellum is considered an evolutionary innovation that occurred at the agnatha-gnathostome transition, cartilaginous fishes represent a key phylogenetic group to gain insight into the ancestral condition of the formation of the cerebellum. In spite of this, only a few studies have been performed dealing with the development of the cerebellum in this animal group.

Among cartilaginous fishes, the lesser spotted dogfish (*Scyliorhinus canicula*) is actually considered as a model species in evolutionary developmental (Evo-Devo) studies. This species presents some features that make it particularly suitable for the study of the development of the cerebellum and its connections, including the presence of a large cerebellum (relative to the total body size) that present a protracted development and the basic anatomical subdivisions found in the cerebellum of all other

gnathostomes. Therefore, we have used *S. canicula* as the animal model to study the development of the cerebellum and the precerebellar nuclei.

The aims of the present Thesis are:

- To know the degree of evolutionary conservation of the gene expression-based regionalization of the isthmus (that is involved in the early cerebellar patterning) by analyzing the genoarchitecture of the rostral hindbrain at pharyngula stages. The comparative analysis of our results with that of other vertebrates could help to understand what genetic changes are at the base of the evolutionary origin of the cerebellum. The results are presented in the **Chapter 1**, entitled: *Genoarchitecture of the rostral hindbrain of a shark: basis for understanding the emergence of the cerebellum at the agnathan-gnathostome transition.*
- To perform a close monitoring of the development of the cerebellum, mainly based on the identification of anatomical landmarks, changes of the gross anatomy and cerebellar compartmentalization throughout development. These results will be framed in discrete developmental periods, which will serve as framework not only for future work in this species, but also to search for anatomical homologies across vertebrates. The results are presented in the **Chapter 2**, entitled: *Origin and development of cerebellum and cerebellum-related structures in a shark.*
- To analyze the development and neurochemical signature of the precerebellar nuclei. Our results will shed light on the basal pattern of cerebellar connectivity and on the degree of evolutionary conservation of this pattern. The results are presented in the **Chapter 3**, entitled: *Development of the cerebellar afferent system in the shark Scyliorhinus canicula: Insights into the basal organization of precerebellar nuclei in gnathostomes.*

- To search for new experimental approaches that can help to solve some challenging questions, as the exact identification of different rhombic lips derivatives from early to late developmental stages. Since genetic fate mapping has been applied in other fishes to investigate this question, we aimed to be acquainted with this technique and explore its possible application in our animal model. A short report on the stay in the laboratory of the Professor Reinhard Köster is presented in the **Appendix 1**.

USC
UNIVERSIDADE
DE SANTIAGO
DE COMPOSTELA

CHAPTER 1

GENOARCHITECTURE OF THE ROSTRAL HINDBRAIN OF A SHARK: BASIS FOR UNDERSTANDING THE EMERGENCE OF THE CEREBELLUM AT THE AGNATHAN-GNATHOSTOME TRANSITION

Some results of the present work appear published in the article:

- Rodríguez-Moldes I, Carrera I, Pose-Méndez S, Quintana-Urzainqui I, Candal E, Anadón R, Mazan S, Ferreiro-Galve S. 2011. Regionalization of the shark hindbrain: a survey of an ancestral organization. Front Neuroanat 5:1-14.

USC
UNIVERSIDADE
DE SANTIAGO
DE COMPOSTELA

Genoarchitecture of the rostral hindbrain of a shark: basis for understanding the emergence of the cerebellum at the agnathan-gnathostome transition

INTRODUCTION

Two prominent external constrictions divide the early vertebrate brain into three main vesicles: hindbrain (or rhombencephalon), midbrain (or mesencephalon), and forebrain (or prosencephalon). The isthmic organizer (IsO), located at midbrain-hindbrain boundary or MHB, is a secondary organizer that controls the formation of optic tectum rostrally and the cerebellum caudally (for review, see Martínez, 2001; Aroca and Puelles, 2005; Nakamura et al., 2008). A complex network of genes is involved in this process. Firstly, the transcription factors *Otx2* and *Gbx2* determine the correct positioning of the isthmic organizer at MHB (Simeone, 2000) and *Lmx1b* is responsible for the initiation and maintenance of *Fgf8* expression, which in turn is the main signaling molecule of the isthmic organizer (O'Hara et al., 2005; Guo et al, 2007). The *Iroquois* and *Engrailed* genes are also related to the isthmic territory and involved in cerebellum development, since *Irx3* and *En2* act as repressor and activator, respectively, of the appearance of the cerebellum (for review, see Gómez-Skarmeta and Modolell, 2002; Hidalgo-Sánchez et al., 2005). These genes have intricate relationships between them, activating and/or inhibiting each other (for review, see Liu and Joyner, 2001), which appear well conserved throughout evolution (Urbach, 2007). As well, these genes execute other important functions. In particular, cells expressing *En2* migrated from the neural crest at isthmic levels to participate in the patterning of the mandibular arch (Knight et al., 2008).

Although an isthmus organizer-like is present from hemichordates (Pani et al., 2012), the cerebellum is an evolutionary innovation of gnathostomes or jawed vertebrates, concurrently with the jaw and, consequently with predation in vertebrates. Because cartilaginous fishes present the most primitive features of gnathostomes, they are closer to the ancestral condition of jawed vertebrates, and may shed light on the emergence of the cerebellum at the agnathan-gnathostome transition. However, the knowledge about the isthmic territory mainly comes from studies in mammals (for review, see Joyner et al., 2000), birds (Hidalgo-Sánchez et al., 2005), amphibians (Glavic et al., 2002) and teleost fishes (Jászai et al., 2003). In basal gnathostomes as cartilaginous fish, circumstantial information about this territory, so closely related to the cerebellum emergence, comes from developmental studies about fin and mesoderm in the shark *Scyliorhinus*, in which the expression of isthmus-related genes as *En-1* and *En-2* is shown (Tanaka et al., 2002; Adachi et al. 2012).

The genoarchitecture corresponds to the description of neural structure in terms of discrete gene expression patterns (for review, see Puelles and Ferrán, 2009). Because understanding the phylogenetic and ontogenetic aspects of the genoarchitecture of the rostral hindbrain and, in particular of this organizer, are fundamental to advance our knowledge on the cerebellum emergence, we have analyzed the genoarchitecture of the rostral hindbrain of the shark *Scyliorhinus canicula* or lesser spotted dogfish by studying the expression pattern of the *ScOtx2*, *ScGbx2*, *ScFgf8*, *ScLmx1b*, *ScIrx1*, *ScIrx3* and *ScEn2* genes and the distribution of Pax6 protein at pharyngula stages. To analyze the degree of evolutionary conservation of the gene expression patterns found in this basal vertebrate, a comparative study was also performed. The similarities with more complex organisms will show the degree of conservation of the gene expression patterns in the isthmic territory and will allow the establishment of subdivisions of the

rostral hindbrain in shark during early patterning of the cerebellum. On the other hand, dissimilarities with respect to simpler organisms (agnatha and invertebrates) could correspond with potential causes of the cerebellar evolutionary innovation in basal gnathostomes.

MATERIAL AND METHODS

Experimental animals and tissue preparation

Embryos of the lesser spotted dogfish (*Scyliorhinus canicula)* were supplied by the Marine Biological Model Supply Service of the CNRS UPMC Roscoff Biological Station (France) and the Estación de Bioloxía Mariña da Graña (Galicia, Spain). Additional embryos and juveniles were kindly provided by the Aquaria of Gijón, O Grove and A Coruña (Spain). A total of 20 embryos at early (stages 19-20) and late (stages 24-25) pharyngula stages were analyzed. Embryos were staged on the basis of their external features according to Ballard et al. (1993). Adequate measures were taken to minimize animal pain or discomfort. All procedures conformed to the guidelines established by the European Communities Council Directive of 22 September 2010 (2010/63/UE) and by the Spanish Royal Decree 53/2013 for animal experimentation, and were approved by the Ethics Committee of the University of Santiago de Compostela.

Specimens were anaesthetized with 0.5% tricaine methane sulphonate (MS-222; Sigma) in seawater. Embryos were fixed by immersion in phosphate buffered 4% paraformaldehyde. Then, the fixative was removed with saline phosphate buffer. Some embryos were cryoprotected with 30% sucrose in phosphate buffer, embedded in NEG 50_{TM} (Thermo Scientific, Kalamazoo, MI), frozen with liquid nitrogen-cooled

isopentane and cut on a cryostat. Parallel series of transverse and sagittal sections (18-20µm thick) were mounted on Superfrost Plus slides (Menzel-Glässer®, Madison, WI).

In situ hybridization on whole mount embryos and on sections

We applied in situ hybridization for *ScFgf8* (Compagnucci et al., 2013), *ScEn2*, *ScGbx2*, *ScIrx1*, *ScIrx3*, *ScLmx1b*, and *ScOtx2* (Germot et al., 2001; Plouhinec et al., 2005) genes. These probes were selected from a collection of *S. canicula* embryonic cDNA library (mixed stages, S9 to 22), submitted to high throughput EST sequencing (coord. Dr. Sylvie Mazan at the Station Biologique de Roscoff, France). cDNA fragments, kindly provided by Dr. Mazan, were cloned in pSPORT vectors. Sense and antisense digoxigenin-UTP-labeled and fluorescein-UTP-labeled probes were synthesized directly by *in vitro* transcription using as templates linearized recombinant plasmid DNA (Otx2 probe) or cDNA fragments prepared by PCR amplification of the recombinant plasmids (*ScFgf8, ScEn2, ScGbx2, ScIrx1, ScIrx3* and *ScLmx1b* probes).

In situ hybridization in whole mount and on cryostat sections was carried out following standard protocols (Coolen et al., 2007). Briefly, sections were permeabilized with proteinase K, hybridized with sense or antisense probes overnight at 65ºC (in sections) or 70ºC (whole mount) and incubated with the alkaline phosphatase-coupled anti-digoxigenin and anti-fluorescein antibody (1:2000, Roche Applied Science, Manheim, Germany) overnigh at 4ºC. The color reaction was performed in the presence of BM-Purple and FastRed tablets (Roche). Control sense probes did not produce any detectable signal.

Immunohistochemistry

Combination of *in situ* hybridization on sections with immunohistochemistry for the rabbit polyclonal anti-Pax6 (Covance) was also carried out at stages 24 and 25 following standard protocols (for details see Rodríguez-Moldes et al., 2011). Details

about the specificity of antibody in *Scyliorhinus canicula* were previously proved by preadsorption with the respective blocking peptide (see Ferreiro-Galve et al., 2012).

Imaging

In toto embryos were analyzed in the Olympus SZX12 stereo microscope fitted with an Olympus DP12 color digital camera. Photomicrographs were taken with an Olympus DP70 color digital camera fitted to a Provis photomicroscope equipped for fluorescence with appropriate filter combinations. For presentation, some color photomicrographs were converted to gray scale, and brightness and contrast adjusted using Adobe Photoshop 7.0. Plate photomontage, schemes and lettering were made with Corel Draw X6 and Adobe Photoshop 7.0.

RESULTS

We have studied the genoarchitectonic aspects at midbrain-hindbrain boundary (MHB) and the most rostral hindbrain during the early regionalization of the cerebellum in the lesser-spotted dogfish. We have focused the study on early and late pharyngula stages (stages 19/20 and 24/25, respectively) because they correspond to the period just before the cerebellar primordium appearance (stages 19/20) and the period when the rhombic lips become evident (stages 24/25), as showed in the further study about the cerebellum morphogenesis (**see Chapter 2**). In addition, equivalences between these developmental stages and those of other vertebrates are based on similarities in the reported gene expression patterns and external morphological features. Here we present the expression pattern of the *ScOtx2, ScGbx2, ScFgf8, ScLmx1b, ScIrx1, ScIrx3* and *ScEn2* genes in the rostral hindbrain and caudal midbrain.

The *in situ* hybridization results obtained from whole mount and cryostat sections, did not yield significant differences between early (stages19/20) and late

(stages 24/25) pharyngula stages as regards the expression of most of the genes studied here in the rostral hindbrain (Figs.1 and 2).

Expression pattern of isthmus related genes in whole mount embryos

At stages 20 and 24 *ScOtx2* and *ScGbx2* positive domains appeared to be complementary. Strong *Otx2* expression was found in the forebrain and midbrain (Fig. 1A,B), while Gbx2 was expressed in the hindbrain (Fig. 1C,D) and thus delimited the boundary between midbrain and hindbrain (MHB; black arrows in Fig. 1). Caudal to the line where *ScOtx2* and *ScGbx2* abutted, a conspicuous band of *ScFgf8* expression was observed at stages 20 and 24 (Fig. 1E,F), similarly to that reported by Compagnucci et al. (2013). At early pharyngula, *ScLmx1b* gene was also expressed in a band of cells in the caudal midbrain, which apparently abutted with that expressing *Fgf8*, though it is also extended marginally in rostral (up to the forebrain) and caudal (along the hindbrain) domains (Fig. 1G). In late pharyngula, the *ScLmx1b* positive band at MHB appeared thinner and partially overlaid the *ScFgf8* band (white arrows in Fig. 1F,H).

The gene *ScIrx1* was expressed rostrally to the MHB. At stages 20 and 24, the caudal limit of the positive domain roughly coincided with that of *ScOtx2*, while it extended rostrally up to the caudal forebrain (Fig. 1I,J). The expression pattern of *ScIrx3*, showed a conspicuous negative gap at MHB and two positive domains, one caudal along the hindbrain, and other rostral, which extended up to the caudal forebrain at stage 20 and more rostrally at stage 24 (Fig. 1K,L). Furthermore, at stage 24 the expression in the midbrain tegmentum decreased and consequently the negative gap appeared enlarged at this level (outlined arrows in Fig. 1K,L).

ScEn2 is highly expressed in the MHB and its expression decreased gradually both rostrally and caudally (Fig. 1M-O). The caudal limit of the domain appeared to coincide with the area of the upper rhombic lip located rostrally to the lateral recess,

while the rostral edge roughly coincided with the rostral limit of the mesencephalic tegmentum (Fig. 1O).

Boundaries among the expression domains of isthmus related genes

To better discern the degree of overlapping among the expression domains of these genes at MHB, we performed single and double labeling on sections. Comparison of the expression patterns of *ScGbx2* and *ScOtx2* allowed us to see that they do not overlap but just abut at MHB (compare midsagittal section in Fig. 2A,B), although a few cells expressing both *ScOtx2* and *ScGbx2* genes were observed in the neuroepithelium (not shown). Likewise, *ScOtx2* domain abutted with *ScFgf8* domain at MHB (Figs. 2C,D), except for a tiny overlapping consisting of a few weakly labeled cells in the neuroepithelium (insets in Fig. 2C,D) and a conspicuous negative gap at parasagittal level (asterisk in Fig. 2E,F). Interestingly, the sequential analysis of sagittal sections from medial to lateral levels revealed that in some sections the isthmic or meso-rhombencephalic fissure and isthmic fovea were located within the *ScOtx2* positive domain and rostrally to the *ScFgf8* positive area (Fig. 1A-F,L).

The *ScGbx2* and *ScIrx1* domains were also abutting at MHB (Fig. 2G,H). The *ScLmx1b* and *ScFgf8* domains abutted at parasagittal levels (Fig. 2I), except for a thin marginal area of expression that extended caudally. However, at midsagittal levels *ScLmx1b* extended rostro-caudally, clearly overlaying the *ScFgf8* domain (Fig. 2J). The *ScFgf8-ScIrx3* combination showed that the rostral limit of the *ScIrx3* domain in the hindbrain roughly coincided with the caudal edge of *ScFgf8* domain (arrowhead in Fig. 2K) except for the median-alar portion, where both genes overlapped (inset in Fig. 2L). On the other hand, the caudal limit of the *ScIrx3* domain in the midbrain appeared adjacent to the anterior limit of *ScEn2* expression (outlined arrows in Fig. 2K,L,M). The

ScEn2 gene showed that the limit of expression extended beyond the MHB (Fig. 2L) both partially in the midbrain and hindbrain. Comparing to Pax6, at stage 24 the Pax6 protein appeared only extended up to the r1-r2 boundary and not abutting with *ScEn2* (compare Fig. 2M,N). Shortly after, at stage 25 the Pax6 protein appeared rostrally extended and roughly abutted (as a meeting of gradients of expression) at the half of r1 with the caudal limit of *ScEn2* positive domain (Fig. 2O,P). Ventrally at parasagittal levels, the *ScEn2*-Pax6 boundary appeared to coincide with the caudal edge of the *ScFgf8* positive area, and not at the half of r1 (compare Fig. 2I,M,O,P).

DISCUSSION

General considerations on the regionalization of the midbrain-hindbrain boundary

There are several models for defining the regionalization around midbrain-hindbrain boundary or MHB. Terminology referring to what is considered isthmic organizer is quite diverse: it has been either defined as the area comprising the most caudal and rostral portions of the midbrain and hindbrain respectively (Matsunaga et al., 2002; Hidalgo-Sánchez et al., 2005; O'Hara et al., 2005), or as the most rostral area of the hindbrain (Aroca and Puelles, 2005). This controversy arises because these authors have found genes with organizer activity both in midbrain (as *Engrailed*) and hindbrain (as *Fgf8*). Although our results cannot ascertain these hypothesis, we consider the isthmic organizer as the territory expressing *ScFgf8*.

The subdivision of the rostral hindbrain is also in open debate and there is no agreement about whether the isthmic organizer is included in the rhombomere 1 or r1 (Zervas et al., 2004) or should be considered separately as rhombomere 0 or r0 (Moens and Prince, 2002; Aroca and Puelles, 2005). Of note, the latter does not obey all the features of a true rhombomere, such as morphologically distinguishable limits from r1.

Moreover, the existence of some migrated cells from the midbrain has been described (Jungbluth et al., 2001), which does not usually occurs across rhombomeres. However, our results about a gene expression compartment in the lesser spotted dogfish (see below) support the existence of a r0 as in other vertebrates (Aroca and Puelles, 2005).

There has been also some controversy about the origin of the cerebellum, whether it emerges from rostral hindbrain and caudal midbrain (Martínez and Alvarado-Mallart, 1989; Hallonet et al., 1990; Hallonet and Le Douarin, 1993; Millet et al., 1996) or exclusively from the rostral hindbrain (for review, see Sotelo, 2004; and Hidalgo-Sánchez et al., 2005). In fact, whether a dual neuromeric origin of the cerebellum exists or not, cannot be completely ascertained because of the existence of an early transient intercompartmental cell mixing (Zervas et al., 2004). However, a reminiscent intermingle of cells also occurs between other rhombomeres (for review, see Zervas et al., 2004). On the basis of present results, and although the cerebellar primordium appeared located exclusively in the area of genes with hindbrain positive domains (as *ScGbx2* gene), we cannot determine whether the origin of the cerebellum is exclusive from the hindbrain or some contribution occurs from the midbrain.

Genoarchitecture of the MHB in *S. canicula.* Comparison to other gnathostomes

The striking morphological resemblance between early embryos of the lesser spotted dogfish (stages 19/20 and 24/25), and those of chick (HH10/14-15 and HH19/20) and mouse (E8,5 and 9,5/10,5), which roughly coincide with the counterpart stages proposed by Rodríguez-Moldes et al. (2011), greatly facilitates the comparative study at these stages. Comparative study to other anamniota, as bony fishes and amphibian was also carried out. In general, we observed that the expression pattern of the isthmus related genes in the lesser spotted dogfish is quite similar to that of other

gnathostomes (see below), as those of mouse published by the Allen Brain Institute (Allen Brain Atlas data portal, http://.brain-map.org). Moreover, double combinations of *in situ* hybridization for the respective *S. canicula* genes also showed similar boundaries among them, and therefore, almost the same expression patterns of isthmus related genes (see below).

The reliability of the *ScOtx2* probe has been previously demonstrated in *S. canicula* in studies on the ear and eye development (Mazan et al, 2000; Plouhinec et al, 2005). Additionally, the present results show that the caudal limit of the brain *ScOtx2* positive domain in forebrain and midbrain coincides just at MHB, as in other gnathostomes [xenopus (Glavic et al., 2002), zebrafish (Jászai et al., 2003), chick (Hidalgo-Sánchez et al., 2005) and mouse (for review, see Joyner and Millet, 2000)]. Although the expression of *ScGbx2* was not previously described in *S. canicula*, its positive domain in the hindbrain, abutting with *ScOtx2* domain, matches with that described in other jawed vertebrates [xenopus (Glavic et al., 2002), zebrafish (Kikuta et al., 2003; Rhinn et al., 2003), chick (Hidalgo-Sánchez et al., 2005) and mouse (for review, see Joyner and Millet, 2000)], although in xenopus and zebrafish *Gbx2* expression is excluded from the posteriormost portion of the embryo (for review Hidalgo-Sánchez et al., 2005). The similarities we observed in *S. canicula* with respect to other gnathostomes allow identifying the location of the MHB in this species (see Fig. 3).

The *Fgf8* positive band observed at pharyngula stages (present results; Compagnucci et al., 2013) and even later (Compagnucci et al., 2013), corresponds to the rhombomere 0 as described Aroca and Puelles (2005). In addition, the interface abutting *Fgf8* and *Otx2* observed in present results matches well with what was described in other gnathostomes [xenopus (Glavic et al., 2002), zebrafish (Inoue et al.,

2008), chick (Hidalgo-Sánchez et al., 2005) and mouse (for review, see Joyner and Millet, 2000)]. Additional similarities were observed, as the overlapping of a few *ScFgf8* positive cells in the *Otx2* positive domain (present results) which has been previously described in chick (Hidalgo-Sánchez et al., 2005). Furthermore, the negative gap between *ScFgf8* and *ScOtx2* could correspond to that observed in mouse (see Fig. 2 in Sotelo, 2004), and transiently in the midbrain of chick (Millet et al, 1996). This negative gap may be involved in morphogenetic movements for the completion of the isthmic constriction, as it has been suggested in chick (Millet et al., 1996; Adams et al., 2000). However, other possibilities cannot ruled out, i.e., it could be an area for free cell intermixing between midbrain and hindbrain (Zervas et al., 2004), or it could be related with the small triangular mass described by Alvarado-Mallard as a part of the mesencephalon giving rise to cerebellum (for review, see Sotelo, 2004).

Some differences were also observed, as the location of the isthmic constriction that in *S. canicula* is located partially within the *ScOtx2* positive area early on development (present results), differently from that occurring in chick and mouse, where it is found caudal to the *Otx2* domain (Millet et al., 1996).

The expression pattern of *ScLmx1b* also appears similar to its ortholog in zebrafish (O'Hara et al., 2005; Cheng et al., 2007), xenopus (Haldin et al., 2003), chick (Adams et al., 2000) and mouse (Mishima et al., 2009; Liu et al., 2010). Furthermore, in chick and mouse, the *Lmx1b* positive domain temporarily covers the MHB and progressively becomes restricted to the caudal midbrain, (Adams et al., 2000; Guo et al., 2007; Mishima et al., 2009). A decrease of expression of *Lmx1b* from early to late pharyngula stages was also observed in *S. canicula* (present results).

The expression of *Iroquois* genes roughly coincides with that reported in other gnathostomes. On one hand, the *Irx3* gene shows two domains (rostral and caudally to

the MHB respectively) and, as in the lesser spotted dogfish (present results), a negative gap in the isthmic area was found in chick (Fig. 2 in Kobayashi et al., 2002), mouse (Bosse et al., 1997; Cohen et al., 2000), and zebrafish (Tan et al., 1999). In xenopus, *Xiro3* was expressed in the MHB at early stages, but its expression becomes reduced in this area later in development (Bellefroid et al., 1998; Rodríguez-Seguel et al., 2009). On the other hand, the rostral domain of expression of *ScIrx1* appears similar to that of other gnathostomes. However, a caudal expression domain was also described in mouse and zebrafish (Cohen et al., 2000; Cheng et al., 2001, 2007), differently from that we observed in the lesser spotted dogfish. Nevertheless, in most of jawed vertebrates this gene is not expressed at MHB (Cohen et al., 2000; Cheng et al., 2001, 2007; present results), except in xenopus, (Glavic et al., 2002).

The great similarity of the expression pattern of isthmus related genes in the lesser spotted dogfish to those of other gnathostomes allowed us to identify the MHB and rhombomere 0, which correspond to the *ScFgf8/ScGbx2/ScEn2*-positive and *ScIrx3*-negative domain, just caudal to the midbrain *ScIrx1/ScOtx2/ScLmx1b*-positive domain (see Fig. 3).

Regionalization of the upper rhombic lip

The expression pattern of the gene *En2* was previously described around the MHB in *Scyliorhinus torazame*, a close related shark species to *S. canicula*, (Adachi et al., 2012). The expression pattern appears to be the same as we observed in the lesser spotted dogfish (present results), as well as in other jawed vertebrates [xenopus (Koenig et al., 2010), zebrafish (Lekven et al., 2003), chick (Hidalgo-Sánchez et al., 2005) and mouse (Liu et al., 1999)]. The expression pattern of a close related gene (*En1*) was also previously described in *S. canicula* (Tanaka et al., 2002), whose positive domain at

MHB appears very similar to that of *ScEn2* (present results). Regarding to the distribution of Pax6 protein in the lesser spotted dogfish, it appeared slightly delayed with respect to the expression of the *ScPax6* gene, as it was described in r1 (Derobert et al., 2002; Ferreiro-Galve, 2010) at earlier stages than the Pax6 protein (present results). Similarly, a delay of Pax6 expression in r1 was described in mouse, in which the Pax6 was firstly observed up to the r1-r2 boundary and progressively appeared in r1 (Takahashi and Osumi, 2011).

The anterior limit of Pax6 roughly abutted with the posterior limit of *ScEn2* positive domain at the half of the rhombomere 1. This result allows the recognition of rostral and caudal regions in this rhombomere (Fig. 3). However, ventrally at parasagittal levels, the boundary abutting *ScEn2*-Pax6 roughly coincides with the caudal edge of rhombomere 0 (Fig. 3), as we previously described (Rodríguez-Moldes et al., 2011). In zebrafish *En2* also appears roughly abutting with *Pax6* (Scholp et al., 2003). Furthermore, the GAD-DCX cells previously described at the most rostral part of r1 or r0-r1 boundary (Rodríguez-Moldes et al., 2011), which may correspond to migrating neuroblasts from the upper rhombic lip or r1 (**see Chapter 3**), appear to abut with the caudal edge of *ScFgf8* expression domain and to overlap with the *ScEn2* positive domain in the rostral half of the r1 (present results). A subdivision of r1 into two halves, as proposed in *S. canicula* (present results), was also established in mammals (Aroca and Puelles, 2005; Liu et al., 2010; Sato and Joyner, 2009).

The fact that both r0-r1 and r1a-r1b boundaries are not clearly defined morphologically could be due to a delay in the morphogenesis of this rostral hindbrain region with respect to more caudal rhombomeres, as previously suggested by Aroca and Puelles (2005).

Comparison to invertebrates and agnatha

As the cerebellum is an evolutionary innovation of gnathostomes, the dissimilarities with respect to simpler organisms could explain why the isthmic organizer acquired the ability to induce the formation of the cerebellum for the first time in evolution, probably in the ancestor of jawed vertebrates.

An isthmic organizer-like exists from hemichordates, although it is not located at *Otx-Gbx* boundary and *En* gene does not overlap with *Fgf8* expression domain (Pani et al., 2012), which is different from shark (present results) and other vertebrates (see above). These genes are also present in basal chordates although their expression patterns are not all the same as those observed in vertebrates (for review, see Holland, 2013). In cephalochordates (amphioxus), an *Otx-Gbx* boundary is present, but signaling molecules as *Fgf8* are expanded and not restricted to the area equivalent to MHB (Holland, 2005, 2013; Castro et al., 2006; Holland and Short, 2008; Bertrand et al., 2011) as they seem to have secondarily lost some developmental mechanisms in comparison to hemichordates (for review, see Pani et al., 2012). The expression patterns of isthmus related genes in urochordates, as ascidia (Ikuta and Saiga, 2007) also showed dissimilarities from what was observed in shark (present results) and other vertebrates (for review, see Castro et al., 2006), such as the loss of the *Gbx* gene and therefore, the absence of a homologous MHB (Wada et al., 2003; Ikuta and Saiga, 2007). Therefore, as Pani et al. (2012) suggested, at least a partial IsO-like signaling center pre-dates vertebrates.

Comparing to agnatha (basal vertebrates), the expression pattern of an array of genes related to the MHB matches well with those of other vertebrates (for review, see Kuratani et al., 2002) and lesser spotted dogfish (present results). For instance, the caudal limit of *Otx* expression in lamprey, coincides at the caudal edge of the midbrain

(Tomsa and Langeland, 1999; Murakami et al., 2001; Suda et al., 2009), the *Fgf8* was restricted to the MHB (Rétaux and Kano, 2010; Sugahara et al., 2011) and the *En* gene was expressed overlaying the MHB (Matsuura et al., 2008; Hammond et al., 2009). However, the *Gbx* gene has not been described in lamprey yet. Nevertheless, dissimilarities between agnatha and gnathostomes also exist. The *IrxA* gene in lamprey, ortholog to the *Irx1/3* of gnathostomes, does not show a negative gap of expression at MHB (Jiménez-Guri and Pujades, 2011), differently from that observed in the lesser spotted dogfish (present results). The *Irx3* has been described as repressor of the cerebellum (for review, see Gómez-Skarmeta and Modolell, 2002). In fact, mice deficient for the expression of *Irx2* (which is involved in the formation of the cerebellum), did not present the negative gap of *Irx3* expression at MHB (Lebel et al., 2003). Besides, *ziro3* in zebrafish appears expressed in the MHB only after the formation of the cerebellum (Tan et al., 1999). Therefore, it cannot be ruled out the possibility that the induction of the cerebellum must be directly or indirectly related to the appearance of new *Iroquois* isoforms due to genetic duplication in gnathostomes (Kerner et al., 2009) and to the down-regulation of *Irx3* at MHB. In addition to the genetic duplications that occur in agnatha-gnathostomate transition (Kerner et al., 2009), our results also support some hypothesis previously proposed for explaining the cerebellar innovation in gnathostomes, such as the absence of *Pax6* expression in the rhombic lip in lamprey, different from that occurs in gnathostomes (for review, see Kuratani et al., 2002). In the lesser spotted dogfish, like in other gnathostomes, *Pax6* is expressed in the rhombic lip and cerebellum (Rodríguez-Moldes et al., 2008, 2011).

To activate the pathways involved in the formation of the cerebellum, it is necessary that some genes reach a high threshold of expression and be expressed long enough, such as in the case of *Fgf8* (Sato and Nakamura, 2004; Sato and Joyner, 2009)

or *Gbx2* (Waters and Lewandoski, 2006). Therefore, though the expression patterns of isthmus related genes appear very similar in agnatha and gnathostomes, it could be possible that the level of expression of the respective genes in lamprey would not be high enough.

Therefore, the emergence of the cerebellum for the first time in the ancestor of gnathostomes might have been a very gradual process from simpler organisms. So, although mostly of isthmus related genes expression patterns coincide between jawless and jawed vertebrates, small differences in the agnatha-gnathostomate transition would be a key for the evolutionary innovation of the cerebellum.

Evidence of concurrent evolutionary innovation of the cerebellum and jaw

It is widely accepted that both the cerebellum and the jaw are a concurrent evolutionary innovation of gnathostomes (for review, see Northcutt, 2002). In fact, the appearance of these structures allowed big changes in the evolutionary history of vertebrates, as the predation and so the necessity of controlling more complex body movements. Nevertheless, whether mechanisms involved in early patterning of both structures are also closely related or not, it is not completely understood yet.

The origin and development of the jaw has been extensively studied. The jaw is mostly derived from the first branchial arch (br1) or mandibular arch, whose cells in turn correspond to neural crest cells that have migrated from isthmic levels (for review, see Logan et al., 1993). Furthermore, in the br1 some isthmus related genes (as *Otx2*, *Fgf8* and *En2*) are also expressed, which are involved in early patterning of the jaw (Logan et al., 1993; Matsuo et al., 1995; Abu-Issa et al., 2002; Knight et al., 2008). Likewise, in cartilaginous fishes, these genes have been described in relation to the br1 and jaw development and also in the MHB (Adachi et al., 2012; Compagnucci et al.,

2013). Therefore, as in the MHB and br1 (mainly derived from neural crest of isthmic levels) an array of genes in common is expressed, data about the expression patterns of isthmus related genes in *S. canicula* (present results; Adachi et al., 2012; Compagnucci et al., 2013) could indicate a high degree of conservation in a possible close relation of genetic networks involved in the early patterning of the cerebellum and jaw.

CONCLUSIONS

Similarities observed between the lesser spotted dogfish and other gnathostomes show the high degree of conservation of the expression patterns of isthmus related genes and support the hypothesis that the chondrychthyan pattern reveals the ancestral condition of cerebellar formation. Additionally, it allowed the recognition of the boundaries between r0-r1 and r1a-r1b in the rostral hindbrain. On the other hand, the dissimilarities found with respect to other anamniota species reveal that those features were secondarily derived.

While invertebrates present particular combinations of various isthmus related genes at the IsO-like signaling center, only vertebrates present a whole set of isthmus related genes with conserved expression patterns. Our results support previously proposed hypothesis for explaining the cerebellar origin. Although more genoarchitectonic studies in basal gnathostomes and agnatha would be necessary, small dissimilarities we observed between them might give a clue to clarify why the isthmic organizer acquired the ability to induce the formation of the cerebellum in the ancestor of jawed vertebrates.

LITERATURE CITED

Abu-Issa R, Smyth G, Smoak I, Yamamura K, Meyers EN. 2002. *Fgf8* is required for pharyngeal arch and cardiovascular development in the mouse. Development 129:4613-4625.

Adachi N, Takechi M, Hirai T, Kuratani S. 2012. Development of the head and trunk mesoderm in the dogfish, *Scyliorhinus torazame*: II. Comparison of gene expression between the head mesoderm and somites with reference to the origin of the vertebrate head. Evol Dev 14:257-276.

Adams KA, Maida JM, Golden JA, Riddle RD. 2000. The transcription factor *Lmx1b* maintains *Wnt1* expression within the isthmic organizer. Development 127:1857-67.

Aroca P, Puelles L. 2005. Postulated boundaries and differential fate in the developing rostral hindbrain. Brain Res Rev 49:179-190.

Ballard WW, Mellinger J, Lechenault H. 1993. A series of normal stages for development of *Scyliorhinus canicula*, the lesser spotted dogfish (*Chondrichthyes: Scyliorhinidae*). J Exp Zool 267:318-336.

Bellefroid EJ, Kobbe A, Gruss P, Pieler T, Gurdon JB, Papalopulu N, 1998. *Xiro3* encodes a *Xenopus* homolog of the *Drosophila Iroquois* genes and functions in neural specification. EMBO J 17:191-203.

Bertrand S, Camasses A, Somorjai I, Belgacem MR, Chabrol O, Escande ML, Pontarotti P, Escriva H. 2011. Amphioxus *FGF* signaling predicts the acquisition of vertebrate morphological traits. Proc Natl Acad Sci USA 108:9160-9165.

Bosse A, Zülch A, Becker MB, Torres M, Gómez-Skarmeta JL, Modolell J, Gruss P. 1997. Identification of the vertebrate *Iroquois* homeobox gene family with overlapping expression during early development of the nervous system. Mech Dev 69:169-181.

Castro LF, Rasmussen SL, Holland PW, Holland ND, Holland LZ. 2006. A *Gbx* homeobox gene in amphioxus: insights into ancestry of the ANTP class and evolution of the midbrain/hindbrain boundary. Dev Biol 295:40-51.

Cheng CW, Hui C, Strähle U. Cheng SH. 2001. Identification and expression of zebrafish *Iroquois* homeobox gene *irx1*. Dev Genes Evol 211:442-444.

Cheng CW, Yan CH, Choy SW, Hui MN, Hui CC, Cheng SH. 2007. Zebrafish homologue *irx1*a is required for the differentiation of serotonergic neurons. Dev Dyn 236:2661-2667.

Cohen DR, Cheng CW, Cheng SH, Hui CC. 2000. Expression of two novel mouse *Iroquois* homeobox genes during neurogenesis. Mech Dev 91:317-321.

Compagnucci C, Debiais-Thibaud M, Coolen M, Fish J, Griffin JN, Bertocchini F, Minoux M, Rijli FM, Borday-Birraux V, Casane D, Mazan S, Depew MJ. 2013. Pattern and polarity in the development and evolution of the gnathostome jaw: Both conservation and

heterotopy in the branchial arches of the shark, *Scyliorhinus canicula*. Dev Biol 377:428-448.

Coolen, M, Sauka-Spengler T, Nicolle D, Le-Mentec C, Lallemand Y, Da Silva C, Plouhinec JL, Robert B, Wincker P, Shi DL, and Mazan, S. 2007. Evolution of axis specification mechanisms in jawed vertebrates: insights from a chondrichthyan. *PLoS ONE* 2, e374. doi: 10.1371/journal. pone.0000374.

Derobert Y, Baratte B, Lepage M, Mazan S. 2002. *Pax6* expression patterns in *Lampetra fluviatilis* and *Scyliorhinus canicula* embryos suggest highly conserved roles in the early regionalization of the vertebrate brain. Brain Res Bull 57:277-280.

Ferreiro-Galve S. 2010. Brain and retina regionalization in sharks: study based on the spatiotemporal expression pattern of Pax6 and other neurochemical markers. Doctoral Thesis, University of Santiago de Compostela, Spain.

Ferreiro-Galve S, Rodríguez-Moldes I, Candal E. 2012. Pax6 expression during retinogenesis in sharks: comparison with markers of cell proliferation and neuronal differentiation. J Exp Zool 318:91-108.

Germot A, Lecointre G, Plouhinec JL, Le Mentec C, Girardot F, Mazan S. 2001. Structural evolution of *Otx* genes in craniates. Mol Biol Evol 18:1668-1678.

Glavic A, Gómez-Skarmeta JL, Mayor R. 2002. The homeoprotein Xiro1 is required for midbrain-hindbrain boundary formation. Development 129:1609-1621.

Gómez-Skarmeta JL, Modolell J. 2002. *Iroquois* genes: genomic organization and function in vertebrate neural development. Curr Opin Genet Dev 12:403-408.

Guo C, Qiu HY, Huang Y, Chen H, Yang RQ, Chen SD, Johnson RL, Chen ZF, Ding YQ. 2007. *Lmx1b* is essential for *Fgf8* and *Wnt1* expression in the isthmic organizer during tectum and cerebellum development in mice. Development 134:317-325.

Haldin CE, Nijjar S, Massé K, Barnett MW, Jones EA. 2003. Isolation and growth factor inducibility of the Xenopus laevis *Lmx1b* gene. Int J Dev Biol 47:253-262.

Hallonet ME, Le Douarin NM. 1993. Tracing neuroepithelial cells of the mesencephalic and metencephalic alar plates during cerebellar ontogeny in quail-chick chimaeras. Eur J Neurosci 5:1145-55.

Hallonet MER, Teillet MA, Le Douarin NM. 1990. A new approach to the development of the cerebellum provided by the quail-chick marker system. Development 108:19-31.

Hammond KL, Baxendale S, McCauley DW, Ingham PW, Whitfield TT. 2009. Expression of *patched*, *prdm1* and *engrailed* in the lamprey somite reveals conserved responses to Hedgehog signaling. Evol Dev 11:27-40.

Hidalgo-Sánchez M, Millet S, Bloch-Gallego E, Alvarado-Mallart RM. 2005. Specification of the meso-isthmo-cerebellar region: The *Otx2/Gbx2* boundary. Brain Res Rev 49:134-149.

Holland LZ. 2005. Non-neural ectoderm is really neural: evolution of developmental patterning mechanisms in the non-neural ectoderm of chordates and the problem of sensory cell homologies. J Exp Zool 304:304-323.

Holland LZ. 2013. Evolution of new characters after whole genome duplications: Insights from amphioxus. Semin Cell Dev Biol 24:101-109.

Holland LZ, Short S. 2008. Gene duplication, co-option and recruitment during the origin of the vertebrate brain from the invertebrate chordate brain. Brain Behav Evol 72:91-105.

Ikuta T, Saiga H. 2007. Dynamic change in the expression of developmental genes in the ascidian central nervous system: revisit to the tripartite model and the origin of the midbrain-hindbrain boundary region. Dev Biol 312:631-643.

Inoue F, Parvin MS, Yamasu K. 2008. Transcription of *fgf8* is regulated by activating and repressive *cis*-elements at the midbrain-hindbrain boundary in zebrafish embryos. Dev Biol 316:471-486.

Jászai J, Reifers F, Picker A, Langenberg T, Brand M. 2003. Isthmus-to-midbrain transformation in the absence of midbrain-hindbrain organizer activity. Development 130:6611-6623.

Jiménez-Guri E, Pujades C. 2011. An ancient mechanism of hindbrain patterning has been conserved in vertebrate evolution. Evol Dev 13:38-46.

Joyner AL, Liu A, Millet S. 2000. *Otx2*, *Gbx2* and *Fgf8* interact to position and maintain a mid-hindbrain organizer. Curr Opin Cell Biol 12:736-741.

Jungbluth S, Larsen C, Wizenmann A, Lumsden A. 2001. Cell mixing between the embryonic midbrain and hindbrain. Curr Biol 11:204-207.

Kerner P, Ikmi A, Coen D, Vervoort M. 2009. Evolutionary history of the *iroquois/Irx* genes in metazoans. BMC Evol Biol 9:74.

Kikuta H, Kanai M, Ito Y, Yamasu K. 2003. *gbx2* Homeobox gene is required for the maintenance of the isthmic region in the zebrafish embryonic brain. Dev Dyn 228:433-450.

Knight RD, Mebus K, Roehl HH. 2008. Mandibular arch muscle identity is regulated by a conserved molecular process during vertebrate development. J Exp Zool 310:355-369.

Kobayashi D, Kobayashi M, Matsumoto K, Ogura T, Nakafuku M, Shimamura K. 2002. Early subdivisions in the neural plate define distinct competence for inductive signals. Development 129:83-93.

Koenig SF, Brentle S, Hamdi K, Fichtner D, Wedlich D, Gradl D. 2010. En2, Pax2/5 and Tcf-4 transcription factors cooperate in patterning the *Xenopus* brain. Dev Evol 340:318-328.

Kuratani S, Kuraku S, Murakami Y. 2002. Lamprey as an evo-devo model: lessons from comparative embryology and molecular phylogenetics. Genesis 34:175-183.

Lekven AC, Buckles GR, Kostakis N, Moon RT. 2003. *Wnt1* and *wnt10b* function redundantly at the zebrafish midbrain-hindbrain boundary. Dev Biol 254:172-187.

Lebel M, Agarwal P, Cheng CW, Kabir MG, Chan TY, Thanabalasingham V, Zhang X, Cohen DR, Husain M, Cheng SH, Bruneau BG, Hui CC. 2003. The *Iroquois* homeobox gene *Irx2* is not essential for normal development of the heart and midbrain-hindbrain boundary in mice. Mol Cell Biol 23:8216-8225.

Liu A, Joyner AL. 2001. EN and GBX2 play essential roles downstream of FGF8 in patterning the mouse mid/hindbrain region. Development 128:181-191.

Liu A, Losos K, Joyner AL. 1999. *FGF8* can activate *Gbx2* and transform regions of the rostral mouse brain into a hindbrain fate. Development 126:4827-4838.

Liu ZR, Shi M, Hu ZL, Zheng MH, Du F, Zhao G, Ding YQ. 2010. A refined map of early gene expression in the dorsal rhombomere 1 of mouse embryos. Brain Res Bull 82:74-82.

Logan C, Khoo WK, Cado D, Joyner AL.1993. Two enhancer regions in the mouse *En-2* locus direct expression to the mid/hindbrain region and mandibular myoblasts. Development 117:905-916.

Martínez S. 2001. The isthmic organizer and brain regionalization. Int J Dev Biol 44:367-371.

Martínez S, Alvarado-Mallart RM. 1989. Rostral Cerebellum Originates from the Caudal Portion of the So-Called 'Mesencephalic' Vesicle: A Study Using Chick/Quail Chimeras. Eur J Neurosci 1:549-560.

Matsunaga E, Katahira T, Nakamura H. 2002. Role of *Lmx1b* and *Wnt1* in mesencephalon and metencephalon development. Development 129:5269-5277.

Matsuo I, Kuratani S, Kimura C, Takeda N, Aizawa S. 1995. Mouse *Otx2* functions in the formation and patterning of rostral head. Genes Dev 9:2646-2658.

Matsuura M, Nishihara H, Onimaru K, Kokubo N, Kuraku S, Kusakabe R, Okada N, Kuratani S, Tanaka M. 2008. Identification of four *Engrailed* genes in the Japanese lamprey, *Lethenteron japonicum*. Dev Dyn 237:1581-1589.

Mazan S, Jaillard D, Baratte B, Janvier P. 2000. *Otx1* gene-controlled morphogenesis of the horizontal semicircular canal and the origin of the gnathostome characteristics. Evol Dev 2:186-193.

Millet S, Bloch-Gallego E, Simeone A, Alvarado-Mallart RM. 1996. The caudal limit of *Otx2* gene expression as a marker of the midbrain/hindbrain boundary: a study using in situ hybridization and chick/quail homotopic grafts. Development 122:3785-3797.

Mishima Y, Lindgren AG, Chizhikov VV, Johnson RL, Millen KJ. 2009. Overlapping function of *Lmx1a* and *Lmx1b* in anterior hindbrain roof plate formation and cerebellar growth. J Neurosci 29:11377-11384.

Moens CB, Prince VE. 2002. Constructing the hindbrain: insights from the zebrafish. Dev Dyn 224:1-17.

Murakami Y, Ogasawara M, Sugahara F, Hirano S, Satoh N, Kuratani S. 2001. Identification and expression of the lamprey *Pax6* gene: evolutionary origin of the segmented brain of vertebrates. Development 128:3521-3531.

Nakamura H, Sato T, Suzuki-Hirano A. 2008. Isthmus organizer for mesencephalon and metencephalon. Dev Growth Differ. 50 Suppl 1:S113-118.

Northcutt RG. 2002. Understanding vertebrate brain evolution. Integr Comp Biol. 42:743-756.

O'Hara FP, Beck E, Barr LK, Wong LL, Kessler DS, Riddle RD. 2005. Zebrafish *Lmx1b*.1 and *Lmx1b.2* are required for maintenance of the isthmic organizer. Development 132:3163-3173.

Pani AM, Mullarkey EE, Aronowicz J, Assimacopoulos S, Grove EA, Lowe CJ. 2012. Ancient deuterostome origins of vertebrate brain signalling centres. Nature 483:289-294.

Plouhinec JL, Leconte L, Sauka-Spengler TS, Bovolenta P, Mazan S, Saule S. 2005. Comparative analysis of gnathostome *Otx* gene expression patterns in the developing eye: implications for the functional evolution of the multigene family. Dev Biol 278:560-575.

Puelles L, Ferrán JL. 2012. Concept of neural genoarchitecture and its genomic fundament. Front Neuroanat 6:47.

Rétaux S, Kano S. 2010. Midline signaling and evolution of the forebrain in chordates: a focus on the lamprey *Hedgehog* case. Integr Comp Biol 50:98-109.

Rhinn M, Lun K, Amores A, Yan YL, Postlethwait JH, Brand M. 2003. Cloning, expression and relationship of zebrafish *gbx1* and *gbx2* genes to *Fgf* signaling. Mech Dev 120:919-936.

Rodríguez-Moldes I, Ferreiro-Galve S, Carrera I, Sueiro C, Candal E, Mazan S, Anadón R. 2008. Development of the cerebellar body in sharks: spatiotemporal relations of *Pax6*-expression, cell proliferation and differentiation. Neurosci Lett 432:105-110.

Rodríguez-Moldes I, Carrera I, Pose-Méndez S, Quintana-Urzainqui I, Candal E, Anadón R, Mazan S, Ferreiro-Galve S. 2011. Regionalization of the shark hindbrain: a survey of an ancestral organization. Front Neuroanat 5:1-14.

Rodríguez-Seguel E, Alarcón P, Gómez-Skarmeta JL. 2009. The *Xenopus Irx* genes are essential for neural patterning and define the border between prethalamus and thalamus through mutual antagonism with the anterior repressors Fezf and Arx. Dev Biol 329:258-268.

Sato T, Joyner AL. 2009. The duration of *Fgf8* isthmic organizer expression is key to patterning different tectal-isthmo-cerebellum structures. Development 136:3617-3626.

Sato T, Nakamura H. 2004. The Fgf8 signal causes cerebellar differentiation by activating the Ras-ERK signaling pathway. Development 131:4275-4285.

Scholpp S, Lohs C, Brand M. 2003. Engrailed and Fgf8 act synergistically to maintain the boundary between diencephalon and mesencephalon. Development 130:4881-93.

Simeone A. 2000. Positioning the isthmic organizer where *Otx2* and *Gbx2* meet. Trends Genet 16:237-240.

Sotelo C. 2004. Cellular and genetic regulation of the development of the cerebellar system. Prog Neurobiol 72:295-339.

Suda Y, Kurokawa D, Takeuchi M, Kajikawa E, Kuratani S, Amemiya C, Aizawa S. 2009. Evolution of *Otx* paralogue usages in early patterning of the vertebrate head. Dev Biol 325:282-295.

Sugahara F, Aota S, Kuraku S, Murakami Y, Takio-Ogawa Y, Hirano S, Kuratani S. 2011. Involvement of Hedgehog and FGF signalling in the lamprey telencephalon: evolution of regionalization and dorsoventral patterning of the vertebrate forebrain. Development 138:1217-1226.

Takahashi M, Osumi N. 2011. Pax6 regulates boundary-cell specification in the rat hindbrain. Mech Dev 128:289-302.

Tan JTY, Korzh V, Gong Z. 1999. Expression of a zebrafish *iroquois* homeobox gene, *Ziro3*, in the midline axial structures and central nervous system. Mech Dev 87:165-168.

Tanaka M, Münsterberg A, Anderson WG, Prescott AR, Hazon N, Tickle C. 2002. Fin development in a cartilaginous fish and the origin of vertebrate limbs. Nature 416:527-531.

Tomsa JM, Langeland JA. 1999. *Otx* expression during lamprey embryogenesis provides insights into the evolution of the vertebrate head and jaw. Dev Biol 207:26-37.

Urbach R. 2007. A procephalic territory in *Drosophila* exhibiting similarities and dissimilarities compared to the vertebrate midbrain/hindbrain boundary region. Neural Dev 2:23.

Wada S, Tokuoka M, Shoguchi E, Kobayashi K, Di Gregorio A, Spagnuolo A, Branno M, Kohara Y, Rokhsar D, Levine M, Saiga H, Satoh N, Satou Y. 2003. A genome wide survey of developmentally relevant genes in *Ciona intestinalis*. II. Genes for homeobox transcription factors. Dev Genes Evol 213:222-234.

Waters ST, Lewandoski M. 2006. A threshold requirement for Gbx2 levels in hindbrain development. Development 133:1991-2000.

Zervas M, Millet S, Ahn S, Joyner A. 2004. Cell behaviors and genetic lineages of the mesencephalon and rhombomere 1. Neuron 43:345-357.

Figure 1. Panoramic and details of lateral views of *S. canicula* embryos at stages 19, 20 and 24 showing in situ hybridization reactions in whole mounts for: *ScOtx2* (A,B), *ScGbx2* (C,D), *ScFgf8* (E,F), *ScLmx1b* (G,H), *ScIrx1* (I,J), *ScIrx3* (K,L) and *ScEn2* (M-O) genes in the rostral hindbrain and adjacent brain areas. Black arrows (in A-L,O) indicate the midbrain-hindbrain boundary. White arrows (in F,H) indicate possible overlapping of Fgf8 and Lmx1b positive domains. Outlined arrows in K,L,M indicate the mesencephalic tegmentum. Note that for any marker, the signal at stage 20 is higher than at stage 24. br1-3, branchial archs 1-3; Mes, mesencephalon; MHB, midbrain-hindbrain boundary; Pros, prosencephalon; Rh, rhombencephalon.

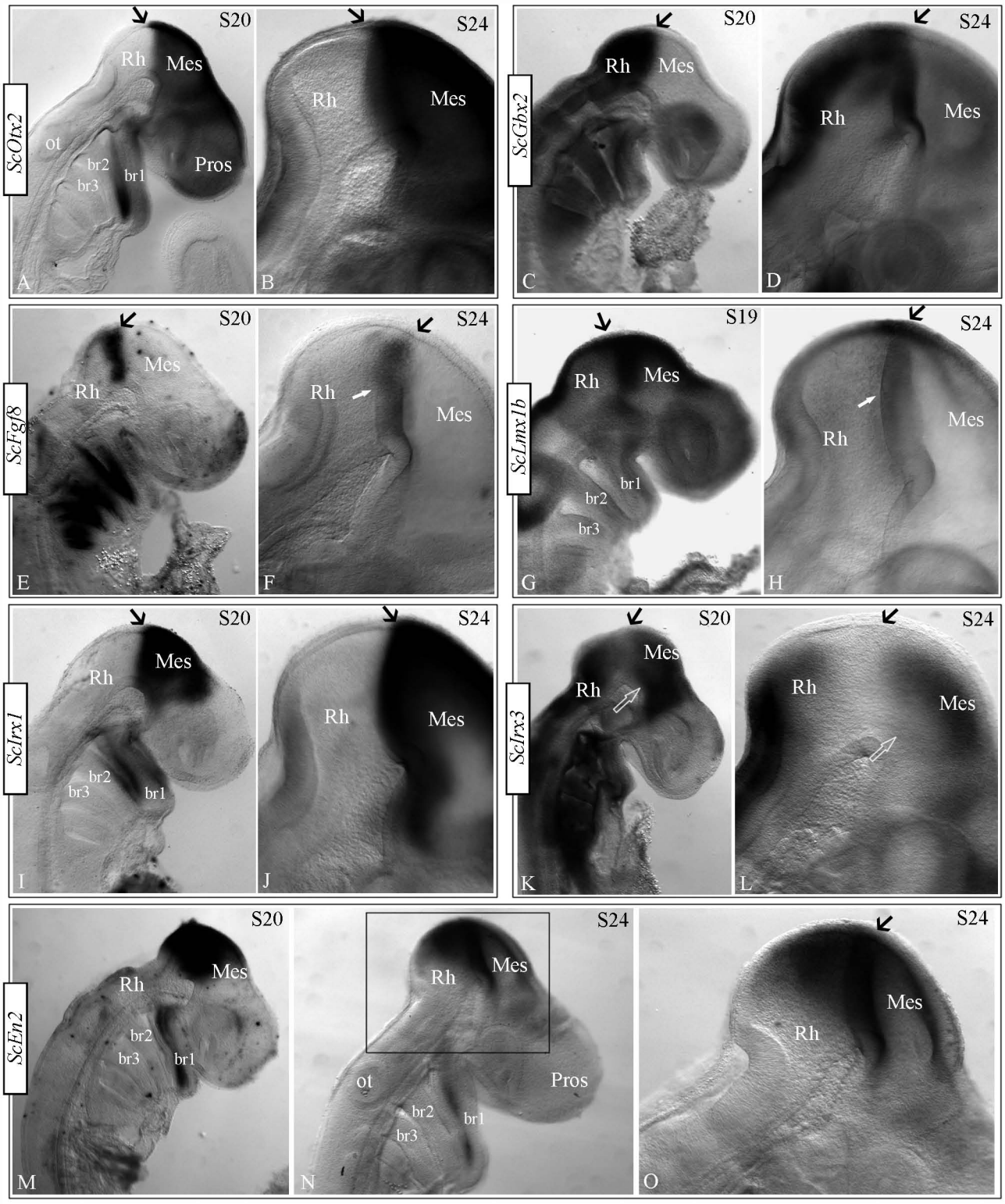
ScOtx2
S20
S24
Rh
Mes
ot
Pros
br2
br3
br1
A
B
ScGbx2
C
D
ScFgf8
E
F
ScLmx1b
S19
G
H
ScIrx1
I
J
ScIrx3
K
L
ScEn2
M
N
O

FIGURE 1

Figure 2. Midsagittal (A-D,J,L) and parasagittal (E-I,K,M-P) sections of *S. canicula* embryos at 24 (G-N) and 25 (A-F,O,P) stages hybridized for the indicated gene markers (upper left). Black arrows indicate the midbrain-hindbrain boundary. **A-F.** Details of *ScGbx2*, *ScOtx2* and *ScFgf8* positive domains. Insets in C and D show a few cells expressing both *ScFgf8* and *ScOtx2* genes. The FastRed labeling was (accidentally) removed after secondarily revealed the Otx2 with BM-Purple (in B,C and F). Asterisk (in E,F) indicates a negative gap for the expression of *ScFgf8* and *ScOtx2*. **G-M.** Details (G-I,K,M) and panoramic views (J,L) of double (G-L) or single (M) labeling of *ScGbx2-ScIrx1* (G,H), *ScFgf8-ScLmx1b* (I,J), *ScFgf8-ScIrx3* (K,L), and *ScEn2* (M) genes. Insets in J and L show overlapping domains of expression. Arrowhead (in K) indicates the interface abutting *ScFgf8* and *ScIrx3* positive domains. Outlined arrows (in K,L,M) indicate the interface roughly abutting *ScIrx3* and *ScEn2* positive domains. **N-P.** Single labeling of the Pax6 protein (N) and double labeling of the expression of the *ScEn2* gene and Pax6 protein (O,P). Cbp, cerebellar plate; Isfo, isthmic fovea; IVv, fourth ventricle; Mes, mesencephalon; MHB, midbrain-hindbrain boundary; mrf, meso-rhombencephalic fissure ; OT, optic tectum; Pros, prosencephalon; r1-4, rhombomeres 1-4; Rh, rhombencephalon; RL, rhombic lip. Scale bar = 200 µm in A-I,K,M-P; 500 µm in J,L.

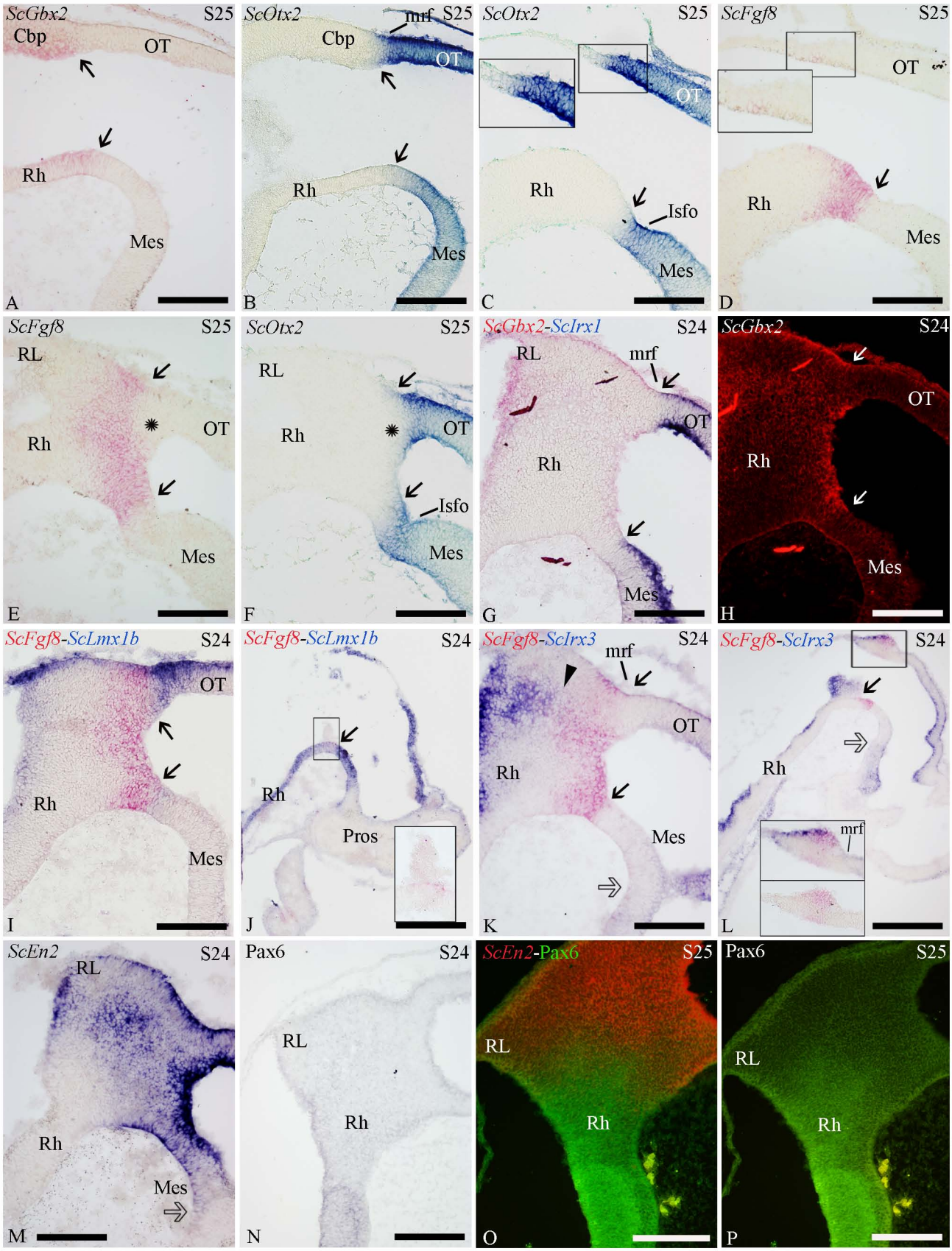
ScGbx2 S25
Cbp
OT
Rh
Mes
A
ScOtx2 S25
mrf
Cbp
OT
Rh
Mes
B
ScOtx2 S25
OT
Rh
Isfo
Mes
C
ScFgf8 S25
OT
Rh
Mes
D
ScFgf8 S25
RL
Rh
OT
Mes
E
ScOtx2 S25
RL
Rh
OT
Isfo
Mes
F
ScGbx2-ScIrx1 S24
RL
mrf
OT
Rh
Mes
G
ScGbx2 S24
OT
Rh
Mes
H
ScFgf8-ScLmx1b S24
OT
Rh
Mes
I
ScFgf8-ScLmx1b S24
Rh
Pros
J
ScFgf8-ScIrx3 S24
mrf
OT
Rh
Mes
K
ScFgf8-ScIrx3 S24
Rh
mrf
L
ScEn2 S24
RL
Rh
Mes
M
Pax6 S24
RL
Rh
N
ScEn2-Pax6 S25
RL
Rh
O
Pax6 S25
RL
Rh
P

FIGURE 2

Figure 3. Schematic drawings of sagittal (A,C) and dorsal (B,D) views of *S. canicula* embryos at stages 24/25 showing the expression pattern of the *ScOtx2*, *ScGbx2*, *ScFgf8*, *ScLmx1b*, *ScIrx1*, *ScIrx3* and *ScEn2* genes. The diagram in E summarizes the distribution of domains of expression in *S. canicula* at midbrain, midbrain-hindbrain boundary, and rostral hindbrain. Bars indicate roughly the extension of the expression domains. Thin line in Lmx1b and Irx3 indicate the rostro-caudal extension of the expression pattern in the marginal zone. Anterior levels correspond the right side. br1-3, branchial archs 1-3; IVv, fourth ventricle; LRL, lower rhombic lip; Mes, mesencephalon; MHB, midbrain-hindbrain boundary; ot, otic vesicle; OT, optic tectum; Pros, prosencephalon; r1-4, rhombomeres 1-4; Rh, rhombencephalon; URL, upper rhombic lip.

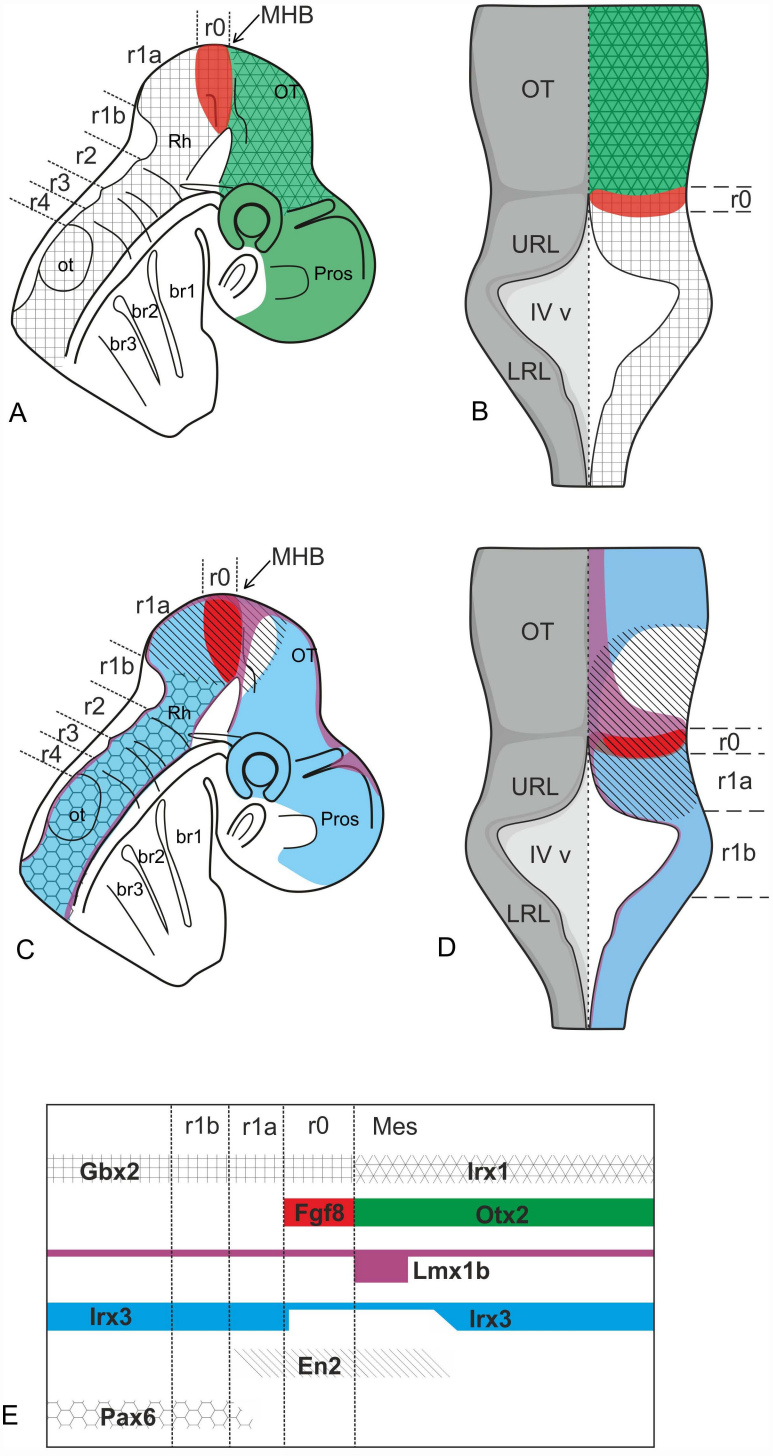
r0
MHB
r1a
r1b
r2
r3
r4
OT
Rh
ot
Pros
br1
br2
br3
A
OT
r0
URL
IV v
LRL
B
r0
MHB
r1a
r1b
r2
r3
r4
OT
Rh
ot
Pros
br1
br2
br3
C
OT
r0
r1a
URL
IV v
r1b
LRL
D
r1b
r1a
r0
Mes
Gbx2
Irx1
Fgf8
Otx2
Lmx1b
Irx3
Irx3
En2
Pax6
E

FIGURE 3

USC
UNIVERSIDADE
DE SANTIAGO
DE COMPOSTELA

CHAPTER 2

ORIGIN AND DEVELOPMENT OF CEREBELLUM AND CEREBELLUM-RELATED STRUCTURES IN A SHARK

USC
UNIVERSIDADE
DE SANTIAGO
DE COMPOSTELA

Origin and development of the cerebellum and cerebellum-related structures in a shark

INTRODUCTION

The cerebellum is a brain structure shared by all gnathostomes or jawed vertebrates. During the anterior-posterior patterning, the alar walls of the metencephalon grow up giving rise to the rhombic lips, which join at the midline to originate the cerebellar anlage. In jawless vertebrates (agnatha), a cerebellar anlage is present but whether it corresponds to a true cerebellum has largely been a matter of debate (for review, see Larsell, 1947; Nieuwenhuys, 1967; Schnitzlein and Faucette, 1969; Butler and Hodos, 2005; Murakami and Watanabe, 2009). The gnathostome-like cerebellum and cerebellar related nuclei are currently thought to have emerged in the gnathostome lineage because agnathans lack the cell types that define the cerebellum, i.e., they lack Purkinje cells (Lannoo and Hawkes, 1997) and granule cells (for review, see Kuratani et al., 2002). Similarities among different vertebrates are observed at early stages and, as development proceeds, many differences arise due to phylogenetic divergence. Paradoxically, this makes the cerebellum extremely variable in size and shape despite its highly conserved basic structure through evolution. In fact, existing cerebellar morphologies are countless (Nieuwenhuys, 1967; Butler and Hodos, 2005). However, a great harmony and preservation leads all through phylogeny both at macroscopic (main cerebellar subdivisions) and microscopic (citoarchitectonic) levels. The basic macroscopic division in all gnathostomes consists on auricles (or floculonodular lobe) and cerebellar body, which are separated by the posterolateral fissure. Though, some groups present special structures, as the lateral hemispheres (conspicuous in mammals and weak in birds) and the cerebellar valvula, present in bony fishes (for review, see

Nieuwhenhuys, 1967; Sarnat and Netsky, 1981; Butler and Hodos, 2005; Voogd and Glickstein, 1998). At microscopic level, the somas of the cerebellar cells are organized in the cerebellar cortex. All vertebrates share the same main cell types distributed in molecular, Purkinje and granular cell layers, although some groups of vertebrates present peculiar cell types in the cerebellar cortex, and the relative location of these layers can vary among different groups of vertebrates (for review, see Sarnat and Netsky, 1981; Álvarez-Otero and Anadón, 1992; Álvarez-Otero et al., 1995; Hibi and Shimizu, 2011). A similar histology to that of the cerebellar cortex is also present in other structures known as cerebellar-like structures that share a common genetic-developmental program (Montgomery et al., 2012) and mainly include parts of the octavolateral and electrosensory systems. It has been suggested that cerebellum-like structures were the evolutionary antecedent of the cerebellum and that the cerebellum arose through a change in this genetic-developmental program (Montgomery et al., 2012). Therefore, there is no complete agreement on whether the cerebellum itself is a cerebellar-like structure or should be considered separately (Devor, 2000; Bell, 2002; Montgomery et al., 2012). What is well known is that the development of these areas is closely related, because both cerebellar body and other cerebellar-like structures emerge from the somatosensorial area of the hindbrain (Bell, 2002).

The study of cerebellar development is essential, not only for understanding its complex framework or the origin of certain diseases (Utsunomiya et al., 1998; ten Donkelaar et al., 2003), but also for evolutionary studies, since the identification of similarities and differences among species throughout development is critical in comparative studies. Cerebellar morphogenesis (i.e., the process for getting the mature shape of the cerebellum) has been widely studied in mammals (Altman and Bayer, 1985; Herrup and Kuemerle, 1997; ten Donkelaar et al., 2003; Triulzi et al., 2005;

Prayer et al., 2006; Sudarov and Joyner, 2007; Cheng et al., 2010) and there are also some studies in other gnathostome groups including fishes (Larsell, 1925, 1934, 1967; Pouwels, 1978; Candal et al., 2005). Cartilaginous fishes or chondrichthyans are a key group in developmental and evolutionary studies about the cerebellum because they represent the earliest vertebrate group with cerebellum. Thus, they could help to explain how the cerebellum of the ancestors of jawed vertebrates could be, i.e., they are closer to the basic pattern present in the earliest gnathostomes. Besides, the cerebellum of cartilaginous fishes, at difference of bony fishes, has not secondarily derived structures and for this, it appears more suitable for understanding the most complex cerebellar organization through the simplest one.

The organization of the cerebellum in chondrichthyans as sharks, skates and rays (elasmobranchs) has been fairly detailed in adults (Schaper, 1898; Houser, 1901; Ariëns Kappers et al., 1936; Larsell, 1967; Nieuwenhuys, 1967; Nicholson et al., 1969; Kuhlenbeck, 1975; Smeets et al., 1983; Álvarez-Otero, 1990; Álvarez-Otero et al., 1995; Anadón et al., 2009), but developmental studies are very scarce in these cartilaginous fishes. Classic developmental studies were mainly focused on the anatomy of cerebellum in squalomorph sharks (Sterzi, 1912; Palgrem, 1921; Rüdeberg, 1961; Larsell, 1967; Nieuwenhuys, 1967) being especially detailed that performed in *Squalus* by Larsell (1967). Nowadays, the galeomorph *Scyliorhinus canicula* is considered a generalized model in evolutionary developmental (Evo-Devo) studies (Coolen et al., 2009). Furthermore, recent studies made evident that this species is especially suitable for studying any aspects of the cerebellar development (Rodríguez-Moldes et al., 2008; Chaplin et al., 2010; **see Chapter 3**), a value that is also strengthened by a fairly good knowledge of the cytoarchitecture, connections and physiology of the cerebellum in this

species (Paul and Roberts, 1975; Smeets et al., 1983; Álvarez and Anadón, 1987, 1992; Álvarez-Otero et al., 1993, 1995; Anadón et al., 2009).

The combination of classical anatomical studies with current molecular techniques provides excellent complementarity to reach a better understanding of the development, as has been illustrated by Puelles and Ferrán (2012), since gene marker analysis solve controversies about the source and development of different brain regions. Genes *Engrailed-2* (*En2*) and *Otx2* are well known by their important roles in the cerebellar patterning since early stages (at midbrain-hindbrain boundary (MHB); Hidalgo-Sánchez et al., 2005), until late in development (in the intracerebellar regionalization; Herrup and Kuemerle, 1997; Frantz et al., 1994). The *HoxA2* gene, which is the only *Hox* gene expressed in the rhombomere 2 (r2; Tümpel et al., 2008; Alexander et al., 2009), may help in the identification of the accurate origin of the auricle (for review, see Wingate and Hatten, 1999; Tümpel et al., 2008), since at present it is not clear if it exclusively comes from r1 (Wingate and Hatten, 1999), or also from r2 (Marín and Puelles, 1995). Although some anatomical markers, such as the isthmic or meso-rhombencephalic fissure, are not always consistent with the limits established by gene markers, others match rather well and, in combination with gene expression, appear to be reliable landmarks for distinguishing different brain territories during development. In fact, the expression of certain genes not only coincides with the anatomical landmarks but also directly influences their formation. That is the case of *En2*, which is critical for the formation of the main fissures during the cerebellar morphogenesis (Cheng et al., 2010).

In the present work a detailed analysis of cerebellar development in *S. canicula* was carried out by using both morphological and gene markers. We describe the gross anatomy of the cerebellum and related structures as well as the morphological

landmarks throughout development and postembryonic stages. Anatomical results were compared with the expression pattern of *Otx2*, *En2* and *HoxA2* genes, which supported particular boundaries within the cerebellum. In order to assess the degree of evolutionary conservation of cerebellar morphogenesis, a comparison of our results with that previously reported in *Squalus* and other vertebrates was also performed.

As cartilaginous fishes were the earliest vertebrate group with cerebellum, the identification of territories in these basal gnathostomes on the basis of gene expression and anatomical landmarks, together with cross-species comparison, will shed light on the ancestral condition of the cerebellum and cerebellar-related structures.

MATERIAL AND METHODS

Experimental animals and tissue preparation

Embryos of the lesser spotted dogfish (*S. canicula)* were supplied by Marine Biological Model Supply Service of the CNRS UPMC Roscoff Biological Station (France) and the Estación de Bioloxía Mariña da Graña (Galicia, Spain). Additional embryos and juveniles were kindly provided by the Aquaria of Gijón, O Grove and A Coruña (Spain). A total of 30 embryos were analyzed (which ranged from stage 20 to prehatching), and staged on the basis of their external features according to Ballard et al. (1993). Additionally, 5 juveniles and 2 adults were studied. Adequate measures were taken to minimize animal pain or discomfort. All procedures conformed to the guidelines established by the European Communities Council Directive of 22 September 2010 (2010/63/UE) and by the Spanish Royal Decree 53/2013 for animal experimentation, and were approved by the Ethics Committee of the University of Santiago de Compostela.

Specimens were anaesthetized with 0.5% tricaine methane sulphonate (MS-222; Sigma) in seawater. Embryos were fixed by immersion in phosphate buffered 4% paraformaldehyde, while prehatching, juveniles and adults were intracardially perfused with the same fixative. For *in toto* analysis of normal material the tissue was preserved in saline phosphate buffer, and the brain was excised in some specimens. In the case of sections, the fixative was removed with saline phosphate buffer. Then tissue was cryoprotected with 30% sucrose in phosphate buffer, embedded in NEG 50_{TM} (Thermo Scientific, Kalamazoo, MI), frozen with liquid nitrogen-cooled isopentane and cut on a cryostat. Parallel series of transverse and sagittal sections (18-20µm thick) were mounted on Superfrost Plus slides (Menzel-Glässer®, Madison, WI). In order to facilitate the identification of morphological landmarks, some sections were stained with haematoxylin-eosin. Furthermore, sections processed with diverse immunohistochemical markers were also used for the analysis of gross anatomy but the results for such labeling were not described.

Immunohistochemistry

Single fluorescent labeling was performed after incubation with goat polyclonal anti-aldolase-C (Aldo-C, Santa Cruz) antibody at stage 34, and double fluorescent labeling with the goat polyclonal anti-doublecortin (DCX, Santa Cruz) and rabbit polyclonal anti-glial fibrillary acidic protein (GFAP, Dako) antibodies in juveniles. Light field labeling was performed after incubation with mouse monoclonal anti-proliferating cell nuclear antigen (PCNA, Sigma) antibody in adult specimens. Source and working dilution of the antibodies is indicated in Table 1. The immunohistochemistry was performed by standard procedures as previously described (for details see Ferreiro-Galve et al., 2010). Details about the specificity of DCX, GFAP

and PCNA antibodies in *S. canicula* brain have been previously published (Quintana-Urzainqui et al., 2012; **see Chapter 3**).

Western blot

The specificity of the goat polyclonal Aldo-C antibody was tested by Western blot analysis of brain protein extracts of adult lesser spotted dogfish by standard procedures (for details about the preparation of brain extracts and blotting procedure, see Anadón et al., 2000; Carrera et al., 2012). In this blot, the Aldo-C antibody stained a single protein band of about 40 kDa (Fig. 1). As a positive control, staining of other antigens was carried out in parallel (**see Chapter 3**). ProSieve protein standards (Lonza, Rockland, ME) were used as molecular weight markers.

In situ hybridization on sections

We applied *in situ* hybridization for *ScHoxA2* (Oulion et al., 2010; Rodríguez-Moldes et al., 2011), *ScEn2* and *ScOtx2* (Germot et al., 2001; Plouhinec et al., 2005). These probes were selected from a collection of *S. canicula* embryonic cDNA library (mixed stages, S9 to S22) submitted to high throughput EST sequencing (coord. S. Mazan). Sense and antisense digoxigenin-UTP-labeled probes were synthesized directly by *in vitro* transcription using as templates linearized recombinant DNA plasmids (*Otx2* probe) or cDNA fragments prepared by PCR amplification (*ScEn2*, *ScHoxA2* probes). *In situ* hybridization on cryostat sections was carried out in stages 31, 32 and prehatching embryos following standard protocols (Coolen et al., 2007). Briefly, sections were permeabilized with proteinase K, hybridized with sense or antisense probes overnight at 65ºC and incubated with the alkaline phosphatase-coupled anti-digoxigenin antibody (1:2000, Roche Applied Science, Manheim, Germany) overnight at 4ºC. The color reaction was performed in the presence of BM-Purple (Roche). Control sense probes did not produce any detectable signal.

Imaging

Anatomical analysis of normal material (*in toto* brains) was studied in the Olympus SZX12 stereo microscope fitted with an Olympus DP12 color digital camera. Photomicrographs were taken with an Olympus DP70 color digital camera fitted to a Provis photomicroscope equipped for fluorescence with appropriate filter combinations. Double labeled samples were studied with a spectral confocal laser scanning microscope (Leica TCS-SP2, Wetzlar, Germany). For presentation, some color photomicrographs were converted to gray scale, and brightness and contrast adjusted using Adobe Photoshop 7.0. Plate photomontage, schemes and lettering were made with Corel Draw X6 and Adobe Photoshop 7.0.

RESULTS

To define boundaries and development of structures related to cerebellum, we basically followed the terminology used by Larsell (1967), Smeets and Nieuwenhuys (1976), Smeets et al. (1983), and Carrera et al (2012). Based on the changes observed in the gross anatomy of the cerebellum of the lesser spotted dogfish through development, we have distinguished three developmental periods that are summarized in Table 2. Main changes in the gross anatomy during these periods can be observed in normal material from dorsal view (see Fig. 2). Upper and lower rhombic lips were roughly discerned one from each other in stage 20 embryos (Fig. 2A).During the first period (Fig. 2B-E), the cerebellar plate or anlage of the cerebellum is formed because of the fusion of the upper rhombic lips. During the second period (Fig. 2F-H) the cerebellar anlage turns into the primordia of cerebellar body and the upper auricle leaf, while the lower auricle leaf is formed from the adjacent somatosensorial area. Finally, the third developmental period (Fig. 2I) mostly corresponds to maturation and growth of the

cerebellar system. A comprehensive study was performed on sagittal and transverse sections throughout these periods (see below), which allowed us to accurately detail when the cerebellar plate turns into the cerebellar body and when the auricles are formed, as well as the progressive rostral-to-caudal formation of four bending points that will serve as anatomical landmarks.

First period: early developmental period of cerebellum (stages 24-29)

Very early on development, the dorsal (alar) part of metencephalon (rostral hindbrain) had progressively grown up to give rise to the upper or rostral rhombic lips (compare Fig. 2A and 2B), which were clearly distinguished in sagittal sections from stages 23-24 (Figs. 3A, B, 4A). The meso-rhombencephalic fissure (mrf) or isthmic constriction was already visible in these early embryos in the anterior limit of the cerebellar primordium, which corresponds to the first point of flexure (number 1 in Figs. 3A, 4A). Shortly after, at stage 25, the onset of the fusion of the rhombic lips took place at rostral levels (Figs. 2C, 4B), which gave rise to an incipient cerebellar plate. Later on, at stage 27, the incipient cerebellar plate extended caudalwards (Figs. 2D, 3C, D). Shortly after (stage 28, Fig. 4C, D), the second point of flexure emerged, which defines the prospective dorsoventral boundary in the anterior part of the cerebellum (number 2 in Fig. 4C).

At stage 29 (Figs. 2B, 4E, F and 5A-E), the paired cerebellar plates extended caudalwards and grew medially so that they increased in size and width (Fig. 2E, 4E), although they were still separated by an ependimary raphe (Fig. 5B). The third point of flexure, which defined the prospective dorsoventral boundary of the posterior part of the cerebellum, started to be distinguished from sagittal view (number 3 in Fig. 4F). Additionally, new sulci were distinguished in transverse sections, which were located

ventrally to the cerebellar plate. We call X to the sulcus that delimit the cerebellar plate and upper rhombic lips at intermediate levels of the cerebellum (Figs. 5B, C), which could correspond to the ventral boundary of the prospective cerebellar cortex. We call X' to the sulcus that delimited the upper rhombic lips at caudal levels (Fig. 5D). At more caudal levels, the intermediate dorsal sulcus and the sulcus of His were also distinguished (Fig. 5E).

Second period: intermediate developmental period of cerebellum

(stages 30 and 31)

From stage 30 (Figs. 2F, 6A-E and 7A) the primordium of the cerebellar peduncle became progressively noticeable (CPp in Figs. 6C, 7A), due to the appearance of the sulcus e. During this stage, the cerebellar plate started to bend, as the first and second points of flexure became more conspicuous, which shaped the cerebellar body rostrally. Additionally, the fourth point of flexure was observed as a weak groove that delimited the boundary between the prospective cerebellar body and upper auricle leaf (Fig. 2F). Because it represents the limit between cerebellar body and upper auricle leaf, it must correspond to the posterolateral fissure.

At stage 31 (Figs. 2G, H, 6F-O, 7B-D, 8A-D) the cerebellar plate and the primordium of upper auricle leaf were progressively turning into the cerebellar body and the upper auricle leaf respectively (compare Figs. 6F-J and 6K-O), in part because the posterolateral fissure and the other points of flexure became more noticeable (numbers 1-4 in Figs. 7B and 8A, C). At early stage 31 the onset of the bending of caudal cerebellar anlage was observed in transverse view as a small elevation (compare Fig. 6G and 6H). As well, the upper auricle leaf primordium began to form, being visible as a small elevation and thinning in transverse sections (Fig. 6I) or as a bending

in sagittal sections (Figs. 7B, 8A, B). Then, at intermediate stage 31, the cerebellar plate continued to bend rostral and caudally by the points of flexure to eventually acquire the mature-like shape of the cerebellar body and upper auricle leaf. The lower auricle leaf was not seen yet, even at lateral level. At the end of this stage, the cerebellum got the mature (caudally closed) shape of cerebellar body (Figs. 2H, 6K-N, 7C, 8C, D), and the protuberance of the cerebellar peduncle became patent (CP in Fig. 6L). In addition, the primordium of the lower auricle leaf emerged, delimited by the sulcus X' and the boundary with the octavolateral area (Fig. 6M-O). The formation of the lower auricle leaf appears to be by a process of eversion of the area located rostrally to the octavolateral area (growing up in a dorso-caudal direction), as seen in a parasagittal view (Figs. 7D, 8D).

Third period: late developmental period of cerebellum (stage 32-adult)

The completion of the mature shape (similar to that observed in juveniles) was already observed at early stage 32 (Figs. 2I, 9A-E, 10A, B). At this stage, a transverse fissure was observed in the external part of the cerebellar body at the level of the cerebellar peduncle (prf in Figs. 2I, 10A). It corresponds to the primary transverse fissure or *fissura prima*, which divides the cerebellum into the anterior (smaller) and posterior (higher) lobes. At early stage 32, the cerebellar cortex became considerably thicker with respect to previous stages. The paramedian granular eminences started to be distinguished as longitudinal paired prominences (Fig. 9A, B) because of the condensation of granular cells (as described by Rodríguez-Moldes et al., 2008) and the upper and lower auricle leaves became patent by the accentuation of the sulcus X' (Fig. 9C-E).

At late stage 32 the longitudinal fissure that divides the cerebellar body into left and right parts became very conspicuous and visible in transverse view as an external median sulcus (Fig. 9F-J). Throughout this period, auricles were progressively much more noticeable (Figs. 9H-J, 10A, B). The upper auricle leaf (that is a caudal prolongation of the cerebellar body; Figs. 10A, B), and the lower auricle leaf (adjacent to the octavolateral area; Fig. 10B), clearly joined laterally (Figs. 9C-E,H-J).

At prehatching stages (stages 33 and 34; Figs. 10C, D and 11A-F), the size of the cerebellum was notably increased with respect to previous stages (Fig. 10C, D) and the auricles were observed as patent paired lateral protuberances (Fig. 11A, D, E). Furthermore, a new small bulge appeared, probably equivalent to the *lobus posticus* described in the developing *Squalus* by Larsell (1967), which is flanked by the caudal cerebellar body and the upper auricle leaf (Lpost in Figs. 10D, 11F).

In postnatal specimens (Fig. 9K-O, 10E, F, 11G-O), the cerebellar cortex became thicker (Figs. 9K-O, 11G-M) and the cerebellar body continued to extend over the optic tectum (Figs. 10E, F, 11H, K). In juveniles, the primary transverse fissure became more noticeable and other small clefts were also observed at marginal level (Figs. 10E, F, 11G, I). To study this fissures more in detail, we performed immunohistochemistry with DCX and GFAP, which have been used as markers of migrating neuroblasts and radial glia, respectively, and are known to be associated to fissuration during cerebellar morphogenesis (Sudarov and Joyner, 2007; Ma et al., 2012). While in the cortex the GFAP-immunoreactive radial glia appeared organized in parallel, in the clef single labelled DCX or GFAP processes appeared in a fan shaped bundle (detail in Fig. 11G').

In adults, clefts were conspicuous, and the cerebellar body became much more extended than in juveniles, both rostral and caudalwards (Fig. 11K). The observation of

the roof of the cerebellar body from ventral view (inner surface) showed that the granular eminences were smooth in juveniles and with striking folds and sulci in adults (compare Fig. 11J and 11L). The two largest folds observed in the adult may correspond to the deepest external grooves observed dorsally (compare asterisks in Figs. 11K and 11L). Immunohistochemistry with a marker of proliferation (proliferating cell nuclear antigen; PCNA) revealed proliferating cells all along the median ventricular zone (a proliferating zone previously described in adult cerebellum by Rodríguez-Moldes et al., 2008), and also within the transversally oriented inner fissures (Fig. 11M). On the other hand, the granular eminences of the ventral part of the cerebellar body appeared smooth, both in juveniles and adults. The auricles were already rostralward tilted in juveniles but, differing from adults, the lower auricle leaf did not appear to be more caudally extended than the upper auricle leaf (detail in Fig. 11N). At adulthood, both auricles appeared to be bigger and much more curved (Fig. 11O).

Gene expression patterns at intermediate and late cerebellar development

We studied the expression pattern of some genes (*ScEn2, ScHoxA2* and *ScOtx2*) at intermediate developmental stages (i.e., when the biggest changes occur in the cerebellum; Figs. 12A-F) and late development (up to completion of the mature shape; Fig. 12G-J), with two main objectives: (1) to assess whether cerebellar auricles are originated from r1 and/or r2; and (2) to investigate to what extent the boundaries of gene expression match with the aforesaid anatomical landmarks.

The *ScHoxA2* gene was previously shown to be expressed in the r2 and to delimit the r1-r2 boundary at pharyngula stages (Rodríguez-Moldes et al., 2011). In the present work we show that the expression of this gene was maintained later on development, at least until stage 32 (Fig. 12A-C, H). This allowed us to identify r2 at

the beginning of the third developmental period of the cerebellum. At early stage 31 (Fig. 12A-C), *ScHoxA2* expression was observed in the rhombencephalic tegmentum, including that of r2 (identified by the position of the trigeminal nerve root); the anterior limit of expression was caudal to the extension of the cerebellum. This expression pattern appeared homogeneous in the median-lateral axis (Fig. 12A-C). Interestingly, there was no expression of *ScHoxa2* in the area identified as the primordium of the upper auricle leaf.

The expression of *En2* gene was previously analysed on early development in other galeomorph species (*Scyliorhinus torazame*) and was reported to be expressed around the midbrain-hindbrain boundary (Adachi et al., 2012). In *S. canicula ScEn2* showed a similar expression pattern early on development (**see Chapter 1**) and until late in development (Fig. 12D, E, G, I, J). At early stage 31, a strong *ScEn2*-expression was observed in the area adjacent to the posterolateral fissure, which had been identified as the upper auricle primordium. As regards the cerebellar plate, the expression of *ScEn2* was not homogeneus in the rostrocaudal axis (the strongest signal was found in the rostral half). However, the level of expression was homogeneous at median and lateral levels, with moderate signal along the entire cerebellum (not shown). Other areas that also expressed *ScEn2* were the caudal portion of the optic tectum, the mesencephalic tegmentum and the rostral rhombencephalic tegmentum (Fig. 12D, E).

ScOtx2, whose expression in the rostral brain was also observed at pharyngula stages (Mazan et al., 2000; Plouhinec et al., 2005; **see Chapter 1**), was also expressed later in development (present results). At intermediate stage 31, when the cerebellar body and upper auricle leaf became clearly distinguishable (Fig. 12F), *ScOtx2* was expressed in the upper auricle leaf from median to lateral levels; two positive areas of expression were also observed at paramedian levels of the cerebellar body, one that

extends through its rostral half and other that extends between the third point of flexure and the posterolateral fissure (Fig. 12F).

Then, at late cerebellar development (stage 32, when the lower auricle leaf was also noticeable), the expression of *ScEn2* was observed in the upper auricle leaf; in the cerebellar body *ScEn2*-expression was caudally extended though the signal was more intense at paramedian levels. At this stage the *ScHoxA2* expression appeared in the rhombencephalic tegmentum and marginally in the cerebellum, but it was not expressed in either upper or lower auricle leaves. As development proceeded, in prehatching embryos, the expression of *ScEn2* was maintained in the upper auricle leaf, and restricted to a single paramedian area in the cerebellar body (Fig. 12I, J). At the same stage most of Purkinje cells were positive for the anti-Aldo-C antibody (Fig. 12K), a marker of Purkinje cells.

DISCUSSION

The present results give evidence of the process of cerebellar morphogenesis in a species representative of galeomorph sharks, characterized by their elaborated (Northcutt, 1977) or Type II brains (which present extensive migration of neuronal cell bodies away from the periventricular surface; for review, see Butler and Hodos, 2005), similar to those of teleosts and amniotes. Our results in *S. canicula*, together with that obtained earlier by Larsell (1967) in a squalomorph shark (with laminated or Type I brains, which present limited migration of cells away from the periventricular surface; see Butler and Hodos, 2005), reveal that the early development of the cerebellum in cartilaginous fishes follows a similar pattern in all gnathostomes: it originates from two lateral swellings or rhombic lips, which make up paired cerebellar plates that bind in the medial region to result in an elongated tube while leaving a small midline ependymal

raphe. Later, the impar cerebellar plate enlarges and undergoes a series of folds to give rise to the cerebellar body and auricles, which form part of the vestibulolateral system. Differences in the mode of growth (evagination, invagination or eversion; for review, see Nieuwenhuys, 1967) and in the bending process will cause the huge variability of the external cerebellar morphology observed among the different groups of gnathostomes (Butler and Hodos, 2005). This wide variability also exists within elasmobranchs, whose dissimilarities are believed to be due to evolutionary divergence and also to differences in their ecology, adapted behaviors or enhanced cognitive capabilities (Yopak et al., 2007; Lisney et al., 2008; Yopak and Montgomery, 2008).

Therefore, while the origin of the cerebellum from the alar region of the hindbrain is very similar in all gnathostomes, the morphology in adults becomes quite different. Accordingly, we wondered at what point in the development of the cerebellum, main differences with respect to other species arise. We also aimed to know if developmental genes that are responsible for the rostral hindbrain patterning and involved in cerebellar regionalization in other vertebrates could play the same role in basal gnathostomes.

Comparison to other elasmobranch species

The developmental stages proposed in *S. canicula* and their counterparts in *Squalus acanthias* (Table 2) were mainly based on changes of the cerebellar morphology throughout the embryonic period and postnatally in both shark species (present results and Larsell, 1967). Early in cerebellar development, Larsell (1967) described a rudimentary cerebellum in 7-8mm-embryos of *Squalus*, which consisted in a thickened area on each side of the midline of the hindbrain roof and immediately behind to the isthmic fold; these bilateral halves were connected across the midline by a

narrow thinner zone. We consider that these stages would be equivalent to the stages 23-24 and 25 of *S. canicula*, when (1) the meso-rhombencephalic fissure and rhombic lips became noticeable and (2) the fusion of rhombic lips begins, respectively.

In addition, we consider that embryos of *S. canicula* at stages 28-29 might be homologous to 22mm-embryos of *Squalus*, on the basis of the similarities noted in the cerebellar shape from sagittal view.

The emergence of the posterolateral fissure as a faint furrow in *S. canicula* stage-30 embryos (at the beginning of the second developmental period) led us to consider embryos of this stage as equivalent to 32mm-embryos of *Squalus*. Furthermore, according to Larsell (1967), the margin of the lateral recess in *Squalus* was observed as a tenial attachment that should demarcate the position of the primordium of the upper auricle leaf, which has been also observed in *S. canicula* at this stage. In *Squalus* the formation of the cerebellar body was next illustrated from the dorsal arching of the cerebellar plate that occurs in 32mm embryos to the elongated bursa observed in 50mm embryos; in its turn, the *pars medialis* (median part of the upper auricle leaf) continues almost horizontally caudalward (Larsell, 1967). Accordingly, embryos of *S. canicula* at early stage 31 may be equivalent to 50 mm-embryos of *Squalus*. In the cerebellum of *Squalus* embryos of 60mm, the swelling in the *pars ventralis* (or *eminentia ventralis cerebellaris*) described by Larsell (1967) could correspond to the incipient swelling of the cerebellar peduncle, that in the lesser spotted dogfish occurred at intermediate stage 31. Although the resemblance of the cerebellar contour is evident, there are some differences between both species at this stage, as the auricles of *Squalus* embryos were ear-like shaped, while in *Scyliorhinus* this was not observed until late S31, coinciding with the onset of the lower auricle leaf formation. Later on, in *Squalus* embryos of 80 mm, the cerebellum was described as the *pars*

medialis submerged beneath a caudal projection of the *corpus cerebelli* (Larsell, 1967), which could correspond to the incipient upper auricle leaf beneath the cerebellar body (as a closed structure) observed in *S. canicula* embryos at late stage 31.

The description of an expansion of the dorsal part of cerebellar body both rostrally and caudally, the reduction of the cerebellar base to a peduncle-like constriction and the apparition of the *sulcus primus* (transverse or primary transverse fissure) in advanced *Squalus* embryos (120mm in length) may correspond to the events we described in *Scyliorhinus* at stage 32. Of note, transverse grooves were not described in classical studies in the cerebellum of *Scyliorhinus canicula* (Nieuwhenhuys, 1967; Smeets et al., 1983), probably due to the fact that they are less conspicuous than in other species. Postnatally, both in newborns specimens of the lesser spotted dogfish and in spiny dogfish pups of 150-170 mm, the auricles were extended dorsalward on either side of the cerebellar body. Later on, as the brain elongated, the auricles tilted forward their longitudinal axis and became nearly horizontal at adulthood in both species (Larsell, 1967; present results).

In summary, similarities in the cerebellar development were noticeable between both species and reveal a high degree of conservation within elasmobranchs. However, a few dissimilarities were observed in stages we proposed as equivalent, mainly due to some disparity in the time of maturation of the auricles with respect to the cerebellar body. These dissimilarities could be at the base of interspecific differences observed in adults.

Comparison to other gnathostomes

The variability of cerebellums in different groups of gnathostomes is enormous. In order to carry out a comparative study on cerebellar morphogenesis we will pay

attention to particular aspects of the development, as the mode of growth (by evagination, invagination or eversion), the presence of the major components of the cerebellum, the ontogeny of the main cerebellar fissures (posterolateral and primary transverse fissures) and when the completion of the mature shape takes place in the different gnathotosmate groups.

The growth of the cerebellum by evagination that we observed in *S. canicula* (present results) appears to be the same as that present in other cartilaginous fishes and in most gnathostomes studied so far (for review, see Niewenhuys, 1967). However, it differs from some reptiles, in which the cerebellum grows by eversion (for review, see Niewenhuys, 1967). The morphology of the cerebellar body then changes from flat (as in turtle) to folded (as in lungfish), curved (in alligator), reverse curved (lizard), double folded (present results in *S. canicula*) or multifolded (pigeon), as has been extensively reviewed by Butler and Hodos (2005). A peculiar cerebellar structure was found in chondrosteans due to the fact that cerebellar anlage folds inward and fuse in the median plane (Vázquez et al., 2002). The cerebellar ventricle also varies from wide (as in cartilaginous fishes; present results and Butler and Hodos, 2005) to virtually obliterated (as in some actinopterygians and sarcopterygians; Nieuwenhuys, 1967; Pouwels, 1978; Butler and Hodos, 2005; Candal et al., 2005).

Most gnathostomes share the major components of the cerebellum, i.e, the cerebellar body and the auricles. Despite this commonness, some additional developmental processes may occur as development progresses, which are particular of some groups. Such is the case of the cerebellum of ray-finned fishes, the rostral part of which grows to give rise to the cerebellar valvula (Nieuwenhuys, 1967; Pouwels, 1978; Butler and Hodos, 2005; Candal et al., 2005). Most actinopterygians and sarcopterygians develop auricles as lateral projections that appear similar to those of

cartilaginous fishes. However, the auricles were absent in teleosts (Nieuwenhuys, 1967; Nieuwenhuys et al., 1998; Vázquez et al., 2002), probably due to secondary evolutionary divergence.

The ontogeny of the fissures also appears roughly well conserved throughout evolution. In *S. canicula*, the meso-rhombencephalic fissure appears first, followed by the posterolateral fissure. The same sequence was observed in bony fishes (Nieuwenhuys, 1967; Pouwels, 1978; Candal et al., 2005), amphibians and reptiles (Larsell, 1934), birds (for review, see Nieuwenhuys, 1967), and mammals (Herrup and Kuemerle, 1997; ten Donkelaar et al., 2003; Triulzi et al., 2005; Prayer et al., 2006). Of note, in some amphibians (anurans) and reptiles, in opposite way to that observed in cartilaginous fishes, the posterolateral fissure is reduced because of the reduction of the vestibulocerebellum as development proceeds. This is related to the disappearance of lateral line organs (during metamorphosis in amphibians), which are absent in not aquatic animals (Larsell, 1934; Nieuwenhuys, 1967; Sarnat and Netsky, 1981).

In *S. canicula* the appearance of the posterolateral fissure is followed by that of the primary transverse fissure or *fissura prima* (present results). The same has been reported in reptiles (Larsell, 1934), chick (Niewenhuys, 1967), rats and humans (Herrup and Kuemerle, 1997; ten Donkelaar et al., 2003; Triulzi et al., 2005; Prayer et al., 2006). In chick it has been additionally pointed that the primordium of the posterolateral fissure is detected near the attachment of the *tela choroidea* when the cerebellum is made up of two bilateral thickenings unfused at the midline, and then temporarily becomes much less apparent than the *fissura prima* (Peña-Melián et al., 1986). In mouse, unlike in *S. canicula* and other mammals, the *fissura prima* was described before the posterolateral fissure (Sudarov and Joyner, 2007; Cheng et al., 2010). These discrepancies could be related to misinterpretations in the identification of

the posterolateral fissure because of its proximity to the attachment of the choroid plexus.

Possible equivalences and/or dissimilarities with other vertebrates were also analyzed with respect to the completion of the mature shape of the cerebellum at birth. In *S. canicula* the posterolateral fissure appears in late stage 30 embryos, the cerebellar body overlays the upper auricle leaf at stage 31 and the cerebellar crest overlays octavolateral area in stage 32 embryos (roughly three months before hatching). These processes in trout have been described at late embryos, hatching and fry fishes, respectively (Candal et al., 2005), which means that the completion of the mature shape occurs postnatally. The completion of the mature shape also occurs postnatally in sturgeon (chondrostean; for review, see Gómez et al., 2004). On the contrary, in birds and mammals it appears that the acquisition of mature shape occurs prenatally (Peña-Melián et al., 1986; ten Donkelaar et al., 2003), as in *S. canicula*.

While the cerebellum begins to differentiate very early on development, it is one of the latest brain structures to mature. Fissuration and foliation have been also utilized as indicator of degree of cerebellar maturation. Indeed, in amniotes there is a progressive augment of fissuration of second and third order (Peña-Melián et al., 1986), which in humans continues for many months after birth (Triulzi et al., 2005; Prayer et al., 2006). In the lesser spotted dogfish (present results), a higher folding was observed in adults with respect to juveniles, both at outer and inner walls.The outer and inner folding observed in the lesser spotted dogfish is consistent with that observed in other cartilaginous fishes, but different from birds and mammals, which present only outer folding (for review, see Nieuwenhuys, 1967). In *S. canicula*, the fan shaped bundle of glial processes in the base of the small fissures could indicate a possible role of glial cells in the fissuration, as in mammals (Ma et al., 2012). However, in mammals, the

granule cells of the external granular layer (secondary proliferative matrix) are also involved in the formation of fissures. Granule cells, influenced by the signal from Purkinje cells, are displaced along the radial glia towards the inner of the cerebellar cortex (Sudarov and Joyner, 2007; Cerri et al., 2010). In *S. canicula* there is not marginal proliferation from stage 32 (Rodríguez-Moldes et al., 2011), when the *fissura prima* emerges, which could indicate a slightly difference in the process of cerebellar fissuration with respect to mammals. A possible explanation could also be by tension forces along parallel fibers, as previously proposed in mammals (Van Essen, 1997).

The features of *S. canicula* cerebellum observed only in adults (folds affecting the entire cerebellar cortex, auricles rostrally tilted, and the lower auricle leaf much more caudally extended than the upper auricle leaf), could correspond to the continuous growth of the cerebellar body and auricles along the lifetime. Indeed, proliferation in the cerebellum up to adulthood has been understood as a feature of fishes in general, since it was described in the cerebellum of adult elasmobranchs (Margotta, 2007; Rodríguez-Moldes et al., 2008) and teleosts (Zupanc et al., 2005; Kaslin et al., 2009).

Origin of the auricles: genoarchitectonic evidence

The expression pattern of the genes studied in the present work was fairly consistent with the anatomical landmarks described above and was similar to that reported in mammals by the Allen Brain Institute (Allen Brain Atlas data portal, http://.brain-map.org).

To date, there is no agreement about which rhombomere is at the source of the auricles, i.e., whether they originate exclusively from r1 (for review, see Wingate and Hatten, 1999; see also Edison et al., 2004), at least in part from r1 (Volkman et al., 2008), or entirely from r2 (Marín and Puelles, 1995). To solve this question, we

analysed the expression of the *En2* and that of *HoxA2* gene, which has been previously used as a marker of r2 since its rostral limit of expression coincides with the r1/r2 boundary (Tümpel et al., 2008; Alexander et al., 2009). Our results about *ScEn2* expression also support the origin of the auricle from r1. The expression of *ScEn2* in the cerebellar area located caudal to the posterolateral fissure confirm our identification of this territory as the upper auricle leaf primordium (at early stage 31) that will give rise to the upper auricle leaf (at stage 32).

In *S. canicula*, *ScHoxA2* is expressed in the rhombencephalic tegmentum including the octavolateral area but not in the upper or lower auricle leaves, which support that they entirely derive from r1 (Fig. 13). Moreover, the lower auricle leaf, located just caudally to the lateral recess of the fourth ventricle (in the most caudal part of r1) appears to correspond to a small *ScHoxA2*-negative area (Rodríguez-Moldes et al., 2011) that is maintained throughout development (present results). Of note, a *ScHoxA2*-positive domain was observed dorsally to the dorsal octaval nucleus (red domain in Fig. 13), which was classically identified as belonging to the auricle, as it contains a dense population of cells that express Pax6 (Ferreiro-Galve, 2010), a marker of granular cells (Rodríguez-Moldes et al., 2008). While this result could indicate that part of the lower auricle leaf derives from r2, we think that this domain actually correspond to a transition cerebellar-like structure in between the auricle and the octavolateral area since this area also presents a low density of serotoninergic fibers (not shown) with respect to the *ScHoxA2* negative area that we identified as lower auricle leaf. In late embryos, *ScHoxA2* was also expressed in r1 derived structures (i.e., in the cerebellar body at stage 32), which could be due to a shift of function of the gene at this advanced developmental stage.

In mammals, a small *HoxA2* negative domain is observed caudally to the upper rhombic lip (Allen Brain Atlas data portal, http://.brain-map.org). However, this domain does not develop as a lower auricle leaf. As this structure mainly receives lateral line imput (Schmidt and Bodznick, 1987), the absence of the lower auricle leaf could imply that it disappears through evolution along with the lateral line system.

Antero-posterior and median-lateral compartmentalization of the cerebellum

The delimitation of domains along the anterior-posterior axis is involved in the development of different functional regions (Frantz et al., 1994). Main domains in the cerebellum, which become compartmentalized under the influence of particular genes, are expected to be conserved throughout evolution. We have accordingly studied if the pattern of expression of *ScEn2* and *ScOtx2* in the cerebellum *S. canicula* is compatible with a role of these genes in the compartmentalization of this structure. Labeling of *ScEn2* was observed in the rostral half of the cerebellum at stage 31. This anterior-posterior distribution of *ScEn2* in *S. canicula* appears very similar to that described in mammals (Herrup and Kuemerle, 1997), where this gene has been reported to be important for the development, compartmentalization and fissuration of the cerebellum (Millen et al., 1994; Cheng et al., 2010; Orvis et al., 2012). Accordingly, we have considered the possibility that *ScEn2* in *S. canicula* can be delimiting the prospective anterior lobe of the cerebellar body and possibly determining the location of the *fissura prima*, which begins to form at paramedian levels.

The *ScOtx2* gene in *S. canicula* was also expressed in different domains along the rostro-caudal axis: one paramedian domain in the rostral half of the cerebellar body, one paramedian domain between the third point of flexure and the posterolateral fissure, and a domain extending through the upper auricle leaf. Except for the most rostral

domain, this pattern of expression is highly reminiscent of that described in mammals, where *Otx2* has been reported to be involved in the anterior-posterior cerebellar patterning (Frantz et al., 1994; Herrup and Kuemerle, 1997; Cheng et al., 2010).

By analysing the expression of *ScEn2*, we also sought to know if it could be involved in the median-lateral compartmentalization of the cerebellum, as has been reported for mammals (for a review, see Herrup and Kuemerle, 1997; Sillitoe et al., 2008). Indeed, in mammals *En2* is widely expressed in many cell types along a wide domain early in development, and later mainly in granule cells distributed into seven parasagittal bands, with the highest level of expression medially (Davis and Joyner, 1988; Davis et al., 1988; Wilson et al., 2011). In *S. canicula*, *ScEn2* it is widely expressed in the cerebellar body at stage 32, and becomes restricted to a single paramedian band (the granular layer), at stage 34. The *ScEn2* positive domain in the lesser spotted dogfish could then correspond to the median *En2* positive area of the cerebellar vermis on mammals. However, contrary to that found in mammals, in *S. canicula* we found no evidence of a longitudinal pattern consisting of parasagittal bands, which is an indication that the median-lateral compartmentalization of the cerebellum of cartilaginous fishes is simpler to that of mammals. Absence of a longitudinal banding pattern for *En2* expression was also observed in the cerebellum of bony fish (Vecino and Ekström, 1991).

The analysis of the expression of Aldo-C (zebrin) in *S. canicula* allowed us to further investigate the presence of a median-lateral compartmentation of the cerebellum, since in birds (Pakan et al., 2007; Marzban et al., 2010) and mammals (Lerlerc et al., 1990; Namba et al., 2011), this marker was reported to be expressed in a zebra-like pattern of parasagittal bands. In *S. canicula*, Aldo-C was observed in a single band consisting of Purkinje cells. Therefore, one *En2* positive band was found paramedially

in the granular layer, while an Aldo-C positive band was found laterally in the Purkinje layer at each side of the cerebellum. This supports the simple median-lateral compartmentalization as inferred by means of *ScEn2*. A single zebrin-ir band was also described in other fishes, including the stingray (Puzdrowski, 1997) and the zebrafish (Meek et al., 1992), which implies that a subdivision in multiple parasagittal bands did not occur in the ancestral cerebellum, as has been previously suggested (Puzdrowski, 1997).

CONCLUSIONS

The classification of cerebellar development in *S. canicula* into three developmental periods allows a more systematic study in this species, which is useful not only from the anatomical point of view, but also as a framework for future immunohistochemical and genoarchitectonic studies about the development of the cerebellum. Significant interspecific differences in cerebellar developmental processes were not observed between *S. canicula* (present results) and *Squalus* (Larsell, 1967), which allowed us identifying possible equivalent embryonic stages between galeomorphs and squalomorphs. The acquisition of the mature shape of the cerebellar body and auricles at stage 32 in *S. canicula* would justify considering this stage as the beginning of the maturity in relation to the morphology of the cerebellum, though the cerebellum continues growing throughout life. However, this does not apply to other jawed vertebrates, because the completion of the mature shape of the cerebellum is acquired later in bony fishes than in dogfish.

The use of fissures as anatomic landmarks during cerebellar development was supported by molecular evidence and comparative studies. Moreover, the order of appearance of the main cerebellar fissures should be considered as an important

developmental feature of the cerebellum in gnathostomes, as it appeared roughly maintained through evolution. On the other hand, the process of cerebellar morphogenesis in the lesser spotted dogfish highly differs from that of bony fishes and some reptiles since early on development, while it appears to be closer to that of mammals. This points to the cerebellum of elasmobranchs as an adequate model to study the possible ancestral condition of jawed vertebrates. The results obtained here by combining anatomical observations with molecular assays led us to propose that both the upper and lower auricle leaves originate from r1. The expression pattern of the genes *ScEn2* and *ScOtx2* also support the anatomical landmarks and provided a subdivision of the cerebellum into transverse domains, which appeared well conserved throughout evolution. On the other hand, the absence of a multiple banding pattern in the median-lateral axis could be indicative of a simple compartmentalization in basal gnathostomes consisting of a single paramedian and two lateral bands.

LITERATURE CITED

Adachi N, Takechi M, Hirai T, Kuratani S. 2012. Development of the head and trunk mesoderm in the dogfish, *Scyliorhinus torazame: II*. Comparison of gene expression between the head mesoderm and somites with reference to the origin of the vertebrate head. Evol Dev 14:257-276.

Alexander T, Nolte C, Krumlauf R .2009. *Hox* genes and segmentation of the hindbrain and axial skeleton. Annu Rev Cell Dev Biol 25:431-456.

Altman J, Bayer SA .1985. Embryonic development of the rat cerebellum. I. Delineation of the cerebellar primordium and early cell movements. J Comp Neurol 231:1-26.

Álvarez-Otero R. 1990. Estudio citarquitectónico y ultraestructural del cerebelo de la pintarroja, *Scyliohinus canicula, L*. Doctoral Thesis, University of Santiago de Compostela.

Álvarez R, Anadón R. 1987. The cerebellum of the dogfish, *Scyliorhinus canicula*: a quantitative study. J Hirnforsch 28:133-137.

Álvarez-Otero R, Anadón R. 1992. GOLGI cells of the cerebellum of the dogfish, *Scyliorhinus canicula* (elasmobranchs): a GOLGI and ultrastructural study. J Hirnforsch 33:321-327.

Álvarez-Otero R, Regueira SD, Anadón R. 1993. New structural aspects of the synaptic contacts on Purkinje cells in an elasmobranch cerebellum. J Anat 182:13-21.

Álvarez-Otero R, Pérez SE, Rodríguez MA, Adrio F, Anadón R. 1995. GABAergic neuronal circuits in the cerebellum of the dogfish *Scyliorhinus canicula* (Elasmobranchs): an immunocytochemical study. Neurosci Lett 187:87-90.

Anadón R, Molist P, Rodríguez-Moldes I, López JM, Quintela I, Cerviño MC, Barja P, González A. 2000. Distribution of choline acetyltransferase immunoreactivity in the brain of an elasmobranch, the lesser spotted dogfish (*Scyliorhinus canicula*). J Comp Neurol 420:139-170.

Anadón R, Ferreiro-Galve S, Sueiro C, Graña P, Carrera I, Yáñez J, Rodríguez-Moldes I. 2009. Calretinin-immunoreactive systems in the cerebellum and cerebellum-related lateral-line medullary nuclei of an elasmobranch, *Scyliorhinus canicula*. J Chem Neuroanat 37:46-54.

Ariëns Kappers C, Huber G, Crosby E. 1936. The comparative anatomy of the nervous system of vertebrates including man. Vol. 2, Hafner Publishing Company.

Ballard WW, Mellinger J, Lechenault H. 1993. A series of normal stages for development of *Scyliorhinus canicula*, the lesser spotted dogfish (*Chondrichthyes: Scyliorhinidae*). J. Exp. Zool. 267:318-336 .

Bell CC. 2002. Evolution of cerebellum-like structures. Brain Behav Evol 59:312-326.

Butler A, Hodos W. 2005. Comparative vertebrate neuroanatomy, evolution and adaption. Wiley-Interscience 180-197.

Candal E, Anadón R, Bourrat F, Rodríguez-Moldes I. 2005. Cell proliferation in the developing and adult hindbrain and midbrain of trout and medaka (teleosts): a segmental approach. Brain Res 160:157-175.

Carrera I, Anadón R, Rodríguez-Moldes I. 2012. Development of tyrosine hydroxylase-immunoreactive cell populations and fiber pathways in the brain of the dogfish *Scyliorhinus canicula*: New perspectives on the evolution of the vertebrate catecholaminergic system. J Comp Neurol 520:3574-3603.

Cerri S, Piccolini VM, Bernocchi G. 2010. Postnatal development of the central nervous system: anomalies in the formation of cerebellum fissures. Anat Rec (Hoboken) 293:492-501.

Chaplin N, Tendeng C, Wingate RJ. 2010. Absence of an external germinal layer in zebrafish and shark reveals a distinct, anamniote ground plan of cerebellum development. J Neurosci 30:3048-3057.

Cheng Y, Sudarov A, Szulc KU, Sgaier SK, Stephen D, Turnbull DH, Joyner AL. 2010. The *Engrailed* homeobox genes determine the different foliation patterns in the vermis and hemispheres of the mammalian cerebellum. Development 137:519-529.

Coolen, M., Sauka-Spengler, T., Nicolle, D., Le-Mentec, C., Lallemand, Y., Da Silva, C., Plouhinec J.-L., Robert, B., Wincker, P., Shi, D.-L., and Mazan, S. 2007. Evolution of axis specification mechanisms in jawed vertebrates: insights from a chondrichthyan. *PLoS ONE* 2, e374. doi: 10.1371/journal. pone.0000374.

Coolen M, Menuet A, Chassoux D, Compagnucci C, Henry S, Lévèque L, Da Silva C, Gavory F, Samain S, Wincker P, Thermes C, D'Aubenton-Carafa Y, Rodriguez-Moldes I, Naylor G, Depew M, Sourdaine P, Mazan S. 2009. The dogfish *Scyliorhinus canicula*, a reference in jawed vertebrates. In: Behringer RR, Johnson AD, Krumlauf RE, editors. Emerging model organisms. A laboratory manual. Vol. 1. Cold Spring Harbor, NY: Cold Spring Harbor Laboratory Press. p. 431-446.

Davis CA, Joyner A. 1988. Expression patterns of the homeo box-containing genes *En-1* and *En-2* and the proto-oncogene *int-1* diverge during mouse development. Genes Dev 2:1736-1744.

Davis CA, Noble-Topham SE, Rossant J, Joyner AL. 1988. Expression of the homeo box-containing gene *En-2* delineates a specific region of the developing mouse brain. Genes Dev 2:361-371.

Devor A. 2000. Is the cerebellum like cerebellar-like structures? Brain Res Rev 34:149-156.

Eddison M, Toole L, Bell E, Wingate RJ. 2004. Segmental identity and cerebellar granule cell induction in rhombomere 1. BMC Biol 2:14.

Ferreiro-Galve S. 2010. Brain and retina regionalization in sharks: study based on the spatiotemporal expression pattern of Pax6 and other neurochemical markers. Doctoral Thesis, University of Santiago de Compostela, Spain.

Ferreiro-Galve S, Rodríguez-Moldes I, Anadón R, Candal E. 2010. Patterns of cell proliferation and rod photoreceptor differentiation in shark retinas. J Chem Neuroanat 39:1-14.

Frantz GD, Weimann JM, Levin ME, McConnell SK. 1994. *Otx1* and *Otx2* define layers and regions in developing cerebral cortex and cerebellum. J Neurosci 14:5725-5740.

Germot A, Lecointre G, Plouhinec JL, Le Mentec C, Girardot F, Mazan S. 2001. Structural evolution of *Otx* genes in craniates. Mol Biol Evol 18:1668-1678.

Gómez A, Durán E, Ocaña FM, Jiménez-Moya F, Broglio C, Domezain A, Salas C, Rodríguez F. 2004. Observation on the brain development of the sturgeon Acipenser naccarii. In: Carmona R, Domezain A, García-Gallego M, Hernando JA, Rodríguez F, Ruiz-Rejón M, editors. Biology, conservation and sustainable development of sturgeons. Springer. p. 155-174.

Herrup K, Kuemerle B. 1997. The compartmentalization of the cerebellum. Annu Rev Neurosci 20:61-90.

Hibi M, Shimizu T. 2011. Development of the cerebellum and cerebellar neural circuits. Dev Neurobiol 72:282-301.

Hidalgo-Sánchez M, Millet S, Bloch-Gallego E, Alvarado-Mallart RM. 2005. Specification of the meso-isthmo-cerebellar region: The *Otx2/Gbx2* boundary. Brain Res Rev 49:134-149.

Houser G. 1901. The neurons and supporting elements of the brain of a selachian. J Comp Neurol 11:65-175.

Kaslin J, Ganz J, Geffarth M, Grandel H, Hans S, Brand M. 2009. Stem cells in the adult zebrafish cerebellum: initiation and maintenance of a novel stem cell niche. J Neurosci 29:6142-6153.

Kuhlenbeck H. 1975. The central nervous system of vertebrates: spinal cord and deuterencephalon. S Karger.

Kuratani S, Kuraku S, Murakami Y. 2002. Lamprey as an evo-devo model: lessons from comparative embryology and molecular phylogenetics. Genesis 34:175-83.

Lannoo MJ, Hawkes R. 1997. A search for primitive Purkinje cells: zebrin II expression in sea lampreys (*Petromyzon marinus*). Neurosci Lett 237:53-55.

Larsell O. 1925. The development of the cerebellum in the frog (*Hyla regilla*) in relation to the vestibular and lateral-line systems. J Comp Neurol 39:249-289.

Larsell O. 1934. Morphogenesis and evolution of the cerebellum. Arch Neurol 31:373-395.

Larsell O. 1947. The cerebellum of myxinoids and petromyzonts including developmental stages in the lampreys. J Comp Neurol 86:395-445.

Larsell O. 1967. The comparative anatomy and histology of the cerebellum from myxinoids through birds. University of Minnesota Press, Minneapolis.

Lerlerc N, Doré L, Parent A, Hawkes R. 1990. The compartmentalization of the monkey and rat cerebellar cortex: zebrin I and cytochrome oxidase. Brain Res 506:70-78.

Lisney TJ, Yopak KE, Montgomery JC, Collin SP. 2008. Variation in brain organization and cerebellar foliation in chondrichthyans: batoids. Brain Behav Evol 72:262-282.

Ma S, Kwon HJ, Huang Z. 2012. Ric-8a, a guanine nucleotide exchange factor for heterotrimeric G proteins, regulates Bergmann glia-basement membrane adhesion during cerebellar foliation. J Neurosci 32:14979-14993.

Margotta V. 2007. PCNA immunoreactivity revealing normal proliferative activity in the brain of an adult Elasmobranch, *Torpedo marmorata*. Ital. J Anat Embryol 112:145-155.

Marín F, Puelles L. 1995. Morphological fate of rhombomeres in quail/chick chimeras: a segmental analysis of hindbrain nuclei. Eur J Neurosci 7:14-38.

Marzban H, Chung SH, Pezhouh MK, Feirabend H, Watanabe M, Voogd J, Hawkes R. 2010. Antigenic compartmentation of the cerebellar cortex in the chicken (*Gallus domesticus*). J Comp Neurol 518:2221-2239.

Mazan S, Jaillard D, Baratte B, Janvier P. 2000. *Otx1* gene-controlled morphogenesis of the horizontal semicircular canal and the origin of the gnathostome characteristics. Evol Dev 2:186-193.

Meek J, Hafmans TG, Maler L, Hawkes R. 1992. Distribution of zebrin II in the gigantocerebellum of the mormyrid fish *Gnathonemus petersii* compared with other teleosts. J Comp Neurol 316:17-31.

Millen KJ, Wurst W, Herrup K, Joyner A. 1994. Abnormal embryonic cerebellar development and patterning of postnatal foliation in two mouse *Engrailed-2* mutants. Development 120:695-706.

Montgomery JC, Bodznick D, Yopak KE. 2012. The cerebellum and cerebellum-like structures of cartilaginous fishes. Brain Behav Evol 80:152-165.

Murakami Y, Watanabe A. 2009. Development of the central and peripheral nervous systems in the lamprey. Dev Growth Differ 51:197-205.

Namba K, Sugihara I, Hashimoto M. 2011. Close correlation between the birth date of Pukrinje cells and the longitudinal compartmentalization of the mouse adult cerebellum. J Comp Neurol 519: 2594-2614.

Nicholson C, Llinás R, Precht W. 1969. Neural elements of the cerebellum in elasmobranch fishes: structural and functional characteristics. Chicago: Am Med Assoc. p. 215-243.

Nieuwenhuys R. 1967. Comparative anatomy of the cerebellum. Prog Brain Res 25:1-93.

Nieuwenhuys R, Ten Donkelaar HJ, Nicholson C. 1998. Chondrostean fishes. In: The Central Nervous System of Vertebrates. Springer: 701-757.

Northuctt RG. 1977. Elasmobranch central nervous system organization and its possible evolutionary significance. Am Zool 17:411-429.

Orvis GD, Barraza LH, Wilson SL, Szulc KU, Turnbull DH, Joyner AL. 2012. The *engrailed* homeobox genes are required in multiple cell lineages to coordinate sequential formation of fissures and growth of the cerebellum. Dev Biol 367:25-39.

Oulion S, Debiais-Thibaud M, d'Aubenton-Carafa Y, Thermes C. Da Silva C, Bernard-Samain S, Gavory F, Wincker P, Mazan S, Casane D. 2010. Evolution of *Hox* gene clusters in gnathostomes: insights from a survey of a shark (*Scyliorhinus canicula*) transcriptome. Mol Biol Evol 27:2829–2838.

Pakan JMP, Iwaniuk AN, Wylie DRW, Hawkes R, Marzban H. 2007. Purkinje cell compartmentation as revealed by zebrin II expression in the cerebellar cortex of pigeons (*Columba livia*). J Comp Neurol 501:619-630.

Palmgren A. 1921. Embryological and morphological studies on the midbrain and cerebellum of vertebrates. Acta Zool 2:1-94.

Paul DH, Roberts BL. 1975. Responses of neurones in the cerebellar corpus of the dogfish (*Scyliorhinus canicula*). J Physiol 244:47-49.

Peña-Melián A, Puerta Fonolla J, Gil Loyzaga P. 1986. The ontogeny of the cerebellar fissures in the chick embryo. Anat Embryol (Berl) 175:119-128.

Plouhinec JL, Leconte L, Sauka-Spengler TS, Bovolenta P, Mazan S, Saule S. 2005. Comparative analysis of gnathostome *Otx* gene expression patterns in the developing eye: implications for the functional evolution of the multigene family. Dev Biol 278:560-575.

Pouwels E. 1978. On the development of the cerebellum of the trout, *Salmo gairdneri. I.* Patterns of cell migration. Anat Embryol (Berl) 152:291-308.

Prayer D, Kasprian G, Krampl E, Ulm B, Witzani L, Prayer L, Brugger PC. 2006. MRI of normal fetal brain development. Eur J Radiol 57:199-216.

Puelles L, Ferrán JL. 2012. Concept of neural genoarchitecture and its genomic fundament. Front Neuroanat 6:47.

Puzdrowski RL. 1997. Anti-Zebrin II immunopositivity in the cerebellum and octavolateral nuclei in two species of stingrays. Brain Behav Evol 50:358-368.

Quintana-Urzainqui I, Rodríguez-Moldes I, Candal E. 2012. Developmental, tract-tracing and immunohistochemical study of the peripheral olfactory system in a basal vertebrate: insights on Pax6 neurons migrating along the olfactory nerve. Brain Struct Funct DOI 10.1007/s00429-012-0486-2.

Rodríguez-Moldes I, Ferreiro-Galve S, Carrera I, Sueiro C, Candal E, Manzan S, Anadón R. 2008. Development of the cerebellar body in sharks: spatiotemporal relations of Pax6-expression, cell proliferation and differentiation. Neurosci Lett 432:105-110.

Rodríguez-Moldes I, Carrera I, Pose-Méndez S, Quintana-Urzainqui I, Candal E, Anadón R, Mazan S, Ferreiro-Galve S. 2011. Regionalization of the shark hindbrain: a survey of an ancestral organization. Front Neuroanat 5:1-14.

Rüdeberg S. 1961. Morphogenetic studies on the cerebellar nuclei and their homologization in different vertebrates including man. Doctoral Thesis Univ of Lund.

Sarnat H, Netsky M. 1981. Evolution of the Nervous System. Oxford University Press. p. 213-242.

Schaper A. 1898. The finer structure of the selachian cerebellum (*Mustelus vulgaris*) as shown by chrome-silver preparations. J Comp Neurol 8:1-20.

Schmidt AW, Bodznick D. 1987. Afferent and efferent connections of the vestibulolateral cerebellum of the little skate, *Raja erinacea*. Brain Behav Evol 30:282-302.

Schnitzlein HN, Faucette JR. 1969. General morphology of the fish cerebellum. En: Neurobiology of cerebellar evolution and development. Llinás R, editor. Chicago: Am Med Assoc. p. 77-106.

Sillitoe RV, Stephen D, Lao Z, Joyner A. 2008. *Engrailed* homeobox genes determine the organization of Purkinje cell sagittal stripe gene expression in the adult cerebellum. J Neurosci 28:12150-12162.

Smeets WJ, Nieuwenhuys R. 1976. Topological analysis of the brain stem of the sharks *Squalus acanthias* and *Scyliorhinus canicula*. J Comp Neurol 165:333-368.

Smeets WJAJ, Nieuwenhuys R, Roberts BL. 1983. The central nervous system of cartilaginous fishes. Structure and functional correlations. Berlin: Springer-Verlag.

Sterzi G. 1912. Il sistema nervoso centrale dei vertebrate. Pesci, vol II. Draghi, Padova.

Sudarov A, Joyner AL. 2007. Cerebellum morphogenesis: the foliation pattern is orchestrated by multi-cellular anchoring centers. Neural Dev 2:26.

ten Donkelaar HJ, Lammens M, Wesseling P, Thijssen HO, Renier WO. 2003. Development and developmental disorders of the human cerebellum. J Neurol 250:1025-1036.

Triulzi F, Parazzini C, Righini A. 2005. MRI of fetal and neonatal cerebellar development. Semin Fetal Neonatal Med 10:411-420.

Tümpel S, Cambronero F, Sims C, Krumlauf R, Wiedemann LM. 2008. A regulatory module embedded in the coding region of *Hoxa2* controls expression in rhombomere 2. Proc Natl Acad Sci USA 105:20077-20082.

Utsunomiya H, Takano K, Ogasawara T, Hashimoto T, Fukushima T, Okazaki M. 1998. Rhombencephalosynapsis: cerebellar embryogenesis. AJNR Am J Neuroradiol 19:547-9.

Van Essen. 1997. A tension-based theory of morphogenesis and compact wiring in the central nervous system. Nature 385:313-318.

Vázquez M, Rodríguez A, Domezain A, Salas C. 2002. Development of the brain of the sturgeon *Acipenser naccarii*. J Appl Ichtyol 18:275-279.

Vecino E, Ekström P. 1991. Expression of the homeobox *engrailed* gene during the embryonic development of the nervous system of the trout (*Salmo fario L.*). Neurosci Lett 129:311-314.

Volkmann K, Rieger S, Babaryka A, Köster RW. 2008. The zebrafish cerebellar rhombic lip is spatially patterned in producing granule cell populations of different functional compartments. Dev Biol 313:167-180.

Voogd J, Glickstein M. 1998. The anatomy of the cerebellum. Trends Neurosci 21:370-5.

Wilson SL, Kalinovsky A, Orvis GD, Joyner A. 2011. Spatially restricted and developmentally dynamic expression of *engrailed* genes in multiple cerebellar cell types. Cerebellum 10:356-372.

Wingate RJ, Hatten ME. 1999. The role of the rhombic lip in avian cerebellum development. Development 126:4395-4404.

Yopak KE, Montgomery JC. 2008. Brain organization and specialization in deep-sea chondrichthyans. Brain Behav Evol 71:287-304.

Yopak KE, Lisney TJ, Collin SP, Montgomery JC. 2007. Variation in brain organization and cerebellar foliation in chondrichthyans: sharks and holocephalans. Brain Behav Evol 69:280-300.

Zupanc GK, Hinsch K, Gage FH. 2005. Proliferation, migration, neuronal differentiation, and long-term survival of new cells in the adult zebrafish brain. J Comp Neurol 488:290-319.

Abbreviations

AMV	anterior medullary velum
Aur	auricles
c	caudal
Cb	cerebellum
CbCr	cerebellar crest
Cbdp	dorsal part of the cerebellar body
Cbp	cerebellar plate or cerebellar primordium
Cbvp	ventral part of the cerebellar body
ChP	choroid plexus
CP	cerebellar peduncle
CPp	cerebellar peduncle primordium
DON	dorsal octaval nucleus
e	sulcus e
ERa	ependymary raphe
FL	fibrous layer
fmi	inferior median fissure
GE	granular eminence
GL	cerebellar granular layer
IIIn	oculomotor nerve
IS	isthmus
Isfo	isthmic fovea
IVv	fourth ventricle
IXn	glossopharyngeal nerve
LAL	lower auricle leaf
lf	longitudinal fissure
LPost	lobulus posticus
LR	lateral recess
LRL	lower rhombic lip
MedE	median eminence
Mes	mesencephalon
MOL	cerebellar molecular layer
MON	medial octaval nucleus
mrf	meso-rhombencephalic fissure
nlla	anterior lateral line nerve
OLA	octavolateral area
OT	optic tectum
PL	Purkinje layer
plf	posterolateral fissure
prf	primary transverse fissure
Pros	prosencephalon
r	rostral
r1-8	rhombomeres 1-8
Rh	rombencephalon
sid	intermediate dorsal sulcus
siv	intermediate ventral sulcus
slH	His sulcus
smi	median inferior sulcus
sms	median superior sulcus
UAL	upper auricle leaf
UALp	upper auricle leaf primordium
URL	upper rhombic lip
VIIIm	magnocellular octaval nucleus
VIIIn	octaval nerve
VIIn	facial nerve
VIS	viscerosensorial area
Vn	trigeminal nerve
X	sulcus X
X’	sulcus X’

Table 1. Primary and secondary antibodies used in this study.

Primary antibody	Source	Working dilution	**Secondary antibody**	Source	Working dilution
DCX	Polyclonal goat anti-DCX Santa Cruz Biotechnology, Santa Cruz, CA	1:100	488-conjugated donkey anti-goat	Alexa Fluor Molecular Probes	1:100
GFAP	Polyclonal rabbit anti-GFAP Dako, Glostrup, Denmark	1:500	546-conjugated donkey anti-rabbit	Alexa Fluor Molecular Probes	1:200
Aldo-C	Polyclonal goat anti-Aldo-C Santa Cruz Biotechnology, Santa Cruz, CA	1:100	488-conjugated donkey anti-goat	Alexa Fluor Molecular Probes	1:100
PCNA	Monoclonal mouse anti-PCNA Sigma, St Louis, MO	1: 1000	goat anti-mouse	Dako, Glostrup, Denmark	1:100

Table 2. Correlation among developmental stages of *Scyliorhinus canicula* accordingly with their external features as proposed by Ballard et al. (1993), age (from "day 1", when they were laid naturally), body size, extent of cerebellar morphogenesis and developmental periods. Counterpart developmental stages of *Scyliorhinus canicula* and *Squalus acanthias* were proposed based on the changes of the gross anatomy of the cerebellum (Larsell, 1967; present results).

Table 2

	Scyliorhinus canicula						***Squalus acanthias*** (Larsell, 1967)
	Stage	**External features** (Ballard et al., 1993)	**Age (days)**	**Body size (mm)**	**External cerebellar morphology during development** (present results)	**Main morphogenetic processes of Cb** (present results)	**Body size (mm)**
FIRST PERIOD	24	Pharyngeal sets C1-C4 are open	30-31,5	10-12	Meso-rhombencephalic fissure becomes noticeable Rhombic lips become noticeable	Joint of rhombic lips and growth of cerebellar plate.	7
	25	Set C5 are open	31-38	13-15	Onset of rhombic lips fusion rostrally		8
	27	Mouth is diamond-shaped Gill filaments buds	42-46	17-20	Cerebellar plate becomes evident		
	28	Mouth is traverse oval shaped	46-51	21-23	Cerebellar plate curvature starts to form rostrally		
	29	Mouth as an arched line Incomplete circle of eye pigment	49-53	23,5-30	Intermedio-caudal flexion of the cerebellar plate starts to form		22
SECOND PERIOD	30	Complete circle of eye pigment	52-60	31-33	Posterolateral fissure as a faint furrow	Formation of the cerebellar body and auricles	32
	31E	Rostrum as a detectable protrusion Yolk begins to be transferred to the internal sac	60-67	34-36	Primordium of cerebellar body rostrally and higher flexion of the caudal cerebellar plate Primordium of the upper auricle leaf		50
	31M		67-74	36-38	Evident incipient cerebellar body and upper auricle leaf Conspicuous cerebellar peduncle		60
	31L	Rostrum increases in size Maximum development of gill filaments	74-80	38-40	Cerebellar body as a closed structure Primordium of the lower auricle leaf		80
THIRD PERIOD	32E	Pigment completely covers eyes	75-92	40-48	Patent cerebellar body and auricles Transverse fissure becomes noticeable Conspicuous longitudinal fissure	Growth and maturation	120
	32M/L	Pigment of the body increases	92-125	49-67	Granular eminences become noticeable		
	PH	The external yolk is shrinking in size (33) The external yolk is button-like (34, hatching)	115-175	68-82	Growth and maturation of cerebellar body and auricles		
	Juv	Posthatching		82→	External folding of the cerebellar cortex		150-170
	Adult	Sexual maturation			Inner folding of the cerebellar cortex		

Figure 1. Immunoblot of SDS-polyacrylamide gel of *S. canicula* adult brain protein extracts stained by anti-aldolase-C (Aldo-C), which showed single band of about 40 kDa.

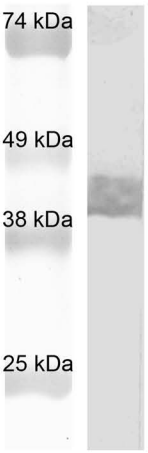

FIGURE 1

Figure 2. Schematic drawings of cerebellar development from dorsal view. For abbreviations, see list. Scale bar = 300 µm in A-C, F-H; 400 µm in I; 600 µm in D, E.

Figure 3. Schematic drawings of sagittal sections of the brain (without telencephalon) at paramedian and parasagittal levels of the cerebellum. The level of the sections in the Figure 5 (grey lines) is also indicated. Number 1 (in red) indicates a bending point or point of flexure in the cerebellum, and grey arrows indicate bending movements in the cerebellar primordium. The exit of some cranial nerves (V, VII and VIII) is also represented. For abbreviations, see list. Scale bar = 200 µm in A-D.

Figure 4. Representative images of the cerebellum in sagittal (A, D, F) and transverse (B) sections, and from dorsal view (C, E) of embryos at stages 24 (A), 25 (B), 28 (C, D) and 29 (E, F). Numbers 1-3 (in red) indicate bending points or points of flexure in the cerebellum. For abbreviations, see list. Scale bar = 300 µm in A, B, D, F; 600 µm in C, E.

Figure 5. Schematic drawings of transverse sections of the cerebellum and rhombencephalon at stage 29. The level of the sections is indicated in Fig. 3C. The exit of the V cranial nerve is also represented. For abbreviations, see list. Scale bar = 500 µm in A-E.

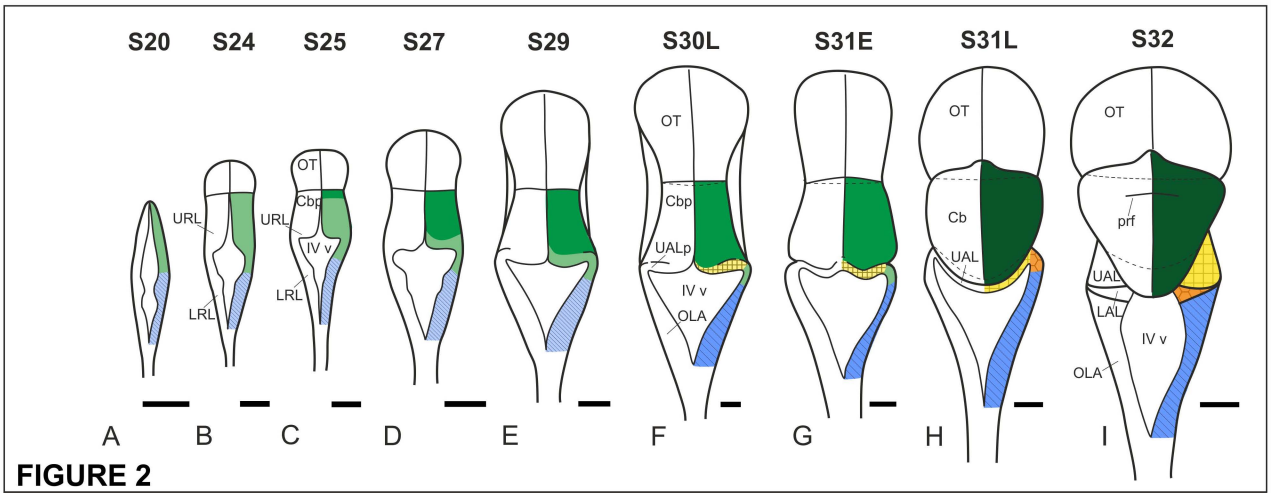

FIGURE 2

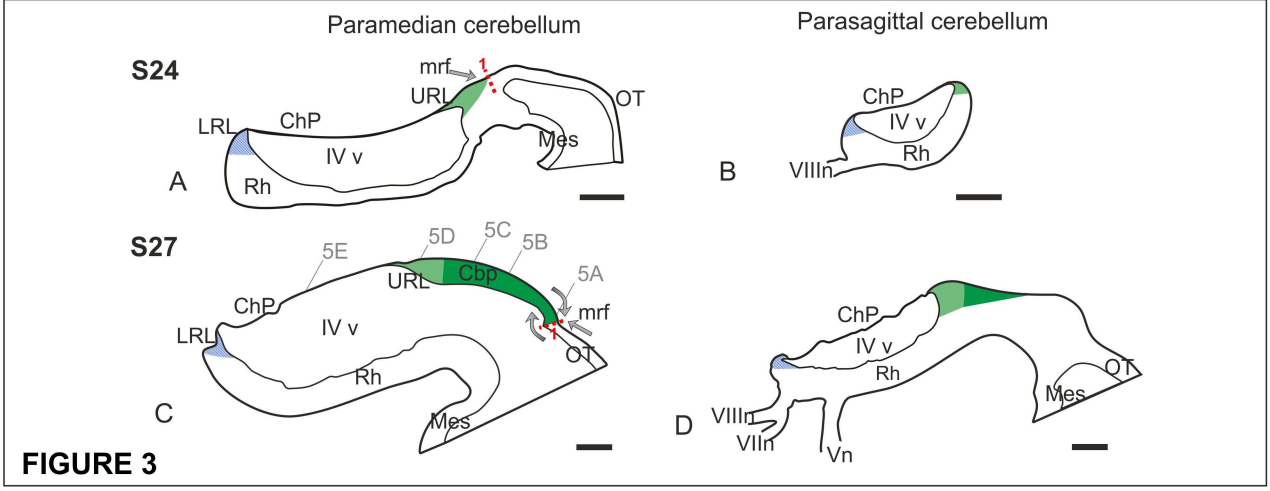

FIGURE 3

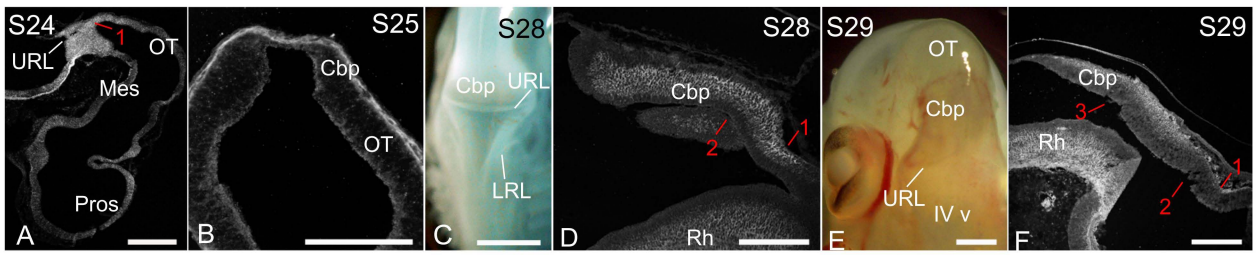

FIGURE 4

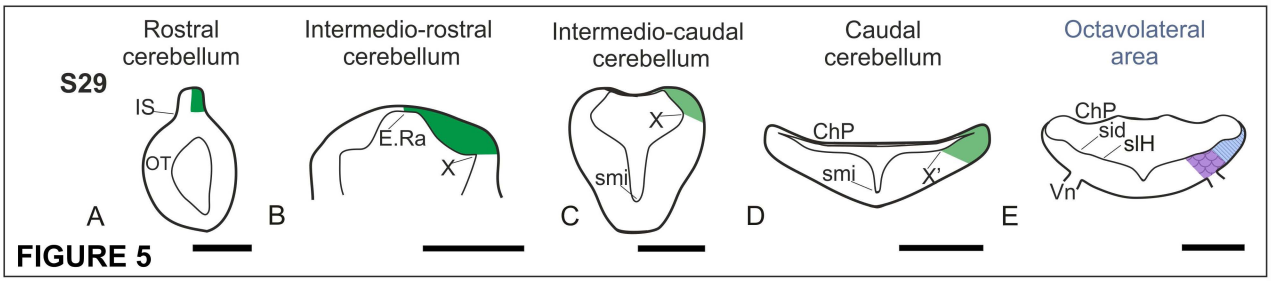

FIGURE 5

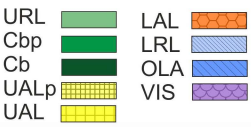

Figure 6. Schematic drawings of transverse sections of the cerebellum and rhombencephalon at stages 30 (A-E) and 31 (F-O). The level of the sections is indicated in Fig. 8A, C. The exit of the V cranial nerve is also represented. For abbreviations, see list. Scale bar = 500 µm in A-O.

Figure 7. Representative images of the cerebellum in transverse (A) and sagittal (B-D) sections of embryos at stages 30 (A) and 31 (B-D). Numbers 2-4 (in red) indicate bending points or points of flexure in the cerebellum. For abbreviations, see list. Scale bar = 200 µm in D; 300 µm in A-C.

Figure 8. Schematic drawings of sagittal sections of the brain (without telencephalon) at paramedian and parasagittal levels of the cerebellum at stage 31. Grey lines indicate the level of the sections in Fig. 6F-O. Numbers 1-4 (in red) indicate bending points or points of flexure in the cerebellum, and grey arrows indicated bending movements in the cerebellar primordium. The exit of some cranial nerves (III and VIII) is also represented. For abbreviations, see list. Scale bar = 500 µm in A-D.

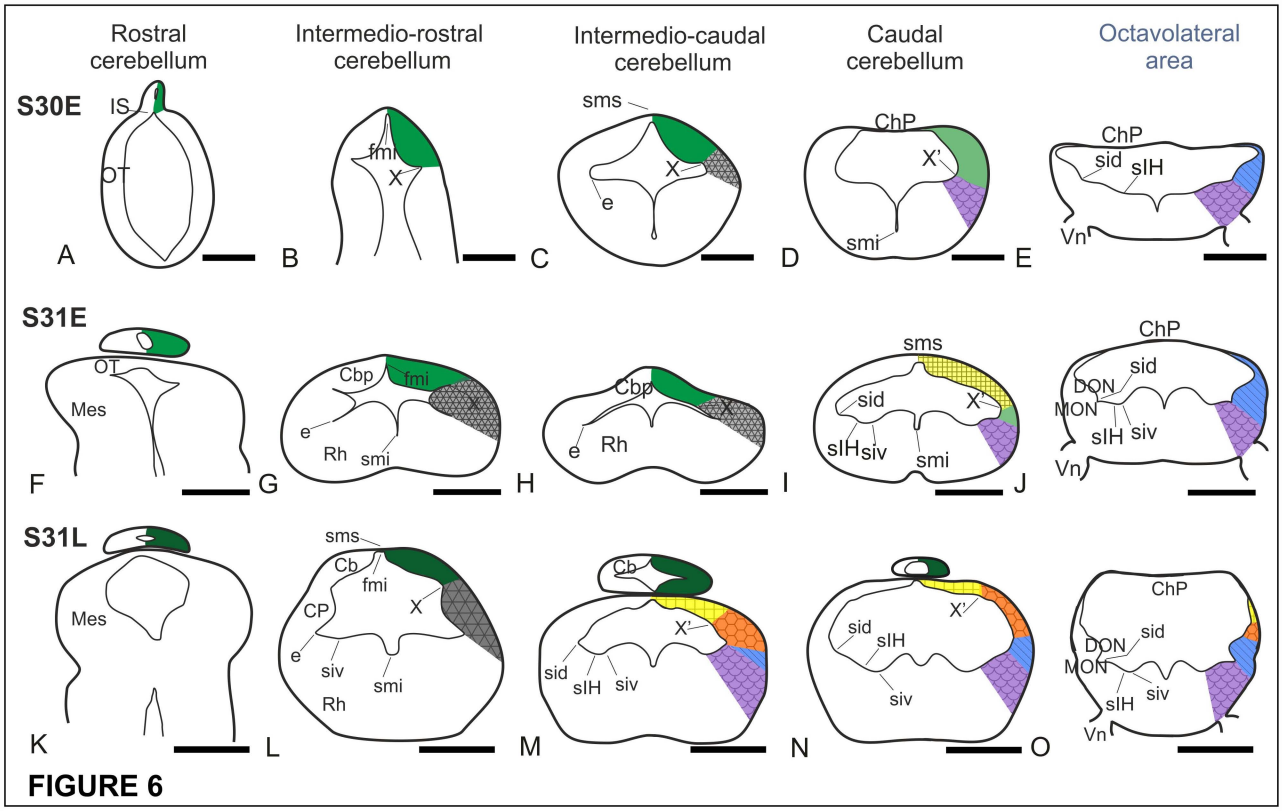

FIGURE 6

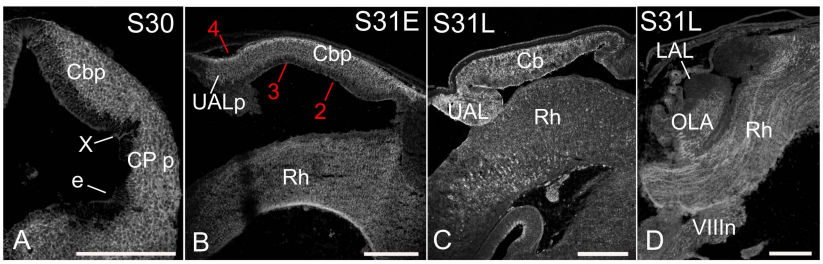

FIGURE 7

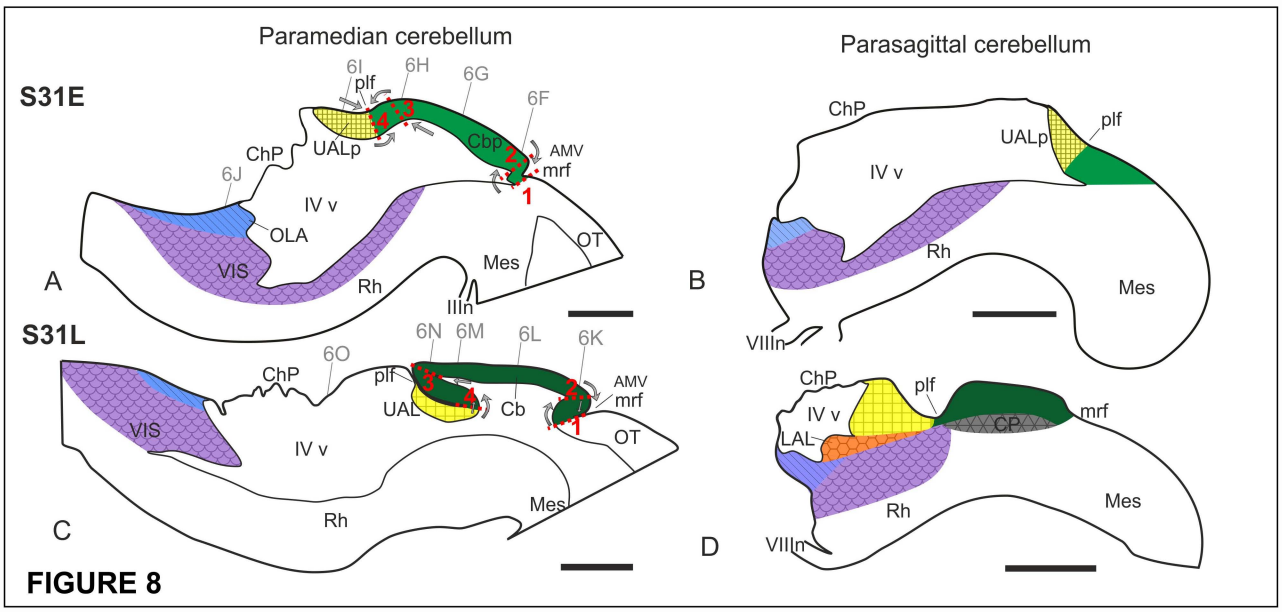

FIGURE 8

Figure 9. Schematic drawings of transverse sections of the cerebellum and rhombencephalon at stages 32 (A-J) and juveniles (K-O). The level of the sections is indicated in Fig. 10A, E. The exit of the IIa and VIII cranial nerve is also represented. For abbreviations, see list. Scale bar = 500 µm in A-O.

Figure 10. Schematic drawings of sagittal sections of the brain (without telencephalon) at paramedian and parasagittal levels of the cerebellum at stage 32 (A, B), prehatching embryos (C, D) and juveniles (E, F). The level of the sections in Fig. 9A-E, and 9K-O is also indicated. Numbers 1-4 (in red) indicate bending points or points of flexure in the cerebellum, and grey arrows indicate bending movements in the cerebellum. The exit of some cranial nerves (VIII, IX and X) is also represented. For abbreviations, see list. Scale bar = 200 µm in A, B; 500 µm in C-F.

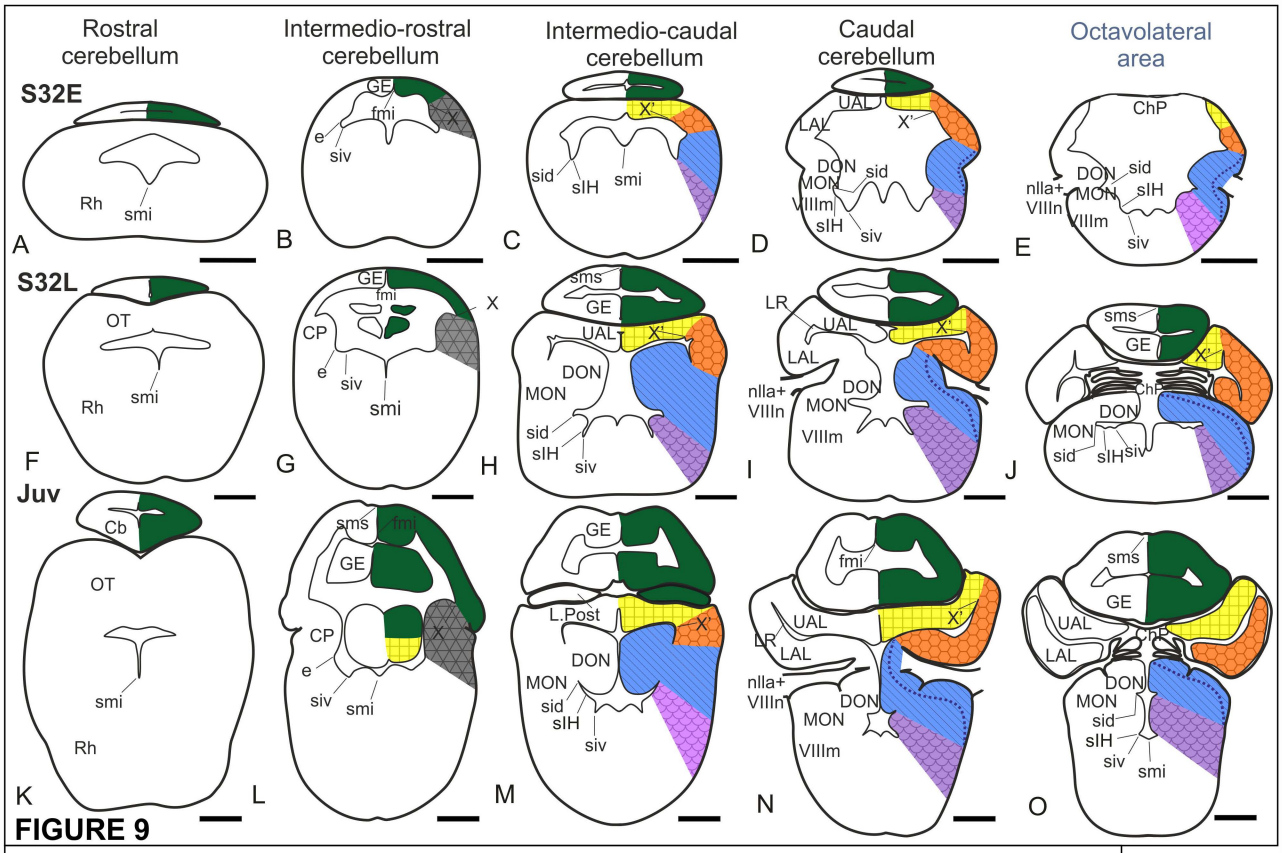

FIGURE 9

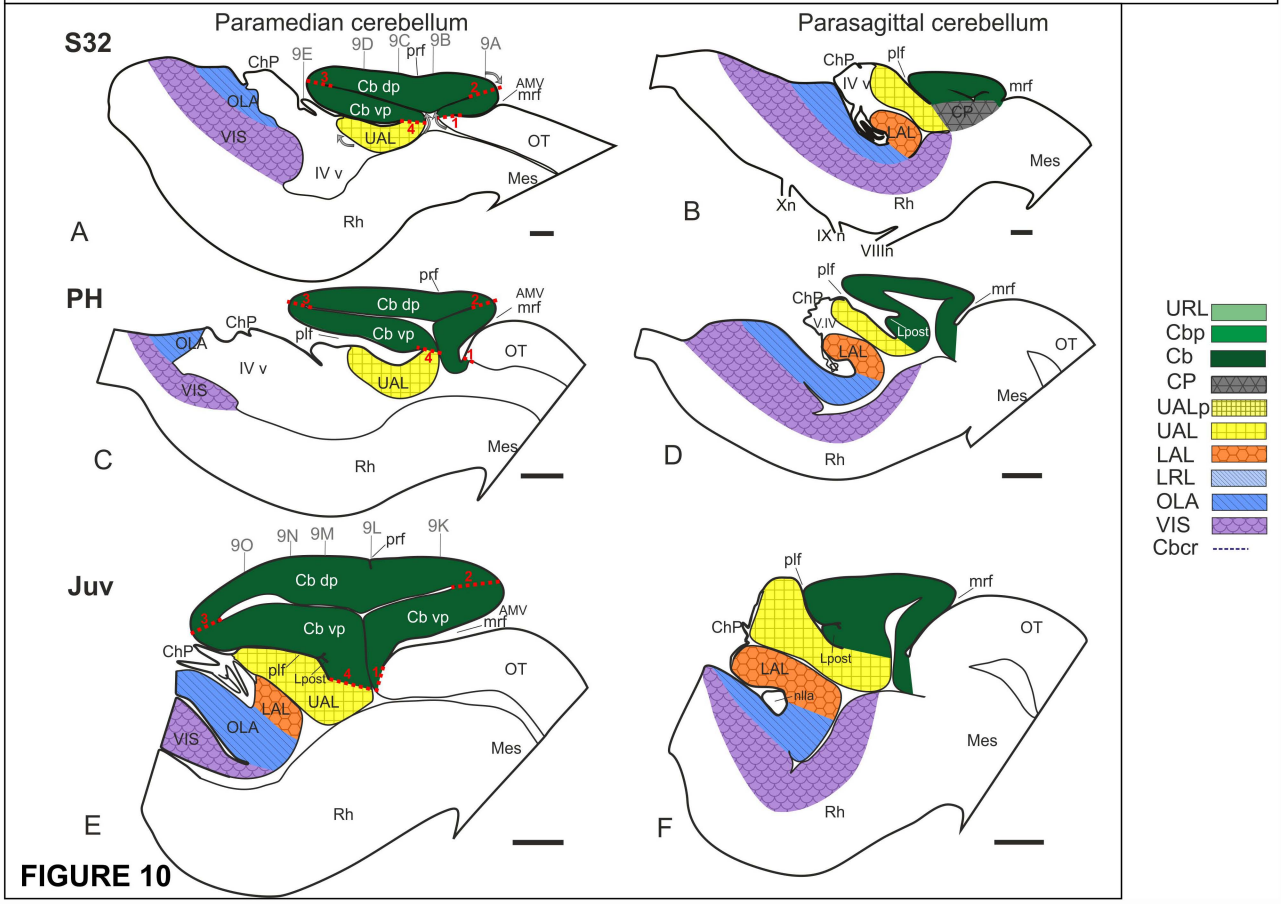

FIGURE 10

Figure 11. Representative images of the cerebellum *in toto* normal material (A, D, E, H-L, N, O), and in horizontal (B, C), transverse (F) and sagittal (G, M) sections, in prehatching embryos (A-F), juveniles (G-J, N) and adults (K-M, O). **A-E.** Images showing the mature ear-like shape of cerebellar auriles. **F.** The level of the section in F is indicated in the scheme. **G.** Section to show DCX- and GFAP-ir processes in a fan shaped bundle. The squared area corresponds to the detail in G'. **H-J.** The cerebellum of a juvenile was dissected as indicated in H to have access to the roof of the cerebellar body from dorsal (I) and ventral (J) views. **K, L.** The cerebellum of an adult was dissected as indicated in K to access the roof of the cerebellum from a ventral (L) view. The asterisks indicate that outer fissures observed in lateral view (K') correspond to inner folds shown in L. **M.** Sagittal section of the cerebellar cortex showing PCNA-ir cells in the inner fissures. A detail is shown in the inset. **N, O.** Ventral part of the cerebellar body of juveniles (N) and adults (O) observed after dissection as indicated in the figures H and K, respectively, to show the auricles. For abbreviations, see list. Scale bar = 150 µm in G; 300 µm in F, M; 500 µm in B, C; 1 mm in A, D, E, H; 2 mm in K, L, O.

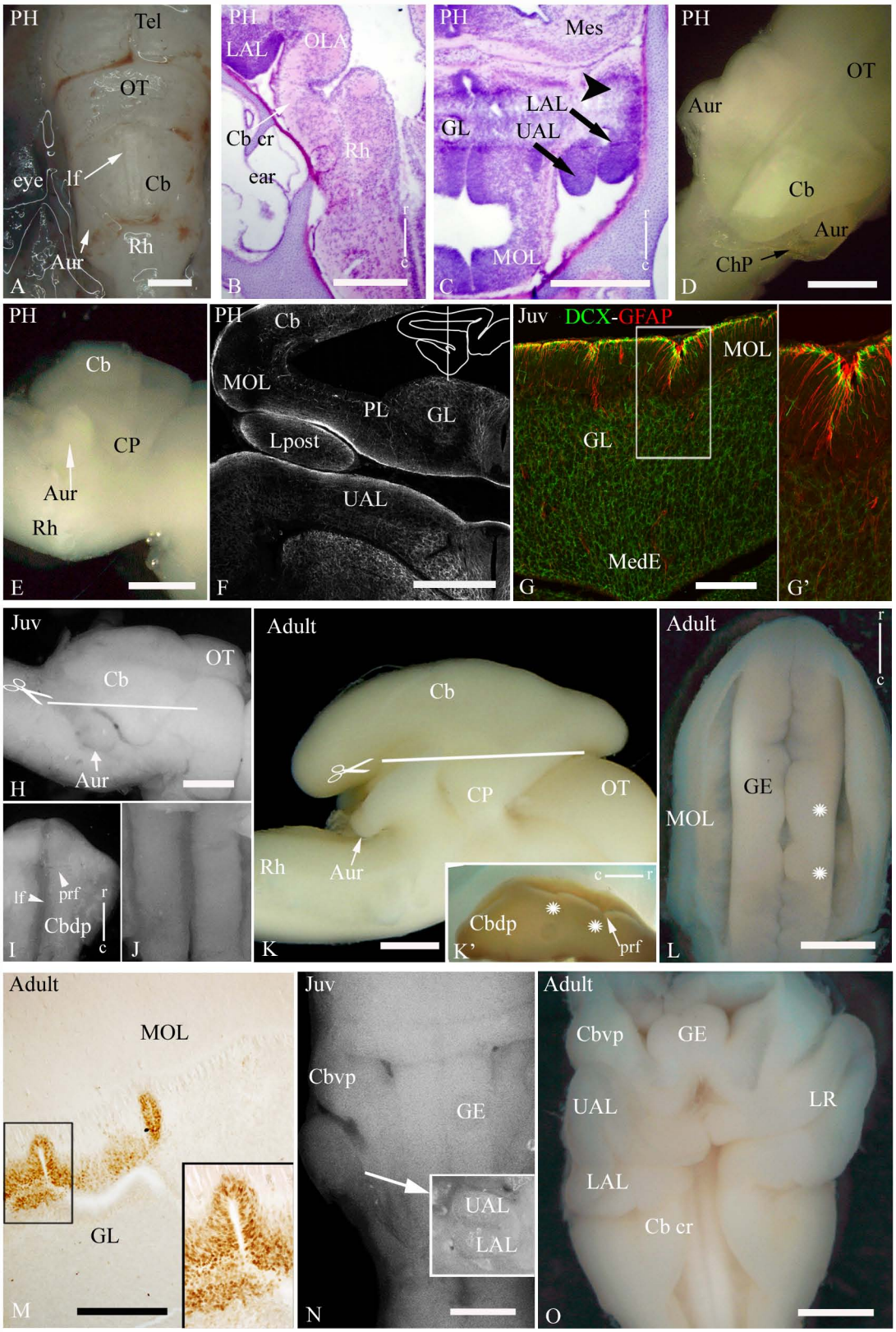
PH
Tel
OT
eye
lf
Cb
Aur
Rh
A
PH
LAL
OLA
Cb cr
ear
Rh
r
c
B
PH
Mes
LAL
UAL
GL
MOL
r
c
C
PH
OT
Aur
Cb
Aur
ChP
D
PH
Cb
CP
Aur
Rh
E
PH
Cb
MOL
PL
GL
Lpost
UAL
F
Juv
DCX-GFAP
MOL
GL
MedE
G
G'
Juv
OT
Cb
Aur
H
Adult
Cb
CP
OT
Rh
Aur
Cbdp
prf
K
K'
Adult
r
c
GE
MOL
L
lf
prf
r
Cbdp
c
I
J
Adult
MOL
GL
M
Juv
Cbvp
GE
UAL
LAL
N
Adult
Cbvp
GE
UAL
LR
LAL
Cb cr
O

FIGURE 11

Figure 12. Photomicrographs of sagittal (A-F) and transverse sections (G-K) of the brain of *S. canicula* after *in situ* hybridization (A-J) and immunohistochemistry (K) at the indicated stages. **A-C.** Panoramic view (A,B) and detail (C) of the rhombencephalon showing the *ScHoxa2* positive domain caudally to the cerebellum at early stage 31. Note the upper auricle leaf primordium *Hoxa2* negative. **D,E.** Panoramic view (D) and detail (E) of *ScEn2* expression pattern at early stage 31. Positivity was observed in the mesencephalic tegmentum, caudal optic tectum and rostral rhombencephalon. Note the moderate intensity in the rostral half of cerebellar plate and high intensity in the upper auricle leaf primordium. **F.** Expression pattern of *ScOtx2* at intermediate stage 31. Note the *Otx2* positive signal in the mesencephalon, rostral and caudal parts of the cerebellar body, and upper auricle leaf. **G.** Expression pattern of *ScEn2* at intermediate stage 32 showing positive domains in the upper auricle leaf and cerebellar body at median and lateral levels. **H.** Expression pattern of *ScHoxa2* at intermediate stage 32 in the rhombencephalic tegmentum and marginally in the cerebellar body. Note that both the upper and lower auricle leaves are negative for *ScHoxA2*. **I,J.** Expression of *ScEn2* at stage 34 paramedially in the upper auricle leaf and cerebellar body. **K.** Aldolase-C labeling was observed in most of Purkinje cells. Scale bar = 150 µm in K; 500 µm in A-J.

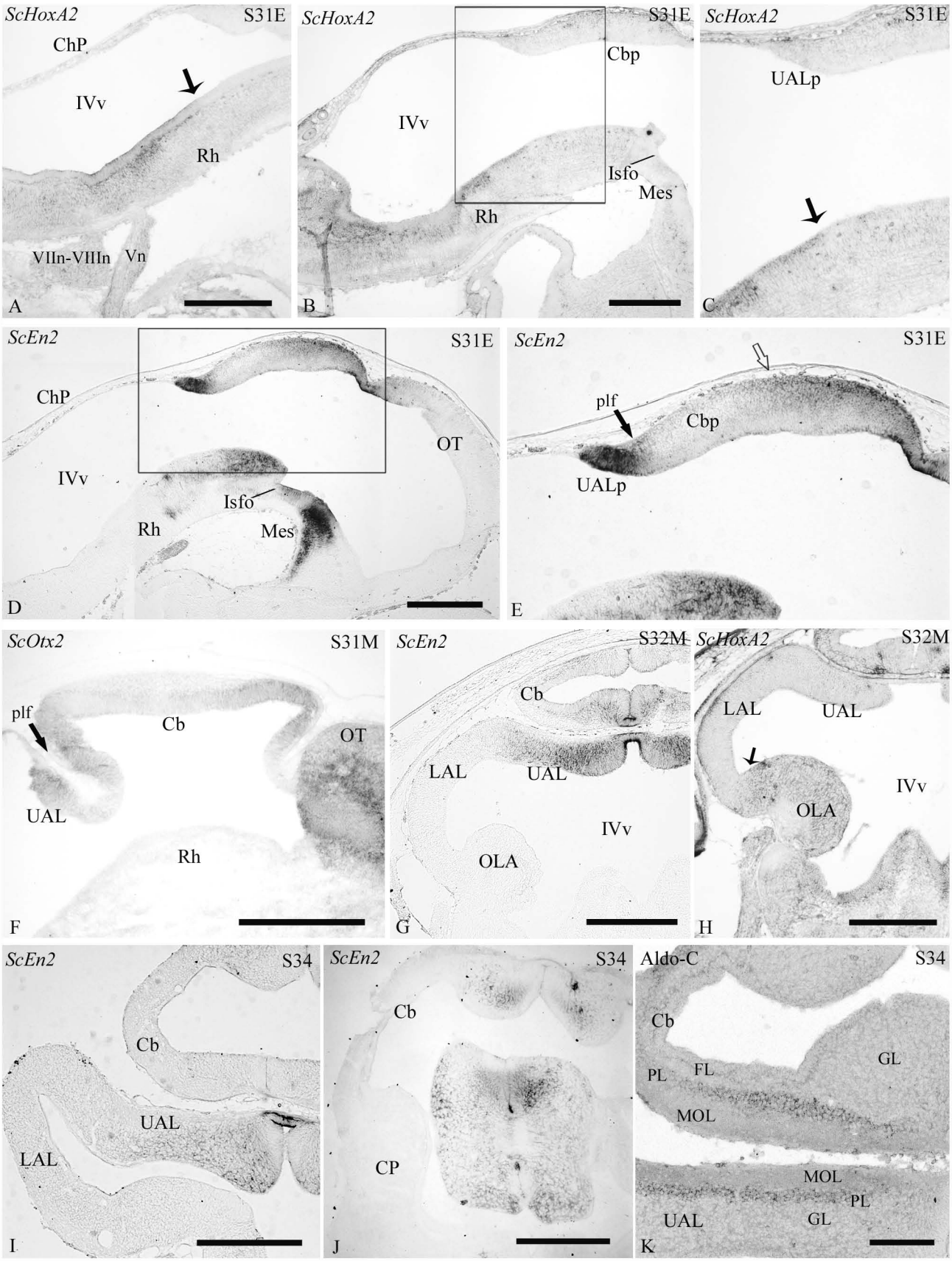
ScHoxA2
S31E
ChP
IVv
Rh
VIIn-VIIIn
Vn
A
ScHoxA2
S31E
Cbp
IVv
Isfo
Mes
Rh
B
ScHoxA2
S31E
UALp
C
ScEn2
S31E
ChP
IVv
Isfo
Rh
Mes
OT
D
ScEn2
S31E
plf
Cbp
UALp
E
ScOtx2
S31M
plf
Cb
OT
UAL
Rh
F
ScEn2
S32M
Cb
LAL
UAL
IVv
OLA
G
ScHoxA2
S32M
LAL
UAL
IVv
OLA
H
ScEn2
S34
Cb
UAL
LAL
I
ScEn2
S34
Cb
CP
J
Aldo-C
S34
Cb
GL
PL
FL
MOL
MOL
PL
UAL
GL
K

FIGURE 12

Figure 13. A. Schematic drawing of a transverse section of the rhombencephalon at intermediate stage 32. The expression patterns of *ScEn2* and *ScHoxA2* are illustrated together with the possible boundaries of auricles and cerebellar-like structures. The *HoxA2* positive area located between the lower auricle leaf and octavolateral area (indicated in red) corresponds to a potential cerebellar-like structure, which also contains a low density of serotoninergic fibers (see text for details). **B.** Diagram indicating the possible origin of the different cerebellar and cerebellar-like structures.

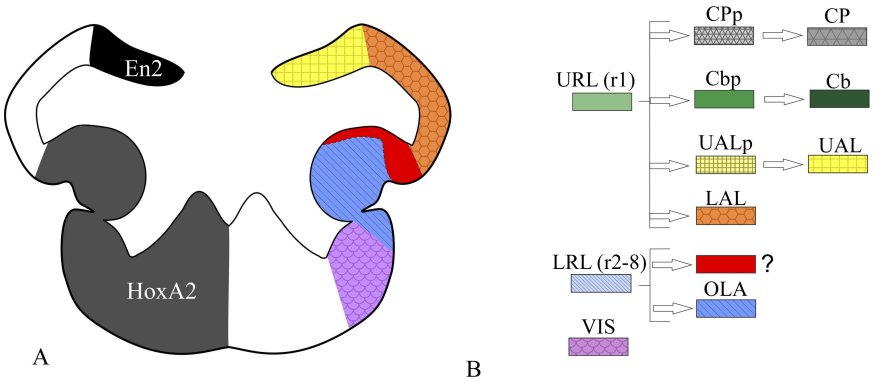

FIGURE 13

USC
UNIVERSIDADE
DE SANTIAGO
DE COMPOSTELA

CHAPTER 3

DEVELOPMENT OF THE CEREBELLAR AFFERENT SYSTEM IN THE SHARK *Scyliorhinus canicula*: INSIGHTS INTO THE BASAL ORGANIZATION OF PRECEREBELLAR NUCLEI IN GNATHOSTOMES

The results of this chapter are included in the article:

Pose-Méndez S, Candal E, Adrio F, Rodríguez-Moldes I. Development of the cerebellar afferent system in the shark *Scyliorhinus canicula*: Insights into the basal organization of precerebellar nuclei in gnathostomes. J Comp Neurol (accepted with minor changes).

USC
UNIVERSIDADE
DE SANTIAGO
DE COMPOSTELA

Development of the cerebellar afferent system in the shark *Scyliorhinus canicula*: Insights into the basal organization of precerebellar nuclei in gnathostomes

ABSTRACT

The cerebellum is recognized as an evolutionary innovation of jawed vertebrates, whose most primitive group is represented by the chondrichthyans or cartilaginous fishes. A comprehensive knowledge of cerebellar connections in these fishes might shed light on the basal organization of the cerebellar system. Although the organization of precerebellar system is known in adults, developmental studies are essential for understanding the origin and evolution of precerebellar nuclei. In the present work we performed a developmental study of cerebellar connections in embryos and juveniles of an advanced shark species, *Scyliorhinus canicula,* by application of tract-tracing in combination with immunohistochemical techniques. Main precerebellar cell populations were located in the diencephalon (pretectum and thalamus), mesencephalon (reticular formation and nucleus ruber), rhombencephalon (cerebellar nucleus, reticular formation and inferior olive) and spinal cord (ventral horn). The order of arrival of cerebellar afferent projections throughout development revealed a common pattern with other jawed vertebrates, which was helpful for comparison of stages of cerebellar development. The neurochemical study of the inferior olive and other precerebellar nuclei revealed many shared features with other gnathostomes. Furthermore, since many precerebellar nuclei originate from rhombic lips, the first analysis of neuronal migrations from these lips was performed with markers of neuroblasts. The shared features of development and organization of precerebellar connections observed between sharks and amniotes, suggest that their basic pattern was established early in gnathostome evolution.

INTRODUCTION

The cerebellum is an evolutionary innovation of jawed vertebrates or gnathostomes, clearly recognizable in cartilaginous fishes or chondrichthyans, which are phylogenetically considered the most primitive group of gnathostomes. The large cerebellum of chondrichthyans consists of cerebellar body (spinocerebellum) and auricles (vestibulocerebellum). The cerebellar cortex of sharks and rays (elasmobranchs) contains the same main cell types as mammals, i.e. Purkinje cells, granule cells, Golgi cells and stellate cells, but it lacks basket cells, Lugaro cells and unipolar brush cells (see Nicholson et al., 1969; Álvarez-Otero, 1990; Álvarez-Otero and Anadón, 1992; Álvarez-Otero et al., 1993, 1995). Cerebellar cells form the basic cerebellar circuitry typical of vertebrates (for review, see New, 2001; Anadón et al., 2009; Montgomery et al., 2012). Afferent and efferent cerebellar connections appear to be conserved throughout evolution (New, 2001) and are crucial to carry out an effective regulation of motor control, although they are also important to maintain body balance and the interrelation between sensorimotor information and motor learning (reviewed in Delgado-García, 2001).

The cerebellar connections have been studied in adults of different species of cartilaginous fishes using normal material or experimental procedures such as axonal degeneration, electrophysiology or tract-tracing methods (reviewed in Nieuwenhuys, 1967; Northcutt, 1978; Smeets et al., 1983; Schmidt and Boznick, 1987; Fiebig, 1988; Smeets, 1998; Puzdrowski and Gruber, 2009). These studies suggest that the cell populations that project to the elasmobranch cerebellum may correspond to the precerebellar nuclei of mammals. Similarly, most afferent fibers end in the cerebellum as mossy fibers (arising from various brain regions) and climbing fibers (arising exclusively from the inferior olive). Both types of afferent fibers have been reported in

adults of the lesser spotted dogfish (Álvarez-Otero et al., 1993). The cerebellar body efferents (Purkinje cell axons) end in the cerebellar nucleus located in the cerebellar peduncle (Paul and Roberts, 1984; Álvarez-Otero et al., 1996), which is considered homologous to the deep cerebellar nuclei of mammals. Hindbrain precerebellar neurons, including nucleo-cortical cells of deep cerebellar nuclei, have deserved special attention in developmental studies in mammals because of their complex migratory behavior from their origin place in the rhombic lips (for review, see Sotelo, 2004; and Sotelo and Chedotal, 2005). Whether similar processes take place in fishes is under discussion (Wingate, 2001; Volkmann et al., 2010; Wullimann et al., 2011; Butts et al., 2011), although there are some evidences of the contribution of the zebrafish rhombic lips to the precerebellar and deep cerebellar nuclei homologs (i.e., eurydendroid cells) (Wullimann et al., 2011). Moreover, recent developmental studies in the lesser spotted dogfish (*Scyliorhinus canicula*) have revealed a high degree of conservation in the patterns of cerebellar development (Rodríguez-Moldes et al., 2008; Chaplin et al., 2010).

The lesser spotted dogfish *S. canicula* is considered as a model species in Evo-Devo studies (Coolen et al., 2009). It is especially advantageous for studying different aspects of the cerebellar development because its relatively slow development enables to perform comprehensive studies, and because the organization of the adult cerebellum is well known (for review, see Smeets et al., 1983; and New, 2001). Knowledge of the development of cerebellar connectivity in chondrichthyans will shed light on the basal pattern of cerebellar organization, i.e., the pattern closest to the ancestral condition. Therefore, we performed an experimental study on the development of the cerebellar afferent system in *S. canicula*. We firstly determined by tract-tracing the postnatal organization of cerebellar connections in *S. canicula* by identifying the different afferent

nuclei to the cerebellar body and then analyzed their order of arrival during development. For a better characterization of precerebellar cells, we analyzed these cells by combining tract-tracing techniques with immunomarkers for neuroactive substances or their synthesis enzyme (serotonin, tyrosine hydroxylase, glutamic acid decarboxylase, glutamate, choline acetyltransferase and calretinin) previously known to be expressed in neurons and fibers of the lesser spotted dogfish cerebellum and brain regions containing precerebellar nuclei (Álvarez-Otero et al., 1995, 1996; Anadón et al., 2000, 2009; Carrera et al., 2008, 2012; Rodríguez-Moldes et al., 2011). We also combined tract-tracing techniques with the neuronal immunomarker NeuN, which has been reported in certain cerebellar and cerebellum-related cell populations in other vertebrates (Ono et al., 2004; Kim et al., 2011; Piper et al., 2011). In addition, we sought to identify rhombic-lip-derived migrating cells that form the hindbrain precerebellar nuclei by combining immunohistochemistry for doublecortin (a marker of migrating neuroblasts) and tract-tracing. This study provides the first description of the development of the cerebellar connections in fishes and gives new information on the basic developmental processes that take place during the formation of cerebellar connections in vertebrates, thus helping to understand how the cerebellum has evolved.

MATERIAL AND METHODS

Experimental animals

Embryos of the lesser spotted dogfish (*Scyliorhinus canicula)* were supplied by Marine Biological Model Supply Service of the CNRS UPMC Roscoff Biological Station (France) and the Estación de Bioloxía Mariña da Graña (Galicia, Spain). Additional embryos and juveniles were kindly provided by the Aquaria of Gijón, O Grove and A Coruña (Spain). Eggs and juveniles from different broods were raised in

fresh seawater tanks in standard conditions of temperature (16-18ºC) and 12:12 hr day/night cycle. The embryos were staged on the basis of their external features according to Ballard et al. (1993). The following stages were analyzed: stage 23 (three branchial arches opened; one embryo), stage 30 (eyeballs circled with black pigment; one embryo), stage 31 (detectable rostrum and long branchial filaments; three embryos), stage 32 (regression of branchial filaments; nine embryos), stage 33 (decreased volume of the yolk sac; three embryos). Of note, when stage 32 begins, the first half of embryonic development has taken place and hatching occurs after the emptying of the external yolk sac in embryos at stage 34. For more information about the relationship of the embryonic stages, body size, gestation length and birth, see Table 1 in Ferreiro-Galve et al. (2010). In addition, five young juveniles were used. Adequate measures were taken to minimize animal pain or discomfort. All procedures conformed to the guidelines established by the European Communities Council Directive of 22 September 2010 (2010/63/UE) and by the Spanish Royal Decree 53/2013 for animal experimentation, and were approved by the Ethics Committee of the University of Santiago de Compostela.

In vitro tracing techniques

A total of 21 animals ranging from stage 30-embryos to juveniles were used (Table 1). The experiments were performed in whole brains under *in vitro* conditions. All specimens were deeply anaesthetized in seawater containing 0.5% tricaine methane sulfonate (MS-222; Sigma, St. Louis, MO). Animals were then immersed in (stages 30 and 31) or transcardially perfused (stages 32, 33 and juveniles) with 30 ml of ice-cooled elasmobranch Ringer's solution (see Ferreiro-Galve et al., 2012) containing 11mM glucose, which was oxygenated with an oxygen aerator to a pH of 7.4. After decapitation, the brain and spinal cord were quickly isolated by removing the overlying

skin and cartilaginous skull and transferred to fresh iced Ringer's solution to proceed with the immediate application of the tracer.

We applied Neurobiotin (322.8 Da molecular weight; Vector Laboratories, Burlingame, CA), an amino derivative of biotin used in neuronal tract-tracing, whose transport efficiency in retrograde labeling has been proved (Barreiro-Iglesias et al., 2008). The tracer was dissolved in distilled water until saturation and recrystallized at the tip of a minute pin (00) according to Morona et al. (2005). The application of the tracer was carried out manually or using a micromanipulator (Narishige, Japan). Brains were accessed by vertical penetrations and all applications were made unilaterally, most of them to the caudal lobe of the cerebellar body; in some cases the tracer was applied to the anterior lobe of the cerebellar body, the lower rhombic lip and the rostral spinal cord (Table 1). After application of the tracer, brains were maintained in continuously oxygenated Ringer's solution containing 11 mM glucose for 2-4 days at 8ºC, and then fixed by immersion in 4% paraformaldehyde in 0.1 M phosphate buffer (PB, pH 7.4) containing 1.75% of urea (elasmobranch PB) for 2 days. The tissue was then cryoprotected with 30% sucrose in PB, embedded in NEG 50^{TM} (Thermo Scientific, Kalamazoo, MI), frozen with liquid nitrogen-cooled isopentane and cut on a cryostat. Parallel series of transverse and sagittal sections (20-25µm thick) were mounted on Superfrost Plus slides (Menzel-Glässer®, Madison, WI).

Neurobiotin visualization

Neurobiotin was visualized by incubating the sections with fluorescein isothiocyanate (FITC)-labeled Avidin-D or Dy-Light^{549} (1:1000, Vector Laboratories) in a humid chamber for 2.5 h at 37ºC. The slides were rinsed in 0.05M Tris-buffered saline (TBS; pH 7.4), then rinsed in distilled water, dried for 30 min at 37ºC, and mounted in Mowiol 4-88 Reagent (Calbiochem MerkKGa, Darmstadt, Germany).

Alternatively, sections were pretreated with H_2O_2 to eliminate the endogenous peroxidase activity and then incubated with the preformed Avidin:Biotinylated enzyme Complex (Vectastain ABC system, Vector Laboratories) following the procedure indicated by manufacturer. The tracer was then visualized with 0.25 mg/mL diaminobenzidine tetrahydrochloride (DAB, Sigma) in TBS pH 7.4 with 2.5 mg/mL nickel ammonium sulfate and 0.00075% H_2O_2. All dilutions were made with TBS containing 0.2% Triton X-100 (Sigma). Sections were then dehydrated and coverslipped.

Combined tract-tracing and immunohistochemistry

The tracer was applied *in vitro* and the tissue processed as described above. Sections were pretreated with 0.01M citrate buffer pH 6.0 for 30 min at 90ºC, for heat induced epitope retrieval. After cooling, sections were rinsed twice in TBS (pH 7.4) for 5 min each and then incubated in primary antibody solutions overnight at room temperature (RT). The primary antibodies used were (for characteristics see Table 2): rabbit polyclonal anti-doublecortin (DCX), rabbit polyclonal anti-serotonin (5-HT), rabbit polyclonal anti-calretinin (CR), rabbit polyclonal anti-glutamate (Glut), rabbit polyclonal anti-glial fibrillary acidic protein (GFAP), goat polyclonal anti-choline acetyltransferase (ChAT), mouse monoclonal anti-human HuC/HuD (HuC/D), mouse monoclonal anti-neuronal nuclear antigen (NeuN), mouse monoclonal anti-tyrosine hydroxylase (TH) and sheep polyclonal anti-glutamic acid decarboxylase (GAD). Secondary antibodies were subsequently incubated for 1 h at RT. The following secondary antibodies were used (Table 3): Alexa Fluor 546 or 488 donkey anti-rabbit, Alexa Fluor 647 donkey anti-mouse, Alexa Fluor 633 donkey anti-sheep and Alexa Fluor 488 or 633 donkey anti-goat IgGs (1:100-200, Molecular Probes, The Netherlands). All antibodies were diluted in TBS containing 15% normal serum of

donkey, the species in which the secondary antibody was raised, 2% bovine serum albumin (BSA, Sigma) and 0.2% Triton X-100 (Sigma). Neurobiotin was visualized with FITC-labeled-avidin-D or with DyLight^{549} as described above. The slides were rinsed in TBS (pH 7.4), then in distilled water, dried for 30 min at 37ºC, and mounted in Mowiol 4-88 Reagent.

In addition, one embryo at stage 23 that had not been previously treated for tract-tracing, was processed as above for double immunohistochemistry with DCX and HuC/D for searching migrating neuroblasts.

Antibody characterization

Table 2 indicates the immunogens, suppliers, catalog numbers, hosts, type and dilution of the primary antibodies used here and Table 3 the secondary antibodies used.

Doublecortin

The polyclonal anti-DCX antibody was produced by immunizing rabbits with a synthetic peptide corresponding to human DCX. The antibody was purified by protein A and peptide affinity chromatography. In Western blots of extracts from mouse and rat brain, this antiserum recognizes one band of approximately 45 kDa (manufacturer's technical information). The same antibody labels immature neurons (neuroblasts) in neurogenic regions of the mouse brain (Dellarole and Grilli, 2008). As a further control of specificity, we performed Western blot analyses of brain extracts of adult lesser spotted dogfish by standard procedures (for details of preparation of brain extracts and blotting procedure, see Anadón et al., 2000; Carrera et al., 2012). In these blots, the DCX antibody stained a single protein band of about 45 KDa (lane 2 in Fig. 1). ProSieve protein standards (Lonza, Rockland, ME) were used as molecular weight markers.

Serotonin

The specificity of the anti-5-HT antiserum was assessed by the manufacturer using standard immunohistochemical methods. In addition, the specificity of the immunoreaction in *S. canicula* was previously tested by preadsorbing the primary antibody with the 5-HT-BSA conjugate used for rabbit immunization (Carrera et al., 2008). The antiserum has been used in this dogfish, and the pattern of staining observed in the present study was the same as previously reported (Carrera et al., 2008).

Calretinin

According to the manufacturer, the antiserum against CR 1) does not cross-react with calbindin D-28k or other known calcium binding-proteins, as determined by immunoblots and by its distribution in the brain; 2) it labels a subpopulation of neurons in the normal brain with high efficiency, but does not stain the brain of CR knock-out mice; 3) it recognizes a band of 29-30 kDa by Western blot. In addition, this antibody was previously characterized by Western blotting in brain extracts of *S. canicula* where it revealed a single protein band of the same molecular weight (29 kDa) as in rat (Graña et al., 2008; lane 3 in Fig. 1).

GFAP

According to the manufacturer, the anti-GFAP antibody recognizes a 50 kDa intracytoplasmic filamentous protein that constitutes a portion of the cytoskeleton in astrocytes, and it has been proved to be the most specific marker for cells of astrocytic lineage. The antibody has been solid-phase absorbed with human and cow serum GFAP proteins, which show 90-95% homology between species. It has been previously used as a glial marker in different elasmobranch species including *Scyliorhinus canicula* (Wasowicz et al., 1999; Kálmán and Gould, 2001; Sueiro et al., 2007; Ari and Kálmán, 2008).

GAD

The GAD65/67 antiserum (GAD 1440) was a gift from Dr. Mugnaini, and was initially produced in the National Institute of Health, Bethesda, MD from a source developed by Drs. Irwin J. Kopin, Wolfgang Oertel, Donald E. Schmechel, and Marcel Tappaz (Oertel et al., 1981), with methodological contributions from the laboratory of Enrico Mugnaini (University of Connecticut, Storrs). Details about the origin and specificity of the GAD 1440 antibody have been previously published (MacLeod et al., 2006). Additional controls for specificity of this antiserum in *S. canicula* and rat brain protein extracts were previously performed by Western blot (Sueiro et al., 2004); similar 65 and 67 kDa bands were observed in *S. canicula* and rat lanes, indicating that the antibody recognized both isoforms of GAD in *S. canicula*. The same antiserum has been used in different vertebrate groups, including fishes (Mugnaini et al., 1984; Carr et al., 1989; Maler and Mugnaini, 1994; MacLeod et al., 2006).

Glutamate

The anti-Glut antiserum was raised against glutamate conjugated to a carrier protein using glutaraldehyde. According to the supplier, 1) in test of monkey, cat, rat and mouse tissues the antibody has successfully localized glutamate and glutamatergic neurons such as retinal photoreceptors and cortical pyramidal cells; and 2) in dot blot assays against a variety of other amino acid conjugates including the standard 20 amino acids found in proteins, the nonprotein amino acids GABA, glutamine, glycine, D-aspartate, serine and arginine, which did not yield significant reactivity. In addition, the antibody was tested by Western blotting with adult *S. canicula* brain protein extracts, and no protein band was stained in these blots (lane 1 in Fig. 1). As a positive control, the CR was immunostained, which showed the presence of a single band of about 29-30 kDa (lane 3 in Fig. 1). The procedure, as cited above, was performed by standard

procedures. A related antibody from the same supplier (Immunosolution, cat. no. IG1007), similarly raised but produced for glutaraldehyde-fixed tissues, did not stain any protein band in lamprey brain protein extracts (Villar-Cerviño et al., 2011) and labeled specific neuronal cell types in the glutaraldehyde-fixed lamprey brain (Villar-Cerviño et al., 2011, 2012).

ChAT

Immunoblotting of mouse NIH/3T3 cell lysates with this antibody revealed a single 68 kDa protein band (manufacturer's technical information). The anti-ChAT antiserum has also been characterized in Western blots of lesser spotted dogfish brain extracts, where it labeled a protein band similar to that labeled in rat brain extracts (Anadón et al., 2000). Moreover, the distribution of cholinergic neurons in the brain of the adult lesser spotted dogfish has been previously reported using this antibody (Anadón et al., 2000).

HuC/D

The mouse monoclonal anti-HuC/D antibody (originally isolated by M. Marusich in the University of Oregon Monoclonal Antibody Facility as mAb 16A11) was raised against a RNA-binding protein originally isolated from humans. According manufacturer, it recognizes the *embryonic lethal abnormal visual* (Elav) family members HuC, HuD and Hel-N1 (all of them neuronal proteins), but not HuR; in immunoblots, it reveals bands of around 40 kDa that correspond to the HuC and HuD proteins (Marusich et al., 1994; Takeda et al., 2008; Vellema et al., 2010). Moreover, this antibody specifically labeled neuronal cells in teleosts, birds and humans (Ekström and Johansson, 2003; Soukkarieh et al., 2007; Takeda et al., 2008). The same antibody labeled different types of neurons in the spinal cord of embryos and juveniles of the lesser spotted dogfish (Sueiro et al., 2004).

NeuN

The anti-NeuN (or Neuronal Nuclei) antibody has been extensively used as neuronal marker as it recognizes a vertebrate neuron-specific nuclear protein (NeuN). Some neurons such as Purkinje cells and inferior olivary neurons are not recognized by the NeuN antibody (Mullen et al., 1992; Wolf et al., 1996). The immunohistochemical staining is primarily found in the nucleus of the neurons with lighter staining of the cytoplasm. The antibody recognized two-three bands ranged between 46-48 kDa that correspond to isoforms of NeuN, as shown by Western blot and electrophoretic separation of crude nuclear fraction of adult mouse brain (Lind et al., 2005). The specificity of the antibody in the lesser spotted dogfish is supported by the labeling of neurons in the granular layer of the cerebellum, similarly to that reported in other vertebrates (Ono et al., 2004; Kim et al., 2011; Piper et al., 2011).

TH

The mouse monoclonal TH antiserum was raised against denatured TH from rat pheochromocytoma. According to the technical information supplied by the manufacturer, in Western blots it recognizes a protein of approximately 59-60 kDa. In addition, the antiserum specificity has been characterized previously by Western blot in brain extracts of the lesser spotted dogfish where it stained a single protein band of about 56-60 kDa (Carrera et al., 2012). The antibody displays wide species cross-reactivity and has been used to demonstrate the catecholaminergic systems in a number of species, including the lesser spotted dogfish (reviewed in Carrera et al., 2012). The antibody did not recognize TH2 in teleosts, thus revealing only the TH1-immunoreactive catecholaminergic neurons (Filippi et al., 2010; Yamamoto et al., 2010).

Imaging

Photomicrographs were taken with an Olympus DP70 color digital camera fitted to a Provis photomicroscope equipped for fluorescence with appropriate filter combinations. Double labeled samples were studied with a spectral confocal laser scanning microscope (Leica TCS-SP2, Wetzlar, Germany). Stack images were acquired separately from each laser channel with steps from 0.5 to 2 µm along the z-axis and collapsed images were obtained from an average of 15 optical sections. Confocal stacks were acquired and processed with LITE software (Leica). Images were sized and optimized for brightness and contrast using Adobe Photoshop 7.0 (San Jose, CA). For presentation, some color photomicrographs were converted to gray scale and inverted, and brightness and contrast adjusted using Adobe Photoshop 7.0. Plate photomontage, schemes and lettering were also made with Adobe Photoshop 7.0.

RESULTS

Unless otherwise stated, the terminology for the main structures of the elasmobranch cerebellar afferent system basically follows that used by Fiebig (1988), Álvarez-Otero et al. (1996), and Carrera et al. (2008, 2012).

To identify the precerebellar nuclei of *S. canicula*, we applied the recrystallized tracer (Neurobiotin) to the cerebellar body of juveniles. This tracer has been mainly used as a retrograde tracer (Barreiro-Iglesias et al., 2008), although it also appeared to be transported anterogradely (Huang et al., 1992). Therefore, there is no doubt that labeled somas after cerebellar applications represent afferent (precerebellar) neurons, but the labeled tracts of fibers could correspond to either afferent or efferent systems. Although we tried to restrict the application of the tracer to only the cerebellar body, some diffusion outside the cerebellar limits occurred in some cases. Accordingly, to

avoid false positives, we only considered those results that were consistently reproduced in all traced specimens. Furthermore, the present study is qualitative and not quantitative, because the labeled precerebellar cells correspond to a portion of each precerebellar nucleus (that project to the area of the cerebellar body affected by the tracer) and not the entire afferent populations (that project to the whole cerebellum).

The study of connections of the vestibulocerebellum in the lesser spotted dogfish exceeds the objectives of the present work. However, the cerebellar afferents to the vestibulocerebellum in the little skate (Schmidt and Bodznick, 1987) are rather different from those projecting to the cerebellar body described here.

In order to facilitate the interpretation of photomicrographs, the basic organization of cerebellar connections observed in juveniles is illustrated in Figure 2, which includes schematic drawings of representative sagittal and transverse sections through the brain. Main results are also summarized in Figure 3. Both in schemes and figures, the right side is ipsilateral with respect to the tracer application site and the left side is contralateral. The developmental pattern of cerebellar connections is displayed in sagittal and transverse schematic representations in Figure 4, summarized in Table 4, and illustrated in detail in Figures 5-10. Subsequently, the neurochemical characterization of precerebellar nuclei is summarized in Table 5 and illustrated in Figures 11-13. Finally, Figure 14 shows putative tangential and radial migrating neuroblasts originated in the upper and lower rhombic lips.

Organization of cerebellar afferent pathways in juveniles of *S. canicula*

We have focused our study on the connections of the cerebellar body and not on cerebellar auricles, the latter being mostly linked to the vestibular nuclei. The distribution of cells projecting to the cerebellar body in juveniles of *S. canicula*

(schematically represented in Figure 2) is roughly similar to that described in adults of the thornback guitarfish *Platyrhinoidis triseriata* (Fiebig, 1988) and the Atlantic stingray *Dasyatis sabina* (Puzdrowski and Gruber, 2009). However, in the present study the topological organization of cerebellar afferent nuclei was examined from a segmental point of view according to the transverse and longitudinal domains described in *S. canicula* by Ferreiro-Galve et al. (2008), Rodríguez-Moldes et al. (2011), and Carrera et al. (2012). These domains are supported by the prosomeric (segmental) model of forebrain organization proposed by Puelles and Rubenstein (2003), and the model that advocates the evolutionary conservation of the segmental rhombencephalic entities (for review, see Nieuwenhuys, 2011).

After application of the tracer to the cerebellar body of juveniles, retrogradely labeled (precerebellar) cells were observed from diencephalic to spinal levels (Fig. 2). In general, the afferents to the cerebellum from more rostral brain regions were ipsilateral and those from caudal regions were mostly contralateral, as shown in Figure 3, which summarizes the major precerebellar groups. Additionally, some fibers were anterogradely labeled in the cerebellar peduncle (see below).

The most rostral retrogradely labeled cells were located in the diencephalon (caudal forebrain), particularly in the derivatives of the alar plate of prosomeres 1 and 2 (pretectum and thalamus, respectively), and most of them were ipsilateral to the tracer application (Fig. 2A,B,K). Labeled precerebellar cells were observed at marginal and intermediate levels of pretectum (lateral and central pretectal nuclei) and thalamus (area of lateral geniculate nucleus and medial thalamus) (Fig.2B).

In the mesencephalon, which consists of tectum and tegmentum, some afferent cells from the optic tectum were identified as belonging to the mesencephalic trigeminal nucleus (Fig. 2A,C,K). Along the mesencephalic tegmentum, scattered precerebellar

reticular cells were observed bilaterally to the tracer application, but they were more abundant ipsilaterally. Near the base of the tegmentum, a conspicuous paramedian ipsilateral group of cells was clearly observed just laterally to the oculomotor nerve root (Fig. 2A,C,K). On the basis of its location it was identified as the nucleus ruber described in *Scyliorhinus* (Smeets, 1982; Smeets et al., 1983).

To describe the different precerebellar cell groups, we have roughly subdivided the rhombencephalon into three parts (rostral, intermediate and caudal). In the rostral rhombencephalon (isthmus), just caudal to nucleus ruber, abundant labeled cells appeared densely grouped in basal regions, mostly ipsilaterally and mainly in the superior reticular formation (Fig. 2A,D,K). At dorsolateral isthmic levels a small ipsilateral group of labeled cells and fibers was identified as the isthmic group (Fig. 2A,E,K). More caudally, in the cerebellar peduncle (Fig. 2A,F,K), a few cells were retrogradely labeled with Neurobiotin (NB) in each one of the three cell subpopulations (subventricular, medial and lateral) previously described in the lesser spotted dogfish cerebellar nucleus (Álvarez-Otero et al., 1996), mainly in the ipsilateral side. Abundant bundles of labeled fibers coursed following a dorsoventral orientation in the cerebellar peduncle, and some turned abruptly toward medial regions of the cerebellar nucleus. The 90 degrees turning of fiber bundles suggested that these fibers were Purkinje cell axons innervating the cerebellar nucleus, which is in agreement with previous experimental observations by Álvarez-Otero et al. (1996).

Precerebellar cells of the caudal rhombencephalon were confined to the viscerosensory column [comprised between the intermediate dorsal sulcus (sid) and sulcus limitans (slH)] and motor areas (ventrally to slH) (Fig. 2A,G-I,K). Caudally to the level of the anterior lateral line and octaval nerve entrances, labeled precerebellar cells were observed along the nucleus of the descending trigeminal root (Fig. 2A,H,K).

Labeled precerebellar cells of the inferior reticular formation (Fig. 2A,G-I,K) were located in lateral (marginal and submarginally, i.e. the lateral reticular area or lateral reticular nucleus), paramedian and median (i.e. the raphe nucleus) levels. They were more abundant ipsilaterally than contralaterally to the tracer application site. Just caudally to these populations, retrogradely labeled cells were observed at the level of the contralateral inferior olive in paramedian location. This olivary population extended from the level of entrance of the first vagal nerve root (Fig. 2I,K) to the hindbrain-spinal cord boundary. Two olivary cell subpopulations were distinguished, one located rostrally and dorsolaterally in the inferior olive and the other located more caudally and ventromedially. Taking into account the morphology of inferior olivary cells, two cell types were observed in juveniles and embryos (see below).

In the rostral spinal cord, very few labeled cells were observed in the ventral horn (Figs. 2A,J,K). Other parts of the rostral spinal cord lacked retrogradely labeled neurons in our experiments. More caudal spinal regions were not checked.

Development of precerebellar cells projecting to the cerebellar body

In order to determine the developmental pattern of cerebellar afferent pathways, applications of tracer to the cerebellar body were systematically carried out in embryos of different sizes (stages 31, 32 and 33). Of note, only precerebellar cells whose axons had reached the cerebellum at these stages would be retrogradely labeled, which allow studying the timing of development of such pathways. An overview of the distribution of the precerebellar neuronal groups that innervated the cerebellar body throughout developmental stages is represented in Figure 4, which also shows the relative density of labeled cells in sagittal (Fig. 4A-D) and transverse sections (Fig. 4E-R) at early stage 32 (when the earliest labeled cells were observed), intermediate and late stage 32 (when

the remainder cerebellar afferents successively develop), and stage 33 (when the precerebellar organization described in juveniles became recognizable). The sequence of appearance of the main precerebellar cell groups projecting to the cerebellar body is represented in Table 4. In the stage 31, the only clearly labeled cells were observed in the cerebellar peduncle, although the existence of any extracerebellar afferent cannot be completely ruled out because of the observation of ascending fibers in the cerebellar peduncle.

At early stage 32, NB labeled cells appeared in the alar domain of prosomere 1 or pretectum (Fig. 4A), in the mesencephalon (Fig. 4A,E), and the rostral rhombencephalon (Fig. 4A,F,G). A few precerebellar cells were clearly labeled in the cerebellar peduncle (Fig. 4A,H), but labeled cells were hardly detected at more caudal rhombencephalic levels (Fig. 4A,I). At intermediate stage 32 (Fig. 4B), the number of labeled cells increased in the pretectum and mesencephalic tegmentum, and the first cells became labeled in the optic tectum (Vme) and the region of the caudal rhombencephalon roughly comprised between rhombomere 6 and the spinal cord. Interestingly, in the caudal rhombencephalon some retrogradely labeled cells were observed in a ventroparamedian location, which could represent the primordium of the inferior olive (Fig. 4B). Later on, the density of cell populations progressively increased and towards the end of this stage (late stage 32) precerebellar neurons were labeled in the thalamic area (Fig. 4C,J), and conspicuous precerebellar nuclei were appreciable in the mesencephalon (nucleus ruber; Fig. 4C,K) and the rhombencephalon. Rhombencephalic precerebellar nuclei included the superior reticular formation, the isthmic group, the three subpopulations of the cerebellar nucleus, the inferior reticular formation (including cells of the lateral reticular area and raphe cells), cells in the nucleus of the descending trigeminal root and the inferior olive (Fig. 4C,L-Q). The first

labeled cells in the spinal cord were also observed at this stage (Fig. 4C,R). At stage 33 (Fig. 4D), the relative number of precerebellar cells was higher than at stage 32 but no new specific cell groups appeared thenceforth, and the pattern of precerebellar nuclei was already very similar to that of juveniles.

To perform a detailed description of the progress of each specific cell group projecting to cerebellar body, i.e. to see when they arise and how they change overtime, we proceed to describe the development by regions along the rostrocaudal axis. Diencephalic projections to the cerebellum from the pretectum and thalamus developed sequentially. First diencephalic precerebellar cells were observed marginally in the pretectum (Fig. 5A). Shortly after (at intermediate stage 32) more diencephalic cells were appreciated marginally in the pretectum and extending to the pretectum-thalamus boundary (Figs. 4B, 5B). At the end of this stage (late stage 32), additional labeled cells were observed in an area that contain a calretinin-immunoreactive cell population (Fig. 5C,D) previously identified as belonging to the thalamus (Ferreiro-Galve et al., 2008). At stage 33, the pretectal and thalamic populations extended throughout the alar domain occupying marginal and intermediate levels (Fig. 5E,F). A similar distribution was observed in juveniles (Fig. 5G,H).

In the mesencephalic tegmentum, some precerebellar reticular cells were first observed concurrently with the pretectal population (early stage 32) (Fig. 5I). As development proceeded, the relative number of mesencephalic cells projecting to the cerebellum progressively increased and the labeled cell population extended at marginal, submarginal and intermediate areas (Fig. 5J-L). On the other hand, the nucleus ruber was not appreciable as a defined group until the end of the stage 32 (Fig. 5M) and became more apparent in later stages (Fig. 5N,O). In the optic tectum, a few labeled cells were observed in the mesencephalic trigeminal nucleus from intermediate

stage 32 onwards, but its number did not increase significantly throughout development (Fig. 6A-C).

In the rostral or isthmic rhombencephalon, the first precerebellar cells of the superior reticular formation were labeled at early stage 32 (Fig. 6D), its relative density increased throughout development (Fig. 6E). In juveniles, reticular cells became a very conspicuous and dense population (Fig. 6F). The small dorsolateral isthmic group of precerebellar cells and fibers also appeared labeled at early stage 32 (Fig. 6G). Later on, the number of cells in this group did not increase significantly, although the density of labeled fibers was higher in juveniles (Fig. 6H,I).

The cerebellar peduncle was the first region showing clearly labeled precerebellar cells. When a ventricular prominence became appreciable in the cerebellar peduncle (stage 31), a few labeled cells and some dorsoventrally oriented labeled fibers were distinguished in the primordial lateral cerebellar subnucleus (arrow in Fig. 7A). At early stage 32, the cerebellar peduncle showed a conspicuous eminence and labeled cells were also observed medially in the primordial medial cerebellar subnucleus (Fig. 7B). At intermediate stage 32, the white matter of the cerebellar nucleus was clearly distinguished and exhibited fiber endings in dorsomedial location (arrow in Fig. 7C), abundant fibers coursed following a dorsoventral orientation (Fig. 7C), and the first fibers turning 90 degrees towards the medial zone. These bent fibers appeared to come from the cerebellar cortex (black arrow in Fig. 7D) and from basal rhombencephalic regions (white arrow in Fig. 7D). At late stage 32, the innervation of the dorsomedial cerebellar peduncle area increased (Fig. 7E). The bent fibers were found in bundles, which contained both types of processes, presumably from dorsal and ventral origins (black and white arrows in the Fig. 7F). At this stage, abundant labeled nucleo-cortical cells were observed in the medial area of the cerebellar nucleus, being scarcer in

subventricular and lateral parts (Fig. 7G). In juveniles, the three precerebellar subpopulations of the cerebellar nucleus were patent (Figs. 7H-J), and scattered labeled cells appeared in the white matter. In these juveniles, the dorsoventrally tracts of fibers, the bundles bent towards the medial portion (Fig. 7H,I) and the innervation of the white matter portion of the cerebellar nucleus (Fig. 7I,J) became conspicuous. Interestingly, in the dorsal zone of the cerebellar peduncle, abundant fiber endings were observed around the unlabeled (extracerebellar projecting) nuclear cells (inset in Fig. 7J).

Noteworthy, NB labeled fibers were observed in the marginal region of the rhombencephalon ascending towards the cerebellar peduncle as early as stage 31 (Fig. 8A). Later on, the number of these fibers increased and formed a conspicuous tract (bulbo-cerebellar tract) (Fig. 8B-F). A few labeled fibers were also observed in the trigeminal ganglion and nerve (trigeminal fibers) at late stage 32 (Fig. 8E). Analysis of sagittal sections allowed showed two longitudinal (rostral and caudal) tracts of labeled fibers that reached the cerebellum after intercrossing at the level of the cerebellar peduncle (Fig. 8G,H).

Regarding to the caudal rhombencephalon, labeled precerebellar cells were observed from the intermediate stage 32 onwards (Fig. 8I). The number of these cells gradually increased, and in late stage 32 different cell groups became recognizable: in the nucleus of the descending trigeminal root (Fig. 8J), and those located at intermediate, lateral (Fig. 8K) and raphe (inset in Fig. 8L) regions of the inferior reticular formation. In juveniles, these cell groups became clearly evident (Fig. 8M,N), although the number of cells in the raphe did not appear to increase (Fig. 8O).

Precerebellar cells of the inferior olive were labeled from intermediate stage 32. In a case of this stage, a single paramedian cell at the level of the vagal nerve root (Fig. 9A) and a pair of cells (also paramedially) at rhombencephalon-spinal cord boundary

(Fig. 9B,C) were observed, probably corresponding to the primordia of rostral and caudal subpopulations of the inferior olive, respectively. A defined olivary organization was not observed until late stage 32 (Fig. 9D), when two cell subpopulations of the inferior olive became distinguishable: a rostral portion containing cells with processes dorsolaterally oriented (Fig. 9E) and a caudal portion with cells located more ventromedially (Fig. 9F). To assess whether these olivary cells were young migrating neuroblasts or already differentiated neurons, we performed double labeling with the tracer and DCX (a marker of migrating neuroblasts) or HuC/D (marker of early neurons) immunohistochemistry. We observed that labeled cells of the inferior olive area were DCX negative and HuC/D positive (Fig. 9G-I), which revealed that they were differentiated neurons. In juveniles, a large number of NB labeled cells was observed in the rostral (Fig. 9J) and caudal (Fig. 9K) subpopulations of the inferior olive. The inferior olive extended to the most caudal rhombencephalon (Fig. 9L), and a dense tangle of labeled processes was observed in the inferior olive neuropil. In embryos and juveniles, the labeled olivary perikarya were mostly round, except for a few that were elongated in shape (Fig. 9G and white arrow in Fig. 9K).

In the spinal cord, labeled precerebellar cells were not observed until the late stage 32 (Fig. 10A). As development proceeded, the number of these labeled precerebellar cells was only slightly increased (Fig. 2J).

Prompted by the scarce spinal cells projecting to cerebellum observed in these experiments, a different experiment was carried out in a few embryos, in which the NB was applied to the spinal cord to check if spino-cerebellar projections were actually established at late stage 32 or earlier. The application of NB to the rostral spinal cord of stages 31 and early 32 would affect most of spinal fibers projecting to the cerebellum, including those from caudal spinal levels. In these experiments, anterogradely labeled

fibers were observed in the cerebellum. At stage 31, only a single labeled fiber was observed in the prospective cerebellar peduncle (Fig. 10B). Shortly after (early stage 32), some labeled fibers reached the ipsilateral cerebellar cortex (Fig. 10C) although they were far more abundant in the cerebellar peduncle (Fig. 10D), and some fibers were detected in the contralateral side (Fig. 10E). Labeled fibers were also observed in the anterior medullary velum (AMV) and in the cerebellum (Fig. 10F) and some appeared to cross to the contralateral side (Fig. 10G). At this stage, fibers from the spinal cord also reached the boundary between the cerebellar body and upper auricular leaf (results not shown).

Neurochemical characterization of cerebellar connections in juveniles

In brain regions where precerebellar nuclei were labeled with the tracer we had previously observed cells and fibers immunoreactive to choline acetyltransferase (ChAT; Anadón et al., 2000, serotonin (5-HT; Carrera et al., 2008), calretinin (CR; Rodríguez-Moldes et al., 2011), and tyrosine hydroxylase (TH; Carrera et al., 2012). To assess the neurochemical profile of precerebellar cells, we performed double labeling with these immunomarkers after application of the tracer to the cerebellum. To increase our knowledge on the nature of the precerebellar nuclei, we also carried out double labeling with antibodies raised against GAD (maker of GABAergic structures), glutamate (Glut) and NeuN, a marker of some neuronal populations associated with the cerebellum. These experiments revealed that precerebellar (retrogradely labeled) neurons in the lesser spotted dogfish were generally located in cell groups containing abundant cells immunoreactive to CR, Glut and NeuN, which were similar in size to the NB positive cells. After double labeling we observed that (see Table 5): 1) all precerebellar cell groups contained NB-CR double labeled cells; 2) in most

precerebellar nuclei there were some Glut immunoreactive (-ir) precerebellar cells; 3) in some precerebellar nuclei, NB positive cells were also NeuN-ir; 4) NB-ChAT and NB-TH double labeling of cells was unusual; and 5) NB labeling was lacking in 5-HT-ir and GAD-ir cells located in regions containing precerebellar neurons, which were generally larger than cerebellar-projecting cells. Immunoreactivity to these immunomarkers, especially to GAD, was observed in processes of the neuropil surrounding most of NB labeled cells.

In the diencephalon, most of the pretectal and thalamic NB labeled precerebellar cells were CR-ir (Fig. 11A,B), but not Glut-ir or NeuN-ir (not shown). The surrounding neuropil showed moderate density of 5-HT-ir fibers, and low density of TH-ir, GAD-ir, and ChAT-ir fibers (Fig. 11C,D).

The labeled precerebellar nuclei of the mesencephalic tegmentum showed similar neurochemical pattern (Figs. 11E-K). The precerebellar cells of both the mesencephalic reticular cell group (Fig. 11E-J) and the nucleus ruber (Fig. 11H-K) appeared among abundant CR-ir, Glut-ir and NeuN-ir tegmental cells. Neurobiotin labeled cells in these precerebellar groups also showed immunoreactivity to these immunomarkers, mainly Glut and CR. Neurobiotin labeled cells appeared in areas with 5-HT-ir fibers in the neuropil, and these fibers surrounded some of the labeled cells (inset in Fig. 11K). These mesencephalic precerebellar populations are neighboring the dopaminergic cells of the ventral tegmental area (VTA) and substantia nigra (SN), and the serotoninergic cells of the rostral reticular formation. Specifically, reticular cells projecting to the cerebellum were lateral to the SN, recognizable by its TH-ir cells and the ChAT-ir and 5-HT-ir neuropil (Fig. 11F,G), although some of them appeared just on the edge of the SN and had similar size as nigral TH-ir cells (inset in Fig. 11J).

Moreover, the nucleus ruber was located in a TH-negative gap between the VTA and SN, and dorsally to a conspicuous GAD positive neuropil (Fig. 11J,K).

In the rostral (isthmic) rhombencephalon, the NB labeled superior reticular cells (Fig. 12A-D) and the NB positive cells and fibers of the dorsolateral small isthmic group (Fig. 12E-H), were mostly CR-ir. Both precerebellar populations showed a neuropil with moderate density of 5-HT-ir fibers, mostly beaded. Nevertheless, we also observed dissimilarities between populations related to the neurochemical nature of cells and neuropil of the adjacent regions. Some NB labeled cells of the superior reticular formation were Glut-ir, and some of them were also NeuN-ir. They were roughly overlapping with a conspicuous group of NeuN-ir cells and with some serotoninergic cells, probably corresponding to the B9 group (Fig. 12B,C), and immersed in neuropil containing weakly GAD-ir or ChAT-ir fibers, and strongly TH-ir fibers (Fig. 12C,D). On the other hand, the small isthmic precerebellar group was located ventrolateral to an isthmic area showing conspicuous serotoninergic innervation, and lateral to the locus coeruleus (LC), as characterized by the presence of TH-ir cells (Fig. 12F-H). The NB positive fiber tracts of this group ran parallel to fibers positive for 5-HT and GAD (Fig. 12G,H). Some NB labeled cells appeared occasionally in the LC (asterisk in Fig. 12G), but colocalization of NB and TH was infrequent (inset in Fig. 12G).

At the level of the cerebellar peduncle, the three precerebellar subpopulations of the cerebellar nucleus were similar in several respects (Fig. 12I-O). Most precerebellar cells showed colocalization with CR or Glut immunoreactivity (yellow cells in Fig. 12I,J), but not with NeuN, even though NeuN-ir cells were observed in the three subpopulations (Fig. 12J). Additionally, the neuropil of the three subpopulations presented some double labeled NB-CR fibers (yellow fibers in Fig. 12I) and abundant

fibers and/or boutons single labeled for 5-HT, GAD, ChAT and TH (Fig. 12K-N). In some cases, faintly NB labeled cells were surrounded by boutons immunoreactive to these immunomarkers (yellow arrows in Fig. 12K,M). In the white matter of the cerebellar nucleus, richly innervated by NB fibers especially in the dorsomedial zone, there were scarce CR-ir and 5-HT-ir fibers (Fig. 12I,K,L), and abundant GAD-ir and ChAT-ir boutons (Fig. 12K-M). The NB positive fibers bent towards the medial cerebellar nucleus appeared to contact Glut-ir cells in this region (Fig. 12J), and some 5-HT-ir fibers coursed in the same bent bundles (outlined arrows in Fig. 12L). Furthermore, dorsoventrally oriented NB positive fibers ran parallel to TH-ir fibers, but double labeled fibers were not observed (Fig. 12M and detail in Fig. 12O).

Neurochemical similarities among different NB labeled precerebellar populations of the caudal rhombencephalon (inferior reticular formation, in Fig. 13A-E; and inferior olive, in Fig. 13F-K) were observed, but also some differences. In the inferior reticular formation, retrogradely labeled cells were located among CR-ir, ChAT-ir, Glut-ir and NeuN-ir cells. Double labeling showed some colocalization of these immunomarkers with NB labeling in cells of the lateral reticular area (Fig. 13A,B). No colocalization of NB and 5-HT was observed in the raphe region, although the NB labeled cells were close to serotoninergic cells, mainly at the level of the raphe magnus (Fig. 13D). The neuropil of the inferior reticular formation generally presented a moderate density of fibers and/or boutons immunoreactive to 5-HT, GAD (Fig. 13C), ChAT and TH (Fig. 13E). Reticular cells adjacent to the inferior olive are Glut-NeuN double labeled cells (Fig. 13G), and 5-HT, TH or NB single labeled cells. Some of these reticular cells extended dendritic processes toward the olivary nucleus (outlined arrows in Fig. 13H,I,K), which contained NB positive cells double labeled with CR (Fig. 13F) and Glut (Fig. 13G). The neuropil surrounding these olivary cells presented abundant

GAD-ir, ChAT-ir and TH-ir boutons and moderate number of 5-HT-ir beaded fibers and boutons (Fig. 13H-K). Interestingly, ChAT-ir and TH-ir neuropil was less dense in the rostral subpopulation of the inferior olive (Fig. 13J) than in the caudal one (Fig. 13K).

In the spinal cord, some NB labeled precerebellar cells were also CR-ir and located near the ChAT-ir cells of the motor column (Fig. 13L). Furthermore, some NB positive cells were also located ventromedially close to 5-HT-ir cells in an area abundantly innervated by 5-HT-ir and GAD-ir fibers (Fig. 13M).

Evidence for early migrating neuroblasts arising from rhombic lips in *Scyliorhinus canicula*

In sagittal sections through the lateral region of the rostral rhombencephalon of a stage 23 embryo, double labeling for DCX (marker of migrating neuroblasts) and HuC/D (marker of early neurons) was observed in the soma and processes of tangentially oriented cells located in the thin marginal zone outside the isthmic mantle zone and intermediate zone (Fig. 14A-C). Some of these cells extending in ventral direction (arrows in Fig. 14B,C), while others located more ventrally were oriented rostrocaudally (outlined arrow in Fig. 14B,C). We identified these DCX-HuC/D double labeled cells as tangentially migrating neuroblasts.

In other experiment carried out later in development (at stage 30), the tracer was applied to the lower rhombic lips, and left to transport for three days (see table 1) and subsequently combined with DCX immunohistochemistry. Double labeled cells (i.e. colocalizing NB and DCX) were observed at different levels in the rhombencephalon. Some tangentially oriented cells were observed at marginal (Fig. 14D) and submarginal (Fig. 14E) ventrolateral regions of the caudal rhombencephalon, and also medially in the floor plate (Fig. 14F). Neurobiotin positive cells with the appearance of actively

migrating neuroblasts, extending short radial processes and colocalizing NB and DCX were also observed (Fig. 14G,H). Some of these cell processes were clearly identified as growth cones (Fig. 14G), and possible leading processes (Fig. 14H). As in this experiment the migrating neuroblasts (i.e. NB-DCX cells) appeared located far from the tracer application site (LRL), they could take the NB there before starting their journey toward ventrolateral regions. Additionally, when NB labeling was combined with immunohistochemistry to glial fibrillary acidic protein (GFAP, a glial marker), some NB positive radial processes were observed close to other GFAP-ir processes (Fig. 14I), suggesting some NB uptake by glial cells close to the tracer application point and/or a radial glia-mediated migration of labeled neuroblasts.

In one embryo at stage 32 that presented NB labeling of precerebellar nuclei after application of tracer to the cerebellum, we have also observed tangentially oriented DCX -HuC/D double labeled cells at marginal levels near the lower rhombic lips (Fig.14J,K). In the same sections, cerebellar projecting (retrogradely labeled) cells were NB-HuC/D double labeled, but DCX negative (Fig. 14L,M), which would correspond to characteristics of differentiated neurons and not to that of migrating neuroblasts.

DISCUSSION

Neurobiotin and its transport in the lesser spotted dogfish brain

The fast tracer used in this study (Neurobiotin) has the advantage that it can be easily combined with immunohistochemical techniques. Furthermore, it shows greater transport efficiency than classical neuronal tracers like horseradish peroxidase (HRP) because of its low molecular weight and similar efficiency to that of other modern tracers, like biotinylated dextranamine (BDA) and 1,1'-dioctadecyl 3,3,3',3' tetramethylindocarbocyanine perchlorate (DiI) (see Barreiro-Iglesias et al., 2008).

Due to the dual transport (anterogradely and retrogradely) of NB by neurons we could demonstrate the reciprocal connections between the cerebellar cortex and the cerebellar nucleus in the same experiment: nucleo-cortical projections (retrogradely labeled cells of the subventricular, medial and lateral cerebellar nucleus) and cortico-nuclear projections (anterogradely labeled bundles of fibers directed towards the medial cerebellar nucleus). The latter represent Purkinje cell fibers, in agreement with results of previous studies in adult sharks using the Bodian silver impregnation method and HRP transport (Larsell, 1967; Paul and Roberts, 1984; Álvarez-Otero et al., 1996). However, the origin of other NB labeled fibers and fiber endings observed in the cerebellar peduncle could not be clearly discerned, since they could represent axons of Purkinje cells, cerebellar afferents or their collaterals.

In relation to the cells of origin of NB labeled fibers observed outside the cerebellum and cerebellar nucleus, they most probably correspond with axons of precerebellar cells. Although classic studies in sharks described some Purkinje cell axons projecting out of the cerebellum (revised in Larsell, 1967; Nieuwenhuys, 1967), experimental studies with tracers and axonal degeneration applied to the cerebellar body so far failed to demonstrate such long projections and Purkinje cell axons were found to project only to the cerebellar nucleus (Ebbesson and Campbell, 1973; Paul and Roberts, 1984; Fiebig, 1988; Álvarez-Otero et al., 1996). The present developmental study indicates that the arrival of some cerebellar afferent projections to the cerebellar body precedes the arrival of Purkinje axons to the cerebellar nucleus. Therefore, all extracerebellar NB labeled fibers after application of the tracer to the cerebellar body may correspond to processes of precerebellar cells.

The cerebellar efferent pathways in sharks under an evolutionary perspective

The concurrent presence in sharks of a cerebellar body with Purkinje cells and the cerebellar nucleus implies the appearance of indirect pathways for the outputs of the cerebellum in the earliest vertebrates with true cerebellum. These pathways (from cerebellar cortex to cerebellar nucleus and then towards extracerebellar regions) have been conserved in the most modern amniotes. Vertebrate groups with a divergent cerebellar evolution, as the actinopterygian fishes, have developed alternative output structures for the cerebellar body (eurydendroid cells) which do not form a definite cerebellar nucleus, but anyway maintained a largely indirect output from the cerebellar cortex (Finger, 1978a; Murakami and Morita, 1987; Huesa et al., 2003; Ikenaga et al., 2005; Folgueira et al., 2006). Furthermore, in teleosts, birds and mammals some Purkinje cells (mainly in the vestibulocerebellum) directly project outside the cerebellum (Arends and Zeigler, 1991; Voogd et al., 1991; Straka et al., 2006), indicating the existence in some gnathostomes of a dual cerebellar cortex circuitry that includes both direct and indirect efferent pathways.

Comparison of cerebellar afferents in the lesser spotted dogfish and other vertebrates

Most of precerebellar nuclei observed in juveniles of the lesser spotted dogfish after NB application (present results) have also been observed in the thornback guitarfish after WGA-HRP (wheat germ agglutinin-horseradish peroxidase) and in the Atlantic stingray after BDA (byotinilated dextran amine) injections in the cerebellar body (Fiebig, 1988; Puzdrowski and Gruber, 2009). Differences were mainly due to differential designations of segmental territories.

In the diencephalon, the precerebellar lateral and central pretectal nuclei we described in the lesser spotted dogfish correspond to similar pretectal nuclei of the two batoids (Fiebig, 1988; Puzdrowski and Gruber, 2009), but a periventricular pretectal nucleus equivalent to that of the guitarfish was not distinguished in the dogfish. In the thalamus, the marginal precerebellar population in *S. canicula* corresponds to the dorsal accessory optic nucleus reported in the thornback guitarfish and Atlantic stingray. In the mesencephalon, reticular cells (probably equivalent to the ventral accessory optic nucleus and nucleus reticularis subcuneiformis of batoids) and cells of the nucleus ruber project to the cerebellar body in the three elasmobranch species. There has been some discrepancy about identification of a nucleus ruber in *S. canicula* because of the absence of a rubro-spinal tract, which is present in ray (Smeets and Timerick, 1981). Nonetheless, its existence was proved by the rubro-tectal pathway and its activation by stimulation of cerebellar nuclear cells (Smeets, 1982; Smeets et al., 1983). Furthermore, the nucleus ruber of non-mammalian vertebrates differs from that of mammals in their connections (Sarrafizadeh and Houk, 1994), but they may be considered homologous owing to their equivalent tegmental location. Some authors have also described a rubro-cerebellar projection (from the nucleus ruber to the cerebellar cortex) in mammals and birds (Dietrichs and Walberg, 1983; Wild, 1992). The precerebellar cells observed in the superior reticular formation of the lesser spotted dogfish correspond to different nuclei described in batoids (Fiebig, 1988; Puzdrowski and Gruber, 2009) as forming part of the mesencephalic reticular formation. Since these batoids precerebellar nuclei were located caudally to the oculomotor nerve root and, on the basis of the segmental model proposed for *S. canicula*, they must actually belong to the rostral rhombencephalon. The lesser spotted dogfish isthmic group might be equivalent to the nucleus F described in batoids. Additionally, in both *S. canicula* and the thornback

guitarfish (but not in the Atlantic stingray) the locus coeruleus appeared to contain precerebellar cells. In *S.canicula*, nucleo-cortical cells were labeled in the subventricular, medial and lateral parts of the cerebellar nucleus; by contrast in the thornback guitarfish precerebellar cells of the cerebellar nucleus were described only in the medial and lateral parts (Fiebig, 1988), and do not appear to be present in the Atlantic stingray (Puzdrowski and Gruber, 2009). In mammals, nucleo-cortical projections arise from all subdivisions of the different cerebellar nuclei (Gould, 1979; Tolbert, 1982; Batini et al., 1989). At caudal rhombencephalic levels, the labeled precerebellar cells of the lateral reticular and the nucleus of the descending trigeminal root areas may be correspondent in all three species (Fiebig, 1988; Puzdrowski and Gruber, 2009; present results). With respect to the inferior olive, the existence of two different subpopulations also coincides in both shark and batoids (Kooy, 1916). Nevertheless, the extension of their subpopulations was different. Therefore, a similar topographic connection between the inferior olive and the cerebellum might occur also in *S.canicula*. The existence of climbing fibers had been questioned in elasmobranchs (for review, see Smeets et al., 1983), but there are morphological evidences of their existence in *S. canicula* (Álvarez-Otero et al., 1996). In the lesser spotted dogfish (present study) and batoids (Fiebig, 1988; Puzdrowski and Gruber, 2009), the demonstration of precerebellar cells in the inferior olive supports the existence of these fibers. Although precerebellar cells in the spinal cord were observed in the three elasmobranch species, cells in dorsal column were only observed in batoids (Fiebig, 1988; Puzdrowski and Gruber, 2009).

Similarities were also noted with regard to cerebellar efferents. In the cerebellum of the thornback guitarfish, Purkinje axons were described generally projecting to medial and lateral parts of the cerebellar nucleus and to an area located dorsally (Fiebig,

1988). Likewise, in lesser spotted dogfish we identified Purkinje axons directed towards the medial part of the cerebellar peduncle, and probably also those directed to its dorsomedial and lateral regions.

Another similarity with results of experimental studies in batoids (Fiebig, 1988; Puzdrowski and Gruber, 2009) is the absence of labeled cells in the lesser spotted dogfish hypothalamus. Even after application of the tracer to the anterior lobe (or rostral part) of the cerebellar body, we have not observed any NB labeling in the hypothalamus. This does not support the existence of a lobo-cerebellar tract in chondrichthyans, as also suggested by Northcutt and Brunken (1984) and Fiebig (1988), and unlike classical descriptions of cells in the inferior hypothalamic lobe projecting to the cerebellum (Ariëns Kappers, 1906; Sterzi, 1912; Smeets and Boord, 1985).

Some differences were also noted in the precerebellar populations of elasmobranchs. On the one hand, labeled cells in the mesencephalic trigeminal nucleus and raphe were not described in the thornback guitarfish or Atlantic stingray. Electrophysiological evidence supports the existence of a trigemino-cerebellar tract in *Scyliorhinus* and *Mustelus* (Roberts and Witkovsky, 1975). On the other hand, other precerebellar nuclei described in the thornback guitarfish and/or Atlantic stingray (such as oculomotor and trochlear nuclei, nucleus of the medial longitudinal fascicle, locus subcoeruleus or octaval nuclei) do not project to the cerebellar body in the lesser spotted dogfish; however, the possibility that they have some equivalence of batoids precerebellar reticular nuclei with the precerebellar groups observed along the *S. canicula* inferior reticular formation should be considered.

Therefore, this study reveals that most of cerebellar body connections of the lesser spotted dogfish are coincident with those of batoids, even using different tract-tracing methods. This allows us to establish a generalized pattern of cerebellar afferents

and efferents in cartilaginous fishes. Furthermore, as the morphology of the cerebellum in the lesser spotted dogfish is simpler than in batoids, afferent projections to the cerebellar body in this species are in all probability closer to the ancestral condition, making *Scyliorhinus canicula* a useful model to study the development of basic cerebellar connections in chondrichthyans.

Comparison of experimental results on the precerebellar nuclei reported in bony fishes with those obtained in elasmobranches indicates that some afferents to the cerebellar body are shared between cartilaginous and bony fishes. Hodological studies reported the afferents to the cerebellar body both in primitive (the Siberian sturgeon *Acipenser baeri*; Huesa et al., 2003) and modern (teleosts: Finger, 1978b; Ito et al., 1982; Meek et al., 1986a,b; Wullimann and Northcutt, 1988; Xue et al., 2004; Folgueira et al., 2006) bony fishes. In teleost species precerebellar neurons were mainly observed in the diencephalon (mainly in pretectal nuclei, which are highly specialized), mesencephalon (mostly in the lateral valvular nucleus, but also in the Edinger-Westphal nucleus and perilemniscular tegmentum) and rhombencephalon (locus coeruleus, descending octaval nucleus, nucleus of the descending trigeminal root, nucleus of the commissure of Wallenberg, raphe nucleus, lateral reticular nucleus, inferior reticular formation and inferior olive), and in the spinal cord. All bony fishes have extensive pretecto-cerebellar projections, as elasmobranchs. Thalamo-cerebellar projections were observed in some teleosts (catfish: Karten and Finger, 1976: sunfish and goldfish: Wullimann and Northcutt, 1988; holocentrids: Xue et al., 2004). Unlike teleosts, which exhibit highly specialized mesencephalic precerebellar nuclei, the precerebellar neurons of the mesencephalon in the *A. baeri* appear scattered without forming defined nuclei (Huesa et al., 2003) and are more similar to those observed in *S. canicula*. On the other hand, most precerebellar populations of the teleost rhombencephalon are comparable to

precerebellar populations observed in the lesser spotted dogfish. The inferior olive is a conspicuous cell group that has been described in all fish groups (Kooy, 1916), although its presence in agnathans has not been definitively proved. Its projections to the cerebellar body have been demonstrated in all groups of bony and cartilaginous fishes (Wullimann and Northcutt, 1988; Fiebig, 1988; Huesa et al., 2003; Xue et al., 2004; Folgueira et al., 2006; present results). Different experimental approaches have demonstrated that in teleosts axons of inferior olivary cells end in the cerebellar body as climbing fibers (Finger, 1983; Xue et al., 2008; Bae et al., 2009), and this is assumed to occur in other jawed fishes, including elasmobranchs (Fiebig, 1988; Álvarez-Otero et al., 1996; Puzdrowski and Gruber, 2009; present results).

Insights into development of cerebellar connections in elasmobranchs

Pretecto-cerebellar connections are largely known to be related to cerebellar control of visual reflexes in amniotes (for review, see De Castro et al., 1998), mediating the optokinetic reflex. This could be also applied to elasmobranchs due to the existence of precerebellar cells in the pretectum and thalamus (Fiebig, 1988; Puzdrowski and Gruber, 2009; present results), which correspond to diencephalic nuclei that receive retinal projections (for review, see Smeets et al., 1983). On the other hand, the maturation of photoreceptors in the retina of the lesser spotted dogfish, which begins at early stage 32 and is completed at the end of this stage (Ferreiro-Galve et al., 2010), is nearly concurrent with the development of pretecto-cerebellar projections (present results). This supports the possibility that the onset of control of visual reflexes by the cerebellum occurs at the beginning of stage 32, which would be related to the functional maturation of the retina.

The observation of bending axons coming from the cerebellar cortex and directed towards the medial part of cerebellar peduncle at intermediate stage 32 is indicative of the onset of Purkinje cells maturation at this moment, which is in support of identification of this type of axons in juveniles (see above). Conversely, the bending fibers coming from rhombencephalic tegmentum observed in embryos could correspond to collateral axonic processes or secondary branches of cerebellar afferents (Ruigrok et al., 1995).

The NB labeled fibers observed in the ganglion of trigeminal nerve could correspond to the trigeminal fibers projecting to cerebellum described in previous studies (for review, see Larsell, 1967). Because the diffusion of the tracer cannot be completely discarded, the possibility that labeled fibers in the trigeminal nerve may come from labeled neurons of mesencephalic trigeminal nucleus may be also considered. However, the labeling of these cells supports the cerebellar projection of these mesencephalic trigeminal cells along the trigeminocerebellar tract demonstrated in *Scyliorhinus* by Roberts and Witkovsky (1975). In the caudal rhombencephalon, reticular cells projecting to cerebellum were not labeled until late embryos, despite the fact that many rhombencephalic nuclei start to differentiate at earlier stages (Rodríguez-Moldes et al., 2011). This observation may be attributed to the completion of the axonal growth being coincident with the establishment of layering in the cerebellar cortex at stage 32 (Rodríguez-Moldes et al., 2008). In fact, the gradual increase in incoming cerebellar afferents observed along the stage 32 (present results) coincides with the progressive growth and maturation of the granular eminences (Rodríguez-Moldes et al., 2008). In adults, these lesser spotted dogfish eminences contain conspicuous mossy fiber rosettes (Álvarez-Otero, 1990; Anadón et al., 2009), the type of fiber terminals produced by most of the cerebellar afferents.

In the inferior olive, the observation of first cells projecting to the cerebellum at intermediate stage 32 indicates that the first climbing fibers reach their cortical targets by this stage, which is concurrent with the observation of the first labeled Purkinje cell axons in the cerebellar peduncle (see above). This suggests that the maturation of the olivo-cerebellar circuit begins when the Purkinje cell layer is well defined at stage 32 (Rodríguez-Moldes et al., 2008; Chaplin et al., 2010). The gradual increase in the number of labeled Purkinje cell axons in the cerebellar peduncle and of retrogradely labeled cells in the inferior olive suggests a progressive maturation of Purkinje cells, and progressive growth of axons of inferior olive cells, too. This is supported by the absence of migrating cells (DCX negative) and the presence of differentiated neuronal somata (HuC/D positive) in the inferior olive area at intermediate stage 32 observed in this work. The inferior olive of fishes has been considered to be homologous to the medial accessory olivary nucleus of mammals (Kooy, 1916; Crosby, 1969), which consists of different cell types (De Zeeuw et al., 1998). Our observations of two morphological precerebellar cell types (mostly round and only a few elongated) both in embryos and in juveniles, and previously reported in adults (for review, see Smeets et al., 1983), would support this equivalence with mammals.

First connections between the spinal cord and cerebellum appeared at the beginning of stage 32, before the onset of the first olivo-cerebellar projections. Furthermore, the presence of labeled fibers in the anterior medullary velum and cerebellar peduncle at early stage 32 after applying the tracer to the rostral spinal cord revealed that the two spino-cerebellar tracts develop rather early. These tracts have been considered as the homologs of the ventral and dorsal spino-cerebellar tracts of higher vertebrates (Ariëns Kappers, 1921). Our developmental observations are consistent with the statement that this ascending spinal system ends mostly ipsilaterally in the

cerebellum (Ariëns Kappers et al., 1936). The contralateral retrogradely labeled cells in the spinal cord of the lesser spotted dogfish could be related with an unsuccessful location of ipsilateral cells or a much caudal location of these cells. An intriguing observation was the labeling of some Rohon-Beard cells located in the dorsal marginal zone of the embryonic spinal cord (not shown). Whether these transient primary sensory cells actually project or not to the cerebellum, cannot be ascertained since the possibility that they took the tracer via dendritic endings in the skin during the application procedure cannot be ruled out.

Our observations reveal the progressive increase in number of NB labeled cells in each precerebellar nucleus over time, which could reflect an increase in the number of synaptic terminals produced by precerebellar fibers during development.

Comparative developmental pattern of precerebellar nuclei

The order of appearance of spino-cerebellar and olivo-cerebellar projections in the lesser spotted dogfish is similar to that reported in birds (Okado et al., 1987; Chedotal et al., 1996; Arakawa et al., 2008)and mammals (Ashwell and Zhang, 1992; Paradies and Eisenman, 1993; Grishkat and Eisenman, 1995). Spino-cerebellar fibers reached its target (at early stage 32 in lesser spotted dogfish, HH33 in chick, E15 in rat and E13/14 in mouse) before cerebellar projecting fibers of the inferior olive (at intermediate stage 32 in lesser spotted dogfish, HH35 in chick, E17 in rat and E15/16 in mouse). The embryonic stage when spino-cerebellar fibers reach the cerebellum, roughly coincides with the transition between the second and third developmental periods proposed by Rodríguez-Moldes et al. (2011). Nevertheless, the cerebellar connection of the different precerebellar nuclei in lesser spotted dogfish happens in a relatively shorter period of time than in chick and rat embryos, as shown in Figure 15.

An extended period of development of cerebellar afferents could allow a further refinement of synaptic connections in amniotes cerebellum, especially in rats, which is probably related to much more complex circuits of control of movements.

The arrival to the cerebellum of inferior olive projections appears to happen at roughly equivalent developmental stages in dogfishes, chicken and rats. Accordingly, it may allow us to establish counterpart or homologous stages with respect to the development of the cerebellar system in the three species, even though at that time, at least in mammals, the cerebellum and more specifically Purkinje cells, have not generally completed their maturation (Ohtsuki and Hirano, 2008; Kaneko et al., 2011). Previous studies describing climbing fiber synapses with Purkinje perikarya in the adult lesser spotted dogfish (Álvarez-Otero et al., 1993) have found similarities with transient phases of synaptogenesis that happens during development in mammals, particularly with the "phase du nid" of Cajal (1911), when climbing fibers start to connect with Purkinje cell perikarya. Our results support the suggestion that the first phase of connections of climbing fibers with Purkinje cells in the rat correspond to the primordial condition observed in elasmobranchs (Álvarez-Otero, 1990).

With regard to the arrival of projections of other precerebellar nuclei, as the lateral reticular nucleus and the nucleus of the descending trigeminal root (spinal tract), they appear after the arrival of spinal and olivary afferents both in rats (Ashwell and Zhang, 1992) and the lesser spotted dogfish . However, in this shark it happens relatively earlier in development (see Fig. 15). Another shared feature is that the appearance of cerebellar connections does not occur in a rostro-caudal direction (Ashwell and Zhang, 1992). In fact, in the lesser spotted dogfish, spinal connections arrive at the cerebellum before those from the caudal rhombencephalon (at early and intermediate stage 32, respectively). However, except for the spinal cord and the nuclei

of the diencephalon, the connections of the rest of precerebellar nuclei present a centrifugal order of arrival at the cerebellum. On the other hand, in the lesser spotted dogfish precerebellar cells of the raphe nuclei were labeled during development, which differs from that reported in the rat (Ashwell and Zhang, 1992).

In *Xenopus laevis*, the arrival at the cerebellum of most of cerebellar afferent connections is concentrated in a quite short period of time (van der Linden and ten Donkelaar, 1987). Nevertheless, the order of arrival differs from the order observed in *S. canicula*, in that the cerebellar afferent connections arising from vestibular nuclei, inferior olive, trigeminal and reticular nuclei arrive first, followed by the connections from spinal cord cells and cells of the region of the motor nucleus of the vagal nerve. These developmental dissimilarities of *Xenopus* with respect to the lesser spotted dogfish and amniotes could be due to the major changes that frog tadpoles suffer during metamorphosis. Additionally, in *Xenopus*, retrogradely labeled precerebellar cells from the mesencephalic tegmentum or inferior raphe nucleus (as in the rat, see above) were not observed during development (van der Linden and ten Donkelaar, 1987).

Neurochemical characterization of precerebellar nuclei in the lesser spotted dogfish: a comparative study

The combined tract-tracing and neurochemical study of precerebellar neurons of *Scyliorhinus canicula* revealed that NB labeled cells mostly colocalized with CR and Glut, the Glut-ir probably corresponding with glutamatergic or excitatory cells. The NB-NeuN double labeling was confined to reticular cells in the mesencephalic and rhombencephalic tegmentum. The neuropil surrounding precerebellar nuclei showed generally numerous GAD-ir processes, which indicates GABAergic (inhibitory) innervation. In addition, some precerebellar nuclei (reticular formation, cerebellar

nucleus and inferior olive) were also innervated by serotoninergic (5-HT-ir), catecholaminergic (TH-ir) and cholinergic (ChAT-ir) fibers.

A noticeable observation in the lesser spotted dogfish was that all precerebellar nuclei contained CR-ir precerebellar cells. CR-ir precerebellar cells were also reported in the pretectum and mesencephalon in birds (De Castro et al., 1998; Iwaniuk et al., 2009), and in the spinal cord in mammals (Fu et al., 2012), suggesting shared features. In anamniotes, although the CR has been identified in nuclei recognized as precerebellar nuclei (Castro et al., 2006; Morona and González, 2009; Graña et al., 2012), its projection to the cerebellum had not been demonstrated by tracer-CR double labeling. So, this is the first study in anamniotes demonstrating that all precerebellar nuclei contain CR-ir cells projecting to cerebellum. In amniotes, CR has been related to protection of neurons from potentially damaging intracytoplasmic concentrations of calcium (De Castro et al., 1998), regulation of calcium pools critical for synaptic plasticity (Schwaller et al., 2002), association to both excitatory and inhibitory cells (Fu et al., 2012), and prevention of overexcitation of the cerebellar-projecting cells (Iwaniuk et al., 2009). CR may play similar roles in fishes.

The NeuN protein, though it is a general neuronal marker, shows a differential expression in the cerebellar system, being present in granule cells and absent in Purkinje cells. In addition, it is present in precerebellar nuclei such as the lateral reticular nucleus but absent in inferior olivary neurons (Mullen et al., 1992; Wolf et al., 1996; Ono et al., 2004). Similar pattern has been observed in the cerebellar body of the lesser spotted dogfish (results not shown) being also a very useful marker to discern the NeuN negative cells of the inferior olive from the NeuN positive precerebellar neurons of the reticular formation.

The cerebellum of the lesser spotted dogfish receives projections from putative glutamatergic and cholinergic cells, as observed by means of NB-Glut and NB-ChAT double labeling. This suggests that most cerebellar afferents are excitatory, which is in agreement with results from electrophysiological studies of evoked potentials in elasmobranch cerebellum in response to peripheral and white matter stimulation (Paul, 1967; Young, 1980; Paul and Roberts, 1983). Excitatory (glutamatergic or cholinergic) inputs from the rhombencephalic reticular cells projecting to the cerebellum were also described in mammals (Wang et al., 1993; Lan et al., 1995).

The presence of monoaminergic (5-HT-ir and TH-ir) precerebellar nuclei differs among vertebrates. In amniotes, retrogradely labeled precerebellar cells showing 5-HT immunoreactivity were found in different regions of the brainstem, although they were generally scant (Ito, 1984; Bishop and Ho, 1985; Walker et al., 1988; Kerr and Bishop, 1991). Precerebellar cells double labeled with different tracers and immunomarkers of catecholamines were also found in the ventral tegmental area, locus coeruleus and reticular formation of amniotes (Tohyama, 1976; Ikai et al., 1992). Nevertheless, in fishes, precerebellar cells do not appear to colocalize with 5-HT or TH immunoreactivity (Meek et al., 1986b), except for some NB-TH double labeled cells reported in the locus coeruleus in the thornback guitarfish (Fiebig, 1988). In the lesser spotted dogfish, despite the abundance of 5-HT-ir and TH-ir fibers in the cerebellar cortex and cerebellar peduncle (Carrera et al., 2008, 2012; present results), we only observed very few NB-TH double labeled cells in the locus coeruleus but any NB-5-HT double labeled cells. A possible explanation for the scant number of monoaminergic precerebellar cells observed in lesser spotted dogfish is that their axons had widespread ramification, as it has been described for some serotoninergic populations in mammals (Bishop and Ho, 1985), making difficult to label them in transport experiments.

Moreover, the existence in dogfish of cerebellar afferents that do not uptake efficiently Neurobiotin cannot be ruled out.

In the lesser spotted dogfish cerebellar nucleus, previous studies have revealed the presence of Glut-ir and GABA-ir cells (Álvarez-Otero et al., 1996). In the present work we show that some Glut-ir nuclear cells actually project to cerebellar cortex (NB-Glut double labeling), suggesting they provide excitatory feedback from the nucleus. Nevertheless, some Glut-ir cells in the subventricular region that contain glutamate may also express GABAergic markers, as suggested in adults (Álvarez-Otero et al., 1996). Thus, the possibility that the lesser spotted dogfish cerebellar nucleus provides GABAergic (inhibitory) feedback to the cerebellar cortex cannot be ruled out. Nucleo-cortical projections from GABAergic and glutamatergic cells to cerebellar cortex have been described in the rat (Tolbert, 1982; Batini et al., 1992).

The inferior olive deserves special attention, because of the functional importance of the olivo-cerebellar climbing fiber system, as it is involved in learning and the timing of movements (De Zeeuw et al., 1998). The neurochemical markers of the olivo-cerebellar system in the lesser spotted dogfish were rather similar to that described in other vertebrates. As in mammals (Barmack et al., 1993), dogfish inferior olivary cells are immunonegative for ChAT (Anadón et al., 2000; present results) but, as in birds, some cells were CR-ir (De Castro et al., 1998; Iwaniuk et al., 2009). Although in the rat some cells of the inferior olive were GAD-ir (Fredette et al., 1992), in the lesser spotted dogfish these cells were not observed in the nucleus although GAD immunoreactivity was clearly distinguished in the surrounding neuropil. In the case of NB-Glut-ir olivary cells, they probably represent glutamatergic cells, as it was shown in mammals (Miyazaki et al., 2003) and birds (Islam and Atoji, 2008).

Concerning the innervation of the lesser spotted dogfish inferior olive we have also found some correspondence with other gnathostomes. The GAD immunoreactivity described in the inferior olive neuropil may correspond with the conspicuous GABAergic innervation of the inferior olive in mammals (Fredette and Mugnaini, 1991). In mammals, the inferior olive largely receives GABAergic projections from the cerebellar nuclei (Monaghan et al., 1986; Schwarz and Schmitz, 1997; Sotelo and Chedotal, 2005). If GABA-ir cerebellar nuclear neurons also project to the inferior olive in the lesser spotted dogfish has not been investigated. Furthermore, in mammals, the inferior olive was also innervated by serotoninergic (Bishop and Ho, 1986), dopaminergic (in the ventrolateral outgrowth of inferior olive, (Toonen et al., 1998) and cholinergic (ChAT-ir associated to the dorsal cap, a small caudal subnucleus of the medial accessory olive; Barmack et al., 1993; Caffe et al., 1996) fibers. Whether neurochemically different neuropil territories are also present in the lesser spotted dogfish has not been investigated, although TH-ir and ChAT-ir boutons are mostly observed in the caudal subpopulation of the inferior olive. The existence of two cell subpopulations in the inferior olive of *S. canicula* receiving different types of innervation, previously suggested with calcitonin gene-related peptide-like (CGRP) in adults (Molist et al., 1995), could be involved in differential topographic olivo-cerebellar projections previously reported in the thornback guitarfish (Fiebig, 1988; Puzdrowski and Gruber, 2009; see above) and bony fishes (Meek et al., 1986b). In mammals, the topographic correspondence between the different parts of inferior olive and cerebellar cortex is much more complex (Sugihara and Shinoda, 2007). Therefore, certain neurochemical similarities seem to be maintained throughout evolution.

The olivary glomeruli are defined as the set of dendritic processes of cells of the inferior olive and their associated excitatory and inhibitory fiber endings arising from

different nuclei (De Zeeuw et al., 1998; Sotelo, 2004; Sotelo and Chedotal, 2005). In the lesser spotted dogfish olivary glomeruli were not anatomically outlined, although tangles of dendrites of NB labeled cells (illustrated in Fig. 9L) and multiple fiber endings positive for the different immunomarkers were observed in the area of the inferior olive. This complex organization suggests that the inferior olive integrates information from different motor and sensorial areas, and that it is involved in timing and learning functions, as reported in mammals. The combined excitatory and inhibitory inputs to dendritic spines of olivary cells are compatible with both the timing and learning hypothesis (De Zeeuw et al., 1998).

Towards the identification of rhombic lip derivatives in shark

We approached the origin of precerebellar neuronal populations in the lesser spotted dogfish rhombencephalon by studying developmental stages with markers for migrating neuroblasts, and by applying NB to the lower rhombic lip *in vitro*. The observation of colocalization of DCX-HuC/D immunoreactivity in cells of the outer layer of the neural tube (rostral hindbrain) in the earliest embryos studied (S23) revealed the presence of tangentially migrating neuroblasts. They could correspond to cells of the tangential migratory stream from the upper rhombic lip (URL), because the neuroblasts appear to migrate dorsoventrally and then change their direction, rostral or caudalwards. This kind of migrations of neuroblasts from the URL has been demonstrated experimentally in zebrafish (Köster and Fraser, 2001; Distel et al., 2010; Volkmann et al., 2010; Wullimann et al., 2011), chick (Lin et al., 2001; Wilson and Wingate, 2006) and mouse (Gilthorpe et al., 2002; Wang et al., 2005). Of note, the onset of migration of some URL derived cell types happens earlier than in those derived from lower rhombic lip (LRL) (Wang et al., 2005), as we have observed in *S. canicula*.

The NB-DCX containing cells observed in the embryonic lesser spotted dogfish rhombencephalon at stage 30, three days after the tracer was applied to the LRL, would correspond to tangentially migrating cells that had taken the tracer in the LRL and then moved away this lip, as suggested by the expression of DCX in these cells. Therefore, these markers provide some evidence of the existence of relatively fast migrations of cells derived from the LRL. According to results of experimental studies in mouse and chick embryos (Ono et al., 2004; Kawauchi et al., 2006; Okada et al., 2007; Watanabe and Murakami, 2009), they could correspond to different prospective precerebellar nuclei, depending on their location. In the case of the migrating cells (NB-DCX double labeled), the marginal cells could correspond to forerunners of reticular cells, while submarginal cells could represent forerunners of the inferior olive, since it has been previously reported that they follow marginal and submarginal pathways, respectively (Kuwako et al., 2010). Then, the migrating neuroblasts located at the floor plate midline and those radially oriented could also correspond to prospective lateral reticular nucleus, because some authors (Kawauchi et al., 2006; Okada et al., 2007) describe this population in mammalian embryos as crossing the midline and secondarily radially migrating. The existence in lesser spotted dogfish embryos of two types of close processes labeled for NB and GFAP shown in Figure 14I provides some evidence of the association of migrating neuroblasts (NB labeled) with radial glia processes (GFAP-labeled) during secondary radial migration, as described in mammals (Kawauchi et al., 2006).

Additionally, the DCX-HuC/D double labeled cells observed at stage 32 embryos in the margin of the rhombencephalon suggest that the tangential marginal migratory stream is maintained during this stage. These cells could be derived from the lower rhombic lip and thus interpreted as precursors of precerebellar nuclei. In fact,

there is evidence that Pax6, a transcription factor present in rhombic lip and in cells migrating away from it to form precerebellar nuclei (Engelkamp et al., 1999), is contained in cells forming a marginal stream in the rhombencephalon of *S. canicula* embryos at stages 31 and 32 (Ferreiro-Galve, 2010). On the other hand, the fact that cerebellar projecting (retrogradely labeled) cells observed at stage 32 embryos were differentiated neurons suggests that NB-DCX double labeled cells observed in stage 30 (Fig. 14D-I) correspond to neuroblasts that had taken the tracer in the application site (LRL) previously to the onset of migration, but not to retrogradely labeled cells via their axonal processes.

Although the existence of tangential migratory streams of neuroblasts from the upper and lower rhombic lips in sharks appears evident, it would be interesting to carry out studies to more accurately characterize these tangential migratory pathways, to genetically identify the rhombic lip derivatives and to elucidate their cell lineage and destination. From a comparative point of view, such studies would improve our knowledge on the evolution of these migratory processes and development of precerebellar nuclei.

CONCLUSIONS

Present results represent the first developmental study of connections of the cerebellar body in fishes. The characterization of precerebellar nuclei in the lesser spotted dogfish done following a segmental model of the brain, reveals similarities with other cartilaginous fishes and also shared traits with other vertebrates. Regarding to the developmental analysis, these results revealed that incoming of cerebellar afferents is concurrent with the establishment of layering in the cerebellum. Then new precerebellar neurons become gradually demonstrable by retrograde transport, which reflects the

progressive maturation of the granular and Purkinje cell layers. The first axons of Purkinje cells reach the cerebellar peduncle at the time when the first precerebellar neurons of the inferior olive became retrogradely labeled (intermediate stage 32), characterizing the onset of Purkinje cells differentiation. Moreover, the knowledge of the development of the olivo-cerebellar projection may allow comparisons with the olivo-cerebellar system of other gnathostomes. The development of the spino-cerebellar projections in the lesser spotted dogfish precedes that of the olivo-cerebellar projection, as in amniotes, suggesting that cerebellar afferents from the spinal cord were involved in early control by the cerebellum of body movements. The similarities reported here between the neurochemical signature of the diverse precerebellar nuclei of the lesser spotted dogfish and those in amniotes probably indicate high degree of evolutionary conservation. Additionally, the existence of tangential and radial migrations of precerebellar cells originated in the rhombic lips in *S. canicula* suggests that the developmental pattern of precerebellar nuclei appeared very early in gnathostome evolution, and has been well preserved in gnathostome phylogeny.

In summary, the findings of the present hodologic, neurochemical and developmental study of precerebellar centers in the lesser spotted dogfish show numerous similarities between this shark and tetrapods, some of which may represent synapormorphies or homologies. Therefore, studies in this species shed light on the ancestral organization of the cerebellar system, and mark again *Scyliorhinus canicula* as a good model organism for developmental studies of cerebellar connections.

LITERATURE CITED

Álvarez-Otero R. 1990. Estudio citarquitectónico y ultraestructural del cerebelo de la pintarroja, *Scyliorhinus canicula L*. Doctoral Thesis, University of Santiago de Compostela, Spain.

Álvarez-Otero R, Anadón R. 1992. GOLGI cells of the cerebellum of the dogfish, *Scyliorhinus canicula* (elasmobranchs): a GOLGI and ultrastructural study. J Hirnforsch 33:321-327.

Álvarez-Otero R, Regueira SD, Anadón R. 1993. New structural aspects of the synaptic contacts on Purkinje cells in an elasmobranch cerebellum. J Anat 182:13-21.

Álvarez-Otero R, Pérez SE, Rodríguez MA, Adrio F, Anadón R. 1995. GABAergic neuronal circuits in the cerebellum of the dogfish *Scyliorhinus canicula* (Elasmobranchs): an immunocytochemical study. Neurosci Lett 187:87-90.

Álvarez-Otero R, Pérez SE, Rodríguez MA, Anadón R. 1996. Organisation of the cerebellar nucleus of the dogfish, *Scyliorhinus canicula L.*: a light microscopic, immunocytochemical, and ultrastructural study. J Comp Neurol 368:487-502.

Anadón R, Molist P, Rodríguez-Moldes I, López JM, Quintela I, Cerviño MC, Barja P, González A. 2000. Distribution of choline acetyltransferase immunoreactivity in the brain of an elasmobranch, the lesser spotted dogfish (*Scyliorhinus canicula*). J Comp Neurol 420:139-170.

Anadón R, Ferreiro-Galve S, Sueiro C, Graña P, Carrera I, Yáñez J, Rodríguez-Moldes I. 2009. Calretinin-immunoreactive systems in the cerebellum and cerebellum-related lateral-line medullary nuclei of an elasmobranch, *Scyliorhinus canicula*. J Chem Neuroanat 37:46-54.

Arakawa T, Iwashita M, Matsuzaki F, Suzuki T, Yamamoto T. 2008. Paths, elongation, and projections of ascending chick embryonic spinal commissural neurons after crossing the floor plate. Brain Res. 1223: 25-33.

Arends JJ, Zeigler HP. 1991. Organization of the cerebellum in the pigeon (*Columba livia*): I. Corticonuclear and corticovestibular connections. J Comp Neurol 306:221-244.

Ari C, Kálmán M. 2008. Evolutionary changes of astroglia in Elasmobranchii comparing to amniotes: a study based on three immunohistochemical markers (GFAP, S-100, and glutamine synthetase). Brain Behav Evol 71:305-324.

Ariëns Kappers CU. 1906. The structure of the teleostean and selachian brain. J Comp Neurol 16: 1-112.

Ariëns Kappers CU. 1921. Vergleichende Anatomie des Nervensystems. Vol. 2. Haarlem: EF Bohn Verlag.

Ariëns Kappers CU, Huber GC, Crosby EC. 1936. The comparative anatomy of the nervous system of vertebrates including man. Vol. 1. New York: Macmillan.

Ashwell KW, Zhang LL. 1992. Ontogeny of afferents to the fetal rat cerebellum. Acta Anat (Basel) 145:17-23.

Bae YK, Kani S, Shimizu T, Tanabe K, Nojima H, Kimura Y, Higashijima S, Hibi M. 2009. Anatomy of zebrafish cerebellum and screen for mutations affecting its development. Dev Biol 330:406-426.

Ballard WW, Mellinger J, Lechenault H. 1993. A series of normal stages for development of *Scyliorhinus canicula*, the lesser spotted dogfish (Chondrichthyes: Scyliorhinidae). J Exp Zool 267:318-336.

Barmack NH, Fagerson M, Errico P. 1993. Cholinergic projection to the dorsal cap of the inferior olive of the rat, rabbit, and monkey. J Comp Neurol 328:263-281.

Barreiro-Iglesias A, Villar-Cerviño V, Anadón R, Rodicio MC. 2008. Descending brain-spinal cord projections in a primitive vertebrate, the lamprey: cerebrospinal fluid-contacting and dopaminergic neurons. J Comp Neurol 511:711-723.

Batini C, Buisseret-Delmas C, Compoint C, Daniel H. 1989. The GABAergic neurones of the cerebellar nuclei in the rat: projections to the cerebellar cortex. Neurosci Lett 99:251-256.

Batini C, Compoint C, Buisseret-Delmas C, Daniel H, Guegan M. 1992. Cerebellar nuclei and the nucleocortical projections in the rat: retrograde tracing coupled to GABA and glutamate immunohistochemistry. J Comp Neurol 315:74-84.

Bishop GA, Ho RH. 1985. The distribution and origin of serotonin immunoreactivity in the rat cerebellum. Brain Res 331:195-207.

Bishop GA, Ho RH. 1986. Cell bodies of origin of serotonin-immunoreactive afferents to the inferior olivary complex of the rat. Brain Res 399:369-373.

Butts T, Chaplin N, Wingate RJ. 2011. Can clues from evolution unlock the molecular development of the cerebellum? Mol Neurobiol 43:67-76.

Caffe AR, Hawkins RK, De Zeeuw CI. 1996. Coexistence of choline acetyltransferase and GABA in axon terminals in the dorsal cap of the rat inferior olive. Brain Res 724:136-140.

Cajal SR. 1909-11. Histologie du Systéme Nerveux de L'Homme et des Vertebrés. Paris: A. Maloine.

Carr CE, Fujita I, Konishi M. 1989. Distribution of GABAergic neurons and terminals in the auditory system of the barn owl. J Comp Neurol 286:190-207.

Carrera I, Molist P, Anadón R, Rodríguez-Moldes I. 2008. Development of the serotoninergic system in the central nervous system of a shark, the lesser spotted dogfish *Scyliorhinus canicula*. J Comp Neurol 511:804-831.

Carrera I, Anadón R, Rodríguez-Moldes I. 2012. Development of tyrosine hydroxylase-immunoreactive cell populations and fiber pathways in the brain of the dogfish *Scyliorhinus canicula*: New perspectives on the evolution of the vertebrate catecholaminergic system. J Comp Neurol 520:3574-3603.

Castro A, Becerra M, Manso MJ, Anadón R. 2006. Calretinin immunoreactivity in the brain of the zebrafish, *Danio rerio*: distribution and comparison with some neuropeptides and neurotransmitter-synthesizing enzymes. II. Midbrain, hindbrain, and rostral spinal cord. J Comp Neurol 494:792-814.

Chaplin N, Tendeng C, Wingate RJ. 2010. Absence of an external germinal layer in zebrafish and shark reveals a distinct, anamniote ground plan of cerebellum development. J Neurosci 30:3048-3057.

Chedotal A, Pourquie O, Ezan F, San Clemente H, Sotelo C. 1996. BEN as a presumptive target recognition molecule during the development of the olivocerebellar system. J Neurosci 16:3296-3310.

Coolen M, Menuet A, Chassoux D, Compagnucci C, Henry S, Lévèque L, Da Silva C, Gavory F, Samain S, Wincker P, Thermes C, D'Aubenton-Carafa Y, Rodriguez-Moldes I, Naylor G, Depew M, Sourdaine P, Mazan S. 2009. The dogfish *Scyliorhinus canicula*, a reference in jawed vertebrates. In: Behringer RR, Johnson AD, Krumlauf RE, editors. Emerging model organisms. A laboratory manual. Vol. 1. Cold Spring Harbor, NY: Cold Spring Harbor Laboratory Press. p 431-446.

Crosby EC. 1969. Comparative aspects of cerebellar morphology. In: Llinás R, editor. Neurobiology of cerebellar evolution and development. Chicago: Amer Med Assoc.

De Castro F, Cobos I, Puelles L, Martínez S. 1998. Calretinin in pretecto- and olivocerebellar projections in the chick: immunohistochemical and experimental study. J Comp Neurol 397:149-162.

De Zeeuw CI, Simpson JI, Hoogenraad CC, Galjart N, Koekkoek SK, Ruigrok TJ. 1998. Microcircuitry and function of the inferior olive. Trends Neurosci 21:391-400.

Delgado-García JM. 2001. Structure and function of the cerebellum. Rev Neurol 33:635-642.

Dellarole A, Grilli M. 2008. Adult dorsal root ganglia sensory neurons express the early neuronal fate marker doublecortin. J Comp Neurol 511:318-328.

Dietrichs E, Walberg F. 1983. Cerebellar cortical afferents from the red nucleus in the cat. Exp Brain Res 50:353-358.

Distel M, Hocking JC, Volkmann K, Köster RW. 2010. The centrosome neither persistently leads migration nor determines the site of axonogenesis in migrating neurons in vivo. J Cell Biol 191:875-890.

Ebbesson SOE, Campbell CB. 1973. On the organization of cerebellar efferent pathways in the nurse shark (*Ginglymostoma cirratum*). J Comp Neurol 152:233-254.

Ekström P, Johansson K. 2003. Differentiation of ganglion cells and amacrine cells in the rat retina: correlation with expression of HuC/D and GAP-43 proteins. Dev Brain Res 145:1-8.

Engelkamp D, Rashbass P, Seawright A, van Heyningen V. 1999. Role of Pax6 in development of the cerebellar system. Development 126:3585-3596.

Ferreiro-Galve S. 2010. Brain and retina regionalization in sharks: study based on the spatiotemporal expression pattern of Pax6 and other neurochemical markers. Doctoral Thesis, University of Santiago de Compostela, Spain.

Ferreiro-Galve S, Carrera I, Candal E, Villar-Cheda B. 2008. The segmental organization of the developing shark brain based on neurochemical markers, with special attention to the prosencephalon. Brain Res Bull 75:236-240.

Ferreiro-Galve S, Rodríguez-Moldes I, Anadón R, Candal E. 2010. Patterns of cell proliferation and rod photoreceptor differentiation in shark retinas. J Chem Neuroanat 39:1-14.

Ferreiro-Galve S, Rodríguez-Moldes I, Candal E. 2012. Pax6 expression during retinogenesis in sharks: comparison with markers of cell proliferation and neuronal differentiation. J Exp Zool (Mol Dev Evol) 318:91-108.

Fiebig E. 1988. Connections of the corpus cerebelli in the thornback guitarfish, *Platyrhinoidis triseriata* (Elasmobranchii): a study with WGA-HRP and extracellular granule cell recording. J Comp Neurol 268:567-583.

Filippi A, Mahler J, Schweitzer J, Driever W. 2010 Expression of the paralogous tyrosine hydroxylase encoding genes th1 and th2 reveals the full complement of dopaminergic and noradrenergic neurons in zebrafish larval and juvenile brain. J Comp Neurol 518:423-438.

Finger TE. 1978a. Efferent neurons of the teleost cerebellum. Brain Res 153:608-614.

Finger TE. 1978b. Cerebellar afferents in teleost catfish (Ictialuridae). J Comp Neurol. 181: 173-181.

Finger TE. 1983. The organization of the teleost cerebellum. In: Northcutt RG, Davis RE, editors. Fish Neurobiology. Vol 1, The University of Michigan Press, Ann Arbor. p 261-284.

Folgueira M, Anadón R, Yáñez J. 2006. Afferent and efferent connections of the cerebellum of a salmonid, the rainbow trout (*Oncorhynchus mykiss*): a tract-tracing study. J Comp Neurol 497:542-565.

Fredette BJ, Mugnaini E. 1991. The GABAergic cerebello-olivary projection in the rat. Anat Embryol (Berl) 184:225-243.

Fredette BJ, Adams JC, Mugnaini E. 1992. GABAergic neurons in the mammalian inferior olive and ventral medulla detected by glutamate decarboxylase immunocytochemistry. J Comp Neurol 321:501-514.

Fu Y, Sengul G, Paxinos G, Watson C. 2012. The spinal precerebellar nuclei: calcium binding proteins and gene expression profile in the mouse. Neurosci Lett 518:161-166.

Gilthorpe JD, Papantoniou EK, Chedotal A, Lumsden A, Wingate RJ. 2002. The migration of cerebellar rhombic lip derivatives. Development 129:4719-4728.

Gould BB. 1979. The organization of afferents to the cerebellar cortex in the cat: projections from the deep cerebellar nuclei. J Comp Neurol 184:27-42.

Graña P, Anadón R, Yáñez J. 2008. Immunocytochemical study of calretinin and calbindin D-28K expression in the retina of three cartilaginous fishes and a cladistian (*Polypterus*). Brain Res Bull 75:375-378.

Graña P, Huesa G, Anadón R, Yáñez J. 2012. Immunohistochemical study of the distribution of calcium binding proteins in the brain of a chondrostean (*Acipenser baeri*). J Comp Neurol 520:2086-2122.

Grishkat HL, Eisenman LM. 1995. Development of the spinocerebellar projection in the prenatal mouse. J Comp Neurol 363:93-108.

Huang Q, Zhou D, DiFiglia M. 1992. Neurobiotin, a useful neuroanatomical tracer for in vivo anterograde, retrograde and transneuronal tract-tracing and for in vitro labeling of neurons. J. Neurosci Methods 41:31-43.

Huesa G, Anadón R, Yáñez J. 2003. Afferent and efferent connections of the cerebellum of the chondrostean *Acipenser baeri*: a carbocyanine dye (DiI) tracing study. J Comp Neurol 460:327-344.

Ikai Y, Takada M, Shinonaga Y, Mizuno N. 1992. Dopaminergic and non-dopaminergic neurons in the ventral tegmental area of the rat project, respectively, to the cerebellar cortex and deep cerebellar nuclei. Neuroscience 51:719-728.

Ikenaga T, Yoshida M, Uematsu K. 2005. Morphology and immunohistochemistry of efferent neurons of the goldfish corpus cerebelli. J Comp Neurol 487:300-311.

Islam MR, Atoji Y. 2008. Distribution of vesicular glutamate transporter 2 and glutamate receptor 1 mRNA in the central nervous system of pigeon (*Columba livia*). J Comp Neurol 511:658-677.

Ito M. 1984. The cerebellum and neural control. New York: Raven Press.

Ito H, Murakami T, Morita Y. 1982. An indirect telencephalo-cerebellar pathway and its relay nucleus in teleosts. Brain Res 249:1-13.

Iwaniuk AN, Pakan JM, Gutierrez-Ibanez C, Wylie DR. 2009. Expression of calcium-binding proteins in cerebellar- and inferior olivary-projecting neurons in the nucleus lentiformis mesencephali of pigeons. Vis Neurosci 26:341-347.

Kálmán M, Gould RM. 2001. GFAP-immunopositive structures in spiny dogfish, *Squalus acanthias*, and little skate, *Raia erinacea*, brains: differences have evolutionary implications. Anat Embryol (Berl) 204:59-80.

Kaneko M, Yamaguchi K, Eiraku M, Sato M, Takata N, Kiyohara Y, Mishina M, Hirase H, Hashikawa T, Kengaku M. 2011. Remodeling of monoplanar Purkinje cell dendrites during cerebellar circuit formation. PLoS One 6:e20108.

Karten HJ, Finger TE. 1976. A direct thalamo-cerebellar pathway in pigeon and catfish. Brain Res 102:335-338.

Kawauchi D, Taniguchi H, Watanabe H, Saito T, Murakami F. 2006. Direct visualization of nucleogenesis by precerebellar neurons: involvement of ventricle-directed, radial fibre-associated migration. Development 133:1113-1123.

Kerr CW, Bishop GA. 1991. Topographical organization in the origin of serotoninergic projections to different regions of the cat cerebellar cortex. J Comp Neurol 304:502-515.

Kim EJ, Hori K, Wyckoff A, Dickel LK, Koundakjian EJ, Goodrich LV, Johnson JE. 2011. Spatiotemporal fate map of neurogenin1 (Neurog1) lineages in the mouse central nervous system. J Comp Neurol 519:1355-1370.

Köster RW, Fraser SE. 2001. Direct imaging of in vivo neuronal migration in the developing cerebellum. Curr Biol 11:1858-1863.

Kooy FH. 1916. The inferior olive in vertebrates. Ph.D. Thesis, University of Groningen. Haarlem: F. Bohn. 165 pp.

Kuwako K, Kakumoto K, Imai T, Igarashi M, Hamakubo T, Sakakibara S, Tessier-Lavigne M, Okano HJ, Okano H. 2010. Neural RNA-binding protein Musashi1 controls midline crossing of precerebellar neurons through posttranscriptional regulation of Robo3/Rig1 expression. Neuron 67:407-421.

Lan CT, Wen CY, Tan CK, Ling EA, Shieh JY. 1995. Multiple origins of cerebellar cholinergic afferents from the lower brainstem in the gerbil. J Anat 186:549-561.

Larsell O. 1967. The comparative anatomy and histology of the cerebellum from myxinoids through birds. Minneapolis: University of Minnesota Press.

Lin JC, Cai L, Cepko CL. 2001. The external granule layer of the developing chick cerebellum generates granule cells and cells of the isthmus and rostral hindbrain. J. Neurosci 21:159-168.

Lind D, Franken S, Kappler J, Jankowski J, Schilling K. 2005. Characterization of the neuronal marker NeuN as a multiply phosphorylated antigen with discrete subcellular localization. J Neurosci Res 79:295-302.

MacLeod KM, Soares D, Carr CE. 2006. Interaural timing difference circuits in the auditory brainstem of the emu (*Dromaius novaehollandiae*). J Comp Neurol 495:185-201.

Maler L, Mugnaini E. 1994. Correlating gamma-aminobutyric acidergic circuits and sensory function in the electrosensory lateral line lobe of a gymnotiform fish. J Comp Neurol 345:224-252.

Marusich MF, Furneaux HM, Henion PD, Weston JA. 1994. Hu neuronal proteins are expressed in proliferating neurogenic cells. J Neurobiol 25:143-155.

Meek J, Nieuwenhuys R, Elsevier D. 1986a. Afferent and efferent connections of cerebellar lobe C1 of the mormyrid fish *Gnathonemus petersi*: an HRP study. J Comp Neurol 245:319-341.

Meek J, Nieuwenhuys R, Elsevier D. 1986b. Afferent and efferent connections of cerebellar lobe C3 of the mormyrid fish *Gnathonemus petersi*: an HRP study. J Comp Neurol 245:342-358.

Miyazaki T, Fukaya M, Shimizu M, Watanabe M. 2003. Subtype switching of vesicular glutamate transporters at parallel fibre-Purkinje cell synapses in developing mouse cerebellum. Eur J Neurosci 17:2563-2572.

Molist P, Rodríguez-Moldes I, Batten TF, Anadón R. 1995. Distribution of calcitonin gene-related peptide-like immunoreactivity in the brain of the small-spotted dogfish, *Scyliorhinus canicula L.* J Comp Neurol 352:335-350.

Monaghan PL, Beitz AJ, Larson AA, Altschuler RA, Madl JE, Mullett MA. 1986. Immunocytochemical localization of glutamate-, glutaminase- and aspartate aminotransferase-like immunoreactivity in the rat deep cerebellar nuclei. Brain Res 363:364-370.

Montgomery JC, Bodznick D, Yopak KE. 2012. The cerebellum and cerebellum-like structures of cartilaginous fishes. Brain Behav Evol 80:152-165.

Morona R, González A. 2009. Immunohistochemical localization of calbindin-D28k and calretinin in the brainstem of anuran and urodele amphibians. J Comp Neurol 515:503-537.

Morona R, Moreno N, López JM, Muñoz M, Ten Donkelaar HJ, González A. 2005. Calbindin-D28k immunoreactivity in the spinal cord of *Xenopus laevis* and its participation in ascending and descending projections. Brain Res Bull 66:550-554.

Mugnaini E, Wouterlood FG, Dahl AL, Oertel WH. 1984. Immunocytochemical identification of GABAergic neurons in the main olfactory bulb of the rat. Arch Ital Biol 122:83-113.

Mullen RJ, Buck CR, Smith AM. 1992. NeuN, a neuronal specific nuclear protein in vertebrates. Development 116:201-211.

Murakami T, Morita Y. 1987. Morphology and distribution of the projection neurons in the cerebellum in a teleost, *Sebastiscus marmoratus*. J Comp Neurol 256:607-623.

New JG. 2001. Comparative neurobiology of the elasmobranch cerebellum: theme and variations on a sensorimotor interface. Environ Biol Fish 60:93-108.

Nicholson C, Llinás R, Precht W. 1969. Neural elements of the cerebellum in elasmobranch fishes; structural and functional characteristics. In: Llinás R, editor. Neurobiology of

cerebellar evolution and development, Chicago: AMA-ERF Institute for Biomedical Research. p 215-243.

Nieuwenhuys R. 1967. Comparative anatomy of the cerebellum. Prog Brain Res 25:1-93.

Nieuwenhuys R. 2011. The structural, functional, and molecular organization of the brainstem. Front Neuroanat 5:1-33.

Northcutt RG. 1978. Brain organization in the cartilaginous fishes. In: Hodgson ES, Mathewson RF, editors. Sensory biology of sharks, skates, and rays. Arlington, VA: Office of Naval Research, Department of the Navy. p 117-193.

Northcutt RG, Brunken WJ. 1984. Cerebellar afferents in the little skate (Batoidea). Soc. Neurosci Abstr 10:853.

Oertel WH, Schmechel DE, Brownstein MJ, Tappaz ML, Ransom DH, Kopin IJ. 1981. Decrease of glutamate decarboxylase (GAD)-immunoreactive nerve terminals in the substantia nigra after kainic acid lesion of the striatum. J Histochem Cytochem 29:977-980.

Ohtsuki G, Hirano T. 2008. Bidirectional plasticity at developing climbing fiber-Purkinje neuron synapses. Eur J Neurosci 28:2393-2400.

Okada T, Keino-Masu K, Masu M. 2007. Migration and nucleogenesis of mouse precerebellar neurons visualized by in utero electroporation of a green fluorescent protein gene. Neurosci Res 57:40-49.

Okado N, Yoshimoto M, Furber SE. 1987. Pathway formation and the terminal distribution pattern of the spinocerebellar projection in the chick embryo. Anat Embryol (Berl) 176:165-174.

Ono K, Yasui Y, Ikenaka K. 2004. Lower rhombic lip-derived cells undergo transmedian tangential migration followed by radial migration in the chick embryo brainstem. Eur J Neurosci 20:914-922.

Paradies MA, Eisenman LM. 1993. Evidence of early topographic organization in the embryonic olivocerebellar projection: a model system for the study of pattern formation processes in the central nervous system. Dev Dyn 197:125-145.

Paul DH. 1967. Electrical activity in the cerebellum of the spiny dogfish (*Squalus acanthias*). J Physiol 191:68P-70P.

Paul DH, Roberts BL. 1983. The activity of cerebellar nuclear neurones in relation to stimuli which evoke a pectoral fin reflex in dogfish. J Physiol 342:465-481.

Paul DH, Roberts BL. 1984. Projections of cerebellar Purkinje cells in the dogfish, *Scyliorhinus*. Neurosci Lett 44:43-46.

Piper M, Harris L, Barry G, Heng YH, Plachez C, Gronostajski RM, Richards LJ. 2011. Nuclear factor one X regulates the development of multiple cellular populations in the postnatal cerebellum. J Comp Neurol 519:3532-3548.

Puelles L, Rubenstein JL. 2003. Forebrain gene expression domains and the evolving prosomeric model. Trends Neurosci 26:469-476.

Puzdrowski RL, Gruber S. 2009. Morphologic features of the cerebellum of the Atlantic stingray, and their possible evolutionary significance. Integr Zool 4:110-122.

Roberts BL, Witkovsky P. 1975. A functional analysis of the mesencephalic nucleus of the fifth nerve in the selachian brain. Proc. R. Soc. Lond B Biol Sci 190:473-495.

Rodríguez-Moldes I, Ferreiro-Galve S, Carrera I, Sueiro C, Candal E, Manzan S, Anadón R. 2008. Development of the cerebellar body in sharks: spatiotemporal relations of Pax6-expression, cell proliferation and differentiation. Neurosci Lett 432:105-110.

Rodríguez-Moldes I, Carrera I, Pose-Méndez S, Quintana-Urzainqui I, Candal E, Anadón R, Mazan S, Ferreiro-Galve S. 2011. Regionalization of the shark hindbrain: a survey of an ancestral organization. Front Neuroanat 5:1-14.

Ruigrok TJ, Cella F, Voogd J. 1995. Connections of the lateral reticular nucleus to the lateral vestibular nucleus in the rat. An anterograde tracing study with *Phaseolus vulgaris* leucoagglutinin. Eur J Neurosci. 7:1410-3.Sarnat H, Netsky M. 1981. Cerebellar system. In: Evolution of the Nervous System. Oxford University Press. p 213-242.

Sarrafizadeh R, Houk JC. 1994. Anatomical organization of the limb premotor network in the turtle (*Chrysemys picta*) revealed by in vitro transport of biocytin and neurobiotin. J. Comp Neurol 344:137-159.

Schmidt AW, Bodznick D. 1987. Afferent and efferent connections of the vestibulolateral cerebellum of the little skate, *Raja erinacea*. Brain Behav Evol 30:282-302.

Schwaller B, Meyer M, Schiffmann S. 2002. 'New' functions for 'old' proteins: the role of the calcium-binding proteins calbindin D-28k, calretinin and parvalbumin, in cerebellar physiology. Studies with knockout mice. Cerebellum 1:241-258.

Schwarz C, Schmitz Y. 1997. Projection from the cerebellar lateral nucleus to precerebellar nuclei in the mossy fiber pathway is glutamatergic: a study combining anterograde tracing with immunogold labeling in the rat. J Comp Neurol 381:320-334.

Smeets WJAJ. 1982. The afferent connections of the tectum mesencephali in two chondrichthyans, the shark *Scyliorhinus canicula* and the ray *Raja clavata*. J Comp Neurol 205:139-152.

Smeets WJAJ. 1998. Cartilaginous fish. In: Nieuwenhuys R, Ten Donkelaar HJ, Nicholson C, editors. The central nervous system of vertebrates. Vol 1, Berlin: Springer-Verlag. p 551-654.

Smeets WJAJ, Boord RL. 1985. Connections of the lobus inferior hypothalami of the clearnose skate *Raja eglanteria* (Chondrichthyes). J Comp Neurol 234:380-392.

Smeets WJAJ, Timerick SJ. 1981. Cells of origin of pathways descending to the spinal cord in two chondrichthyans, the shark *Scyliorhinus canicula* and the ray *Raja clavata*. J Comp Neurol 202:473-491.

Smeets WJAJ, Nieuwenhuys R, Roberts BL. 1983. The central nervous system of cartilaginous fishes. Structure and functional correlations. Berlin: Springer.

Sotelo C. 2004. Cellular and genetic regulation of the development of the cerebellar system. Prog Neurobiol 72:295-339.

Sotelo C, Chedotal A. 2005. Development of the olivocerebellar system: migration and formation of cerebellar maps. Prog Brain Res 148:1-20.

Soukkarieh C, Agius E, Soula C, Cochard P. 2007. Pax2 regulates neuronal-glial cell fate choice in the embryonic optic nerve. Dev Biol 303:800-813.

Sterzi G. 1912. Il sistema nervoso centrale dei vertebrate. Pesci, vol II. Draghi, Padova .

Straka H, Beck JC, Pastor AM, Baker R. 2006. Morphology and physiology of the cerebellar vestibulolateral lobe pathways linked to oculomotor function in the goldfish. J Neurophysiol 96:1963-1980.

Sueiro C, Carrera I, Molist P, Rodríguez-Moldes I, Anadón R. 2004. Distribution and development of glutamic acid decarboxylase immunoreactivity in the spinal cord of the dogfish *Scyliorhinus canicula* (elasmobranchs). J Comp Neurol 478:189-206.

Sueiro C, Carrera I, Ferreiro S, Molist P, Adrio F, Anadón R, Rodríguez-Moldes I. 2007. New insights on saccus vasculosus evolution: a developmental and immunohistochemical study in elasmobranchs. Brain Behav Evol 70:187-204.

Sugihara I, Shinoda Y. 2007. Molecular, topographic, and functional organization of the cerebellar nuclei: analysis by three-dimensional mapping of the olivonuclear projection and aldolase C labeling. J Neurosci 27:9696-9710.

Takeda A, Nakano M, Goris RC, Funakoshi K. 2008. Adult neurogenesis with 5-HT expression in lesioned goldfish spinal cord. Neuroscience 151:1132-1141.

Tohyama M. 1976. Comparative anatomy of cerebellar catecholamine innervation from teleosts to mammals. J Hirnforsch 17:43-60.

Tolbert DL. 1982. The cerebellar nucleocortical pathway. In: Palay SL, Chan-Palay V, editors. The cerebellum. New vistas. Berlin: Springer-Verlag. p 296-319.

Toonen M, van Dijken H, Holstege JC, Ruigrok TJ, Koekkoek SK, Hawkins RK, Teune TM, vd Burg J, De Zeeuw CI. 1998. Light microscopic and ultrastructural investigation of the dopaminergic innervation of the ventrolateral outgrowth of the rat inferior olive. Brain Res 802:267-273.

van der Linden JA, ten Donkelaar HJ. 1987. Observations on the development of cerebellar afferents in *Xenopus laevis*. Anat Embryol (Berl) 176:431-439.

Vellema M, van der Linden A, Gahr M. 2010. Area-specific migration and recruitment of new neurons in the adult songbird brain. J Comp Neurol 518:1442-1459.

Villar-Cerviño V, Barreiro-Iglesias A, Mazan S, Rodicio MC, Anadón R. 2011. Glutamatergic neuronal populations in the forebrain of the sea lamprey, *Petromyzon marinus*: an in situ hybridization and immunocytochemical study. J Comp Neurol 519:1712-1735.

Villar-Cerviño V, Barreiro-Iglesias A, Fernández-López B, Mazan S, Rodicio MC, Anadón R. 2013. Glutamatergic neuronal populations in the brainstem of the sea lamprey, *Petromyzon marinus*: An In situ hybridization and immunocytochemical study. J Comp Neurol 521:522-57.

Volkmann K, Chen YY, Harris MP, Wullimann MF, Köster RW. 2010. The zebrafish cerebellar upper rhombic lip generates tegmental hindbrain nuclei by long-distance migration in an evolutionary conserved manner. J Comp Neurol 518:2794-2817.

Voogd J, Epema AH, Rubertone JA. 1991. Cerebello-vestibular connections of the anterior vermis. A retrograde tracer study in different mammals including primates. Arch Ital Biol 129:3-19.

Walker JJ, Bishop GA, Ho RH, King JS. 1988. Brainstem origin of serotonin- and enkephalin-immunoreactive afferents to the opossum's cerebellum. J Comp Neurol 276:481-497.

Wang Z, Liu RH, Fung SJ, Reddy VK, Barnes CD. 1993. Immunohistochemical localization of glutamate-containing neurons in the lateral reticular nucleus projecting to the cerebellar vermis in the kitten. Neurosci Lett 164:117-120.

Wang VY, Rose MF, Zoghbi HY. 2005. Math1 expression redefines the rhombic lip derivatives and reveals novel lineages within the brainstem and cerebellum. Neuron 48:31-43.

Wasowicz M, Ward R, Reperant J. 1999. An investigation of astroglial morphology in torpedo and scyliorhinus. J Neurocytol 28:639-653.

Watanabe H, Murakami F. 2009. Real time analysis of pontine neurons during initial stages of nucleogenesis. Neurosci Res 64:20-29.

Wild JM. 1992. Direct and indirect "cortico"-rubral and rubro-cerebellar cortical projections in the pigeon. J Comp Neurol 326:623-636.

Wilson LJ, Wingate RJ. 2006. Temporal identity transition in the avian cerebellar rhombic lip. Dev Biol 297:508-521.

Wingate RJ. 2001. The rhombic lip and early cerebellar development. Curr Opin Neurobiol 11:82-88.

Wolf HK, Buslei R, Schmidt-Kastner R, Schmidt-Kastner PK, Pietsch T, Wiestler OD, Blumcke I. 1996. NeuN: a useful neuronal marker for diagnostic histopathology. J Histochem Cytochem 44:1167-1171.

Wullimann MF, Northcutt RG. 1988. Connections of the corpus cerebelli in the green sunfish and the common goldfish: a comparison of perciform and cypriniform teleosts. Brain Behav Evol 32:293-316.

Wullimann MF, Mueller T, Distel M, Babaryka A, Grothe B, Köster RW. 2011. The long adventurous journey of rhombic lip cells in jawed vertebrates: a comparative developmental analysis. Front Neuroanat 5:1-27.

Xue HG, Yamamoto N, Yang CY, Imura K, Ito H. 2004. Afferent connections of the corpus cerebelli in holocentrid teleosts. Brain Behav Evol 64:242-258.

Xue HG, Yang CY, Yamamoto N. 2008. Afferent sources to the inferior olive and distribution of the olivocerebellar climbing fibers in cyprinids. J Comp Neurol 507:1409-1427.

Yamamoto K, Ruuskanen JO, Wullimann MF, Vernier P. 2010. Two tyrosine hydroxylase genes in vertebrates. New dopaminergic territories revealed in the zebrafish brain. Mol Cell Neurosci 43:394-402.

Young W. 1980. Field potential analysis in elasmobranch cerebellum. Brain Res 199:101-112.

Abbreviations

AMV anterior medullary velum
bc blood cell
bv blood vessel
Cb cerebellum
cc central canal
CN cerebellar nucleus
CP cerebellar peduncle
CPdm dorsomedial zone of the cerebellar peduncle
Di diencephalon
e sulcus e
fr fasciculus retroflexus
GR cerebellar granular layer
Ha habenula
III oculomotor nucleus
IIIn oculomotor nerve
IO inferior olive
IOc caudal part of the inferior olive
IOr rostral part of the inferior olive
IP interpeduncular nucleus
ir immunoreactive
ISg isthmic group
ISn isthmic nucleus
IVn trochlear nerve
IXn glossopharyngeal nerve
Juv juvenile
L lateral region of the cerebellar nucleus
LAL lower auricle leaf
LC locus coeruleus
LRL lower rhombic lip
LRn lateral reticular nucleus
M medial region of the cerebellar nucleus
Mes mesencephalon
MOL molecular layer
nlla anterior lateral line nerve
OT optic tectum
p1-3 prosomeres
Pc posterior commissure
pi pineal organ
Pret pretectum
PretC pretectal central nucleus
Pro posterior recess organ
PTh prethalamus
r1-8 rhombomeres
Ra raphe nucleus
ret reticular cells
RetI inferior reticular formation
RetS superior reticular formation
Rh rhombencephalon
Rub nucleus ruber
S subventricular region of the cerebellar nucleus
sid sulcus intermedius dorsalis
slH sulcus limitans of His
SN substantia nigra
Spc spinal cord
Th thalamus
Thm medial part of the thalamus
UAL upper auricular leaf
URL upper rhombic lip
Vd descending trigeminal root nucleus
VH ventral horn
VI abducens nerve
VIIn facial nerve
VIIIn octaval nerve
Vme mesencephalic trigeminal nucleus
Vn trigeminal nerve
VTA ventral tegmental area
W white matter of cerebellar nucleus
Xn vagal nerve

Table 1. Number of embryos and juveniles used in tract-tracing experiments. The tracer was applied to the caudal lobe of the cerebellar body, except for those marked with one, two and three asterisks in which tracer was applied to the lower rhombic lip, spinal cord and anterior lobe of the cerebellar body, respectively.

Developmental stages (range size in cm)	**S30 (3.1-3.3)**	**S31 (3.4-4)**	**S32E (4-4.8)**	**S32M (4.9-5.7)**	**S32L (5.8-6.7)**	**S33 (6.8-7.8)**	**Juv (8.2→)**
Length of animals (cm) used in transport experiments and time of transport in days (in parenthesis)	3.3 (3) *	3.5 (4)	4.1 (4)	4.9 (4)	5.8 (3)	6.8 (4)	9 (3)
		3.6 (4) **	4.3(4)**	4.9 (3)	6 (2.5)	6.9 (4)	9.8 (2)***
		3.7 (4)	4.4 (3)	5.2 (4)		7.5 (3)	9.9 (4)
				5.4 (2)			10 (3)***
							10 (3)

.

Table 2. Primary antibodies used

Antibody	Inmunogen	Producer	Catalog number	Host	Batch code (Lot No)	Type	Working dilution
DCX	Synthetic peptide corresponding to human DCX coupled to keyhole limpet hemocyanin (KLH)	Cell Signaling Technology, Beverly, MA	4604	Rabbit	N/A	Polyclonal	1/300
5-HT	5-HT coupled to bovine serum albumin (BSA) with paraformaldehyde	DiaSorin/ Immunostar,Hudson, WI; previously IncStar, Stillwater, MN	20080	Rabbit	924005	Polyclonal	1/2500
CR	Recombinant human calretinin containing a 6-his tag at the N-terminal	Swant, Bellinzona, Switzerland	7699/3H	Rabbit	18299	Polyclonal	1/250
GFAP	Human and cow serum proteins	Dako Cytomation	Z0334	Rabbit	00003628	Polyclonal	1/300
Glut	GLU-porcine thyroglobin conjugate	Immunosolution	IG1006	Rabbit	2907	Polyclonal	1/500
ChAT	Human placental enzyme	Millipore, Billerica, MA	AB144P	Goat	JC1663901	Polyclonal	1/100
HuC/D	Human HuD peptide (QAQRFRLDNLL N-C)-KLH conjugate	Molecular Probes, Eugene, OR	A-21271	Mouse	16A11	Monoclonal	1/100
NeuN	Purified cell nuclei from mouse brain	Millipore, Billerica, MA	MAB377	Mouse	LV1427917	Monoclonal	1/250
TH	TH purified from PC12 cells	Millipore, Billerica, MA	MAB318	Mouse	NG1899912	Monoclonal	1/500
$GAD_{65/67}$	L-GAD partially purified from rat brain synaptosomes	Drs. I. Kopin and W. Oertel	N/A	Sheep	N/A	Polyclonal	1/20000

Table 3. Secondary antibodies used.

Antibody	Producer	Catalog number	Host	Working dilution
Alexa Fluor 546 donkey anti-rabbit IgG	Molecular Probes	A10040	Donkey	1/150
Alexa Fluor 488 donkey anti-rabbit IgG	Molecular Probes	A21206	Donkey	1/200
Alexa Fluor 647 donkey anti-mouse IgG	Molecular Probes	A31571	Donkey	1/100
Alexa Fluor 633 donkey anti-sheep IgG	Molecular Probes	A-21100	Donkey	1/100
Alexa Fluor 488 donkey anti-goat IgG	Molecular Probes	A11055	Donkey	1/100
Alexa Fluor 633 donkey anti-goat IgG	Molecular Probes	A21082	Donkey	1/100

Table 4. Sequence of appearance of the main neuronal groups projecting to cerebellum during development revealed by application of tracer to the cerebellar body. The onset of spino-cerebellar connections was also studied by application of the tracer to the rostral spinal cord in early stage 32 (white star).

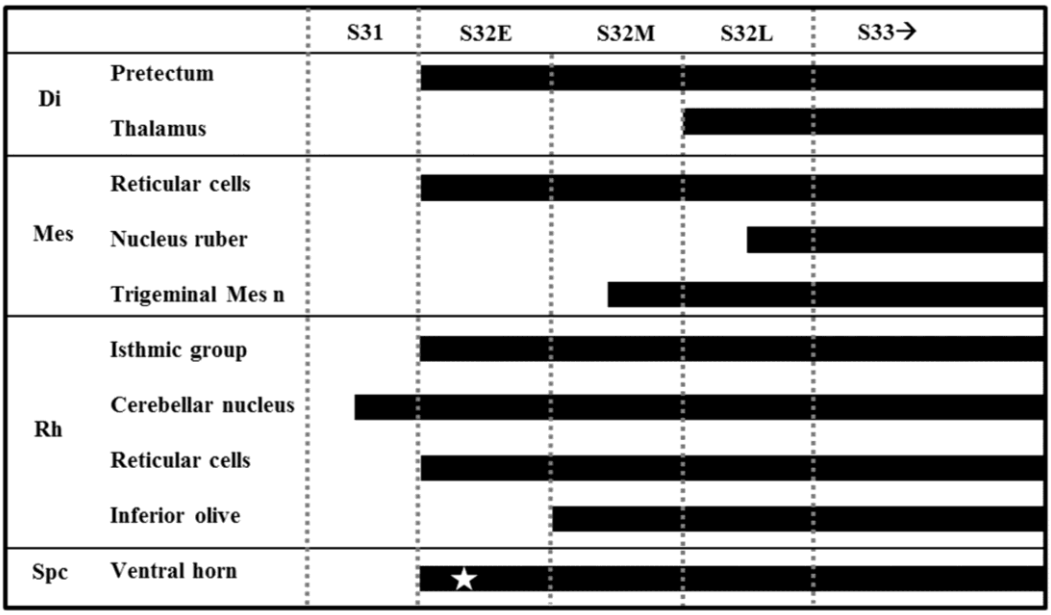

Table 5. Summary of neurochemical characterization of precerebellar cell groups in juveniles after application of tracer to the cerebellar body and subsequent combination with different immunohistochemical neuronal markers (CR, Glut, NeuN, ChAT, 5-HT, TH and GAD). (+) indicates neuronal colocalization (double labeled cells), (-) no colocalization and (ND) not determined. Asterisk indicates very low frequency of colocalization. For abbreviations, see list.

	Pret/Th (Di)	**ret (Mes)**	**Rub (Mes)**	**RetS (Rh)**	**ISg (Rh)**	**LC (Rh)**	**CN (Rh)**	**RetI (Rh)**	**IOr (Rh)**	**IOc (Rh)**	**VH (Spc)**
CR-ir cells	+	+	+	+	+	ND	+	+	+	+	+
Glut-ir cells	-	+	+	+	ND	ND	+	+	+	+	ND
NeuN-ir cells	-	+	-	+	ND	ND	-	+	-	-	ND
ChAT-ir cells	-	-	-	-	-	-	-	+	-	-	-
5-HT-ir cells	-	-	-	-	-	-	-	-	-	-	-
TH-ir cells	-	-	-	-	-	+*	-	-	-	-	ND
GAD-ir cells	-	-	-	-	-	-	-	-	-	-	-

Figure 1. Immunoblots of SDS-polyacrylamide gel of *S. canicula* adult brain protein extracts stained by anti-glutamate (Glut, lane 1), anti-doublecortin (DCX, lane 2) and anti-calretinin (CR, lane 3) antibodies. DCX and CR lanes showed single bands of about 45 kDa and 29–30 kDa, respectively, whereas no protein band was stained in glutamate lane.

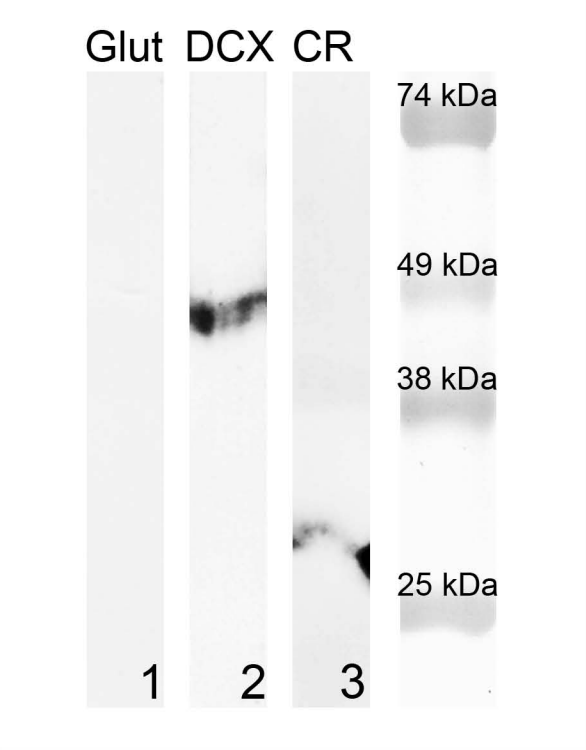

FIGURE 1

Figure 2. Schematic drawings of sagittal (A, K) and selected transverse (B-J) sections of the brain (without telencephalon) of juvenile *Scyliorhinus canicula*, showing the distribution of retrogradely labeled (cerebellar afferent) cells (black circles) from diencephalic to spinal levels and the main afferent pathways (K), after application of the tracer to the cerebellar body (shaded area in A and G). Grey circles in A correspond to nucleo-cortical projecting cells in the cerebellar peduncle. In the sagittal representations it is also indicated: the level of transverse sections schematized in this figure (B-J) and the level of photographs in figures 5-9 (black lines in A); the interprosomeric, diencephalo-mesencephalic, mesencephalo-rhombencephalic and interrhombomeric boundaries (white dashed lines in A and K); and the alar-basal boundary (grey dotted line in A and K). The exit of some cranial nerves (III, V, VI, VII, VIII, IX and X) is also represented (A, C, G, I, K). For abbreviations, see list.

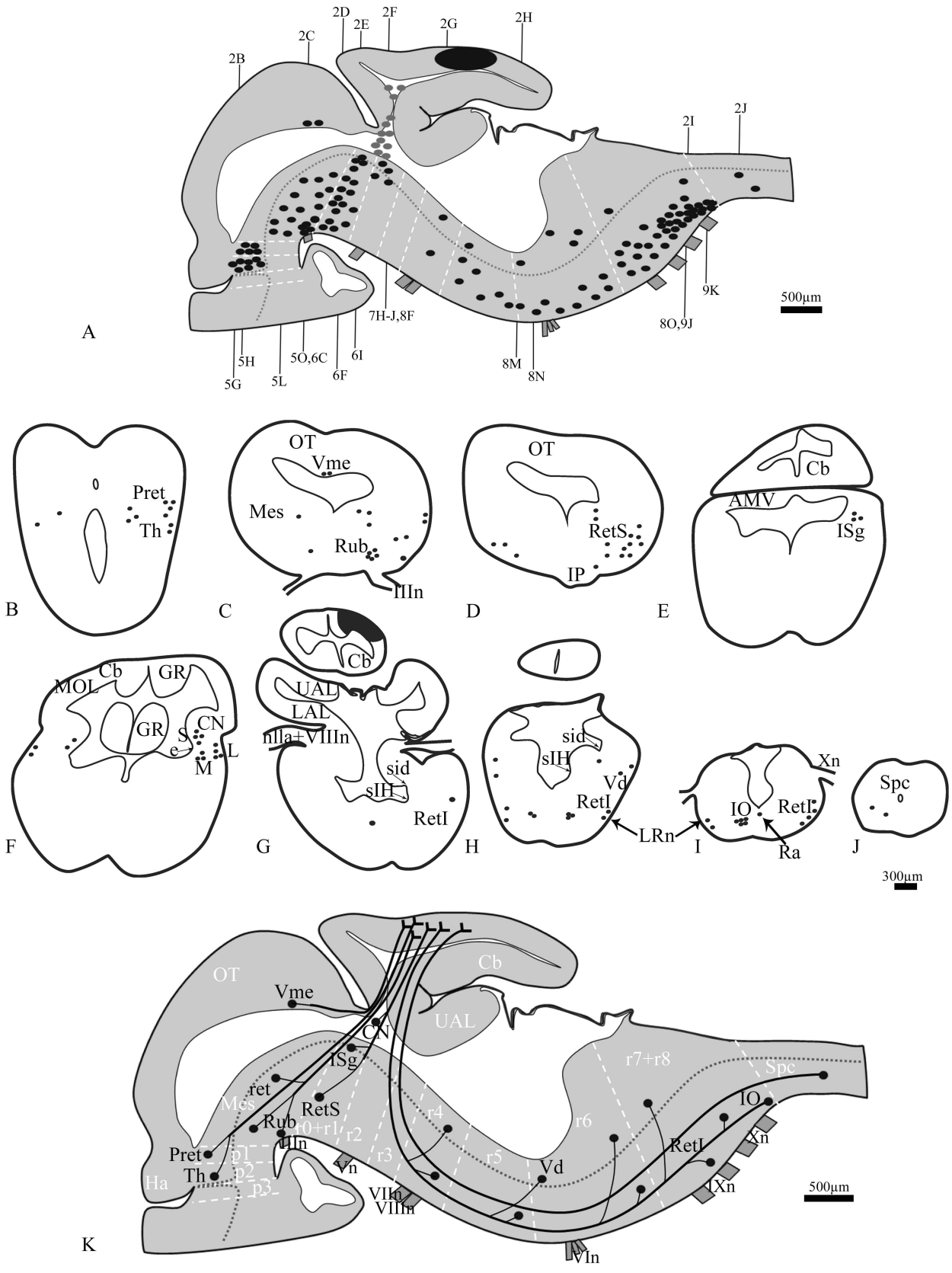
A
2B
2C
2D
2E
2F
2G
2H
2I
2J
5G
5H
5L
5O,6C
6F
6I
7H-J,8F
8M
8N
8O,9J
9K
500µm
B
Pret
Th
C
OT
Vme
Mes
Rub
IIIn
D
OT
RetS
IP
E
Cb
AMV
ISg
F
Cb
GR
MOL
GR
CN
S
e
M
L
G
Cb
UAL
LAL
nIIa+VIIIn
sid
sIH
RetI
H
sid
sIH
Vd
RetI
LRn
I
Xn
IO
RetI
Ra
J
Spc
300µm
K
OT
Vme
Cb
UAL
CN
ISg
r7+r8
Spc
ret
Mes
RetS
Rub
r0+r1
r2
r4
r6
IO
Xn
RetI
IXn
IIIn
Pret
p1
p2
p3
Th
Ha
r3
r5
Vn
Vd
VIIn
VIIIn
VIn
500µm

FIGURE 2

Figure 3. Summary of the ipsilateral (right side) and contralateral (left side) cerebellar afferents observed in juveniles of *S. canicula*. Median structures are represented in the middle. The relative density of cells in each neuronal population is also indicated [(**), abundant; (*), scarce].

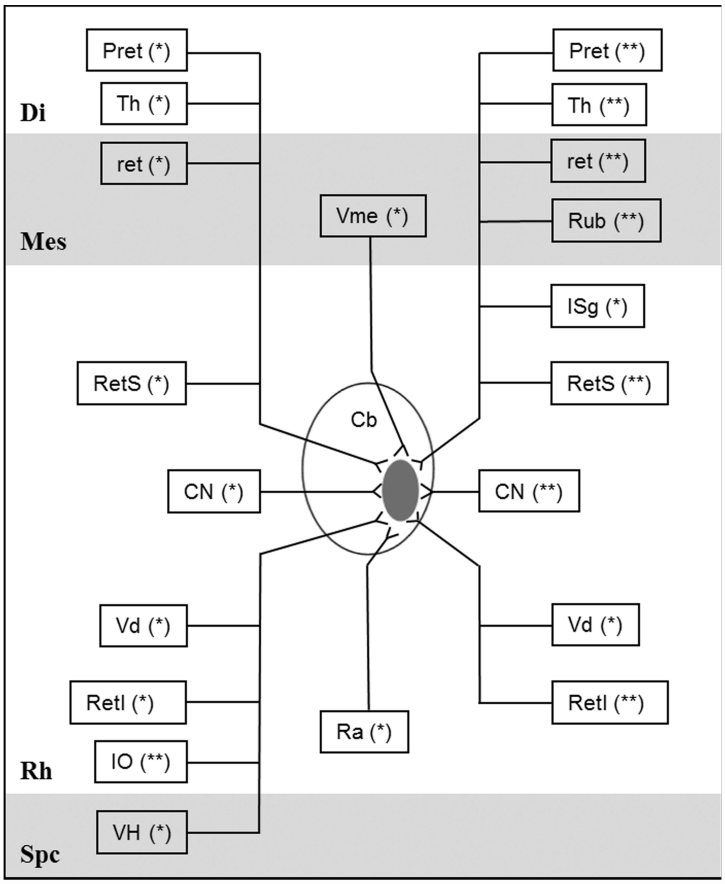
Pret (*)
Th (*)
ret (*)
Vme (*)
Pret (**)
Th (**)
ret (**)
Rub (**)
ISg (*)
RetS (*)
RetS (**)
Cb
CN (*)
CN (**)
Vd (*)
RetI (*)
IO (**)
VH (*)
Ra (*)
Vd (*)
RetI (**)
Di
Mes
Rh
Spc

FIGURE 3

Figure 4. Schematic representations of sagittal (A-D) and transverse (E-R) sections of the brain (without telencephalon) of *S. canicula* embryos at early (A,E-I), intermediate (B) and late (C,J-R) 32 stages and at 33 stage (D), showing the distribution of retrogradely labeled neurons (black circles) after application of the tracer to the cerebellar body (shaded area in A-D,I,O). Grey circles correspond to nucleo-cortical cells in the cerebellar nucleus. In the sagittal schemes it is also represented: the level of transverse sections in this figure (E-R) and of photographic details in Figures 5-10 (black lines in A-D), the interprosomeric, diencephalo-mesencephalic, mesencephalo-rhombencephalic and interrhombomeric boundaries (white dotted lines in A-D) as well as the alar-basal boundary (grey dotted line in A-D). The exit of some cranial nerves (III, V, VI, VII, VIII, IX and X) is also represented (A-D,K,M-Q).

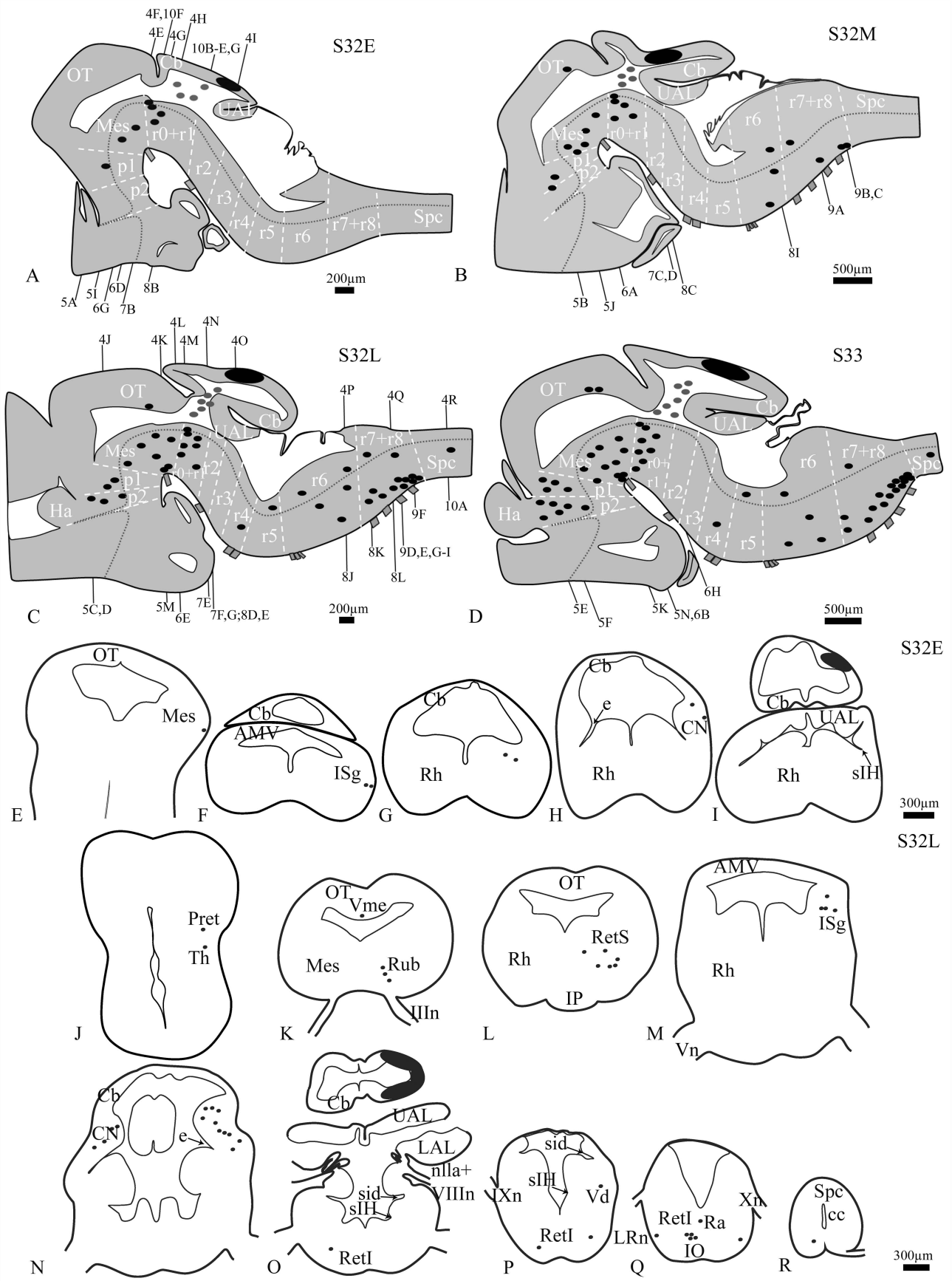
S32E
S32M
S32L
S33
OT
Cb
UAL
Mes
r0+r1
p1
p2
r2
r3
r4
r5
r6
r7+r8
Spc
Ha
Rh
AMV
ISg
sIH
CN
e
Pret
Th
Vme
Rub
IIIn
RetS
IP
Vn
LAL
nIIa+
VIIIn
sid
LXn
Vd
RetI
LRn
Ra
IO
Xn
cc
200µm
500µm
300µm

FIGURE 4

Figure 5. Transverse sections through the diencephalon and mesencephalon of embryos at early 32 (A,I), intermediate 32 (B,J), late 32 (C,D,M) and 33 stages (E,F,K,N), and of juveniles (G,H,L,O), after application of the tracer to the cerebellar body. The level of the sections is indicated in Figures 2A and 4A-D. **A-H,** NB fibers and cells were located in the pretectum and thalamus. Comparisons of parallel sections in C and D shows that NB labeled cells D occupy the region where the thalamic calretinin-immunoreactive cell group is located. **I-L,** NB labeled reticular mesencephalic cells at different developmental stages. **M-O,** Sections through the level of the oculomotor nerve root showing NB labeled cells in the nucleus ruber at different developmental stages, and some scattered cells in the tegmentum of a late embryo (N). For abbreviations, see list. Scale bar = 150 µm in G-O; 200 µm in C; 500 µm in A,B,D-F.

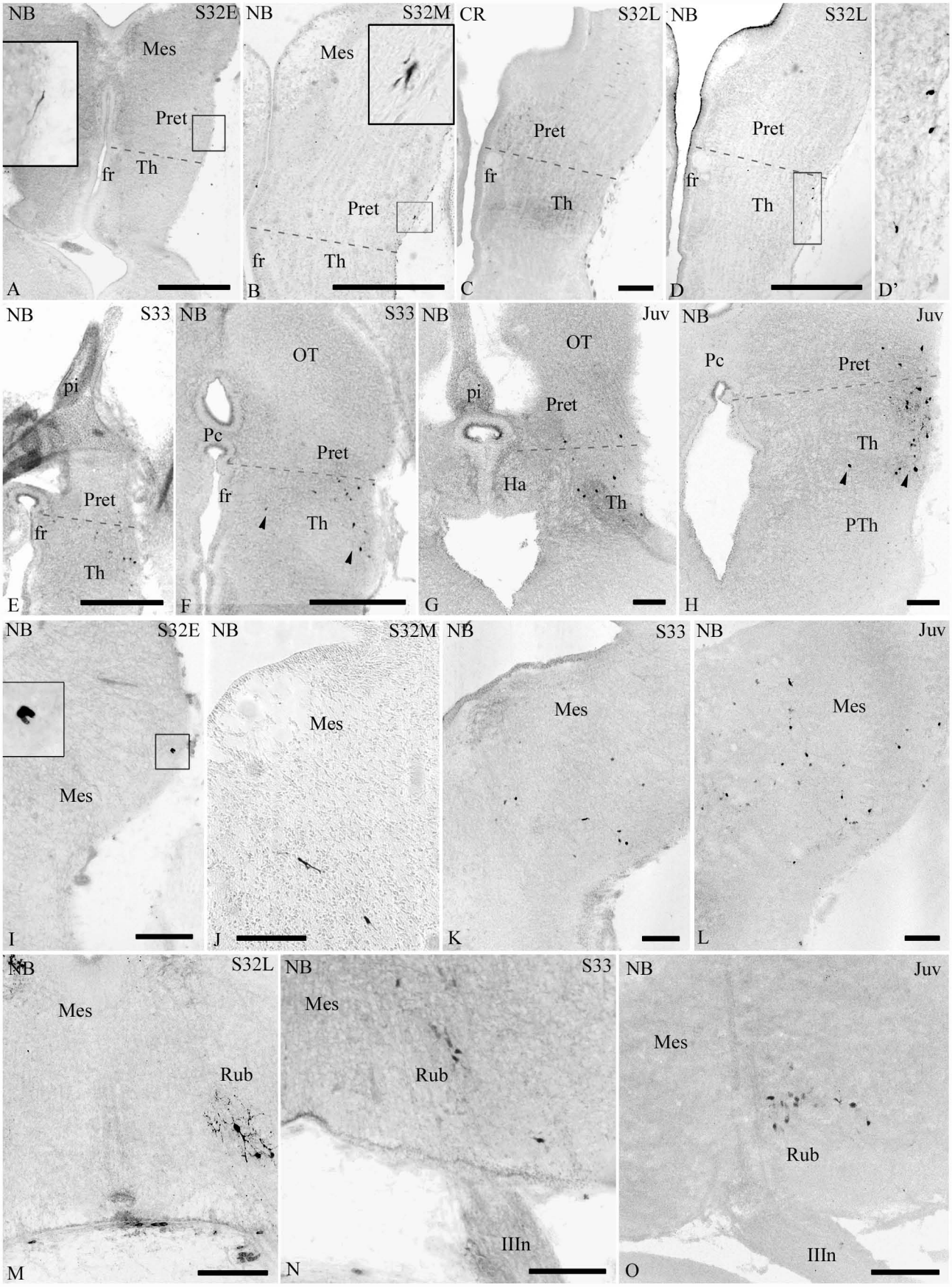
NB
S32E
Mes
Pret
fr
Th
A
NB
S32M
Mes
Pret
fr
Th
B
CR
S32L
Pret
fr
Th
C
NB
S32L
Pret
fr
Th
D
D'
NB
S33
pi
Pret
fr
Th
E
NB
S33
OT
Pc
Pret
fr
Th
F
NB
Juv
OT
pi
Pret
Ha
Th
G
NB
Juv
Pc
Pret
Th
PTh
H
NB
S32E
Mes
I
NB
S32M
Mes
J
NB
S33
Mes
K
NB
Juv
Mes
L
NB
S32L
Mes
Rub
M
NB
S33
Mes
Rub
IIIn
N
NB
Juv
Mes
Rub
IIIn
O

FIGURE 5

Figure 6. Transverse sections through the optic tectum (A-C) and rostral rhombencephalon (D-I) of embryos at early (D,G), intermediate (A) and late (E) 32 stage, 33 stage (B,H), and of juveniles (C,F,I) after application of the tracer to the cerebellar body. The level of sections is indicated in Figures 2A, and 4A-D. **A-C,** Labeled cells in the mesencephalic trigeminal nucleus. **D,** Rostral rhombencephalon showing two NB labeled cells in the superior reticular formation primordium. **E,F,** Section through the rostral reticular rhombencephalon , just posterior to nucleus ruber showing NB labeled cells. **G-I,** Photomicrographs of the rostral rhombencephalon showing labeled cells and dorsolaterally located fibers in the isthmic group. For abbreviations, see list. Scale bar = 100 µm in A-C; 150 µm in D-I.

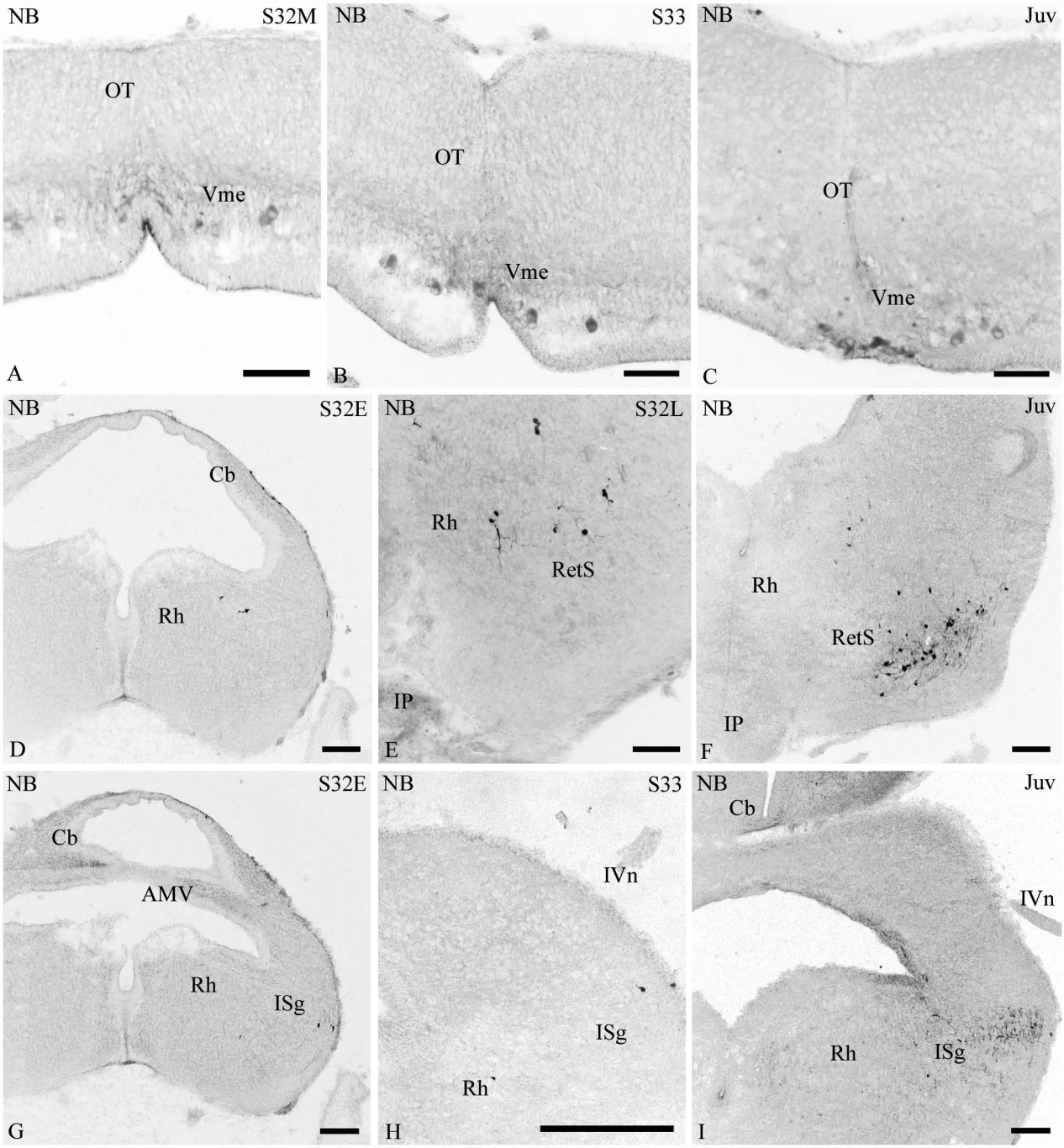
NB
S32M
OT
Vme
A
NB
S33
OT
Vme
B
NB
Juv
OT
Vme
C
NB
S32E
Cb
Rh
D
NB
S32L
Rh
RetS
IP
E
NB
Juv
Rh
RetS
IP
F
NB
S32E
Cb
AMV
Rh
ISg
G
NB
S33
IVn
ISg
Rh
H
NB
Juv
Cb
IVn
Rh
ISg
I

FIGURE 6

Figure 7. Transverse sections of the cerebellar peduncle of 31 stage (A), early (B), intermediate (C,D) and late (E-G) stage 32 embryos, and juveniles (H-J) after application of tracer to the cerebellar body. The level of sections is indicated in Figures 2A and 4A-C. **A,** Primordial cerebellar peduncle showing a submarginal NB labeled cell (arrow) and fibers at the level indicated in the scheme. **B,** Detail of two labeled cells in the medial zone of the cerebellar peduncle (arrows) and fibers that coursed following a dorsoventral orientation. **C,** Some labeled fibers and fiber endings in the dorsomedial zone of the cerebellar peduncle and abundant submarginal fibers that coursed following a dorsoventral orientation. **D,** Detail of the area squared in C showing some fibers bending towards the medial zone, apparently coming from the cerebellar cortex (black arrow) and from rhombencephalic tegmentum (white arrow). **E,** Dorsomedial zone of the cerebellar peduncle (cerebellar nucleus) showing abundant labeled fibers and fiber endings. **F,** Detail of the medial zone of the cerebellar peduncle showing some bending fibers arising apparently from the cerebellar cortex (black arrows) and from the rhombencephalic tegmentum (white arrow). **G,** Cerebellar nucleus showing abundant nucleo-cortical cells in the medial zone and some cell in subventricular and marginal or lateral areas. **H-J,** Cerebellar nucleus of juveniles showing abundant labeled cells in the subventricular (arrow in H), lateral (arrow in I) and medial (arrow in J) areas; scattered cells in the white matter (I); profuse dorsoventrally oriented submarginal fibers (H,I); conspicuous bundles of fibers bending towards the medial region (H,I); and abundant fibers (I) and fiber endings (J) in the dorsomedial zone or white matter surrounding unlabeled (non-cerebellar projecting) nuclear cells (inset in J). For abbreviations, see list. Scale bar = 75 µm in A,B,E,F; 150 µm in C,G-J.

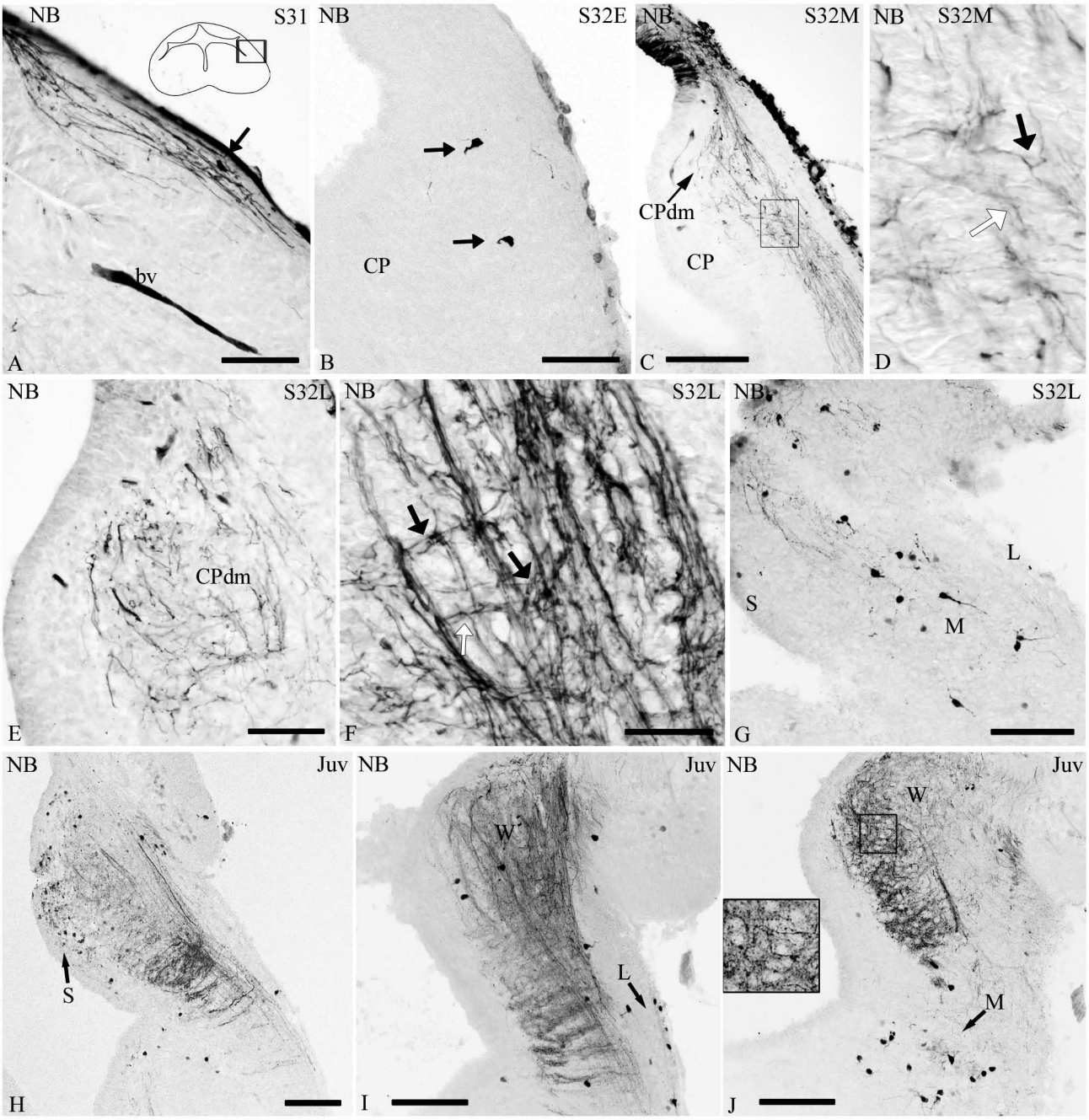
NB
S31
bv
A
NB
S32E
CP
B
NB
S32M
CPdm
CP
C
NB
S32M
D
NB
S32L
CPdm
E
NB
S32L
F
NB
S32L
L
S
M
G
NB
Juv
S
H
NB
Juv
W
L
I
NB
Juv
W
M
J

FIGURE 7

Figure 8. Transverse (A-F,I-O) and sagittal (G,H) sections through the rhombencephalon of stage 31 (A), early (B), intermediate (C,I) and late (D,E,J-L) 32 stage embryos, and of juveniles (F-H,M-O) showing labeled structures after application of the tracer to the cerebellar body. The transverse sections correspond to the region ventral to cerebellar peduncle (A-F) and the caudal rhombencephalon (I-O), as indicated in Figures 2A and 4A-C. **A,** Detail of labeled fibers (arrow) ventral to the cerebellar peduncle at the level indicated in the scheme. **B,** Panoramic view of the cerebellar peduncle showing some labeled fibers (arrow) coursing in the marginal lateral region. **C,** Detail at the level indicated in the scheme, showing labeled marginal and submarginal fibers. **D,** Detail of labeled marginal and submarginal fibers coursing at the level indicated in the scheme. **E,** Detail of the trigeminal nerve entrance showing some labeled fibers in the subpial region (arrow) and in the trigeminal ganglion (arrowheads). **F,** Panoramic view of the cerebellar peduncle and detail (inset) showing labeled fibers ascending from the rhombencephalic tegmentum. Note fiber endings in the cerebellar nucleus. **G,** Sagittal view of the cerebellar peduncle showing two labeled crossed cerebellar afferent tracts (detail in the inset). Note one of them ascending from the mesencephalon and isthmal region (arrow). **H,** Just lateral sagittal view of the cerebellar peduncle to show labeled cerebellar afferent tracts from the rhombencephalon (arrow). **I,** Panoramic view of the caudal rhombencephalon showing two labeled cells located laterally (detail in the inset). **J,** Detail of a retrogradely labeled cell in the nucleus of the descending trigeminal root. **K,** Detail of labeled cells of the inferior reticular formation (in the lateral reticular area or likely the lateral reticular nucleus). **L,** Detail of the caudal rhombencephalon showing labeled cells in the inferior olive and raphe nucleus (detail in the inset). **M,** Detail of a labeled cell in the nucleus of the descending trigeminal root and some cells in the lateroventral inferior reticular formation (lateral reticular nucleus). **N,** Detail of labeled cells in the lateral reticular nucleus and intermediate reticular areas at the caudal rhombencephalon. **O,** Panoramic view of the caudal rhombencephalon showing a labeled cell in the raphe nucleus (detail in the inset). For abbreviations, see list. Scale bar = 75 µm in A,E,K; 150 µm in B-D,F,J,L-O; 500 µm in G-I.

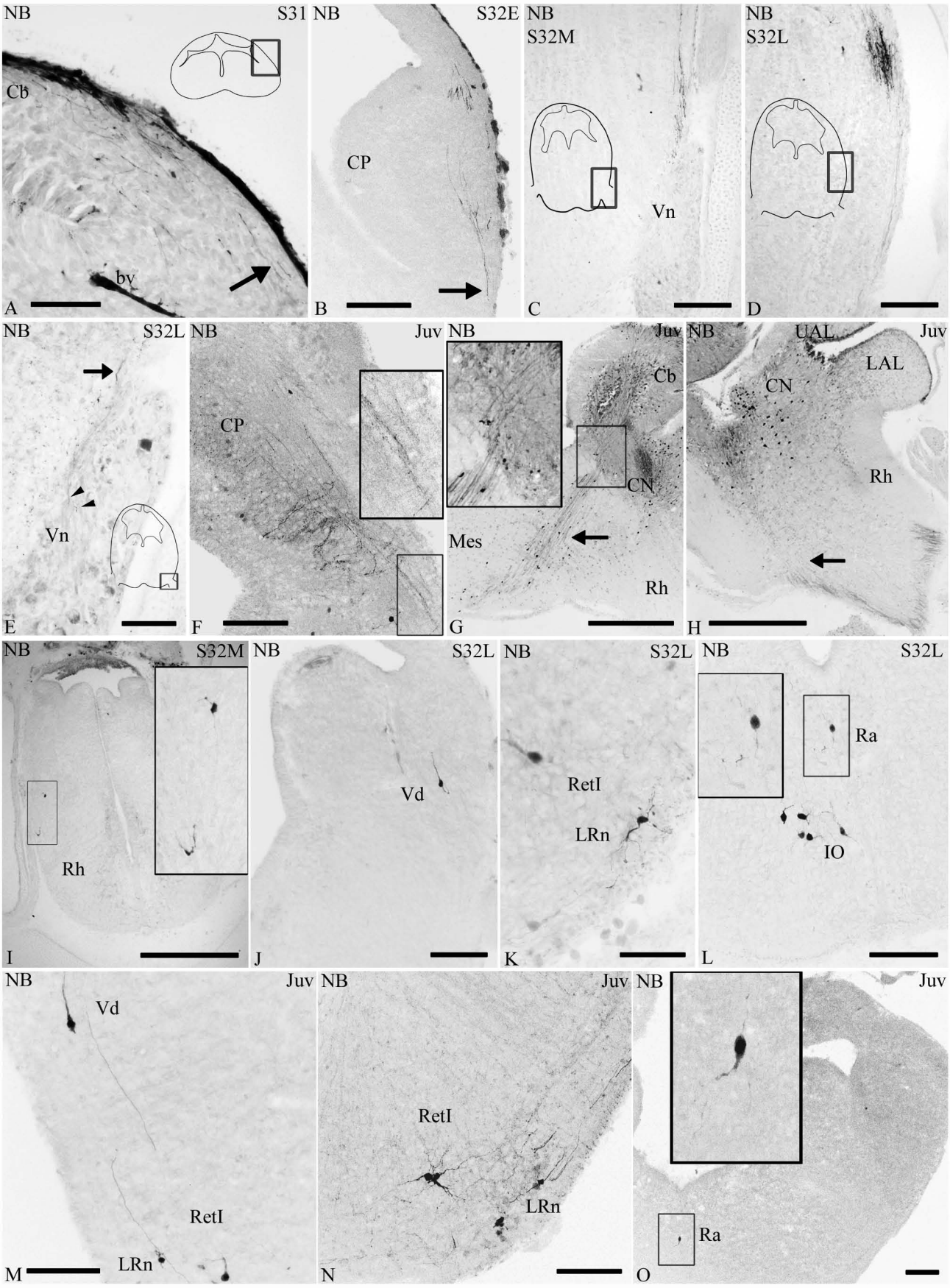
NB
S31
Cb
by
A
NB
S32E
CP
B
NB
S32M
Vn
C
NB
S32L
D
NB
S32L
Vn
E
NB
Juv
CP
F
NB
Juv
Cb
CN
Mes
Rh
G
NB
UAL
Juv
LAL
CN
Rh
H
NB
S32M
Rh
I
NB
S32L
Vd
J
NB
S32L
RetI
LRn
K
NB
S32L
Ra
IO
L
NB
Juv
Vd
RetI
LRn
M
NB
Juv
RetI
LRn
N
NB
Juv
Ra
O

FIGURE 8

Figure 9. Transverse (A-K) and sagittal (L) sections of the caudal rhombencephalon of intermediate 32 (A-C) and late 32 (D-I) embryos, and of juveniles (J-L) showing cells labeled after application of the tracer to the cerebellar body. The level of the transverse sections is indicated in Figures 2A and 4B,C. **A,** Panoramic view at the level of the vagal nerve root showing a labeled cell (detail in the inset) in the rostral inferior olive primordium. **B,** Panoramic view of the rhombencephalon-spinal cord boundary showing two labeled cells, likely in the caudal inferior olive primordium. **C,** Detail of area squared in B showing paramedian labeled cells. **D,** Panoramic view of the rhombencephalon of a late stage 32 at the level of the vagal nerve root showing labeled cells in the rostral inferior olive (detail in the inset). **E,F,** Details of labeled cells in the rostral (E) and caudal (F) subpopulations of the inferior olive. **G-I,** Detail of the inferior olive showing rounded or elongated NB labeled cells (G) that are DCX negative (H; compare black arrows in G'and arrowheads in H') and HuC/D positive (I; compare black arrows in G' and I'). G-I corresponds to color Figure 14M. **J,K,** Details of adjacent sections showing that labeled cells in the rostral subpopulation (J) of the inferior olive are located dorsally to the caudal subpopulation (K). Note that cells are mostly rounded and some elongated (white arrow in K). **L,** Sagittal view of the inferior olive showing abundant labeled cells in the two subpopulations (rostral and caudal), and a dense tangle of dendrites and fibers in the neuropil. For abbreviations, see list. Scale bar = 75 µm in C,E-I; 150 µm in B,J,K; 500 µm in A,D,L.

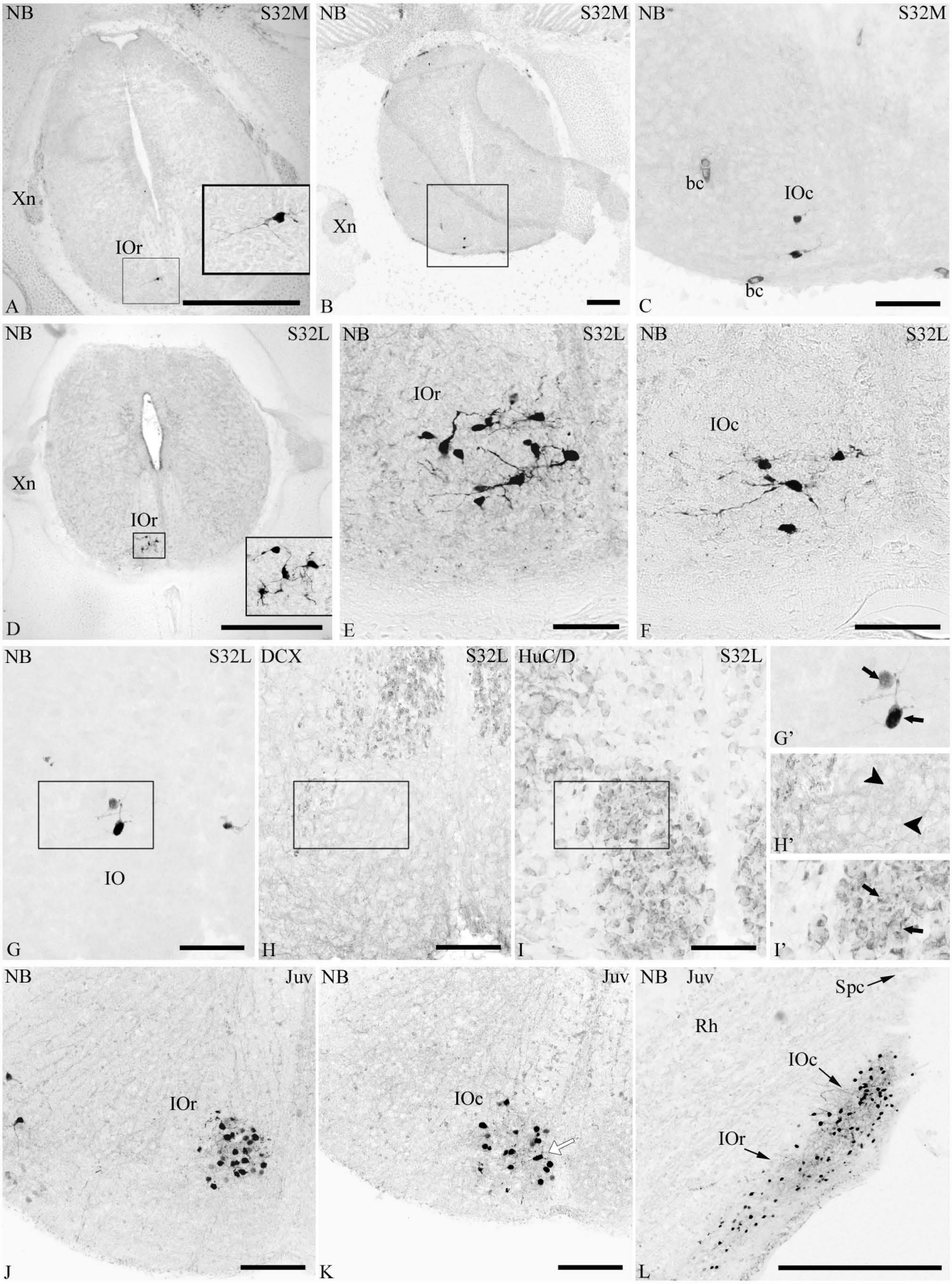
NB
S32M
Xn
IOr
A
B
bc
IOc
C
S32L
D
E
F
DCX
HuC/D
IO
G
H
I
G'
H'
I'
Juv
J
K
Spc
Rh
L

FIGURE 9

Figure 10. Transverse sections at embryonic stages 31 (B), early 32 (C-G) and late 32 (A) after application of the tracer to the cerebellar body in A (black area in the scheme in A) and to the rostral spinal cord in B-G (black area in the schemes in B and C). The level of the sections is indicated in Figure 4A,C. **A,** Section through the rostral spinal cord showing a labeled cell (arrow) in the ventral horn. **B,** Cerebellar peduncle primordium showing an anterogradely labeled fiber (arrow). **C-E,** Some labeled fibers in the cerebellar cortex (arrows in C), and ipsilateral (arrow in D) and contralateral cerebellar peduncle (arrow in E). **F,** Section through isthmic levels showing labeled fibers in the anterior medullary velum and cerebellum. **G,** Labeled fibers at the median cerebellar cortex (arrow in the inset). For abbreviations, see list. Scale bar = 75 µm in B,C,G; 150 µm in A,D-F.

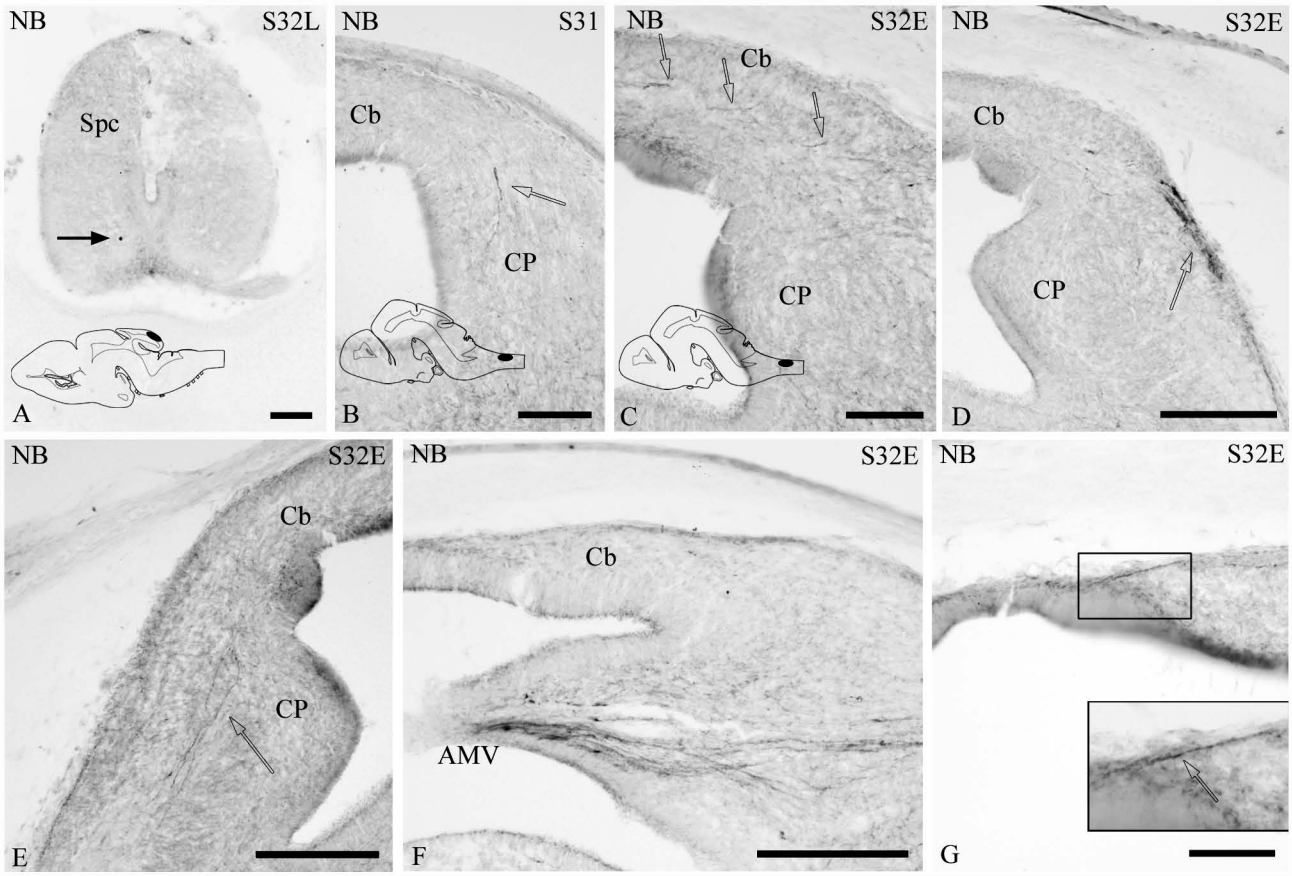
NB
S32L
Spc
A
NB
S31
Cb
CP
B
NB
S32E
Cb
CP
C
NB
S32E
Cb
CP
D
NB
S32E
Cb
CP
E
NB
S32E
Cb
AMV
F
NB
S32E
G

FIGURE 10

Figure 11. Transverse sections of the diencephalon (A-D) and mesencephalon (E-K) of juveniles of *S. canicula* after application of the tracer to the cerebellar body and subsequent immunohistochemistry with the markers indicated by the color code. White arrows point double labeled cells (colocalization of NB and immunomarkers), arrowheads indicate single labeled cells (not colocalization of NB with immunomarkers) and outlined arrows point to NB positive reticular cells in the mesencephalic tegmentum. **A,** Panoramic view showing NB and CR-ir cells in the pretectum and thalamus. **B,** Detail of area squared in A, showing some NB-CR double labeled cells (displayed in the inset). **C,** NB labeled thalamic and pretectal cells intermingled with 5-HT-ir and scarce GAD-ir fibers. **D,** NB labeled thalamic cells intermingled with scarce TH-ir fibers. Note the low density of ChAT immunoreactivity. **E,F,** NB labeled reticular cells of the mesencephalic tegmentum intermingled with Glut-ir and NeuN-ir cells. Some cells were triple NB-Glut-NeuN (inset in E), and double NB-Glut or NB-CR labeled (insets in E and F). **G,** NB positive reticular cells located laterally to the substantia nigra (TH-ir cells) and intermingled with abundant 5-HT-ir fibers. **H,I,** Details of NB positive cells in the nucleus ruber and the reticular area lateral to it, which are among Glut-ir, NeuN-ir and CR-ir cells. Some NB positive cells of the nucleus ruber present double labeling: NB-Glut (inset in H) or NB-CR (inset in I). **J,** Panoramic view showing the most rostral NB positive cells of the nucleus ruber between the ventral tegmental area and the substantia nigra (TH-ir areas), and NB positive reticular cells laterally to the substantia nigra (detail of cells in the inset). **K,** Detail showing the most caudal NB positive cells of the nucleus ruber located among abundant 5-HT-ir fibers, mostly beaded (surrounding a weak NB labeled cell, yellow arrow in the inset). These NB positive cells are located dorsally to a GAD-ir area and near the most rostral 5-HT-ir reticular cells of the rhombencephalon. For abbreviations, see list. Scale bar = 150 μm in A-K.

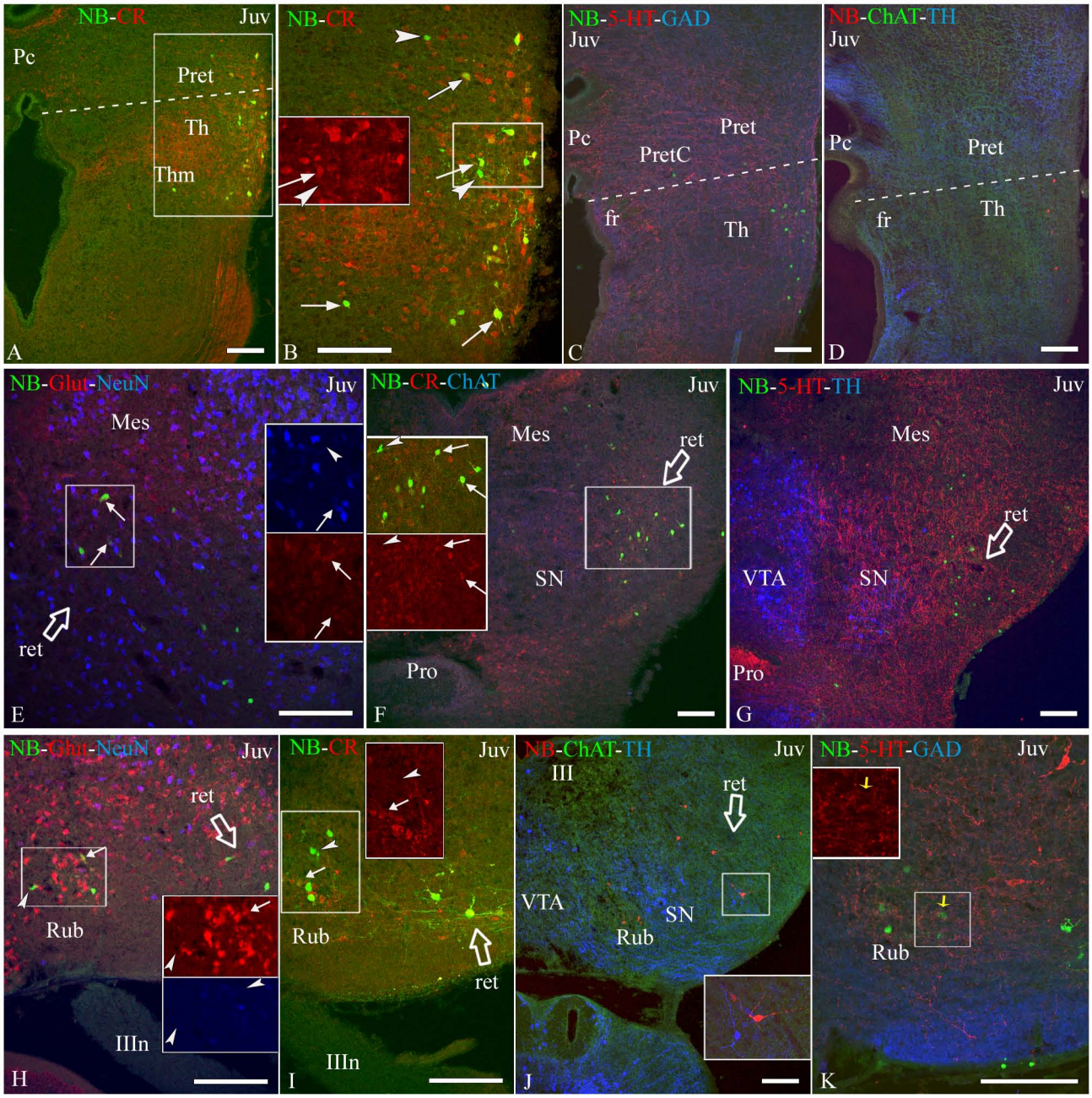
NB-CR
Juv
Pc
Pret
Th
Thm
A
NB-CR
B
NB-5-HT-GAD
Juv
Pc
Pret
PretC
fr
Th
C
NB-ChAT-TH
Juv
Pc
Pret
fr
Th
D
NB-Glut-NeuN
Juv
Mes
ret
E
NB-CR-ChAT
Juv
Mes
ret
SN
Pro
F
NB-5-HT-TH
Juv
Mes
ret
VTA
SN
Pro
G
NB-Glut-NeuN
Juv
ret
Rub
IIIn
H
NB-CR
Juv
Rub
ret
IIIn
I
NB-ChAT-TH
Juv
III
ret
VTA
SN
Rub
J
NB-5-HT-GAD
Juv
Rub
K

FIGURE 11

Figure 12. Transverse sections of rostral rhombencephalic tegmentum (A-H) at the levels indicated in the schemes in Figs. A and E, and cerebellar peduncle (I-O) of juveniles showing labeled structures after application of the tracer to the cerebellar body and subsequent immunohistochemical combinations. While white arrows indicate double labeled cells (colocalization of NB with immunomarkers), arrowheads point single NB labeled cells (no colocalization with immunomarkers). **A-D,** Details of NB labeled cells of the superior reticular formation (at ventral and intermediate levels) located among abundant CR-ir, Glut-ir and NeuN-ir cells and near 5-HT-ir cells. Note double labeled NB-CR (A) and NB-Glut (B) cells and some triple labeled NB-Glut-NeuN cells (B). The surrounding neuropil shows abundant 5-HT-ir and TH-ir fibers, but scarce GAD-ir or ChAT-ir fibers (C,D). **E-H,** Details of the NB labeled cells of the isthmic group, mostly NB-CR double labeled (E), which are lateral to the locus coeruleus (TH-ir cells) (F,G) and latero-ventral to the isthmic nucleus densely innervated by 5-HT-ir fibers (F,H). Note a few NB labeled-TH-negative cells in the locus coeruleus (asterisk in G), and a TH-ir cell with weak staining for NB (inset in G). Moreover, NB positive fibers of the isthmic group run in parallel with 5-HT-ir and GAD-ir fibers (H). **I-O,** Panoramic views and details of NB labeled cells and fibers in the cerebellar peduncle. **I,** NB-CR double labeled cells in the medial and subventricular parts of cerebellar nucleus. Note double labeled fibers in the white matter region. **J,** NB labeled cells of subventricular, medial and lateral cerebellar nucleus intermingled with abundant Glut-ir cells and some NeuN-ir cells. Some NB-Glut double labeled cells were observed in the medial and lateral (inset) parts. **K,** NB labeled fibers in the dorsomedial or white matter parts of the cerebellar nucleus appear intermingled with GAD-ir neuropil, whereas NB positive cells in the medial part appear intermingled with abundant 5-HT-ir fibers (yellow arrow in the inset). **L,** The abundant NB labeled fibers and 5-HT-ir fibers show a separate distribution in the cerebellar nucleus. Note a few 5-HT-ir fibers (outlined arrows) among outstanding bundles of NB labeled fibers. The NB positive cells in the lateral part of cerebellar nucleus are located among abundant 5-HT-ir fibers. **M,** NB labeled cells in the subventricular, medial and lateral parts of cerebellar nucleus are intermingled with abundant TH-ir fibers and ChAT-ir fiber endings (yellow arrows). **N,** Subventricular part of the cerebellar nucleus showing abundant NB labeled cells, in addition to fibers and fiber endings singly positive for NB, ChAT and TH. **O,** Detail of the cerebellar peduncle corresponding to the area squared in M showing no colocalization of NB and ChAT-ir in fibers. Note NB labeled and TH-ir fibers coursing in parallel following a dorsoventral orientation. For abbreviations, see list. Scale bar = 50 μm in O; 75 μm in A,E,N; 150 μm in B,C,D,F-M.

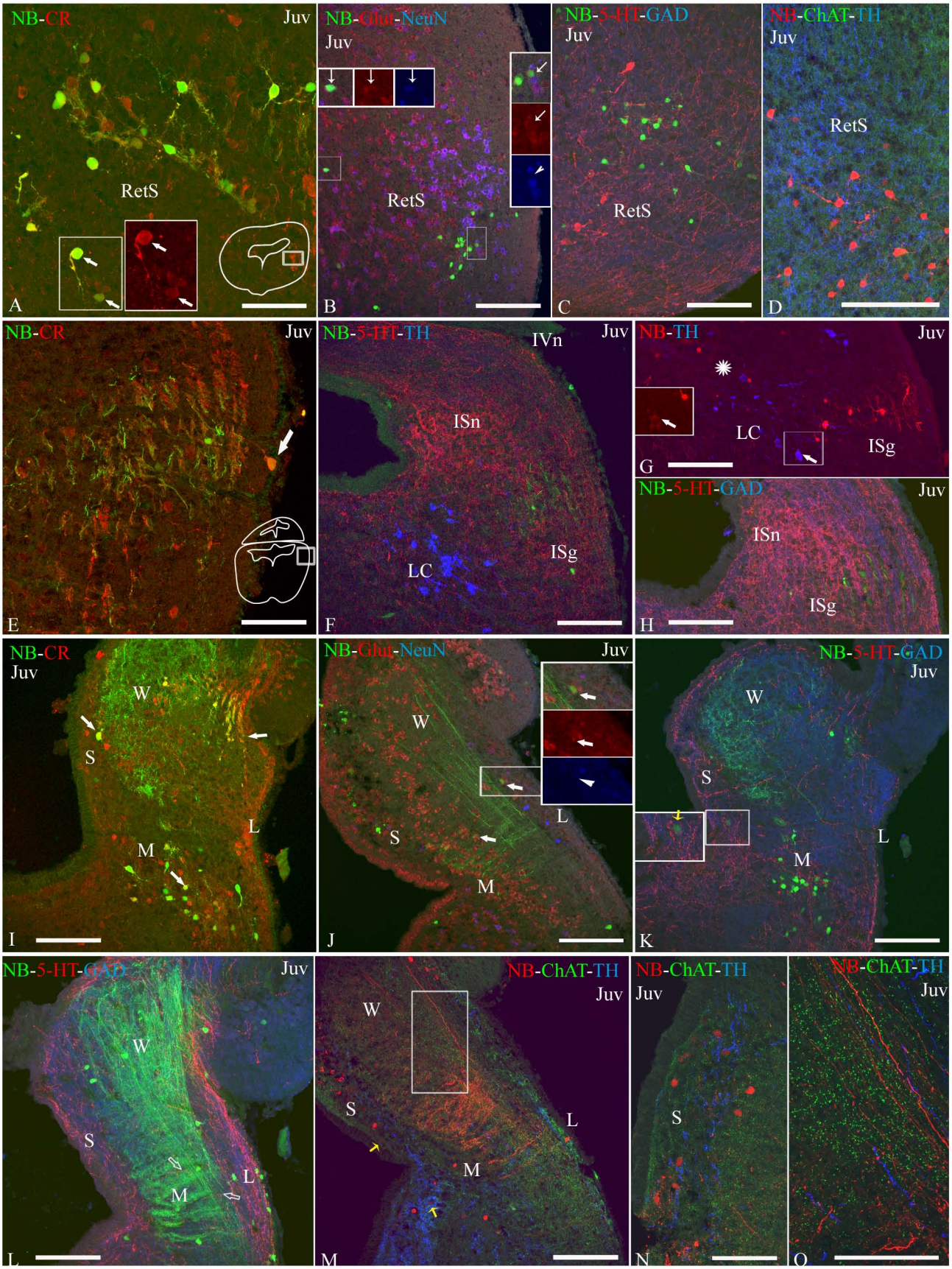
NB-CR
Juv
RetS
A
NB-Glut-NeuN
Juv
RetS
B
NB-5-HT-GAD
Juv
RetS
C
NB-ChAT-TH
Juv
RetS
D
NB-CR
Juv
E
NB-5-HT-TH
IVn
Juv
ISn
LC
ISg
F
NB-TH
Juv
LC
ISg
G
NB-5-HT-GAD
Juv
ISn
ISg
H
NB-CR
Juv
W
S
L
M
I
NB-Glut-NeuN
Juv
W
S
L
M
J
NB-5-HT-GAD
Juv
W
S
L
M
K
NB-5-HT-GAD
Juv
W
S
L
M
L
NB-ChAT-TH
Juv
W
S
L
M
M
NB-ChAT-TH
Juv
S
N
NB-ChAT-TH
Juv
O

FIGURE 12

Figure 13. Transverse sections through the caudal rhombencephalon (A-K) and spinal cord (L,M) of juveniles after application of the tracer to the cerebellar body and combination with immunohistochemistry. White arrows indicate double labeled cells and arrowheads indicate single labeled cells. **A-E,** NB positive precerebellar cells in the inferior reticular formation located at paramedian (in A,E), submarginal (lateral reticular area or lateral reticular nucleus, in A-C,E) and raphe (in D) areas. Note that some of them are NB-CR-ChAT (inset in A) and NB-Glut-NeuN (inset in B) triple labeled cells but 5-HT negative (C and inset in D). The NB labeled cells are located in areas with relative moderately dense neuropil immunoreactive to 5-HT, GAD (C,D), TH and ChAT (E). **F-K,** Panoramic view (F) and details (G-K) of the inferior olive, showing colocalization in NB retrogradely labeled olivary cells with CR (inset in F) and Glut (G); the inferior olive is surrounded by Glut-NeuN (G) double labeled, TH-ir (H) and 5-HT-ir (H,I) reticular cells. Note also some NB positive cell of the inferior reticular formation close to the inferior olive (inset in I) and the different neurochemical content (H-K) of the dendritic processes (outlined arrows in H,I,K), beaded fibers, and boutons (yellow arrow in I) that innervate the inferior olivary area. **L,M,** NB labeled cells in the ventral horn of the spinal cord. Note a NB-CR double labeled cell (arrow in L) close to ChAT-ir motoneurons and a NB positive cell close to 5-HT-ir cells and intermingled with GAD-ir and 5-HT-ir fiber endings near the spinal cord floor plate (in M). For abbreviations, see list. Scale bar = 75 µm in G-K; 150 µm in A-F,L,M.

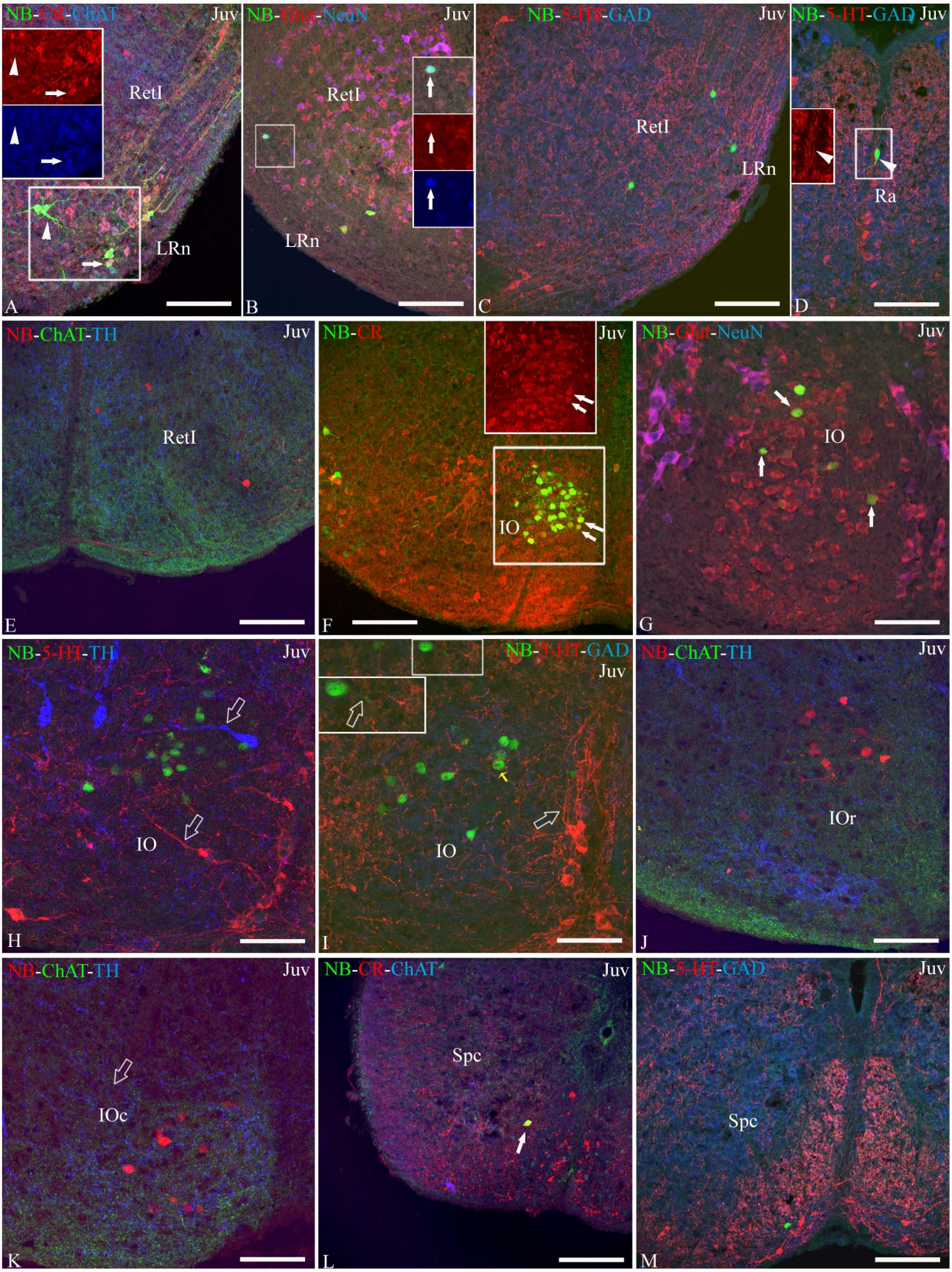
NB-CR-ChAT
Juv
RetI
LRn
A
NB-Glut-NeuN
Juv
RetI
LRn
B
NB-5-HT-GAD
Juv
RetI
LRn
C
NB-5-HT-GAD
Juv
Ra
D
NB-ChAT-TH
Juv
RetI
E
NB-CR
Juv
IO
F
NB-Glut-NeuN
Juv
IO
G
NB-5-HT-TH
Juv
IO
H
NB-5-HT-GAD
Juv
IO
I
NB-ChAT-TH
Juv
IOr
J
NB-ChAT-TH
Juv
IOc
K
NB-CR-ChAT
Juv
Spc
L
NB-5-HT-GAD
Juv
Spc
M

FIGURE 13

Figure 14. Sagittal (A-C) and transverse (D-M) sections through the rhombencephalon at embryonic stages 23 (A-C), 30 (D-I) and late 32 (J-M) to show cellular migrations from the rhombic lips. White arrows point double labeled cells and processes, and arrowheads indicate single labeled processes. The color code in each photomicrograph indicates the markers used. **A-C,** Panoramic view (A) and detail (B,C) of the isthmus showing DCX and HuC/D double labeled neuroblasts tangentially oriented to the brain surface and apparently coursing in dorsoventral (arrows in B,C) and rostro-caudal (outlined arrow in B,C) directions. **D-I,** Details of caudal rhombencephalon after tracer application in the lower rhombic lips (white area in the scheme in D) at stage 30 and subsequent immunohistochemistry with different markers (D-F,H,I). **D-F,** Details of NB-DCX double labeled neuroblasts tangentially oriented at marginal (D), submarginal (E) and floor plate (F) levels. Locations of photomicrographs are indicated in the schemes in D and F. **G-I,** Details of radially oriented processes of NB labeled neuroblasts located in the area indicated in the schemes in G and I, showing a growth cone containing NB (outlined arrow in G), a process double labeled with NB and DCX (H), and two close processes labeled for NB and GFAP, respectively (I). **J-M,** Panoramic view (J) and details (K-M) of the caudal rhombencephalon after application of the tracer to the cerebellar body. Note DCX-HuC/D double labeled cells in the marginal zone of the rhombencephalon (K corresponds to the area squared in J), and NB-HuC/D double labeled cells in the lateral reticular area (L) and in the inferior olive (M corresponds to merged Figure 9G-I). For abbreviations, see list. Scale bar= 50 µm in F,G; 75 µm in B-E,H,I,K-M; 150 µm in A,J.

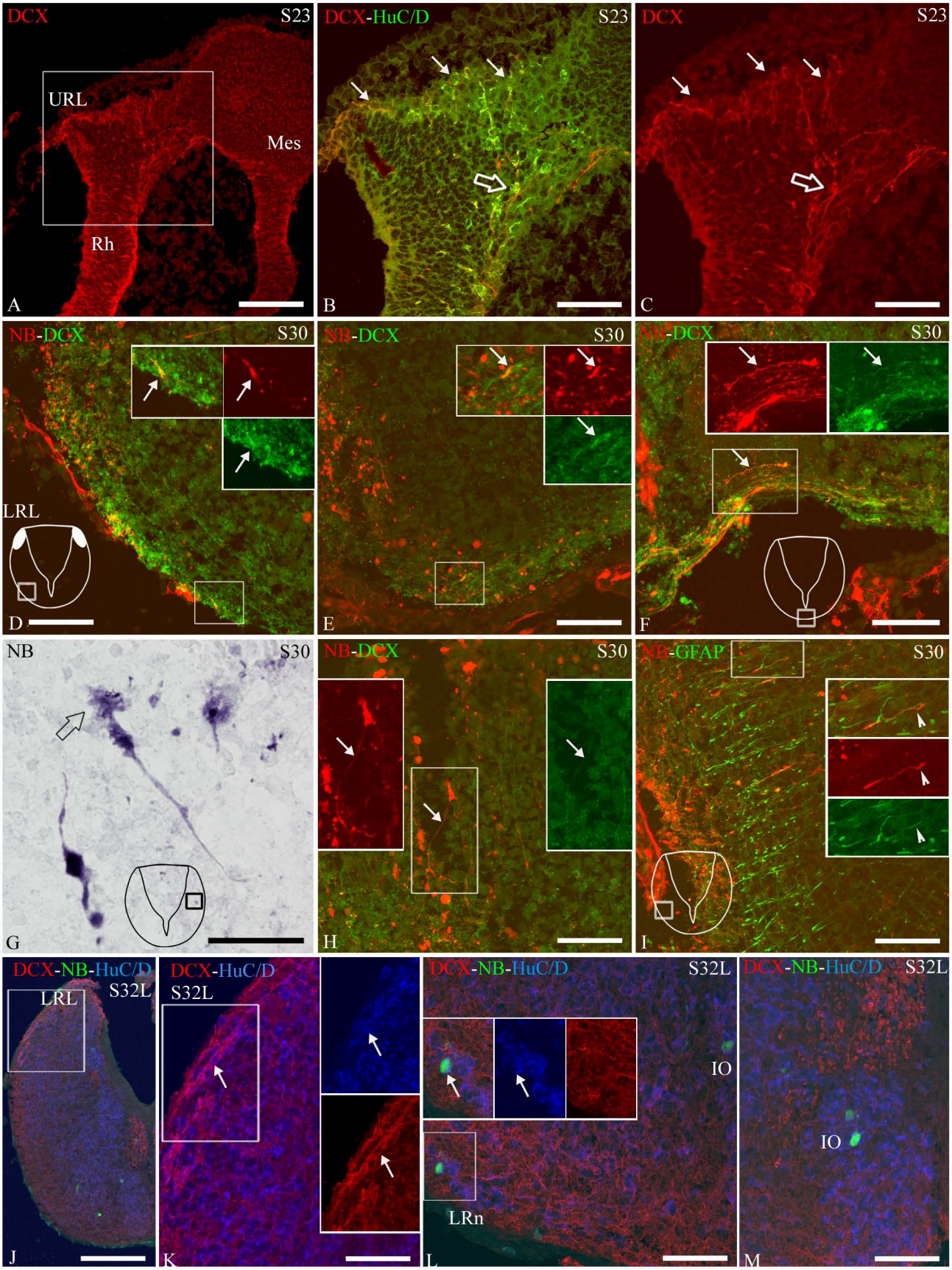
DCX
S23
URL
Mes
Rh
A
DCX-HuC/D
S23
B
DCX
S23
C
NB-DCX
S30
LRL
D
NB-DCX
S30
E
NB-DCX
S30
F
NB
S30
G
NB-DCX
S30
H
NB-GFAP
S30
I
DCX-NB-HuC/D
S32L
LRL
J
DCX-HuC/D
S32L
K
DCX-NB-HuC/D
S32L
IO
LRn
L
DCX-NB-HuC/D
S32L
IO
M

FIGURE 14

Figure 15. Schematic representation of the order of appearance of connections of some precerebellar nuclei of the rhombencephalon and spinal cord in the lesser spotted dogfish, rat and chick; the relative percentage of embryonic development was taken into account.

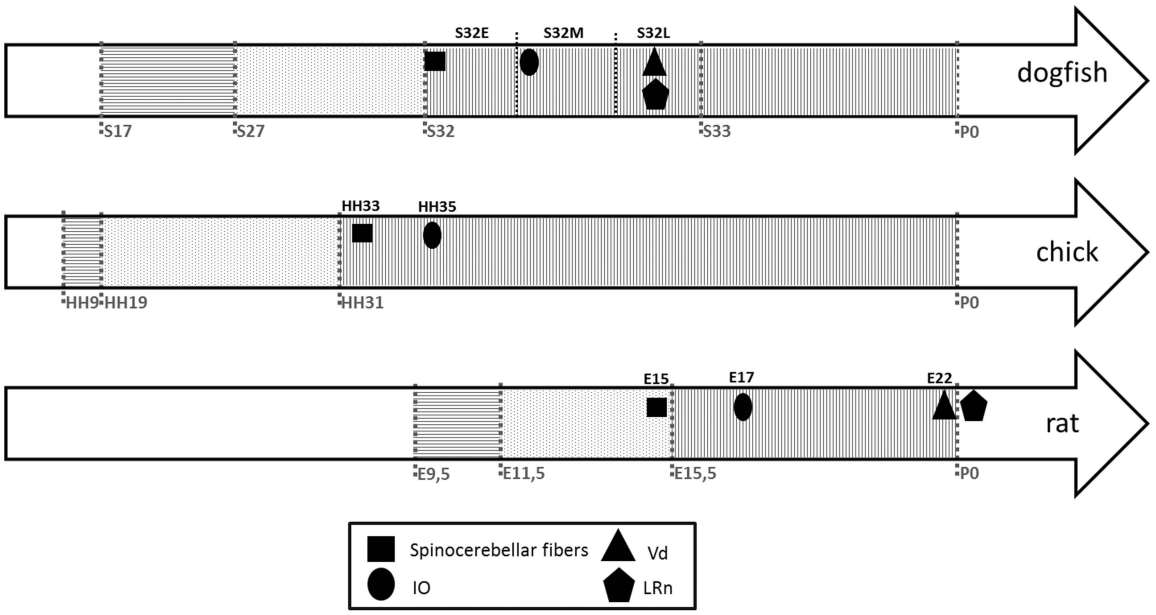
S32E
S32M
S32L
dogfish
S17
S27
S32
S33
P0
HH33
HH35
chick
HH9
HH19
HH31
P0
E15
E17
E22
rat
E9,5
E11,5
E15,5
P0
Spinocerebellar fibers
Vd
IO
LRn

FIGURE 15

USC
UNIVERSIDADE
DE SANTIAGO
DE COMPOSTELA

GENERAL DISCUSSION

USC
UNIVERSIDADE
DE SANTIAGO
DE COMPOSTELA

GENERAL DISCUSSION

As it has been described throughout this work, although cartilaginous fishes represent a key phylogenetic group because of the evolutionary innovation of the cerebellum at the agnathan-gnathostome transition, only a few studies have been concerned to the cerebellar development in these fishes (Larsell, 1967; Rodríguez-Moldes et al., 2008; Chaplin et al., 2010).

In the present work we have performed the first genoarchitectonic study of the rostral hindbrain of the shark *Scyliorhinus canicula* (Chapter 1). Because we have focused our attention to pharyngula stages, characterized by the cerebellar primordium appearance, our results may help to better understand the early cerebellar patterning in basal gnathostomes. This study has led us to distinguish the segmental identity of the region where the cerebellar primordium is located. As the gene expression patterns of the rostral hindbrain appears very similar to that described in amniote species (Aroca and Puelles, 2005), we could clearly discern the midbrain-hindbrain boundary as well as the distinct identity of rhombomere 0 and rhombomere 1. These results could give the basis for explaining some changes in gene expression that could have caused the evolutionary innovation of the cerebellum in the ancestor of gnathostomes. Indeed, though the isthmic genoarchitecture in *S. canicula* mostly coincides with that of agnatha (reviewed in Kuratani et al., 2002), small differences in gene expression patterns could explain why the isthmic organizer only induces the formation of a true cerebellum in jawed vertebrates. Interestingly, genes involved in the earliest patterning of the cerebellum and the jaw appear to be closely related. Both the cerebellum and jaw are considered evolutionary innovations in the ancestor of the gnathostome lineage, a fact that has been related to the appearance of new ways of feeding and more active locomotion (reviewed in Northcutt, 2002).

Developmental studies are essential for understanding the different morphogenetic processes that give rise to an adult cerebellum. So far, the most meticulous description about the cerebellar morphogenesis in chondrichthyans is that reported by Larsell (1967). Nevertheless, we have delved deeper into this aspect. The comprehensive developmental analysis we carried out in *S. canicula* to identify anatomical landmarks and cerebellar compartmentalization was performed on the three spatial axis (rostro-caudal, dorso-ventral and medio-lateral) of the developing cerebellum (Chapter 2). Moreover, molecular markers supplemented and supported the information obtained by analyzing anatomical landmarks. It should be noted that while early on development the position of the isthmic or meso-rhombencephalic fissure does not exactly coincides with the midbrain-hindbrain boundary based of gene expression data (see Chapter 1), the location of other cerebellar fissures and main subdivisions appeared to coincide, respectively with the limits and domains of expression of certain genes, respectively. These results emphasize the importance of combining descriptive classic studies with modern molecular techniques, as well as their usefulness in comparative neuroanatomy, as has been nicely illustrated by Puelles and Ferrán (2012). Furthermore, present genoarchitectonic and morphogenetic analysis (Chapters 1 and 2) allowed us to define when, where and how each part of the cerebellum is formed, and to characterize three developmental periods which provided the basis for the analysis of other aspects of the cerebellar development in this species and for the comparative neuroanatomical study performed (Chapter 3). These analysis have shown evidence that main developmental events we have observed in the cerebellum of *S. canicula* appear well conserved through evolution.

The realization of this work helped us to solve some major questions but has raised new ones. On the one hand, when analyzing from what rhombomere the different

parts of the cerebellum are formed, we found some evidence that the cerebellum is formed exclusively from the rhombomere 1. Of note, *ScHoxA2* (that is expressed in the rhombomere 2) was found in a domain that was classically identified as belonging to the lower auricle leaf. This result could indicate that part of the lower auricle leaf derives from r2. However, we think that this *ScHoxA2* (r2) domain does not belong to the auricle because of the neurochemical differences found between these two regions. Further studies will be necessary for undeniably identifying the different rhombomeric derivatives.

On the other hand, our results about a very simple median-lateral compartmentalization in the cerebellar cortex of *S. canicula* support the absence of multiple parasagittal bands in basal gnathostomes, as previously suggested (Puzdrowski, 1997). Since in mammals different compartments are associated with different functionalities and, therefore, with a topographic map of the cerebellar afferents (Sillitoe et al., 2010), the existence of a paramedian *ScEn2* positive and two lateral *En2* negative bands in *S. canicula* could be directly or indirectly related with the parasagittal topography of the olivocerebellar projection described by Fiebig (1988) in other elasmobranch species. The analysis of other compartmentalization markers, as well as hodologic studies, will be useful tools to further explore this hypothesis.

Because the complexity of the cerebellar system is related to its set of connections, we also carried out a hodologic study in *S. canicula* (Chapter 3). The evidence of a possible topographic projection from the inferior olive similar to that reported in other elasmobranch (Fiebig, 1988) could be related to the basic median-lateral compartmentalization described on the basis of the expression of *ScEn2* (Chapter 2). The afferent and efferent system appeared very similar to that previously described in batoids (Fiebig, 1988; Puzdrowski and Gruber, 2009). Because the cerebellum of the

lesser spotted dogfish is simpler to that of batoids, and for this closer to the ancestral condition, we could generalize a set of cerebellar connections among cartilaginous fishes. Additionally we have characterized the precerebellar nuclei according following a segmental model of the brain.

The results about the orderliness of cerebellar afferents arrival, which represent the first developmental study of connections of the cerebellar body in fishes, showed that the incoming of cerebellar afferents is mostly concurrent with establishment of the layering in the cerebellar cortex, previously reported by our group (Rodríguez-Moldes et al., 2008). Additionally, it coincides with the completion of the mature shape of the cerebellum that occurs at stage 32 (Chapter 2). However, some afferent cells from the cerebellar nucleus were observed earlier, at stage 31. Interestingly, at this stage although the cerebellar body has not yet achieved its mature shape, the protuberance of the cerebellar peduncle became already patent (Chapter 2).

Also noteworthy is the fact that the arrival of spinal fibers to the cerebellar cortex before than that climbing fibers, appeared to be a highly conserved trait throughout evolution. Besides, the observation of the onset of Purkinje cells maturation at intermediate stage 32 may be used to establish the correspondence among equivalent developmental stages of other vertebrates.

Because we have observed a high degree of conservation in the order of arrival of the different cerebellar afferents to the cerebellar cortex, we suggest that this orderliness could be indicative of the onset of different control systems by the cerebellum throughout development. For instance, as regards the control of visual reflexes, the detection of the first pretectal afferents was concurrent with the onset of the maturation of the photoreceptors in the retina (Ferreiro-Galve et al., 2010). In fact the

developmental timing of the retina (described by Ferreiro-Galve et al., 2010) and that of the cerebellum appear to be roughly concurrent.

The evidence of rhombic lips derivatives that migrate tangentially along the migratory pathways of precerebellar nuclei precursors (see Sotelo and Chedotal, 2005) led us to propose that the precerebellar nuclei of *S. canicula* arise from the rhombic lips or somatosensorial area of the hindbrain, as was the case of the cerebellum (Chapter 1 and 2). Furthermore, by comparing the location of cells that migrate tangentially from the upper rhombic lip (Chapter 3), to that of the expression domain of *ScFgf8* (Chapter 2), we could verify that they are located in the rostral part of the rhombomere 1 (or upper rhombic lip). The comparative analysis of our result with those described in other gnathostomes (Sotelo and Chedotal, 2005; Wullimann et al., 2011), revealed a high degree of evolutionary conservation also in the origin of precerebellar nuclei.

To more accurately characterize these tangential migratory pathways in *S. canicula*, it should be necessary at least to genetically identify the rhombic lip derivatives and to elucidate their cell lineage and destination. We aimed then to search for new techniques that help to solve this question. Since techniques for monitoring cell lineages have been successfully carried out in other fish species (Wullimann et al., 2011) we aimed to become familiar with these experimental approaches and explore their possible application in *S. canicula*. In a short stay in the laboratory of the Professor Reinhard Köster at the Technische Universität Braunschweig (Braunschweig, Germany), I have the opportunity of being trained in the generation of transgenic lines and electroporation techniques, which allowed transfecting plasmids in late zebrafish embryos. The application of these techniques to our animal model could open possibilities for further comparative neuroanatomical studies.

LITERATURE CITED

Aroca P, Puelles L. 2005. Postulated boundaries and differential fate in the developing rostral hindbrain. Brain Res Rev 49:179-190.

Chaplin N, Tendeng C, Wingate RJ. 2010. Absence of an external germinal layer in zebrafish and shark reveals a distinct, anamniote ground plan of cerebellum development. J Neurosci 30:3048-3057.

Ferreiro-Galve S, Rodríguez-Moldes I, Anadón R, Candal E. 2010. Patterns of cell proliferation and rod photoreceptor differentiation in shark retinas. J Chem Neuroanat 39:1-14.

Fiebig E. 1988. Connections of the corpus cerebelli in the thornback guitarfish, *Platyrhinoidis triseriata* (Elasmobranchii): a study with WGA-HRP and extracellular granule cell recording. J Comp Neurol 268:567-583.

Kuratani S, Kuraku S, Murakami Y. 2002. Lamprey as an evo-devo model: lessons from comparative embryology and molecular phylogenetics. Genesis 34:175-83.

Larsell O. 1967. The comparative anatomy and histology of the cerebellum from myxinoids through birds. University of Minnesota Press, Minneapolis.

Northcutt RG. 2002. Understanding vertebrate brain evolution. Integr Comp Biol 42:743-756.

Puelles L, Ferrán JL. 2012. Concept of neural genoarchitecture and its genomic fundament. Front Neuroanat 6:47.

Puzdrowski RL. 1997. Anti-Zebrin II immunopositivity in the cerebellum and octavolateral nuclei in two species of stingrays. Brain Behav Evol 50:358-368.

Puzdrowski RL, Gruber S. 2009. Morphologic features of the cerebellum of the Atlantic stingray, and their possible evolutionary significance. Integr Zool 4:110-122.

Rodríguez-Moldes I, Ferreiro-Galve S, Carrera I, Sueiro C, Candal E, Manzan S, Anadón R. 2008. Development of the cerebellar body in sharks: spatiotemporal relations of Pax6-expression, cell proliferation and differentiation. Neurosci Lett 432:105-110.

Sillitoe RV, Vogel MW, Joyner AL. 2010. *Engrailed* homeobox genes regulate establishment of the cerebellar afferent circuit map. J Neurosci 30:10015-24.

Sotelo C, Chedotal A. 2005. Development of the olivocerebellar system: migration and formation of cerebellar maps. Prog Brain Res 148:1-20.

Wullimann MF, Mueller T, Distel M, Babaryka A, Grothe B, Köster RW. 2011. The long adventurous journey of rhombic lip cells in jawed vertebrates: a comparative developmental analysis. Front Neuroanat 5:1-27.

GENERAL CONCLUSIONS

USC
UNIVERSIDADE
DE SANTIAGO
DE COMPOSTELA

GENERAL CONCLUSIONS

1. The analysis of the genoarchitecture of the rostral hindbrain in *Scyliorhinus canicula* showed that the expression pattern of isthmus related genes is very similar to that of other jawed vertebrates. This high degree of evolutionary conservation allowed us to discern the midbrain-hindbrain boundary as well as the boundaries between r0-r1 and r1a-r1b in the rostral hindbrain.
2. While invertebrates present particular combinations of various isthmus related genes at the IsO-like signaling center, only vertebrates present a whole set of isthmus related genes with conserved expression patterns. Changes in the expression pattern of these genes observed in the agnatha-gnathostome transition (by the comparison between the lesser spotted dogfish and lamprey), might give a clue to clarify why the isthmic organizer only induces the formation of a true cerebellum in jawed vertebrates.
3. The comprehensive study of the morphogenesis of the cerebellum in the shark *S. canicula* and the classification of its cerebellar development into three developmental periods permitted a more systematic study of developmental processes and comparative studies. The comparison of cerebellar morphogenesis in the galeomorph shark *S. canicula* with that of the squalomorph *Squalus* allowed the identification of equivalent embryonic stages between both sharks. Comparing to other gnathostome groups, we have observed that the process of cerebellar morphogenesis in the lesser spotted dogfish appeared to be closer to mammals than to bony fishes, which points to the cerebellum of elasmobranchs as an adequate model to study the ancestral condition of jawed vertebrates.
4. The combined analysis on the gross anatomy and the gene expression patterns in this model species allowed us to identify cerebellar fissures as consistent

anatomical landmarks. Their order of emergence appeared to be roughly maintained through evolution, and therefore should be considered as an important developmental feature of the cerebellum in gnathostomes. Such genoarchitectonic analysis led us to discern the possible basal median-lateral compartmentalization of the cerebellum and to provide evidence of the exclusive cerebellar origin from r1.

5. The characterization of precerebellar nuclei in *S. canicula* done following a segmental model of the brain revealed that this species share traits with other vertebrates. The developmental analysis revealed that the incoming of cerebellar afferents is concurrent with the establishment of layering in the cerebellum and that, later on, new precerebellar neurons become gradually demonstrable by retrograde transport, which reflects the progressive maturation of the granular and Purkinje cell layers.
6. The hodologic and developmental study allowed the identification of key events as the onset of Purkinje cells maturation, which provides a reliable reference to establish correspondences among equivalent developmental stages of other vertebrates.
7. The knowledge gained on the development of the olivo-cerebellar projection in *S. canicula* allows comparisons with the olivo-cerebellar system of other gnathostomes and supports hypothesis that involve this system in the timing of movements. This developmental analysis also showed that the spino-cerebellar projections, which precede the olivo-cerebellar projection, could be involved in early control of body movements by the cerebellum.

8. Similarities observed in the neurochemical signature of precerebellar nuclei between *S. canicula* and amniotes reveal a high degree of conservation of the organization of the cerebellar system.
9. The evidence of tangential and radial migrations of rhombic lips derivatives in *S. canicula*, similar to that observed in other jawed vertebrates, suggests that migrating pathways of precerebellar nuclei precursors from rhombic lips appeared very early in gnathostome evolution.
10. The results obtained in the present work show that common features between *S. canicula* and other gnathostomes in relation to the cerebellar development may represent the basal mechanisms necessary for the formation of more complex cerebella, thus revealing the ancestral organization of the cerebellar system.

USC
UNIVERSIDADE
DE SANTIAGO
DE COMPOSTELA

CONCLUSIONES GENERALES

1. El análisis de la genoarquitectura del rombencéfalo rostral en *Scyliorhinus canicula* mostró que el patrón de expresión de genes relacionados con el istmo es muy similar al de otros vertebrados mandibulados. Este alto grado de conservación evolutiva nos permitió discernir el límite mesencéfalo-rombencéfalo así como los límites entre r0-r1 y r1a-r1b en el rombencéfalo rostral.
2. Mientras que los invertebrados presentan combinaciones particulares de varios genes relacionados con el istmo en el símil a un organizador ístmico, sólo los vertebrados presentan un conjunto de genes relacionados con el istmo con patrones de expresión conservados. Cambios en el patrón de expresión de estos genes observados en la transición agnatos-gnatóstomos (mediante la comparación entre la pintarroja y lamprea), podría dar una pista para clarificar por qué el organizador ístmico solo induce la formación de un verdadero cerebelo en vertebrados mandibulados.
3. El estudio detallado de la morfogénesis del cerebelo en el tiburón *S. canicula* y la clasificación de su desarrollo cerebelar en tres periodos de desarrollo permitió un estudio más sistemático de los procesos de desarrollo y estudios comparativos. La comparación de la morfogénesis cerebelar en el tiburón galeomorfo *S. canicula* con el del escualomorfo *Squalus* permitió la identificación de estadios embrionarios equivalentes entre ambos tiburones. En la comparación con otros grupos de gnatóstomos, hemos observado que el proceso de morfogénesis cerebelar en la pintarroja parece más próximo al de mamíferos que al de peces óseos, lo que señala al cerebelo de elasmobranquios como un modelo adecuado para estudiar la condición ancestral de vertebrados mandibulados.

4. El análisis combinado de la anatomía y los patrones de expresión de genes en esta especie modelo nos permitió identificar a las fisuras cerebelares como marcadores anatómicos consistentes. Su orden de emergencia parece mantenerse a lo largo de la evolución, y por lo tanto debería ser considerada como una característica importante del desarrollo del cerebelo en gnatóstomos. Dicho análisis genoarquitectónico nos llevó a discernir la posible compartimentalización basal medio-lateral del cerebelo, así como aportar evidencias del origen cerebelar exclusivo de r1.
5. La caracterización de los núcleos precerebelares en *S. canicula* realizados siguiendo un patrón segmentario del encéfalo reveló que esta especie comparte rasgos con otros vertebrados. El análisis del desarrollo reveló que la llegada de aferencias cerebelosas es concurrente con el establecimiento de las capas en el cerebelo y que, más tarde, nuevas neuronas precerebelares llegan a ser gradualmente demostrables mediante transporte retrógrado, lo que refleja la maduración progresiva de las capas granular y de Purkinje.
6. El estudio hodológico y del desarrollo permitió la identificación de sucesos clave, tales como el comienzo de la maduración de las células de Purkinje, lo que aporta una referencia consistente para establecer correspondencias entre estadios del desarrollo equivalentes de otros vertebrados.
7. El conocimiento adquirido sobre el desarrollo de la proyección olivo-cerebelar en *S. canicula* permite comparaciones con el sistema olivo-cerebelar de otros gnatóstomos y apoya la hipótesis que involucra a este sistema en la sincronización de movimientos. Este análisis del desarrollo también mostró que las proyecciones espino-cerebelosas, las cuales preceden a la proyección olivo-cerebelosa, podrían estar implicadas en el control temprano de movimientos corporales por el cerebelo.

8. Similitudes observadas en la naturaleza neuroquímica de los núcleso precerebelosos entre *S. canicula* y amniotas revelan un alto grado de conservación de la organización del sistema cerebelar.
9. La evidencia de migraciones tangenciales y radiales de derivados de los labios rómbicos en *S. canicula*, similar a lo observado en otros vertebrados mandibulados, sugiere que las rutas de migración de los precursores de núcleos precerebelosos desde los labios rómbicos aparecieron muy pronto en la evolución de los gnatóstomos.
10. Los resultados obtenidos en el presente trabajo muestran que las características comunes entre *S. canicula* y otros gnatóstomos en relación al desarrollo cerebelar pueden representar los mecanismos basales necesarios para la formación de cerebelos más complejos, revelando así la organización ancestral del sistema cerebelar.

USC
UNIVERSIDADE
DE SANTIAGO
DE COMPOSTELA

RESUMEN DE LA TESIS

USC
UNIVERSIDADE
DE SANTIAGO
DE COMPOSTELA

RESUMEN DE LA TESIS

Estudio del desarrollo del cerebelo de peces cartilaginosos: hacia la identificación de las características primitivas de la formación del cerebelo de vertebrados gnatóstomos

El cerebelo o "pequeño cerebro" se encarga, entre otras funciones, de integrar la información sensorial y motora y está implicado en la coordinación y regulación de la actividad muscular, así como del mantenimiento del tono muscular y el balance. Pero además participa en el aprendizaje motor (en el que juega un papel importante la oliva inferior) y procesos cognitivos, los cuales han sido descritos incluso en peces óseos, así como en el análisis de la información de la línea lateral y electrorrecepción.

Aunque la estructura cerebelar más compleja se encuentra en aves y mamíferos, todos los gnatóstomos o vertebrados mandibulados presentan una estructura básica en común. Existe un elevado grado de conservación, tanto de la estratificación de la corteza cerebelosa (capas molecular, de Purkinje y granular), como de la mayor parte de los principales tipos celulares (células estrelladas, de Purkinje, granulares y de Golgi). En agnatos (peces sin mandíbula), la presencia o no de un primordio de cerebelo está bajo debate. Sin embargo, dado que no presenta la estructura típica de la corteza cerebelosa (debido a la ausencia de los principales tipos celulares), no se considera un verdadero cerebelo. Dado que el cerebelo es reconocido como una innovación evolutiva de los gnatóstomos, es concurrente con la innovación evolutiva de la mandíbula, y en consecuencia, significó grandes cambios evolutivos, como la aparición de nuevos medios de alimentación (depredación) en vertebrados.

Los condrictios o peces cartilaginosos son reconocidos como el grupo con características más primitivas del cerebelo, y por lo tanto, claves para la búsqueda de la condición ancestral del cerebelo. El tiburón *Scylorhinus canicula*, comúnmente conocido como pintarroja, es un pez cartilaginoso actualmente considerado una especie modelo en Evo-Devo, el nuevo campo que relaciona estudios evolutivos y del desarrollo. En adultos, el cerebelo muestra un cuerpo cerebeloso y un par de aurículas laterales con dos láminas, una superior ubicada dorsomedial y otra inferior ventrolateralmente (ambas unidas rostrolateralmente). En la parte interna, el cerebelo muestra un amplio ventrículo, que se corresponde a una extensión del cuarto ventrículo. En la corteza cerebelosa se distinguen, desde la zona marginal a la ependimaria, las capas: molecular (que contiene células estrelladas), de Purkinje (con las células de Purkinje) y capa de fibras (que contiene axones de Purkinje y prolongaciones de aferencias cerebelosas). La capa granular (que contiene células de Golgi y granulares) está restringida a niveles paramediales, donde se encuentra agrupada en un par de eminencias paramediales, también conocidas como eminencias granulares. Estas eminencias se extienden rostro-caudalmente desde el velo medular anterior hasta los niveles más caudales, donde continúan en la aurícula. Además, en esta especie se conoce bien la ultraestructura y quimioarquitectura de la corteza cerebelosa, habiéndose mostrado que los componentes del cerebelo en mamíferos están representados primariamente en estos peces.

El desarrollo del cerebelo ha sido ampliamente estudiado en mamíferos, no sólo porque es crucial para una mejor comprensión de la compleja estructura cerebelosa en adultos o el origen de muchas anomalías cerebelosas, sino que también lo es para conocer su historia evolutiva, pues la identificación de semejanzas y diferencias entre especies a lo largo del desarrollo es esencial para estudios comparativos. Este tipo de

estudios han permitido saber que a pesar de que el cerebelo es la estructura encefálica con aparentemente mayor variabilidad, todos los vertebrados mandibulados parecen presentar procesos de desarrollo similares y una red neuronal básica en común. Por lo tanto, para explicar lo más complejo, basarse en lo más simple puede servir para revelar la organización básica, elemental, que es común y esencial para todos los grupos. Sin embargo, en los peces cartilaginosos, a pesar de ser un grupo clave desde el punto de vista filogenético, los estudios realizados sobre el desarrollo del cerebelo en este grupo son escasos.

Para una aproximación a la condición ancestral del cerebelo, y por las razones antes mencionadas, *S. canicula* es un candidato adecuado para estudiar el desarrollo cerebelar. Por ello, en el presente trabajo estudiamos el patrón de regionalización temprana del cerebelo, analizando la genoarquitectura de la región de donde surge el cerebelo, el rombencéfalo rostral, en etapas tempranas del desarrollo (cuando se forma el primordio del cerebelo), para así poder determinar su grado de conservación evolutiva. También se ha llevado a cabo un análisis detallado de los procesos morfogenéticos que tienen lugar durante el desarrollo del cerebelo, complementando la información de marcadores anatómicos y genéticos.

Por otra parte, puesto que un conocimiento detallado de las conexiones cerebelares en este grupo de peces podría arrojar luz sobre la organización basal del sistema cerebelar, se ha realizado un estudio hodológico del cerebelo postnatal y durante el desarrollo embrionario (distinguiendo el orden de llegada de las distintas aferencias a la corteza cerebelosa). Además se ha caracterizado la naturaleza neuroquímica de los distintos núcleos precerebelosos. Para comprobar si el origen y desarrollo de los núcleos precerebelosos (a partir de los labios rómbicos) también muestran un elevado grado de conservación evolutiva, se ha desarrollado una primera

aproximación al estudio de las migraciones neuronales derivadas de los labios rómbicos.

CAPÍTULO 1. Genoarquitectura del rombencéfalo rostral de un tiburón: base para comprender la emergencia del cerebelo en la transición entre vertebrados agnatos y gnatostomados.

El cerebelo se origina a partir de la región alar del rombencéfalo rostral. Se forma debido a la inducción por parte del organizador ístmico, que se encuentra localizado en el límite entre mesencéfalo-rombencéfalo o MHB (por las siglas en inglés referidas a *midbrain-hindbrain boundary*). El conocimiento sobre el territorio ístmico procede sobre todo de estudios realizados en mamíferos, aves, anfibios y peces óseos, pero se carece de estudios en peces cartilaginosos. Aunque un símil a organizador ístmico se ha descrito en hemicordados, la capacidad de inducir la formación de un cerebelo es una innovación evolutiva de vertebrados mandibulados o gnatóstomos.

Puesto que los peces cartilaginosos son considerados un grupo filogenético clave por presentar las características más primitivas de gnatóstomos, el análisis comparativo del patrón de expresión de genes reguladores en el límite mesencéfalo-rombencéfalo (MHB) es esencial para encontrar diferencias que pudieran conducir a cambios evolutivos importantes. De hecho, diferencias en la expresión génica en relación al MHB de peces cartilaginosos con respecto a lo descrito en vertebrados sin mandíbulas o agnatos, podrían desvelar por qué el organizador ístmico adquiere la capacidad de inducir la formación del cerebelo.

En el presente trabajo hemos analizado el patrón de expresión de una variedad de genes (*ScOtx2, ScGbx2, ScFgf8, ScLmx1b, ScIrx1, ScIrx3* y *ScEn2*) mediante técnicas de hibridación *in situ*, así como la distribución de la proteína Pax6 en el

cerebelo en desarrollo del tiburón *Scyliorhinus canicula*. La ubicación de estos productos génicos en embriones tempranos (en etapa de faríngula) demostró una gran semejanza con lo descrito en mamíferos, revelando un patrón altamente conservado. Por consiguiente, las subdivisiones principales del rombencéfalo rostral de *S. canicula* han podido ser reconocidas. Nuestros resultados apoyan la existencia de un rombómero 0, identificado como el dominio *ScFgf8/ScGbx2/ScEn2*-positivo y *ScIrx3*-negativo, que se encuentra justo caudalmente al dominio del mesencéfalo *ScIrx1/ScOtx2/ScLmx1b*-positivo. La expresión diferencial de *ScEn2* y del anticuerpo anti-Pax6 en el rómbomero 1 reveló una subdivisión en una mitad anterior (*ScEn2*-positiva) y otra posterior (Pax6-positiva). En el estudio comparativo, hemos observado que los patrones de expresión de los genes *ScFgf8*, *ScOtx2* y *ScEn2* parecen bastante similares a sus homólogos descritos en agnatos. Sin embargo, se observaron diferencias en relación a la expresión de los genes *Irx*, pues en la pintarroja, al igual que en mamíferos, pero a diferencia de lo descrito en agnatos, el área del MHB es negativa para este gen. Aunque serían necesarios más estudios genéticos, estas diferencias podrían haber conducido a importantes cambios evolutivos, quizá relacionados con la aparición del cerebelo y con el hecho de que la duplicación de genes *Irx* ocurrió en el linaje de los gnatóstomos, después de la separación del linaje de agnatos.

CAPÍTULO 2. Origen y desarrollo del cerebelo y estructuras relacionadas en un tiburón.

Una vez determinada la ubicación del cerebelo, y durante la regionalización del eje antero-posterior del cerebro, las paredes alares del rombencéfalo rostral crecen dando lugar a los labios rómbicos, los cuales se unen en la línea media para originar el primordio cerebelar. Semejanzas entre los diferentes vertebrados se observan en etapas

tempranas, pero conforme avanza el desarrollo surgen muchas diferencias, mayormente debido a la divergencia filogenética. Paradójicamente, esto convierte al cerebelo en una estructura extremadamente variable en tamaño y forma a pesar de su organización básica altamente conservada a lo largo de la evolución.

Por consiguiente, nos preguntamos en qué momento del desarrollo del cerebelo de pintarroja se establecen las principales diferencias con respecto a otras especies. También intentamos averiguar si genes responsables del desarrollo, que participan en el establecimiento del patrón del rombencéfalo rostral y en la regionalización intracerebelosa en otros vertebrados, jugarían el mismo papel en gnatóstomos basales como los peces cartilaginosos.

Para una mejor comprensión de los procesos de desarrollo del cerebelo en un gnatóstomo basal, realizamos un análisis exhaustivo de los cambios en la anatomía macroscópica de estructuras cerebelosas en el tiburón galeomorfo *Scyliorhinus canicula* que nos llevó a distinguir tres períodos de desarrollo. Un primer período o etapa de desarrollo temprano, en el que la placa cerebelosa se forma por la fusión de los labios rómbicos; un segundo período o etapa intermedia durante la cual el primordio cerebeloso se convierte en cuerpo cerebeloso y aurícula superior, mientras la aurícula inferior se forma a partir del área somatosensorial adyacente; y un tercer período o etapa tardía el cual mayormente se corresponde con el crecimiento y maduración del sistema cerebelar. Esta clasificación es útil no sólo desde el punto de vista anatómico, sino que también para crear un marco para un estudio más sistemático del desarrollo del cerebelo desde otros puntos de vista, así como para facilitar el estudio comparativo con otras especies.

En el análisis detallado del paso de formación del primordio cerebelar a cuerpo cerebeloso y aurícula, pudimos distinguir cómo tenía lugar la progresiva formación (de

rostral a caudal) de cuatro puntos de flexión, que nos han servido de referencias anatómicas. El primero se encuentra en el límite entre techo óptico y cerebelo (correspondiéndose con la fisura meso-rombencefálica). Los puntos segundo y tercero establecen los límites rostral y caudal entre las partes dorsal y ventral del cuerpo cerebeloso; y el cuarto se encuentra en el límite entre el cuerpo cerebeloso y la aurícula superior, correspondiéndose el último con la fisura posterolateral.

La comparación del desarrollo cerebeloso en este tiburón galeomorfo (grupo caracterizado por poseer cuerpos cerebelosos complejos) con lo descrito previamente en un tiburón del grupo de los escualomorfos (con cuerpos cerebelosos más sencillos) reveló muchas similitudes interespecíficas, lo que nos ha permitido reconocer etapas embrionarias equivalentes. Además, la comparación con otros vertebrados mandibulados destacó el alto grado de conservación de los marcadores anatómicos en el proceso de morfogénesis cerebelosa. La adquisición de la forma madura del cuerpo cerebeloso y aurículas en el estadio 32 en *S. canicula* justifica el hecho de considerar este estadio como el inicio de la madurez en relación a la morfología del cerebelo, a pesar de que el cerebelo continúa creciendo a lo largo de toda la vida. Sin embargo, esto no se aplica a otros vertebrados con mandíbulas, pues en peces óseos, por ejemplo, la adquisición de la forma madura se adquiere más tarde que en la pintarroja.

El orden de aparición de las fisuras posterolateral y primaria transversa debe ser considerado como una característica importante del desarrollo del cerebelo en gnatóstomos, dado que parece mantenerse en la mayoría de los vertebrados mandibulados. Por otro lado, el proceso de morfogénesis cerebelar en la pintarroja difiere bastante del de peces óseos y reptiles desde etapas tempranas del desarrollo, mientras que parece más próximo al de mamíferos. Así, los peces óseos desarrollan una estructura exclusiva de este grupo denominada válvula cerebelosa, y en algunos reptiles

el crecimiento del cerebelo es por eversión, a diferencia de peces cartilaginosos y demás gnatóstomos, en los que se produce por evaginación. Esto señala al cerebelo de condrictios o peces cartilaginosos como un modelo adecuado para el estudio de la posible condición ancestral de vertebrados mandibulados.

Con el fin de complementar los datos anatómicos, también realizamos técnicas inmunohistoquímicas y de hibridación *in situ*. Para resolver cierta controversia sobre si las aurículas cerebelosas se originan a partir del rombómero 1 y/o del rombómero 2, se analizó el patrón de expresión del gen *ScHoxA2* (marcador del rómbomero 2). Interesa destacar que las aurículas cerebelosas, tanto la lámina superior como la inferior, resultaron ser negativas para este gen, lo que sugiere un origen del cerebelo exclusivamente del primer rombómero. No obstante, una pequeña zona situada entre el área octavo-lateral y el área identificada como aurícula inferior, presenta características peculiares que nos han llevado a caracterizarla como una posible zona de transición entre ambas estructuras.

Por otra parte, los patrones de expresión de los genes *ScEn2* y *ScOtx2* revelaron una compartimentalización antero-posterior del cerebelo similar a la de los mamíferos y apoya el hecho de que las fisuras (comúnmente utilizadas para definir dominios cerebelosos) sean utilizadas como marcadores o puntos de referencia anatómicos fiables. Además, la expresión de *ScEn2* en el plano de la medio-lateral demostró un único dominio positivo paramedial, lo que apoya hipótesis previas sobre la aparición de un patrón de bandas múltiples más tarde en la evolución. Esto también viene apoyado por el marcaje del anticuerpo anti-aldolasa-C observado, con ausencia de múltiples bandas parasagitales.

Estos resultados enfatizan la importancia de combinar estudios clásicos anatómico descriptivos con actuales técnicas moleculares en un vertebrado mandibulado basal para estudiar la evolución, y en la búsqueda de la condición ancestral del cerebelo.

CAPÍTULO 3. Desarrollo del sistema cerebelar aferente en el tiburón *Scyliorhinus canicula*: avances en los conocimientos de la organización basal de los núcleos precerebelosos en gnatóstomos.

Un conocimiento exhaustivo de las conexiones cerebelosas en los peces cartilaginosos podría arrojar luz sobre la organización básica del sistema cerebeloso, de nuevo, partiendo de la base de que el cerebelo es reconocido como una innovación evolutiva de vertebrados mandibulados (cuyo grupo más primitivo está representado por los condrictios o peces cartilaginosos). La organización del sistema precerebelar de peces cartilaginosos ha sido previamente descrita por otros autores en adultos. Dichos estudios sugieren que las poblaciones celulares que proyectan al cerebelo pueden corresponderse con los núcleos precerebelosos de mamíferos. Además, fibras musgosas y trepadoras también han sido previamente descritas en adultos de la pintarroja o *S. canicula*. No obstante, no es posible entender el origen y evolución de los núcleos precerebelosos sin la perspectiva del desarrollo.

Por ello, en el presente trabajo se ha realizado un estudio del desarrollo de las conexiones cerebelosas en embriones y juveniles de *S. canicula*, mediante la aplicación de técnicas de trazado en combinación con técnicas inmunohistoquímicas. El trazador utilizado ha sido la Neurobiotina, el cual presenta una acción mayormente retrógrada, pero también puede ser transportado anterógradamente. Sobre la base de este transporte dual hemos podido distinguir las conexiones recíprocas entre la corteza cerebelosa y el núcleo cerebeloso en el mismo experimento: proyecciones nucleo-corticales, con células

del núcleo cerebeloso retrógradamente marcadas, y proyecciones cortico-nucleares, con paquetes de fibras dirigidos hacia el núcleo cerebeloso anterógradamente marcados. Estos últimos representan los axones de las células de Purkinje.

Las principales poblaciones celulares precerebelosas que hemos podido determinar gracias a este estudio hodológico se encuentran situadas en el diencéfalo (pretecho y tálamo), mesencéfalo (formación reticular y núcleo ruber), rombencéfalo (núcleo cerebeloso, formación reticular y oliva inferior) y la médula espinal (asta ventral), siendo esta distribución muy semejante a las previamente descritas en otros peces cartilaginosos por otros autores. En cuanto al análisis a lo largo del desarrollo, se observó que la entrada del sistema cerebelar aferente es concurrente con el establecimiento de las capas del cerebelo. Más tarde, la proyección de nuevas neuronas precerebelosas alcanza progresivamente la corteza cerebelosa, lo que refleja la progresiva maduración de las capas granular y de Purkinje. El orden de llegada de los distintos sistemas aferentes podría ser indicativo de la aparición de diferentes sistemas de control por el cerebelo a lo largo del desarrollo. Por ejemplo, la maduración de los fotorreceptores de la retina en *S. canicula* (previamente descrito), que comienza en el estadio 32 temprano y se completa al final de este estadio, ocurre prácticamente de forma simultánea con el desarrollo de proyecciones pretecto-cerebelosas. Esto apoya la posibilidad de que el inicio del control de los reflejos visuales por el cerebelo se produce al principio del estadio 32, lo que estaría relacionado con la maduración funcional de la retina.

Los primeros axones de las células de Purkinje alcanzan el pedúnculo cerebeloso coincidiendo con el momento en que se marcan retrógradamente las primeras neuronas de la oliva inferior (estadio 32 intermedio), caracterizando así el comienzo de la diferenciación de las células de Purkinje. Por otra parte, el conocimiento del desarrollo

de la proyección olivo-cerebelosa puede permitir hacer comparaciones con el sistema olivo-cerebelar de otros gnatóstomos. El desarrollo de las proyecciones espino-cerebelosas en la pintarroja precede, al igual que en amniotas, a la proyección olivo-cerebelosa, sugiriendo que las aferencias de la médula espinal participarían en el control temprano de movimientos corporales por el cerebelo. Este patrón común del orden de llegada de las distintas aferencias al cerebelo entre vertebrados mandibulados podría resultar útil para la comparación de las etapas de desarrollo cerebeloso.

Una observación destacable en la caracterización neuroquímica (mediante combinación del trazador y técnicas inmunohistoquímicas) es que todos los núcleos precerebelosos contienen células precerebelosas inmunorreactivas a calretinina.

La oliva inferior merece especial atención debido a la importancia funcional del sistema de fibras trepadoras olivo-cerebelar, ya que está involucrado en el aprendizaje y sincronización de movimientos. Los marcadores neuroquímicos del sistema olivo-cerebelar en la pintarroja son bastante similares a los descritos en otros vertebrados. La existencia de dos subpoblaciones en la oliva inferior de *S. canicula* recibiendo diferentes tipos de inervación podría estar relacionado con proyecciones olivo-cerebelosas topográficas diferenciales, lo que coincide con lo descrito previamente en otro pez cartilaginoso.

Las similitudes que observamos en la caracterización neuroquímica de los diversos núcleos precerebelosos de la pintarroja y los amniotas probablemente indican un alto grado de conservación evolutiva. Además, la existencia de migraciones tangenciales y radiales de las células precerebelosas originadas en los labios rómbicos en *S. canicula* sugiere que su patrón básico pudo ser establecido muy temprano en la evolución de los gnatóstomos.

En conjunto, los resultados obtenidos en el presente trabajo muestran que las características comunes observadas a lo largo del desarrollo del cerebelo entre *Scyliorhinus canicula* y otros gnatóstomos revelan el marco o armazón básico sobre el que se organizan cerebelos más complejos, y que podría corresponder a la organización ancestral del sistema cerebelar.

APPENDIX 1

USC
UNIVERSIDADE
DE SANTIAGO
DE COMPOSTELA

APPENDIX 1

Training stay in the laboratory of the Professor Reinhard Köster

(Cell Physiology-Zoological Institute, Technische Universität Braunschweig, Germany)

The realization of this work helped us to solve some major questions regarding the origin and development of the cerebellum in elasmobranch fishes. However, it also raised new challenging questions, some of which have not been entirely resolved such as, for example, if the cerebellum arises exclusively (or not) from rhombomere 1 (see Chapter 1), or the identification of rhombic lips derivatives as precursors of different precerebellar nuclei (see Chapter 3). We think that these questions could be solved by cell lineage tracking of the rhombomere 1 and lower rhombic lip derivatives, respectively. Therefore, we aimed to approach to this technique, which has been successfully used in other fish species (see, for example, Volkmann et al., 2010; Wullimann et al., 2011; Hocking et al., 2013; and Fig. 1).

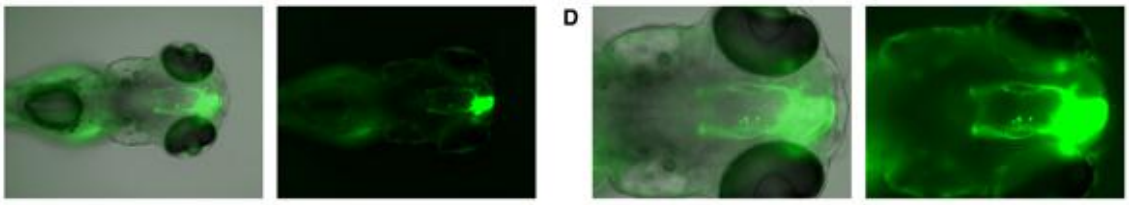

Figure 1. Plasmid driven GFP-expression 4 days post-electropration. Taken from Hoegler et al. (2011).

The stay in the laboratory of the Prof. Köster (University of Braunschweig) has represented to me a great opportunity to be familiar with a number of techniques, including: (1) *in vivo* imaging, by using crossed transgenic lines and studying the combined distribution of different cell types in cerebellum through development; (2) microinjection of various GFP-tagged plasmids and anterograde tracers at one cell stage; (3) electroporation of GFP-tagged plasmids and anterograde tracers in the cerebellum of embryos at 24 and 48 hours post fertilization.

In the course of this stay I managed to electroporate specific cell types in zebrafish, even at late embryonic stages, which allowed the tracing of individual neurons.

Since I have been successful in applying these techniques in late embryos of zebrafish, I consider they can be applicable to *S. canicula*, whose embryos are easily accessible and can be maintained out of the eggshell for several days. The application of these techniques to our animal model could ease the way for further comparative neuroanatomical studies.

Literature cited

Hocking JC, Distel M, Köster RW. 2013. Studying cellular and subcellular dynamics in the developing zebrafish nervous system. Exp Neurol 242:1-10.

Hoegler KJ, Distel M, Köster RW, Horne JH. 2011. Targeting olfactory bulb neurons using combined in vivo electroporation and Gal4-based enhancer trap zebrafish lines. J Vis Exp 54. pii: 2964. doi: 10.3791/2964.

Volkmann K, Chen YY, Harris MP, Wullimann MF, Köster RW. 2010. The zebrafish cerebellar upper rhombic lip generates tegmental hindbrain nuclei by long-distance migration in an evolutionary conserved manner. J Comp Neurol 518:2794-817.

Wullimann MF, Mueller T, Distel M, Babaryka A, Grothe B, Köster RW. 2011. The long adventurous journey of rhombic lip cells in jawed vertebrates: a comparative developmental analysis. Front Neuroanat 5:1-27.

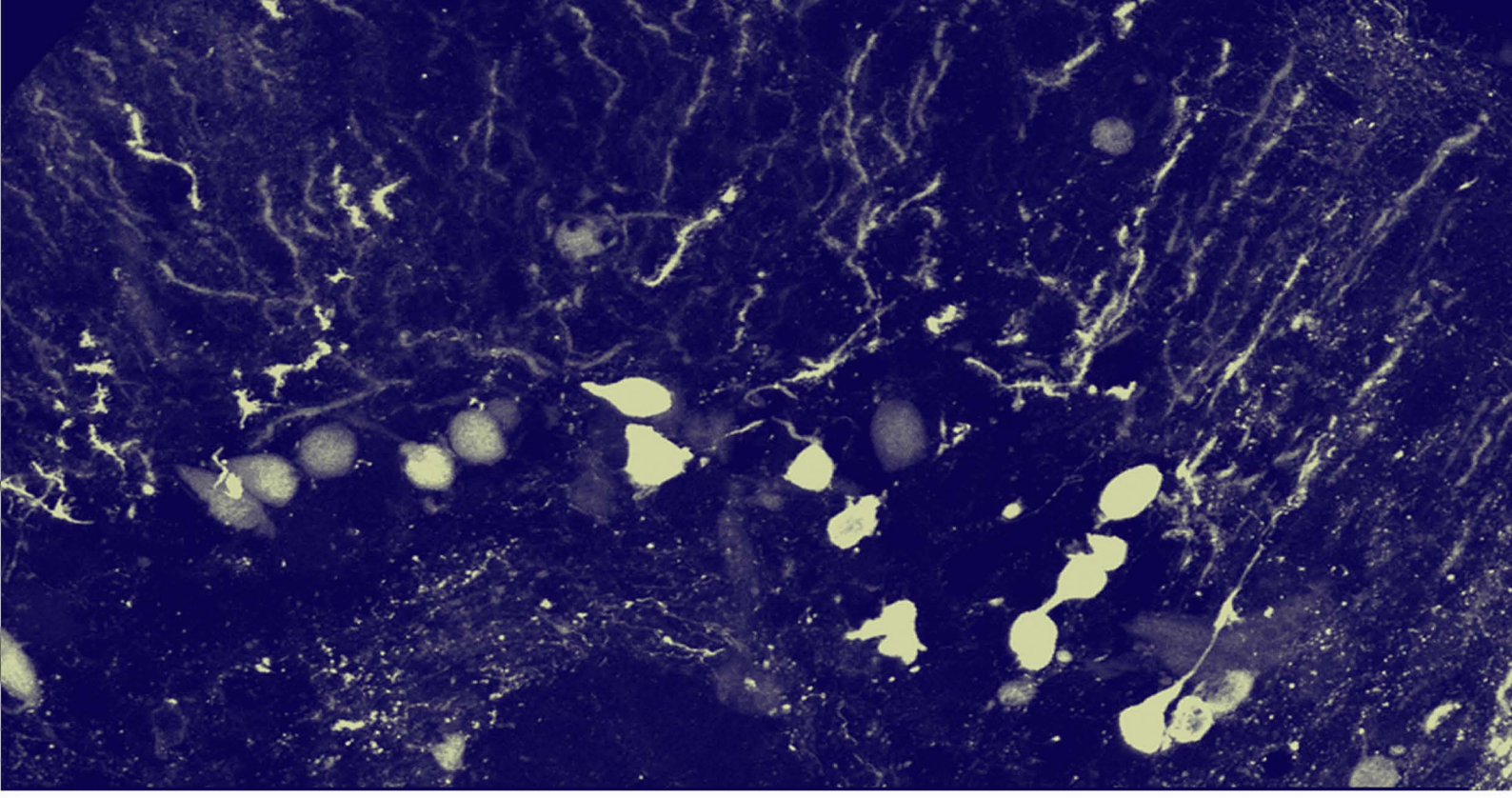

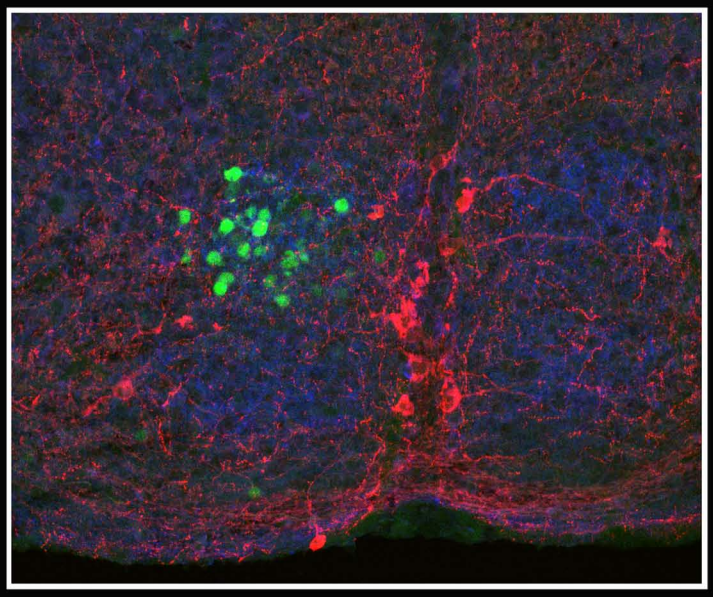

UNIVERSIDAD DE SANTIAGO DE COMPOSTELA